The University Of Sheffield.

A Novel Method for the Characterisation of Human Upper Limb Workspace with Respect to Dexterity

Ulises Daniel Serratos Hernandez

A thesis submitted for the degree of Doctor of Philosophy in the Department of Mechanical Engineering, University of Sheffield

June 2021

ACKNOWLEDGEMENTS

Firstly, I would like to express my sincere gratitude to my supervisors Dr. Jennifer Rowson and Dr. Rob Barthorpe for their continuous support and patience throughout my Ph.D. Their guidance and assistance at every stage of my research was invaluable.

I am deeply grateful to all my colleagues for their support, insightful comments, and suggestions, especially to Carlos Luna Ortiz, Victor Gonzalez Sanchez, and Noe Martinez Sanchez. I would like to extend my sincere thanks to the volunteers that participated in the experiments. Likewise, I would like to thank CONACYT for their financial support.

My sincere thanks also go to my friends for their support, they have made my academic and personal life in the UK a lovely adventure.

Last but not the least, I am enormously grateful to my mother, brother, and sister for their unconditional encouragement and love. In particular, to my mother, the person I admire and love the most.

ABSTRACT

Human dexterity is a complex phenomenon associated to physiological and cognitive factors that affect the execution of precise movements. Dexterity is strongly linked to upper limb (UL) functionality and performance, and its study is important for clinical analysis, ergonomics, sports biomechanics, design, rehabilitation, and human-machine interactions. However, its understanding is quite limited. Dexterity is commonly assessed through time-dependent dexterity tests that can determine the successful completion of tasks on test boards paced in front of the participant. However, such tests cannot inform about participant performance in other regions of the corresponding UL workspace volume (WV), and they can only collect data related to specific tasks, and therefore, cannot predict UL performance for the execution of other tasks.

This thesis establishes a time-independent novel method for the characterisation of UL workspace with respect to dexterity; the "Dexterity Analysis Method" (DAM), which is based on the manipulability analysis method (used in robotics to quantify robot manipulability). The DAM is flexible, versatile, and scalable. It can be used to analyse real and virtual individuals or populations using direct measures or statistical data. Moreover, the DAM allows adding human factors, and to assigning their weights for adjustment and calibration. Hence, the DAM is a powerful tool that can help to evaluate performance, assess healthiness, optimise implants and prosthetics, design ergonomic workplaces and homes, develop assistive devices, and conduct pre- and post-surgery evaluations. Moreover, this work, as implemented in the DAM, promotes the use of WV as an objective reference to map performance, healthiness, and dexterity. Finally, the DAM contributes to closing the knowledge gaps on the understanding and quantification of UL motion, workspace, and dexterity. However, the DAM still needs to be fully validated as the experimental results obtained in this research with such purpose were not conclusive.

A real-life application of the DAM is illustrated in Chapter 7 of this work, which analyses the effects of reverse shoulder arthroplasty (RSA) on WV and dexterity. The results indicate that WV for healthy people can be around 32% larger than those for people with RSA. However, it was found that greater WV do not necessarily translate into larger high dexterity regions, and the effects of reductions in ROM on WV depend on the extreme at which such reductions occur. For instance, a decrease of 15° in elbow extension reduces 2% of 2-D reachability, whereas a decrease of 15° in elbow flexion only reduces it by 10.8%. Therefore, surgeons should carefully consider such factors when making decisions during joint surgery, reconstruction, and implant position optimisation.

Key words: *upper limb, dexterity, performance, limb functionality, workspace, manipulability, human movement science, biomechanics.*

NOMENCLATURE

General Terms

a	Distance on the x axis
a	Acceleration, when referring to motion
A_i	Homogeneous transformations from i to $i-1$
Al	Arm length
$atan$	Inverse trigonometric function of the tangent function
b	Distance on the y axis
c	Distance on the z axis, when referring to a displacement
c	Cosine, when referring to trigonometric functions
C_j	Number of constraints of the j joint
c_{ijk}	Christoffel symbols
$Comfort_\theta$	Comfort with respect to range of motion
$Comfort_{Mo}$	Comfort with respect to torques perceived at the shoulder
$Comfort_{w_k}$	Comfort with respect to work needed to rise the limb
d	Distance
D	Inertial matrix
D_x	Dexterity measure
f	Force
F	Number of degrees of freedom, when referring to degrees of freedom
Fl	Forearm length
g	Gravity
H	Homogeneous matrix
$h_{i,j}$	Element i,j of the homogeneous matrix H
Hl	Hand length
I	Moment of inertia

j	Number of joints
J	Jacobian
J_v	Linear velocity part of the Jacobian
J_ω	Angular velocity part of the Jacobian
K	Kinetic energy
L	Used to refer to The Lagrangian equation
m	Constant
m	Mass of the body, when analysing forces
M_o	Moment of inertia, torque
n	Number of rigid bodies, when referring to DOF
n	Constant
o_i	Origin of frame i
o_j^i	Coordinates of the origin j relative to the frame i
P	Position vector, when referring to position-orientation
P	Potential energy, when referring to forces and energy
q	Joint angle
$\dot{q}$	First derivative of q; angular velocity
$\ddot{q}$	Second derivative of q; angular acceleration
r	Radius, when referring to distance
r_{ci}	Coordinates of the centre of mass of link i
$r_{i,j}$	Element i, j of the rotation matrix R
R	Rotation matrix
R_j^i	Orientation of the frame j relative to the frame i
$Rot_{x,\alpha}$	Rotational matrix representing an angular displacement α with respect to the x axis
$Rot_{y,\beta}$	Rotational matrix representing an angular displacement $\beta\ with$ respect to the y axis
$Rot_{z,\gamma}$	Rotational matrix representing an angular displacement $\gamma\ with$

	respect to the z axis
s	sine
T_j^i	Homogeneous matrix for the representation of position and orientation of the frame j with respect to the frame i
$Trans_{x,a}$	Matrix representing a displacement a on the x axis
$Trans_{y,b}$	Matrix representing a displacement b on the y axis
$Trans_{z,c}$	Matrix representing a displacement c on the z axis
x_i	x axis of frame i
y_i	y axis of frame i
z_i	z axis of frame i
α	Angle of rotation with respect to the x axis
β	Angle of rotation with respect to the y axis
γ	Angle of rotation with respect to the z axis
θ_i	Rotational angle of joint i
$\theta_{i\,min}$	Minimum allowed angle of the i joint
$\theta_{i\,max}$	Maximum allowed angle of the i joint
$\dot{\theta}$	Derivative of θ; angular velocity
ξ	Total body velocity
τ	Torque
υ	Linear velocity
ω	Weight, when describing moments and forces
ω	Angular velocity, when describing motion
w	Manipulability measure
w_k	Work, the k subscript here is to avoid confusion as w without subscript refers to manipulability

Abbreviations

2D	Two dimensional
3D	Three dimensional
ADL	Activities of daily living
ASB	American Society of Biomechanics
BBT	Box and block test
CT	Computed tomography
DH	Denavit-Hartenberg, normally followed by convention or method
DOF	Degree of freedom
EMG	Electromyography
ESB	European Society of Biomechanics
GRS	Global reference system
ISB	International Society of Biomechanics
LRS	Local reference system
MRI	Magnetic resonance imaging
PPT	Perdue pegboard test
REA	Reach envelope area
ROM	Range of motion
SD	Standard deviation

LIST OF FIGURES

Figure 7.6. Estimated workspace volumes (grey) and high dexterity regions (yellow) for: an individual with optimal implant position in reverse shoulder arthroplasty (top row) and a healthy individual (bottom row). Three views: Coronal, Sagittal and Transverse planes.

LIST OF TABLES

1 INTRODUCTION

Humans execute movement even unconsciously. However, motion is a complex phenomenon. It requires the cooperation of different systems of the body. Conscious motion involves recollecting information about the current environment (through the senses), sending such information to the brain to process it, sending commands to the muscles to execute movement, sensing for feedback, and making corrections.

This research is interested in one of the motion qualities that relates to precision called "dexterity". Nikolai Aleksandrovich Bernstein, a Soviet neurophysiologist considered as one of the greatest scientists of the 20th century, described dexterity as a motor ability to execute accurate movements with a determined purpose under any environmental condition [1]. Thus, dexterity is a relevant characteristic human motion as having at least some level of dexterity is required to successfully perform activities of daily living, as well as, to conduct precise tasks for work or recreation purposes. People with low dexterity can become highly dependent on others as in some cases they cannot perform basic tasks or even feed themselves. Likewise, people with low dexterity could be rejected from some job positions that require fine manipulations. Moreover, in some sports and recreation activities such as ping pong, hockey, archery, fencing, crafting, drawing, writing, and painting, dexterity is also an important factor to be successful. Hence, the importance of understanding and characterising dexterity. However, up until now, the understanding of human dexterity is quite limited, and its characterisation challenging.

Up until this research, the most common approach to evaluate upper limb dexterity is through time-dependent dexterity tests such as the Box and Block Test (BBT), Perdue Pegboard Test (PPT), Motor-free Visual Perceptual Test, Functional Dexterity Test, and Strength Dexterity Test [2-10]. Such tests are relatively accessible and easy to administer; however, such tests only evaluate the execution of specific tasks such as matching objects to their corresponding shapes/positions, as well as moving objects from point a to point b. Although, such tests allow to quantify certain aspects of dexterity including grasp patterns and the ability to perform tasks over specific periods of time, they cannot distinguish movement consistency and movement variations among participants, and they cannot inform about the joint angles needed to complete a task, regions of high dexterity, or participant performance in other regions of the corresponding upper limb reachable space. Therefore, a participant can potentially have good performance in a traditional dexterity test even if the person cannot rise the hand to heights other than the test hight due to injuries or diseases. More importantly, such kind of dexterity tests cannot determine if participants are able to perform other activities not evaluated during the test, which is relevant information for prescribing an adequate rehabilitation therapy,

as well as for adjusting the environment of impaired people to improve their lives. Likewise, dexterity tests are time-dependent, and therefore, performing poorly in such tests do not necessarily mean that the individual has low dexterity, as such low performance could be linked to inherent participant behaviour to be slow, or the participant may not be used to perform tasks at high-speed tasks.

In robotics, an equivalent to dexterity is called “manipulability”, which is defined as the ease of changing the position and orientation of the end-effector of a manipulator (robotic arm) [11]. Yoshikawa [11, 12] proposed a manipulability analysis method to quantify the manipulation capabilities of robotic arms. Such method encodes the mechanical properties of the robotic arm and mathematically describe how capable the robotic arm is for specific configurations and at different positions in space. Although a robotic arm and an upper limb may seem to be completely different systems, for the study of motion, both can be modelled as kinematic chains (systems composed of rigid elements interconnected through joints). Therefore, this research explores the applicability of the manipulability analysis to the characterisation of upper limb dexterity, as such method provides relevant information on the ability to perform fine movements given the mechanical properties of the extremity. A few researchers have previously used the manipulability analysis to evaluate specific tasks in the design of user-friendly rehabilitation systems [13], the evaluation of wheelchair propulsion [14], and the assessment of upper limb performance during grasping [15].

One of the most important mechanical elements of the upper limb in terms of motion is the joints, without them, the extremity would be a rigid body uncapable to perform movements. The range within joints can move is called “joint range of motion”, whereas the independent directions in which motion can be performed are called “degrees of freedom”. The combination of joint range of motion and the degrees of freedom at each joint allow the upper limb to perform movements within a specific 3-dimiensional space or “workspace volume”. Workspace volumes have been mostly employed for the study of human-machine interactions [16], the design of exoskeletons [17, 18], ergonomics design [19], and the development of rehabilitation systems [20]. However, workspace volumes are not commonly used as a standard reference to characterise upper limb performance, healthiness, and dexterity. Nonetheless, in recent years, due to the technological advancements, some researchers have attempted to introduce and recommend the use of workspace as a reference for upper limb functionality within the clinical context [21-23]. Thus, this work will explore the use of such workspace volumes to map upper limb dexterity within its corresponding 3-dimensional reachability.

Finally, this research aims to establish a time-independent novel method capable of characterising upper limb workspace with respect to dexterity. As a method of such characteristics would help to close the knowledge gaps on human motion and dexterity and would facilitate the assessment of upper limb performance across the 3-dimensional space. Thus, the novel method is expected to help to evaluate performance, assess healthiness, optimise implants and prosthetic devices, design ergonomic workplaces and homes, develop assistive devices, and conduct pre- and post-surgery evaluations.

1.1 Aims and objectives

The aim of this study is to establish a novel method for the characterisation of upper limb workspace with respect to dexterity. Such method should be able to quantify upper limb workspace and dexterity for healthy and non-healthy individuals or populations, and similar quantitative information that can contribute to the understanding of dexterity and for human motion investigations. Furthermore, the novel method is foreseen as a flexible method that allows parametric adjustment and the inclusion and exclusion of variables related to dexterity.

The specific objectives to achieve the aim of this study are:

i. Development of a general kinematic model for the study of upper limb motion.
ii. Development of a method for the quantification of upper limb workspace
iii. Exploratory study of the manipulability analysis method as a technique for the characterisation of human dexterity.
iv. Study, identification, and integration of human factors associated with upper limb dexterity.
v. Development of a novel method for the characterisation of upper limb workspace with respect to dexterity
vi. Validation of the proposed novel method through experimental analysis.
vii. Demonstration of the applicability of the novel method to real life situations.

1.2 Scope of the study

The scope of this study is limited to the characterisation of upper limb workspace with respect to dexterity including kinematic and dynamic variables associated with joint range of motion, upper limb reachability, joint torques, and work. Therefore, this study does not investigate other factors that may affect dexterity such as energy, muscle strength, muscle activation, joint stability, sensorial aspects, cognitive factors, or healthiness.

However, having established the model, such factors could then be added subsequently to investigate their influences on dexterity.

Likewise, as most of the work conducted in this research is computational, most of the input values used throughout this study were obtained from published human normative data. Such normative data is in many cases confusing, difficult to compare, incomplete or inexistent. Therefore, future work should consider extending the scope of this research study and, when possible, acquiring more accurate normative data for the input parameters.

1.3 Research drivers

The characterisation of upper limb workspace with respect to dexterity would be of significant value to surgeons, rehabilitation therapists, and workplace and home designers.

Surgeons evaluate patient upper limbs, pre- and post-surgery, through medical and functional tests. In cases where joints or bones are highly injured, surgeons replace such elements with medical implants. Conducting such kind of surgeries is not an easy task, it requires pre-operative assessment to determine joint and bone health, bone geometry, and joint range of motion. The information obtained from the pre-operative assessment is used to choose the most appropriate implant and to optimise implant position. The optimisation of joint implant position is commonly based on the maximisation of joint range of motion. However, joint range of motion values by themselves cannot determine the overall 3-dimensional reachability of the extremity. Surgeons habitually have to decide which joint range of motion to sacrifice given the limitations of implants. If the impact of reducing range of motion on upper limb 3-dimensional reachability is unknown, how can surgeons optimise implant position? Is it enough to optimise implants based only on joint range of motion without consideration of 3-dimentional reachability? Therefore, novel human computational models are required to predict the impact of reductions joint range of motion on upper limb reachability, and more importantly, to investigate the impacts of such reductions on human dexterity. Such models would be beneficial for surgeons as they would make informed decisions that could provide the best outcome for patients.

Rehabilitation therapists play an important role in patient recovery. As surgeons, rehabilitation therapists evaluate patients through medical and functional tests that provide a measure of upper limb functionality. Such measure is used as a reference to indicate recovery speed and the status of total recovery. Upper limb performance is commonly evaluated through dexterity tests such as the Box and Block Test (BBT), Perdue

Pegboard Test (PPT), Motor-free Visual Perceptual Test, Functional Dexterity Test, and Strength Dexterity Test. However, such traditional dexterity tests can only evaluate the functionality of the limb for the execution of specific tasks at a fixed position of upper limb workspace (3-D reachability). Those tests cannot determine upper limb performance for the execution of non-evaluated tasks or for other non-evaluated positions of the workspace. Therefore, a patient can obtain a good score in a dexterity test and a poor performance for the execution of other tasks. Similarly, a patient can achieve a score comparable to the population mean or a score similar to a score previously achieved by the same patient, which can be a false diagnostic because there is a chance that the patient could previously perform well during the execution of tasks at any position of the workspace, and that now he can only perform well at the fixed position where the dexterity test takes place. Therefore, human models for the characterisation of upper limb workspace with respect to dexterity would augment the understanding of upper limb motion and functionality and can potentially provide new measures that account for limb performance at all positions within upper limb workspace.

Workplace and home designers interested in including ergonomic factors for the design of optimal workplaces and homes depend on the available scientific data and knowledge. Since decades ago, designers have studied human anthropometry and human motion to develop ergonomic products that can prevent occupational diseases and that can augment productivity and comfort. Although ergonomics researchers have studied and approximated upper limb workspace volumes, they commonly provide information about healthy people and for specific populations. Therefore, the design of workplace and ergonomic products for minority populations or for non-healthy people is limited by the lack of information for such populations. Such data can be obtained through experimental or computational analysis. However, sometimes the corresponding experimental analysis is expensive and the access to such populations limited. Conversely, computational models can potentially approximate workspace volumes and estimate regions where the upper limb can have high performance for the execution of any given task for those minorities and specific populations. As the aim of this research is focused on the development of computational models that can characterise upper limb workspace with respect to dexterity, it is believed that the outcome of this research will significantly benefit workplace and home designers.

1.4 Research hypothesis

Dexterity is a complex phenomenon of which little is known. Due to the lack of knowledge on the subject, it was difficult to propose specific research questions to

answer. This research work rather focused on contributing to the understanding and characterisation of human upper limb dexterity.

However, at the beginning of this investigation it was hypothesised that upper limb workspace volume is directly affected by segment lengths and joint range of motion, and therefore, that workspace volume grows as limb lengths and joint range of motion grow. Nevertheless, it was unknown if all these factors equally affect workspace volume. Likewise, it was believed that regions of high dexterity are proportional to workspace volumes. In addition, it was theorized that workspace volumes and high dexterity regions for healthy populations are larger than those for non-healthy populations as joint range of motion is affected by aging, diseases, injuries, and surgeries. Finally, it was suspected that people performance is affected by the position of the task relative to upper limb workspace.

1.5 Thesis structure

The thesis work presented in this document is composed of 9 chapters logically organised as follows.

Chapter 1 (current chapter) provides an introduction to the research work presented in this thesis including background, aim and objectives, scope, and thesis structure.

Chapter 2 centres on a comprehensive literature review to identifying the current state-of-the-art and research gaps in the study of human motion and dexterity. The literature review includes upper limb anatomy and physiology, hand-object interaction, human motion modelling, upper limb workspace analysis, dexterity analysis, manipulability analysis, uncertainty analysis, and sensitivity analysis.

Chapter 3 introduces the upper limb kinematic model used throughout this research to analyse upper limb motion. The model represents the upper limb as a kinematic chain (system composed of rigid elements interconnected through joints). Once the number of segments and joints to represent the system are defined, global and local frames of reference are assigned to each degree of freedom. Finally, a system of equations is created to describe motion in both cartesian and joint spaces.

Chapter 4 focuses on the development of a model for the analysis and quantification of upper limb reach envelope area (2-dimensional reachability) and workspace volume (3-dimensional reachability), for which the input values are upper limb segment lengths and joint range of motion for each degree of freedom. Additionally, the chapter studies and quantifies the effects of reductions in joint range of motion and identifies the most influential factors.

Chapter 5 introduces and establishes the proposed novel method for the characterisation of upper limb workspace with respect to dexterity. The chapter starts with the definition of the manipulability analysis method (widely used in robotics [11, 12, 24-27]) and the demonstration of the applicability of such method for the quantification of human manipulability. Finally, this chapter establishes the novel method proposed in this thesis (Dexterity Analysis Method), which firstly defines upper limb workspace volume and secondly determines high dexterity regions within such workspace volume through a modified version of the manipulability analysis method that incorporates factors associated with human comfort.

Chapter 6 focuses on upper limb experimental analysis to determine the accuracy of the proposed dexterity method. The experiments consisted of performing linear and circular trajectories on a new custom test board. Participant movements were recorded with a motion capture system (10 optimal cameras), according to a new custom motion capture protocol. Three measurements were computed for this experimental analysis: prediction (dexterity analysis), performance (deviation from the task), and perception (relative participant perception of comfort). Finally, a correlation analysis was conducted to quantify the level of agreement between the computational and experiments analysis.

Chapter 7 demonstrates the applicability of the proposed novel method (Dexterity Analysis Method) to real life situations. Therefore, this chapter centres on the study of human upper limb workspace with respect to dexterity in reverse shoulder arthroplasty (based on the scientific paper published by Keener et al. [28]). Likewise, this chapter provides a qualitative comparison of upper limb workspace and dexterity for a healthy and a non-healthy individual (individual with implant).

Chapter 8 discusses the results, findings, applicability and limitations of the method, and some relevant research gaps in human motion science.

Chapter 9, the final chapter of this thesis, provides the final conclusions, summarises the contributions of this research work to the understanding of dexterity and indicates venues for future work.

2 LITERATURE REVIEW

The aim of this chapter is to provide a comprehensive literature review to identify the current state-of-the-art and research gaps for the study of human dexterity and the investigation of general human motion. The literature review was divided into 3 main groups: anatomy and physiology of the human upper limb, human hand grasp and object interaction, and human motion modelling. The importance of this chapter relies on defining the upper limb structure and functionality to understand the capabilities of the extremity in terms of motion, as well as, on identifying the current state-of-the-art for the assessment and characterisation of upper limb workspace and dexterity.

2.1 Anatomy and physiology of the human upper limb

It is impossible to describe a system or phenomenon if the elements that compose them, their functionality, and their capabilities are unknown. Firstly, upper limb motion is commonly described through kinematic models that represent the extremity as a system composed of rigid elements interconnected through joints (kinematic chains) [29-35], where the rigid and articulated elements of the limb are the bones and joints, respectively. It is well known that Anatomy and Physiology are the fields of science that study the structure and functionality of each element of the body, therefore, this section centres on the review of the anatomy and physiology of the human upper limb. Additionally, this section provides a literature review on range of motion normative data to understand the joint limits to perform movement.

2.1.1 Anatomy and physiology

As the research focus of this thesis is the study of upper limb workspace and dexterity, this section only centres on the description of the anatomy and physiology of the upper limb as a system composed of rigid and articulated elements, bones and joints, respectively. Therefore, other anatomical and physiological elements of the extremity, as well as, the forces and factors that drive motion, are not addressed in this section as the study of those factors is not part of the scope of this research.

Bones are the structural elements of the body that provide frame. They are composed of spongy and hard tissue depending on their size, shape and functionality [36]. Joints are elements that connect two bones, bone and cartilage, or bone and teeth, which can be structurally classified into fibrous (dense connective tissue rich in collagen fibres), cartilaginous (bones held together by cartilage), and synovial (bones connected by an articular capsule, synovial cavity and often accessory ligaments) [36]. Likewise, joints can be classified according to functionality as synarthrosis (immovable), amphiarthrosis

(slightly movable), and diarthrosis (freely movable synovial joints) [36]. As this thesis work is focused on human movement, synovial joints are the joints of interest as they allow movements such as shoulder abduction-adduction or elbow flexion-extension. Synovial joints are enclosed in a synovial capsule and are covered by articular cartilage which is a surface of hyaline to reduce friction and absorb shock [36]. The synovial capsule is composed of fibrous membranes that provide flexibility, whereas fibre bundles called ligaments provide stability and prevent dislocation [36]. Therefore, for gross movements such as elbow flexion-extension or shoulder abduction-adduction, human motion models commonly assume joints to be frictionless due to the properties of the cartilage and the synovial fluid as a highly efficient elements to reduce friction at the joint.

Joints allow motion within a limited range called “joint range of motion” (ROM). Such range of motion is limited by the shape of the bones, the tissue surrounding the joint such as the synovial capsule, the ligaments (which provide stability to the joint), the tendons, and even the body fat surrounding the joint. An example of range of motion limitations can be observed in elbow extension where motion is limited by the collision of the ulnar head with the olecranon fossa. Likewise, forearm pronation is limited by the collision of the radius with the ulna, whereas supination is constrained by the ligaments and the interosseous membrane between the radius and ulna [37]. Therefore, diseases, injuries, and deformations affecting such elements of the body have a direct impact on joint range of motion.

Synovial joint movements are generally classified as [36]:

i. Gliding: nearly flat bone surfaces move back-and-forth and side-to-side with respect to each other within a relatively limited range.

ii. Angular: displacement increasing or decreasing the angle between two bones.

iii. Rotational: rotational movement of the bone around its own longitudinal axis.

iv. Special: movements of particular joints including elevation, depression, protraction, retraction, supination, pronation, and opposition [36].

Therefore, the combination of gliding, angular, rotational, and special movements of the synovial joints allow humans to perform motion.

The upper limb is composed of the scapula, clavicle, humerus, ulna, radius, carpals, metacarpals and phalanges (a total of 32 bones) interconnected through the shoulder, elbow, wrist, carpometacarpal, metacarpophalangeal, and interphalangeal joints (see Figure 2.1) [36].

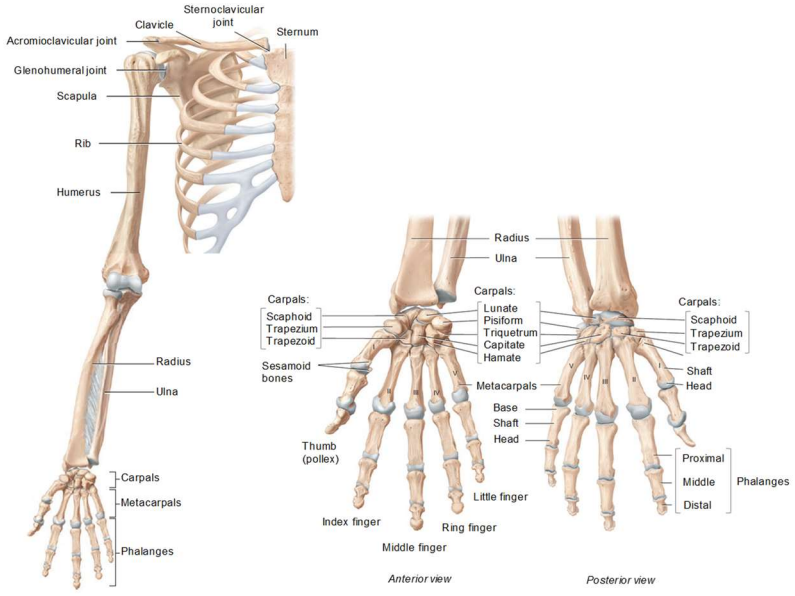

Figure 2.1. Bones of the upper limb. Copyright © 2009, John Wiley & Sons[1].

2.1.1.1 The Shoulder

The shoulder is the joint of the human body with the greatest range of motion and is considered as the main contributor to upper limb reachability, without it, upper limb motion would be tremendously limited. Although the shoulder is commonly thought of and modelled as a ball-and-socket joint, the shoulder is actually a complex system composed of the clavicle, scapula, the head of the humerus, and the joints that interconnect each of these elements. In some cases, the sternum is also considered as part of the shoulder complex.

The shoulder complex consists of five internal joints: the sternoclavicular, acromioclavicular, coracoclavicular, glenohumeral and scapulothoracic joints (see Figure 2.2) [38]. However, the acromioclavicular and coracoclavicular joints are generally assumed to be fixed (as they are just fibrous tissues with extremely limited motion). The sternoclavicular joint connects the clavicle with the sternum and is usually modelled as ball-and-socket joint (with 2-DOFs or 3-DOFs). The glenohumeral joint connects the head of the humerus with the glenoid fossa of the scapula, whereas the scapula connects to the thorax. The combined movements of the glenohumeral and scapulothoracic joints produce the greatest motion in the body. However, the movements of those joints are

[1] Republished with permission of John Wiley & Sons, from "A Photographic Atlas of the Human Body", Tortora, G.; Derrickson, B., 2nd Edition, 2009; permission conveyed through Copyright Clearance Center, Inc.

commonly modelled as a simple ball-and-socket joint with 3-DOFs. Finally, all this shoulder joints combined allow flexion, extension, hypertension, abduction, adduction, horizontal abduction, horizontal adduction, medial and lateral rotation (see Figure 2.3) [38].

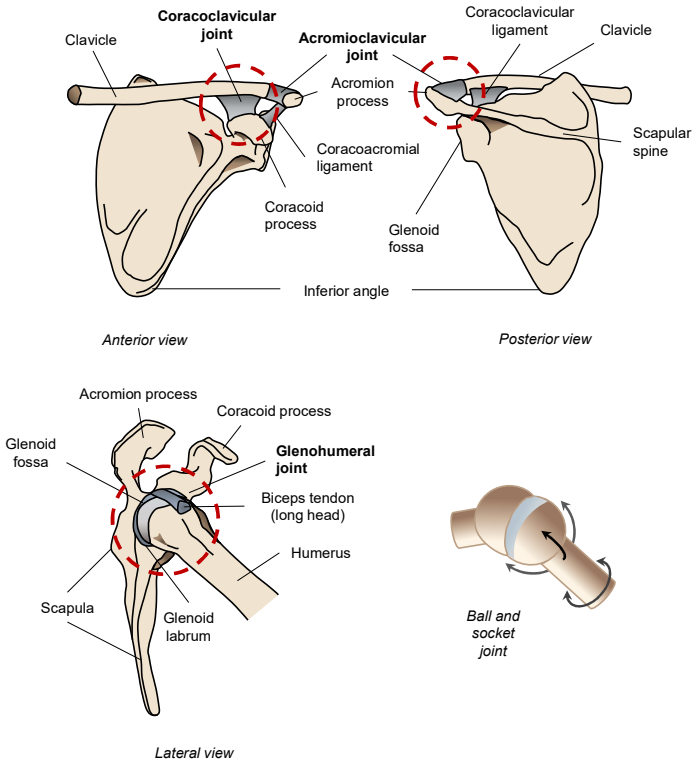

Figure 2.2. Coracoclavicular, acromioclavicular and glenohumeral joints. Adapted from [37] Copyright © 2011, McGraw Hill LLC[2]

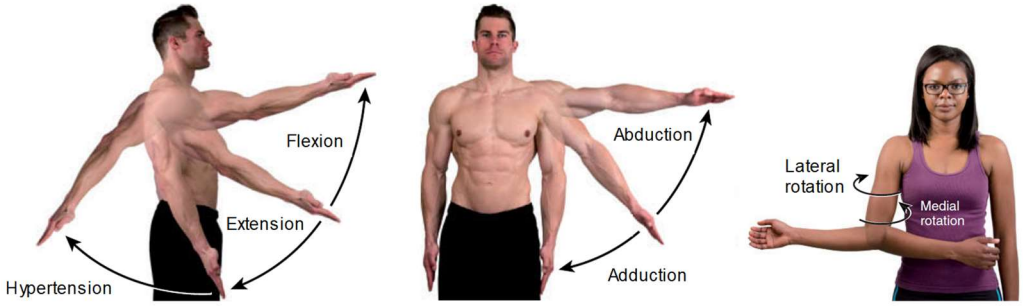

Figure 2.3. Shoulder flexion-extension (left), abduction-adduction (middle), medial-lateral rotation (right). Adapted from [36] Copyright © 2014, John Wiley & Sons[3].

[2] Republished with permission of McGraw Hill LLC, from "Basic Biomechanics", Hall, Sussan J., 6th Edition (International), 2011; permission conveyed through Copyright Clearance Center, Inc.

2.1.1.2 The Elbow

The elbow is considered as a hinge joint that connects the humerus, the radius and the ulna bones. This joint is composed of the humeroulnar, humeroradial, and proximal radioulnar joints (see Figure 2.4). For the study of motion, the humeroulnar and humeroradial joints are usually modelled together as a 1- DOF hinge joint. The range of motion of this hinge joint is constrained by the ligaments, muscles, and the collision of the ulnar bones with the olecranon fossa.

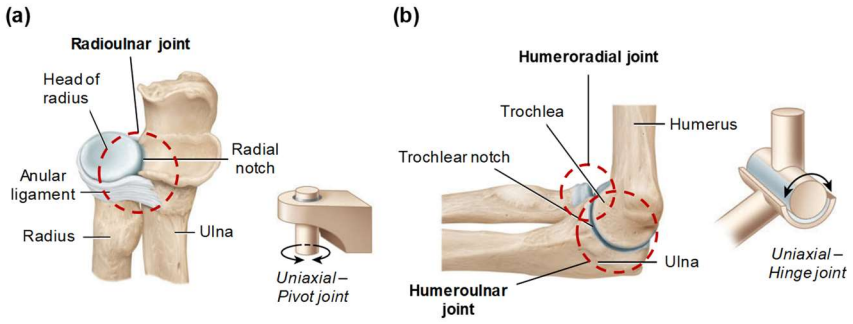

Figure 2.4. Joints of the elbow: (a) Radioulnar (pivot) joint, (b) Humeroulnar (hinge) and Humeroradial (gliding) joints. Adapted from [36] Copyright © 2014, John Wiley & Sons [3].

The proximal radioulnar joint is a 1- DOF pivot joint that allows pronation (palm posterior) and supination (palm anterior) (see Figure 2.5). The range of motion of this joint is constrained by the collision of the radius with the ulna for pronation, and by the ligaments and membranes for supination [37]. Pronation-supination is an interesting upper limb motion that allow the hand to face anteriorly and posteriorly and is believed to highly contribute to limb performance as it increases hand reachability and manipulation.

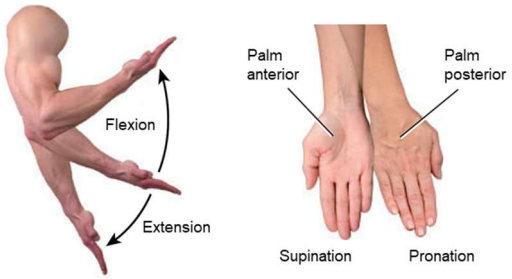

Figure 2.5. Movements of the elbow. Adapted from [36] Copyright © 2014, John Wiley & Sons[3]

---

[3] Reproduced with permission of John Wiley & Sons Limited, from Principles of Anatomy & Physiology, Tortora, G., 14th Edition, 2014; permission conveyed through PLSclear.

2.1.1.3 The Wrist

The wrist is a complex set of small irregular bones called carpals, which are arranged in two rows and which articulate at the radiocarpal and intercarpal articulations (see Figure 2.1) [36]. The wrist is modelled as a 2-DOFs joint that allow flexion, extension, hypertension, ulnar and radial deviation (see Figure 2.6). The range of motion of the wrist is constrained by the ligaments encapsulating the joint. The combination of pronation-supination with wrist flexion, extension, deviation provide a wide number of configurations for hand-object manipulation.

2.1.1.4 The Hand

The Hand is divided into the palm (metacarpal bones) and the fingers (phalanges). The fingers or digits can perform flexion-extension and deviation at the metacarpophalangeal joints(2-DOFs), and flexion-extension at the interphalangeal joints (1-DOF). The thumb can execute flexion-extension, abduction-adduction, and opposition and is the digit with the greatest range of motion (see Figure 2.6) [36]. The opposition movement is an especial movement that permits precise manipulation of objects and increases in hand dexterity.

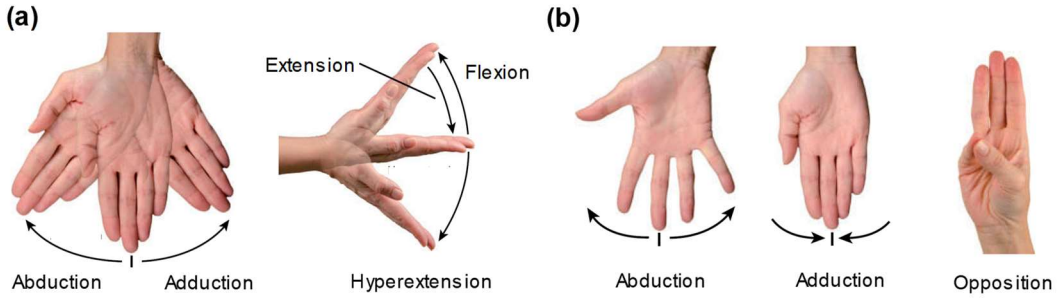

Figure 2.6. Movements of the wrist and hand: (a) abduction-adduction and flexion-extension of the wrist, (b) abduction-adduction and opposition of the fingers. Adapted from [36] Copyright © 2014, John Wiley & Sons[3].

2.1.2 Joint range of motion

Joints are the articulated elements that interconnect bones to allow motion within a limited range called joint "range of motion" (ROM). Joint range of motion is one of the main variables for human motion modelling. However, published normative data for range of motion is confusing, unclear, and difficult to compare [39-42]. Researchers assess range of motion using different methods, instruments, body landmarks and limb configurations. Furthermore, some authors assess range of motion actively (participants move limbs by themselves) [39], some passively (researchers move participant limbs) [41], and some actively and passively [40]. Some researchers believe that passive

assessment provides a better estimate of joint range of motion as active assessment can be affected by pain and weakness in the limb [41].

Table 2.1. Comparison of Range of Motion Data (Means). The values provided are joint range of motion in degrees.

Range of Motion	*Side*	*Glanville (a) (1937)*	*AAOS (b) (1965)*	*Boone (c) (1979)*	*Chang (d) (1988)*	*Stubbs (e) (1993)*	*Gunal (f) (1996)*	*Gunal (f) (1996)*	*Soucie (g) (2011)*
		-	-	-	-	-	*Active*	*Passive*	*Passive*
		N=10	-	*N= 109*	*N=10*	*N=15*	*N=1000*	*N=1000*	*N=114*
		Age 20-40	-	*Age avg. 22.4*	*Age avg. 28*	*Age 25-34*	*Age 18-22*	*Age 18-22*	*Age 22-44*
GH abduction	(Right)	129.3	180.0	184.0	-	176.3	-	165.7	-
	(Left)	130.3			-	178.2	-	168.2	
GH forward flexion	(Right)	179.0	180.0	166.7	-	179.6	-	-	168.8
	(Left)	179.9			-	178.5	-	-	
GH backward extension	(Right)	55.2	60.0	62.3	-	66.3	-	-	-
	(Left)	60.0			-	65.4	-	-	
GH horizontal flexion	(Right)	-	135.0	140.7	-	133.8	116.7	121.3	-
	(Left)	-			-	135.6	122.9	125.1	
GH horizontal extension	(Right)	-	60.0	45.4	-	53.9	27.7	-	-
	(Left)	-			-	54.4	30.7	-	
GH external rotation / side	(Right)	-	60.0	-	-	60.6	-	-	-
	(Left)	-			-	63.7	-	-	
GH external rotation / abduction	(Right)	82.7	90.0	103.7	-	103.4	-	-	-
	(Left)	83.5			-	97.3	-	-	
GH internal rot abduction	(Right)	94.1	70.0	68.8	-	70.8	-	-	-
	(Left)	100.0			-	82.4	-	-	
Elbow flexion	(Right)	138.3	150.0	142.9	148.9	147.3	140.0	142.8	144.6
	(Left)	144.2			146.8	148.5	142.4	145.6	
Elbow extension	(Right)	-	-	-	-	-	182.8	183.8	179.2
	(Left)	-			-	-	184.5	186.0	
Forearm supination	(Right)	99.4	80.0	82.1	87.8	101.1	86.5	90.4	85.0
	(Left)	100.6			88.8	101.4	88.2	93.0	
Forearm pronation	(Right)	91.1	80.0	75.8	84.6	86.2	-	-	76.9
	(Left)	93.0			84.3	86.6	-	-	
Wrist flexion	(Right)	95.0	80.0	76.4	64.8	70.2	-	-	-
	(Left)	90.0			66.6	70.9	-	-	
Wrist extension	(Right)	54.1	70.0	74.9	54.1	76.5	59.4	68.5	-
	(Left)	95.7			50.0	80.0	69.0	78.4	
Radial deviation	(Right)	27.1	20.0	21.5	-	24.5	17.6	18.6	-
	(Left)	31.1			-	23.1	21.3	24.3	
Ulnar deviation	(Right)	66.1	30.0	36.0	-	51.1	-	-	-
	(Left)	66.1			-	51.1	-	-	

(a-e) Stubbs [42].
(f) Gunal [40]. Some information was not presented.
(g) Soucie [41]. The elbow extension was adapted for compatibility (the original angle presented by the author was 0.8).

However, active range of motion seems to be a more reasonable measure as this is the real range in which participants can perform motion by themselves. Table 2.1 provide male joint range of motion from selected published data to illustrate the inconsistencies among researchers. Another factor that complicates the use of ROM normative data is that some authors only evaluate females or males, young or old, healthy or non-healthy, a particular ethnicity, and only some joints or degrees of freedom [39-43]. Similarly, not all authors report statistical information such as sample size, sampling methods, and standard deviation [39-43]. Consequently, future work should focus on the development of standard methods for the assessment of joint range of motion and to provide reliable normative data that can be used for human modelling.

It is important to understand that joint range of motion can be affected by aging, deformations, diseases, injuries, and surgeries. Therefore, some researchers have studied the effects of such factors on joint range of motion: Welsh [44] investigates the impacts of joint dislocation and instability on ROM, Willing [45] studies how bone-on-bone impingement affect ROM, Gutierrez [46] analyses how bone geometry and joint centre of rotation for reverse shoulder implants affect abduction (see Figure 2.7), and Keener et al. [28] optimises implant position with respect to ROM for reverse shoulder arthroplasty.

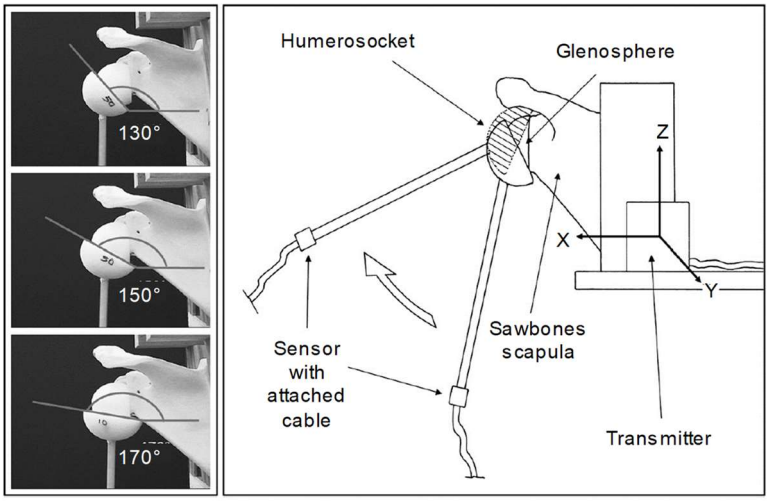

Figure 2.7. Effects of variations in the geometry and joint centre of rotation for reverse shoulder implants. On the left side, 3 different humeral neck -shaft angles. On the right, experimental setup for adduction-abduction range of motion measurements. Copyright © 2008, Elsevier [4].

[4] Reprinted from Journal of Shoulder and Elbow Surgery, vol.17, no.4, Gutierrez, S. et al., "Evaluation of abduction range of motion and avoidance of inferior scapular impingement in a reverse shoulder model", pp. 608-615, copyright (2008), with permission from Elsevier.

Joint range of motion has been used as a measure of upper limb functionality to determine if people are able to perform activities of daily living [47-49]. Gates, Walters, Cowley, Wilken, and Resnik [47] quantified the required joint range of motion of 8 activities of daily living: box of shelf, can of shelf, deodorant, drinking from a cup, hand to back pocket, perineal care, donning and zipping pants, and box of ground. Similarly, Oosterwijk, Nieuwenhuis, van der Schans, and Mouton [48] published a comprehensive and up to date systematic review of shoulder and elbow range of motion required to perform activities of daily living. Taylor, Kedgley, Humphries, and Shaheen [49] evaluated the use of simulated tasks in upper limb assessments in comparison to functional movements and concluded that simulated tasks do not replicate the movements required to perform ADLs.

Several studies investigated of the upper limb kinematics and joint range of motion for movement performance required to execute activities of daily living [47-49], and to perform movements in sports [50-54]. Such studies analyse the effects of pathologies, wear, and injuries on range of motion, as well as define minimum, maximum, or average limb kinematics, required for the successful performance of relevant tasks. However, studies that investigate the separate effects of reductions in range of motion of each independent joint or degree of freedom and their contributions to upper limb performance in a hierarchical and structured manner is lacking in literature. For instance, it is unknown whether a decrease in shoulder adduction would has a greater negative effect on upper limb dexterity and functionality across multiple tasks compared to a similar reduction in shoulder abduction. In other words, how can a surgeon decide if a reduction in elbow extension is less negative than a reduction in elbow flexion during the optimisation of implant placement? Published work rather focuses on the effects of such reductions on upper limb performance for specific tasks relevant to their subjects. Furthermore, this author has not found any published work that provides a quantitative measure describing the negative effects of reductions in range of motion on the overall upper limb dexterity and functionality. Such measure would be tremendously beneficial for a more objective clinical assessment of upper limb healthiness and functionality. Therefore, future work should focus on the study and classification of the separate effects of reductions in joint range of motion of individual joints or degrees of freedom on the overall upper limb performance.

Finally, the understanding and quantification of joint range of motion, as well as minimum range of motion required to execute activities of daily living are vital for the creation of human models that can mimic real human motion. Although the studies mentioned aim to contribute to the study of joint range of motion, standard methods, accurate

normative data, and defining standard activities for the evaluation of upper limb functionality are still needed.

2.2 Human hand grasp and object interaction

Humans have gone through many years of adaptation to the environment that surround them (the evolution). During such time, humans have been interacting with objects, starting with holding sticks and throwing rocks. Years passed by and humans learnt to use those objects as tools to facilitate their lives and to accomplish more advanced tasks, including the development of more sophisticated tools. Thus, scientists argue whether human hands evolved first in adaptation to the use of raw materials to make tools, or if the hands adapted to such tools [55]. Evolutionary changes, particularly in the hand, have made humans distinctive from other species. A clear distinction of humans compared to any other primates is that humans possess the longest thumb relative to the second finger, which was important for the prehistoric tool making [55]. Those anatomical characteristics combined with finger opposition allowed humans to manipulate simple tools that facilitated the development of more complex instruments. The hand-object interaction has been formally investigated, or at least studied with more attention, since late fifties and early sixties [56-58]. Investigations from late fifties to early nineties, commonly focused on the identification and classification of hand grasp patterns, particularly prehensile movements [55, 57-60]. Research on hand object interaction from late nineties to date has diversified, where some of the sub subjects of interest are motor control of the hand, kinematics, dynamics, tribology, postural hand synergies, gasp frequency in ADLs, ergonomic design, hand prosthetics, on so on. Therefore, the study of grasp patterns and hand-object interaction is of relevance to understand full manipulability of the upper limb; likewise, to the characterisation of dexterity. Hence, a literature review on human hand interaction including hand grasp patterns and hand object interaction is presented in this section.

2.2.1 Hand grasp patterns and classification

The human hand can perform movements of two types, prehensile and non-prehensile. In prehensile movements the object is held partially or completely in the hand, whereas, non-prehensile movements present no grasping but rather pushing or lifting whether with the hand or the fingers [57].

However, non-prehensile movements have been of less attention. In this research project, prehensile movements are the only ones of interest. A particular characteristic of prehensile movements is that the object needs to be grasped in a secure and stable fashion before further manipulation [57]. Thus, a hand grasp can be generally defined as a

hand posture in which an object can remain secure independently of the position and orientation of the hand. Grasp stability can be accomplished by using power or precision grips.

According to Napier [57], a power grip is such in which the object is held by partially flexed fingers and the palm with counterpressure by the thumb, whereas, in a precision grip the object is supported between the flexor parts of the fingers and the thumb (see Figure 2.8). Another important observation by Napier [57] is that the posture of the hand with respect to the forearm during precision grip is between ulnar and radial deviation and partially extended, whereas, in power grip the hand presents ulnar deviation and the wrist is in neutral position between flexion-extension and the long thumb axis seems to coincide with the forearm. Likewise, the author mentions that the thumb is commonly in adduction fashion during power grip, whereas, in precision grip the thumb is abducted [57]. In the later observation, Napier [57] states that in intermediate positions between adduction and abduction, the thumb is unstable due to the anatomical characteristics of the carpometacarpal joint.

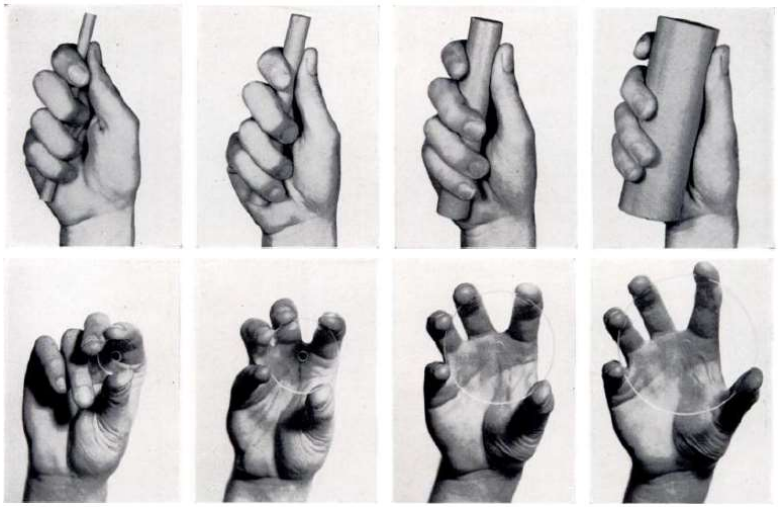

Figure 2.8 – Hand grip for different object sizes. Top: power grip, bottom: precision grip. Copyright © 1948, British Editorial Society of Bone & Joint Surgery[5]

A later work by Kamakura [59] explores static prehension patterns in normal hands of 7 participants holding 98 objects, identifying 14 patterns into 4 categories:

[5] Republished with permission of British Editorial Society of Bone & Joint Surgery, from "The prehensile movements of the human hand", Napier, J., vol. 38-B, no. 4, 1956; permission conveyed through Copyright Clearance Center, Inc.

a) Power grip: a wide area of the palm and the volar sides of the fingers make contact with the object.

b) Intermediate grip: the fingers are in moderate flexion, the contact areas with the object are the pulp of the thumb and the radial aspects of mainly the index and middle fingers. No palm contact is presented.

c) Precision grip: the object is held between the volar aspects of the fingers and the pulp of the thumb.

d) Grip involving no thumb: the object is held between adjacent fingers with no thumb participation in the grip. [59]

On the other hand, Cutkosky [60] studied grasps used by machinists with the aim of predicting human grasps, and as a result he created a hierarchical grasp taxonomy (see Figure 2.9) [60, 61].

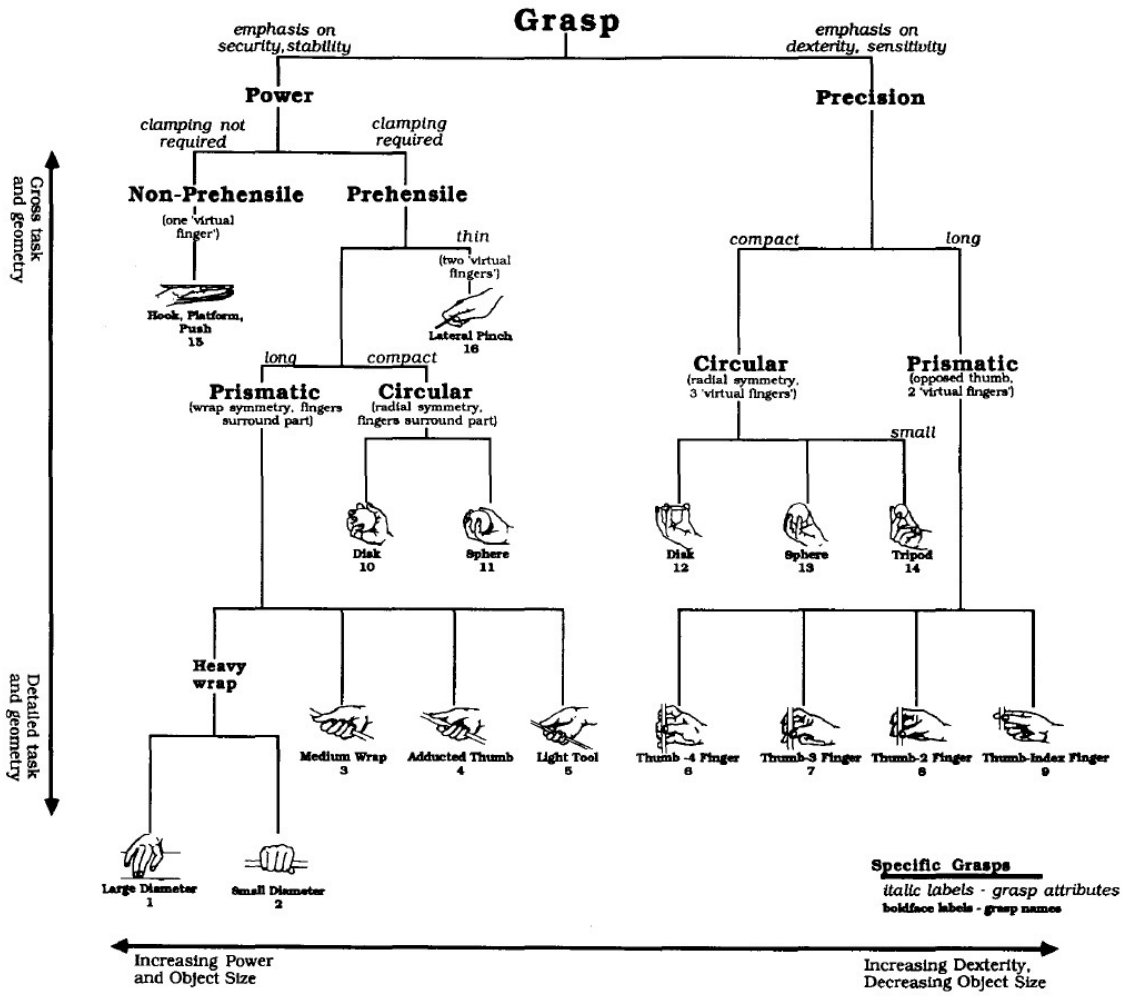

Figure 2.9 – Partial taxonomy of manufacturing grasps (hand grasp hierarchical classification). [60] Copyright © 1989, IEEE.

This hierarchical classification of hand grips seems to be particularly relevant for making decisions about hand grasp patterns to choose depending on the geometry of the object and the grasping required force. Nevertheless, the author states that the choice of grasp is more influenced by the task to be accomplished rather than by the size and shape of the object [60].

Likewise, Cutkosky [60] observed that power grips are characterised by the use of large contact areas between the object and the fingers, with limited or no motion of the fingers, and where the manipulation seems to depend mostly on the wrist. This factor could somehow compromise the dexterity of the hand during the manipulation of the object and suggests that the wrist is, in many cases, responsible for the manipulability of the object.

Moreover, variations on grasp patterns are believed to be affected by personal preferences, object size and shape, and individual hand strength. Cutkosky [60] points out that is the relative size of the object with respect to the hand, geometric constraints and relative individual force play an important role in the decision-making process to determine the type of hand grasp preferred by the participant. This last characteristic related to relative hand-object dimensions seems to be less explored by researchers. It might be of relevance to investigate on the matter for the understanding of hand-object manipulation.

A more recent work on human hand grasp is presented by Feix [62], in which the author analysed and compared existing information and research on human grasp taxonomies and synthesized them into a new classification called “the GRASP taxonomy” after a project (GRASP) founded by the European Commission (see Figure 2.10).

Feix [62] states that hand motion and functionality depend not only on the intrinsic movements of the hand but also on the complementary movements of the arm and the body. Additionally, the author mentions that in power grip the object and the hand are rigidly coupled, and the position-orientation of the object strongly depend on the arm, whereas, in precision grip, the object can be moved by intrinsic movements of the hand [62].

Thus, for modelling purposes, and particularly for power grip, it seems reasonable to represent hand grasp as a static position once the formation of the grip was finalised. However, for precision grip modelling, and depending on the scope of the investigation, it would be necessary to define if the grip would be considered as static during the manipulation of the object.

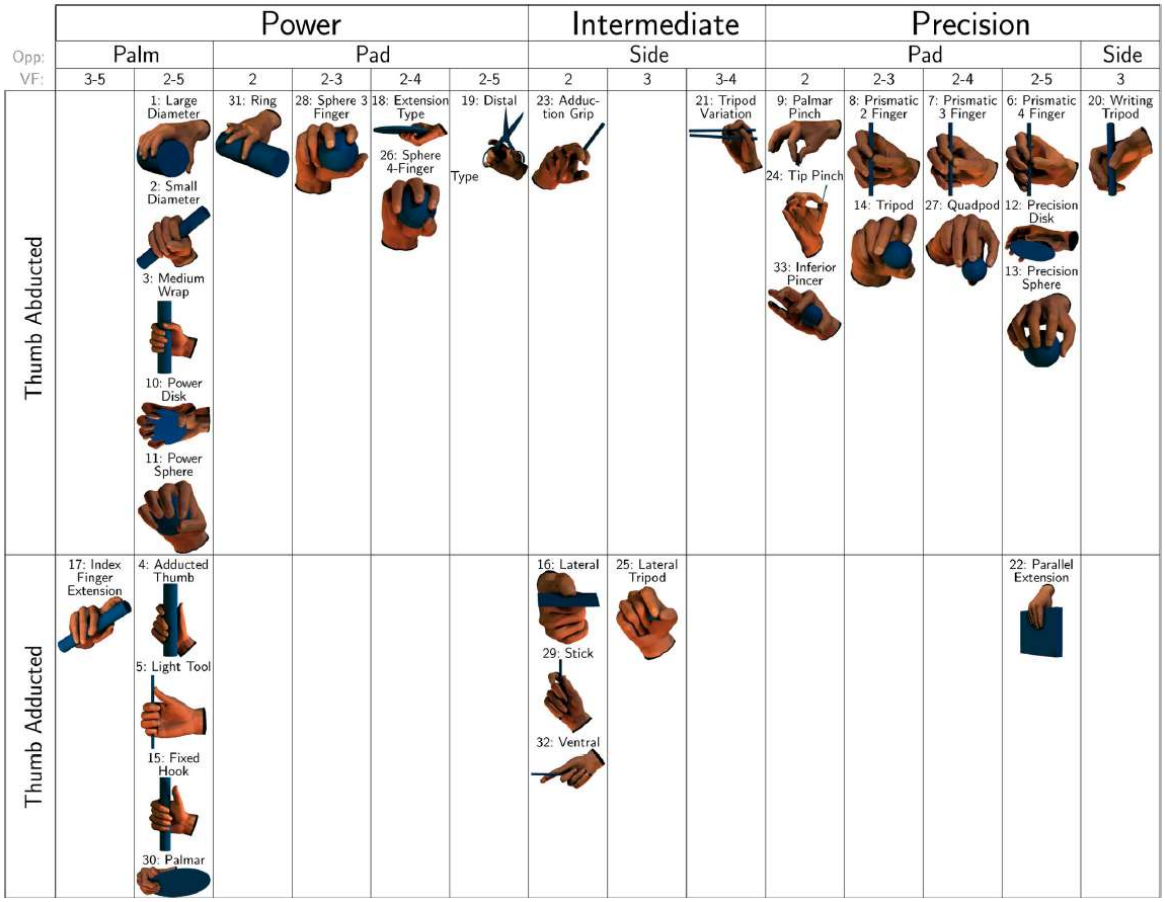

Figure 2.10 – The GRASP taxonomy of human grasp types. [62] Copyright © 2016, IEEE.

The fingers and some aspects of the hand exert forces in different directions depending on the contact areas with the object, such postures are called opposition types (see Figure 2.11) and are divided into [62]:

a) Pad opposition: grasp between the pad surfaces of the thumb and the fingers

b) Palm opposition: grasp between hand surfaces and the fingers

c) Side opposition: grasp between the thumb and the side of the index finger (commonly), although in some cases it could be supported by the side of other fingers. [62]

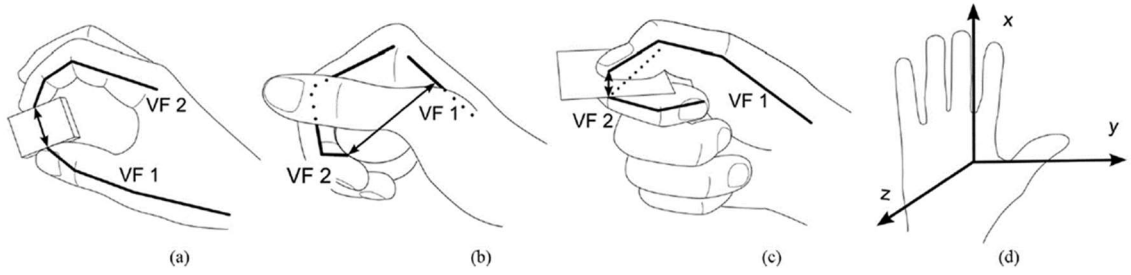

Figure 2.11 – Opposition types of hand grasp. [62] Copyright © 2016, IEEE.

In some hand grip postures, the fingers work together as a single unit exerting forces in similar directions, this synergic collaboration of a set of fingers is called virtual finger (VF) and can serve in some cases as a simplified representation of the fingers for hand grasp [62]. Moreover, Feix [62] points out that most of the grasping types are used for light weight objects (less than 500g), and that such grasping positions require hand openings of 5cm or less.

2.2.2 Hand-Object Interaction

In recent years, research on hand-object interaction and the application of such knowledge to Activities of Daily Living (ADLs) has been gaining interest. It might be due to technological advancements and the demand of generating knowledge for rehabilitation, prosthetics, ergonomics, product design, and robotics. Although, hand grip by itself can be considered mostly static, it is also composed of other dynamical factors which affect hand-object interaction and its applications to real life. According to Smeets [63], the selection of a hand grip to hold and object is influenced by visual information about its position-orientation, as well as, by the shape and size of the object. Furthermore, as objects are not always symmetrical, changes in the orientation of the object can force the participant to adjust grip aperture, size, and orientation (see Figure 2.12) [63]. It suggests that during the manipulation of an object, participants could slightly change hand posture to adapt to each particular circumstance.

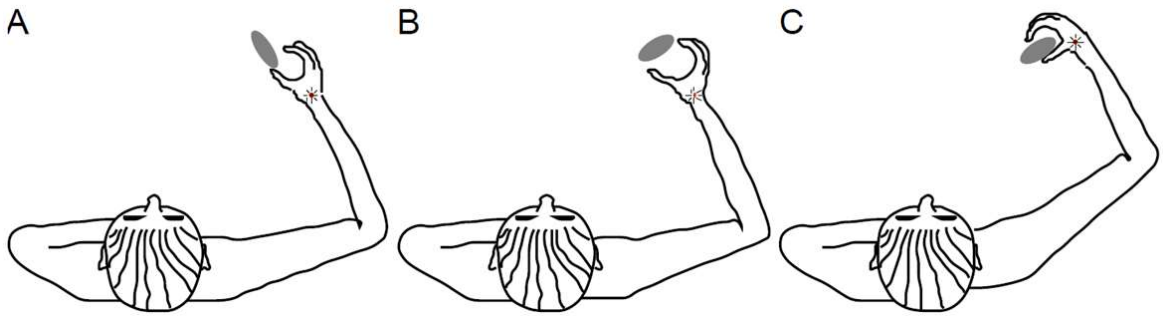

Figure 2.12 – Hand grasp of an object located in the same position but with a different orientation. Copyright © 1999, Human Kinetics, Inc. [6]

Moreover, Smeets [63] state that a stable grasp requires to hold the object in a manner that the line connecting both fingers (or virtual fingers) form a perpendicular line to the

[6] Republished with permission of Human Kinetics, Inc., from "A new view on grasping", Smeets, J.B.; Brenner, E., vol. 3, no. 3, 1999; permission conveyed through Copyright Clearance Center, Inc.

surface of the object, and that such line should go through the centre of gravity of the object. On the other hand, the pre-shape finger movements are performed by the extrinsic muscles that attach on the forearm, whereas the intrinsic hand muscles are responsible for the finalisation of the grip just after touching the object [63, 64]. It implies that the hand is translated and pre-positioned by the arm, whereas the responsibility of the hand is mostly grasping the object and in-hand manipulation. Likewise, the selection of the grasp type, the speed of grip formation, and grasp stability are directly affected by the effective contact area with the object, as well as, by its intrinsic properties such as roughness and weight [63]. Additionally, the author suggests that visual information affect grip aperture and speed patterns during reach out.

Santello [65] published an investigation related to postural hand synergies for tool usage in which the author asked participants to shape the right hand as if to grasp and use objects. The author measured the angular positions of 15 joint angles and processed the information by using discriminant analysis, regression analysis, and principal component analysis. Similarly, Gonzales [66] conducted principal component and trajectory analysis of finger movement, the author suggests that synergies can be used to identify finger movement patterns during manipulative tasks. Thus, principal component analysis, correlation analysis, and hand and finger synergy analysis, have been some of the most common techniques for object-hand interaction analysis. Such kind of analysis can help to identify patterns that could be used for example in robotics to mimic human hand behaviour, and even in the prediction of hand intentions.

The understanding of hand-object interaction for ADLs is of great relevance as the performance of the limb for the execution of such tasks can determine the level of independency of the participant. In other words, when a person fails to perform basic ADLs, the person needs assistance and therefore becomes dependent. Such interactions were explored by Yoxall [67], in which the author analysed participants interacting with packings such as jars, water bottles, yoghurt pots and a flexible crisp packets. As a result, the author found that spherical and box hand grips are more commonly used to open large and medium jars, whereas, lateral and spherical are more popular for small jars [67].

Additionally, Yoxall [67] noticed that lateral grip was commonly used for water bottles and lateral pinch for yoghurt pots. Another interesting observation is that most grips were performed with the elbow flexed and the shoulder slightly abducted [67]. A later article by the same author investigated shear stresses in the digit joints when opening a jar container, showing as a result that participants tend to use lateral grips when possible due to lower joint stresses, and that small participants have lower physical strength and are more likely to suffer from pain discomfort [68]. This suggests that the dimensions of

the hand play an important role in the interaction with the object as it affects the necessary individual finger forces for a particular task, which might be related to the object contact area and the dynamics of the hand.

A similar study by Rowson [69] investigates consumer grip choices during food container opening. The author suggests that the factors affecting the ability to open a container are such as age, gender, grip strength, coefficient of friction, wrist strength and the dimensions of the container [69]. Likewise, the author distinguished a clear difference in torque forces between females and males, where females generally produce lower torques [69]. Furthermore, Rowson [69] identified that during jar container opening, females tend to prefer spherical grip, whereas, males use a larger range of hand grips for the same purpose. That research work provides of substantial information about differences between males and females in both strength forces and grip preferences, which seem to be related. Other authors have focused on identifying grasp patterns and grasp frequency for ADLs and work activities. Zheng [70] and Bullock [71] investigated prehensile human hand use during daily work activities of housekeepers and machinists. Bullock [71] identified that the most frequent hand grips were medium wrap, spherical or precision disk, and lateral pinch. The author noticed that medium wrap was commonly used for large cylindrical objects and during longer duration activities, whereas, spherical (or precision disk) was used mostly for jars, disks, and miscellaneous [71]. Likewise, lateral pinch was used for smaller knobs, flat objects and to pick objects [71]. However, the results presented by Zheng [70] and Bullock [71] are limited to housekeeping and machinist tasks, therefore, it cannot be assumed that the same grasp patterns are used in other professions.

Another area of science interested in hand-object interaction is robotics. For instance, Deimel [72] focuses on compliant and under actuated robotic hands for dexterous grasping. In such study, the author presents soft robotic hand designs that are clearly based on human hand grasp taxonomies (see Figure 2.13). Moreover, the author states that soft hands are inexpensive to manufacture, morphologically easy to adapt, and still able to accomplish a wide diversity of grasps, which are based on human hand grasp patterns [72]. Thus, interdisciplinary research combining robotics and biomechanics can help to develop more efficient and practical human-like robotic hands.

This section addressed hand grasp classifications and grasp pattern use frequency. As a result of this review, it has been identified that the factors that affect hand grasp choice can be divided into four groups: object related, person related, object purpose, and feedback. Each of those groups are described as follows:

a) Object related: factors related to the intrinsic properties of the object such as size, shape, function, weight, texture, wetness, symmetry, and centre of gravity.

b) Person related: factors related to the person such as age, gender, height, hand size, strength, habits, experience, tiredness, and health.

c) Object purpose: as an object can be used for many purposes, participants might base their hand grasp choice on the manipulation intention.

d) Feedback: factors related to the perception of the individual based on sensorial information (feedback), which include object position-orientation, visual and tactile information.

Figure 2.13. Soft robotic hand mimicking the dexterous grasping taxonomy. Copyright © 2016, SAGE Publications.

Furthermore, it is common to investigate the upper limb as an extremity composed of segments of the arm, forearm, and the hand without considering finger interaction and in-hand motion; or as the hand and fingers modelled only from the wrist without consideration of the arm motion contributions. Selecting the elements to be considered in the analysis of upper limb motion depends on the scope of the study. However, in order to understand full limb motion performance, future investigations should include all the elements of the extremity.

The most updated nomenclature and classification for hand grasp taxonomy found in this literature review is the one proposed by Feix [62]. However, the virtual finger (VF) approach seems to be a good technique for a simplified representation of the fingers for hand-object interactions.

2.3 Human motion modelling

The development of human models that can mimic real human behaviour is challenging. Therefore, this section provides a thorough literature review to identify possible challenges, current state-of-the-art, appropriate methods, and techniques for the development of human models to study upper limb workspace and dexterity. Such review includes human motion and dexterity, human biomechanics, upper limb kinematic modelling, workspace, motion redundancy, computational methods, data acquisition, and uncertainty and sensitivity analysis.

2.3.1 Human motion, dexterity, and manipulability

Humans perform movements even unconsciously. Such movements can be studied at different structural levels of the human body to understand each element and its function. This research is interested in general conscious movements such as touching, reaching, grasping, and manipulating objects. However, the study of human motion is complex as this phenomenon depends on the collective and organised participation of different physiological mechanisms called “cooperative synergies” to produce motion, also known as “motor control” [1]. Cooperative synergies are the interaction of the bones, joints, muscles, senses, nervous system and the brain. Moreover, the body is equipped with special organs called “sensory organs”[1]. Such organs help to provide information and feedback to choose the trajectories for motion and to make any corrections whilst executing movement.

According to Bernstein [1] the accuracy of performing a task can be improved by repeating a movement to gain experience in solving a problem, which is called

"exercisability". Exercisability is commonly confused with dexterity. Nevertheless, exercisability and dexterity are different concepts.

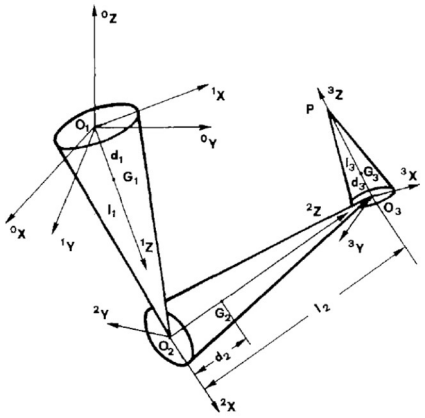

Figure 2.14. Schematized mechanical structure of the humanoid arm. Frame 0 is the GFR, frames 1,2,3, are the LFR. $l_1 l_2 l_3$ are the limb lengths, $G_1 G_2 G_3$ are the centres of mass, and P is the end effector of the kinematic chain. Copyright © 1980, Springer Nature [7]

In the early eighties, fundamental principles of manipulation, dexterity and neurophysiological factors affecting motion were studied by Benati [73], who modelled the arm as a kinematic chain (see **Error! Reference source not found.**). In the publication the author states that dexterity can be considered as a measurement of manipulation, where manipulation depends on the visual and motor processes.

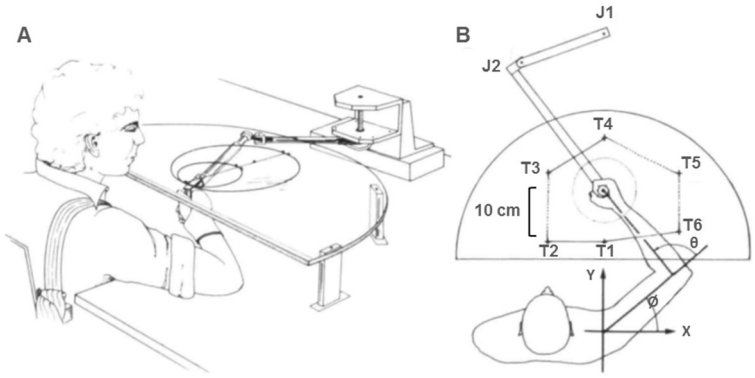

Figure 2.15. Set up for the analysis of planar hand space trajectories. Copyright © 1982, Oxford University Press[8]

[7] Reprinted from Biological Cybernetics, vol. 38, no. 3, Benati, M. et al., "Anthropomorphic robotics", pp. 125-140, copyright (1980), with permission from Springer Nature.
[8] Reprinted from Brain, vol. 105, no. 2, Abend, W. et al., "Human arm trajectory formation", pp. 331-348, copyright (1982), with permission from Oxford University Press.

Later in 1981, Morasso published a research work addressing spatial control of arm movements in which he states that the arm can be described in terms of spatial trajectories of the hand or angular curves of the joints [35]. A year later, the author published a complementary experimental work, concluding that the hands tend to follow straight paths even when participants are asked to produce curved paths (see **Error! Reference source not found.**) [74].

Morasso [35] and Abend [74] concluded that hand speed profiles for the execution of straight lines are normally bell-shaped. In a later study, Morasso [75] investigated three dimensional arm trajectories by using a mechanical arm and cinematography methods to record motion to see if the previous observations in two dimension analysis held in three dimensions (see Figure 2.16**Error! Reference source not found.**). The results confirmed that point-to-point movements at natural speed produce approximately straight trajectories with bell-shape velocity profiles as in studies of planar movements [35, 74, 75].

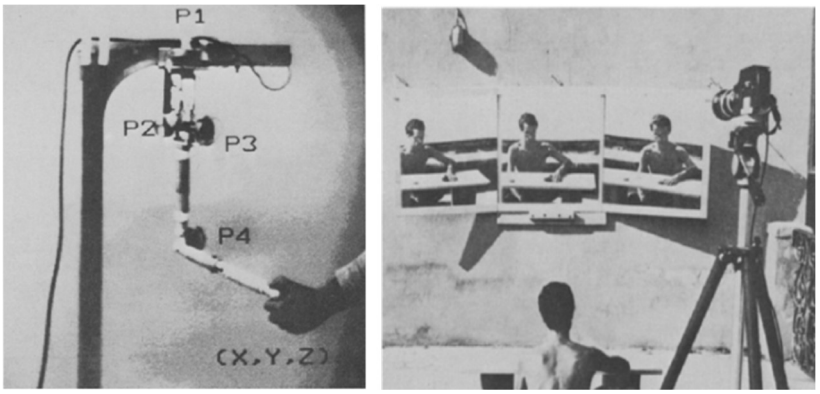

Figure 2.16. Hand trajectory recording methods. Goniometric method (left) and cinematographic method (right). Copyright © 1983, Springer Nature [9]

In the nineties, motor control gained more interest and researchers started focusing on more specific characteristics of motor control. For instance, Redding [76] published a study focused on the effects of visual disturbances on the trajectories of the hand, and Kawato [77] investigated how previous experiences are stored in internal model modules and can be accessed later for the execution of similar motor tasks.

In the last two decades, the investigation of motor control has increased. The technological advancements and the interest in specific aspects of motor control have

[9] Reprinted from Biological Cybernetics, vol. 48, no. 3, Morasso, P., "Three dimensional arm trajectories", pp. 187-194, copyright (1983), with permission from Springer Nature.

pushed researchers to investigate even more specific areas of motor control. Some recent studies have focused on the study of cortical activity for motor control [78], brain-machine interfaces [79], posture-based models for motor problems [80], control performance and kinematic synergies [81], sensory feedback in upper limb prosthetics [82], selective voluntary motor control [83], and neural controlled robotic arms [84]. These investigations are essential for the understanding of motor control and its relationship to human motion. The acquisition of knowledge related to neurological and motor control strategies will improve the development of models that can characterise human movement more accurately.

Dexterity can be defined as the ability to find quick solutions to unexpected new situations by using motor combinations, in other words, a motor ability to perform precise movement with a determined purpose independently of the environmental changing conditions [1]. Therefore, performing dexterous movements depends on the combination of various physiological and cognitive factors and the surrounding conditions. Moreover, dexterity is affected by aging, diseases, injuries, and surgeries. Hence, the development of human models that can capture all those factors is significantly challenging.

Dexterity is commonly evaluated through time dependent tests such as the Box and Block Test (BBT), Perdue Pegboard Test (PPT), Motor-free Visual Perceptual Test, Functional Dexterity Test, and Strength Dexterity Test [2-10]. Such kind of tests can determine if participants can successfully complete tasks, within a given time frame, on test boards placed in a fixed position in front of the participants and at a reachable distance. However, traditional dexterity tests are limited as they cannot provide data related to movement consistency, joint angles required to execute the task, regions of high dexterity, participant performance in other regions of the corresponding upper limb reachable space, and more importantly, dexterity tests cannot determine if participants are able to perform other activities non-evaluated during the test.

In recent years, researchers have used motion capture systems (see Section 2.3.7) to study and quantify upper limb dexterity by analysing kinematic and motor control variables such as joint angles, velocity, acceleration, movement coordination, and motion trajectories [4, 5, 85-89]. As the understanding of such aspects of upper limb motion is essential for prescribing an adequate rehabilitation therapy, as well as for adjusting work and home spaces to facilitate the performance of activities of daily living.

However, traditional dexterity tests and most of the studies mentioned above only analyse and quantify dexterity. Although such data can be used to evaluate and compare upper limb performance for healthy and non-healthy populations, such data without

computational models cannot be used to predict upper limb dexterity. Therefore, computational models to characterise and predict upper limb dexterity are required.

In robotics, an equivalent to human dexterity is called “manipulability”, an ability associated with object manipulation. Manipulability can be described as the ease of changing the position and orientation of the end-effector of a kinematic chain [12]. Yoshikawa [12] proposes the use of manipulability ellipsoids to assess the capability of a manipulator to execute a certain task. This approach uses the system of equations employed to model upper limb kinematics to compute a metric that describes the level of manipulability of the system for a determined task [90]. Although the manipulability analysis method is mostly used in robotics, a few researchers have already used it for the study of the human limb motion [13, 15, 27, 91]. Therefore, this research will explore the use of the manipulability analysis method for the characterisation of upper limb workspace with respect to dexterity.

2.3.2 Upper limb dexterity and functionality

The past subsection introduced and defined dexterity, as well as described the complexity of its study as it involves the coordinated cooperation of all the body systems. On the other hand, Section 2.1.2 addressed joint range of motion and its role on the successful performance of activities of daily living (ADLs). Although many factors affect upper limb functionality, it can be easy observed that both dexterity and joint range of motion are two important components of upper limb functionality. First, the segments of the upper extremity connected by joints can be seen as the physical structure that allow the execution of tasks in 3-dimensional space (upper limb workspace, see Section 2.3.5), where the upper limb reachability is dependent on segment lengths and joint range of motion. Whereas dexterity relates to fine movements involving perception, planning, control, and execution. Research studies on investigating joint range of motion and its relationship to the execution of activities of daily living have demonstrated that the functionality of the extremity can be directly affected by changes in joint range of motion due to aging, injury, degenerative diseases, surgery [28, 44-49] (see Section 2.1.2). For instance, an injury that reduces shoulder flexion and abduction to a maximum range of 80 degrees could constrain the person to reach from a shelf, comb their hair, change their cloths, or touch the back of their heads. Likewise, dexterity and functionality in the clinical context are commonly seen as one, and dexterity tests are frequently used for the assessment of upper limb healthiness and functionality [2-10]. A person that performs poorly in a dexterity test is believed to be limited in the execution of daily tasks as they may not be able to even control a spoon, which is basic for eating. Therefore, it can be easily seen that reductions in joint range of motion or dexterity decrease upper limb

functionality. Although joint range of motion and dexterity are two important components of functionality and have been separately assessed with the aim of defining upper limb healthiness and functionality, this author has not found any scientific publication that combines the assessment of both joint range of motion and dexterity to provide a more complete evaluation of the upper extremity functionality. Therefore, the novel method proposed in this research work can help to close this gap by providing a method that can also be used to assess upper limb functionality in terms of dexterity, and joint range of motion, described here as workspace volume (see Section 2.3.5 for workspace)

2.3.3 Human biomechanics

Biomechanics is the science that studies the Mechanics applied to biological systems, where biological systems refer to living beings, and Mechanics is the science that study motion, forces, and the causes of them [92]. Biomechanics can be generally divided into Kinematics, Kinetics and Statics. Kinematics study motion without reference to mass and force, whereas Kinetics study motion including mass and the forces that produce motion. Finally, Statics investigates the forces that can potentially cause motion.

A complete biomechanical analysis involves the study of Kinematics, Kinetics and Statics. However, this research is mostly interested in the kinematic analysis of the human upper limb, which is represented as a system composed of rigid elements interconnected through joints (a kinematic chain).

The upper limb is a biomechanical system, and as all natural systems, implies dealing with nonlinearities due to the nature of the anatomy and physiology of the limb: muscle contraction and relaxation to perform motion [93], tendon and ligament structural properties, motor control [1, 35, 77, 94-97], and so on. Describing nonlinear systems is challenging as no universal methodology is applicable, which requires the use of combined approaches, techniques, and mathematical tools [98]. In some cases, such systems can be represented by linear models using ordinary linear differential equations (linearization). However, some linearization techniques deviate from real system behaviour and affect the accuracy of the models. Some common methods for nonlinear modelling are the use of state-space representation (i.e. representation of the system as a set of first order differential equations), functional series expansion, and block oriented techniques [99, 100].

Upper limb motion can be analysed in cartesian and joint spaces. Although the upper relationship between movements in cartesian and joint spaces is not linear, homogeneous matrices can be used to linearize such relationship.

2.3.4 Upper limb kinematic modelling

The upper limb is commonly represented as a kinematic chain (a system composed of rigid elements interconnected through joints) for the study of human motion [32, 34, 73, 101-103]. The general assumptions for the study of kinematic chains are that links are infinitely rigid, and joints are frictionless elements that allow motion in some directions and constraint it in other. This representation allows deriving a system of equations that can map movements in both cartesian and joint spaces. Such kinematic models can also be used to determine the position and orientation of any given element (commonly the end-effector) with respect to another (normally a global frame of reference). Moreover, the velocities and accelerations of each element of the system can be obtained by deriving position with respect to time.

A general approach for the analysis of upper limb kinematics is presented in Figure 2.17, in which Raikova [34] represents the upper limb as a simplified 3-link kinematic chain (arm, forearm and hand) with 7 degrees of freedom (DOFs).

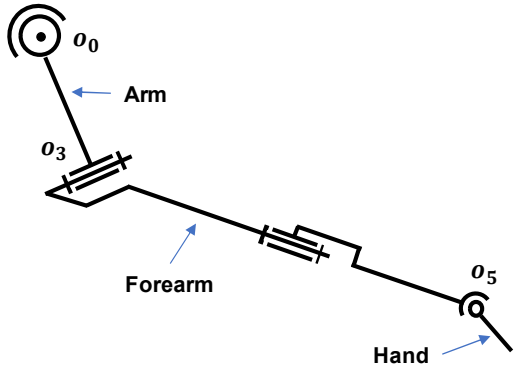

Figure 2.17. Upper limb represented as a 3-link kinematic chain with 7-DOFs. O_0, O_3, O_5 represent the centres of rotation of the shoulder, elbow and wrist respectively. Based on [34] Copyright © 1992, Elsevier [10]

Representing the upper limb as a kinematic chain is quite beneficial as this modelling approach provide essential information about the relationship of motion in both cartesian and joint domains. Hence, kinematic models can help to characterise limb motion [30, 104-106]. Furthermore, this modelling approach is compatible with the study of motion of other systems. Consequently, the information obtained from these models can be used

[10] Reprinted from Journal of Biomechanics, vol. 25, no. 8, Raikova, R., "A general approach for modelling and mathematical investigation of the human upper limb", pp. 857-867, copyright (1992), with permission from Elsevier.

to create robotic arms that can mimic human motion, to develop rehabilitation systems, to create assistive devices, prosthetic limbs, and exoskeletons [107-110].

One of the most important things during the development of a kinematic model is to select a number of segments and degrees of freedom that can accurately represent the upper limb according to the scope of the study and the level of precision needed for the analysis. For instance, the shoulder complex is composed of the clavicle, scapula, and the head of humerus. Creating a kinematic model composed of all those 3 elements and their corresponding degrees of freedom increase the complexity of upper limb models, therefore, the shoulder complex is commonly simplified as a ball-and-socket joint with 3-DOFs. Another aspect to be considered is the location of the centre of rotation for each joint as in some cases such centres of rotation are asymmetric. It is important to contemplate that the more segments and the more DOFs, the more complex the model.

2.3.5 Upper limb workspace

Human upper limbs can perform a wide variety of tasks from moving objects from point A to point B, to executing fine dexterous movements such as writing, painting, drawing, and sewing. However, upper limb movements are limited by joint range of motion (see Section 2.1.2). Such range of motion is commonly measured with the limb segments in a single configuration (normally in neutral configuration). Nevertheless, joint range of motion cannot fully capture upper limb capability to reach objects within a well-defined 3-dimentional space. Such 3-dimentional reachable space is also known as the "workspace volume". In robotics, the computation and understanding workspace volume is essential for the study of robot motion, as successful task execution depends on the ability of the robot to reach a determined region.

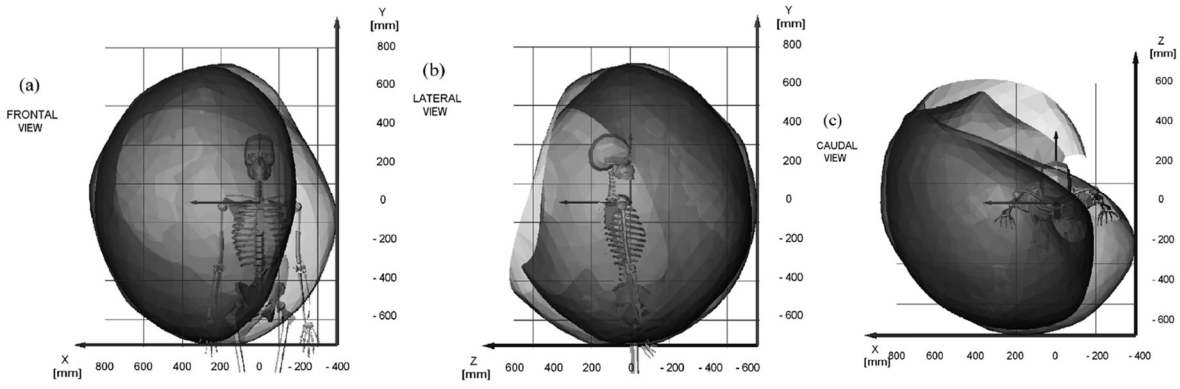

Figure 2.18. Workspace volumes for a human upper limb and an upper-arm exoskeleton. [17] Copyright © 2006, IEEE.

In biomechanics, upper limb workspace volumes are mostly employed in the study of human-machine interactions [16], the design of exoskeletons [17, 18], ergonomics design

[19], and the development of rehabilitation systems [20]. Venema and Hannaford [16], uses a stochastic approach for the computation of human workspace for the design of human interface mechanisms. Schiele and van der Helm [17] computes workspace volumes of a mechanical device and an upper limb for the development and evaluation of an upper-arm exoskeleton (see Figure 2.18). Chaffin [19], provides a comprehensive review (from the year 1970 to 2008) of the use of Digital Human Models (DHM) for workspace design and ergonomics, which demonstrates that workspace volumes for human modelling have been mostly used for workspace and ergonomic design. Piña-Martínez, Roberts, Leal-Merlo, and Rodriguez-Leal [18] compares the anatomic limb workspace for the user with the exoskeleton workspace for the development of and enhanced workspace upper limb exoskeleton. Laribi, Carbone, and Zeghloul [20] focuses on design optimisation (based on workspace volume) of a cable driven parallel robot intended for upper limb rehabilitation.

However, workspace volumes are not commonly used as a standard reference for the evaluation of upper limb dexterity, rehabilitation therapy, sports biomechanics, comparative biomechanics, and clinical analysis. In recent years, due to the technological advancements, some researchers have attempted to introduce and recommend the use of workspace as a reference for upper limb functionality. Kurillo et al. [21] evaluates upper extremity workspace in patients with neuromuscular diseases through the use of a low-cost stereo camera to assess upper limb functional impairment. Similarly, Matthew, Kurillo, Han, and Bajcsy [22] uses a low-cost depth camera to estimate workspace volume as the author aims to introduce the use of workspace volumes in quantitative medicine for the evaluation of patients with muscular disorders. Likewise, Bai and Song [23] compute reachable workspace for post-stroke patients for clinical evaluation and for comparison with the upper limb Fugl-Meyer score provided by a therapist. The research papers previously mentioned indicate that workspace volumes can provide considerable numerical and visual information about upper limb reachability, which can be used as a reference for comparison and optimisation purposes. Therefore, this research work explores the use of workspace volumes as a reference for human motion and for the assessment of dexterity within such volumes (see Chapter 4).

2.3.6 Upper limb motion redundancy

Humans perform hundreds of movements every day. It is known that limb segment angles and trajectories can vary even for the execution of cyclic tasks. However, such angle and trajectory variability does not necessarily translate in poor task performance. This demonstrates that, in some cases, the task can be performed using different motion strategies, and that in such cases, there are many solutions for the execution of the task.

This concept of having more than one possible solution for the execution of a task is known as redundancy. The upper limb joints allow the extremity to move freely within a reachable volume, and many points of such volume can be reached by the limb using different configurations. One example is holding a mug in front of the shoulder, the mug can be hold in a fixed position whilst the segments of the upper extremity can still move without affecting the position of the mug. Likewise, upper limb redundancy can be observed when a person has a disease that affects joints or tissue constraining joint range of motion, as the disease progresses and reduces mobility, the person makes corrections to their movements in order to perform their activities of daily living. Such corrections to the upper limb movements are possible due to upper limb redundancy; the joint configurations can be adjusted to comply with the requirements of the task regardless of the loss of mobility.

Upper limb movement redundancy plays an important role in trajectory planning, upper limb motion prediction, human-machine and human-object interaction. Researchers have investigated upper limb redundancy for upper arm orientation during kinematically redundant movements [111], the development rehabilitation devices [112], and for the development of exoskeletons [108, 113-116]. However, the investigation of upper limb redundancy for upper limb performance and dexterity is lacking in literature. Therefore, research work on the role of redundancy on upper limb motion is needed.

2.3.7 Computational tools for human motion data acquisition and modelling

Computational models are an immensely powerful tool that can be used to analyse real or unreal scenarios. Computational models are particularly helpful in situations in which experimental analysis is expensive or there is no access to large groups of participants, participants from particular populations, with specific anthropometric characteristics, or even with extreme or unseen features. Fortunately, recent years have provided several technological tools and software packages that can be used for the development of computational models. Some of the most common software packages for human motion analysis are Adams, AnyBody Modeling System™, MADYMO®, Articulated Total Body (ATB), 3D Static Strength Program (3DSSP), Abaqus, OpenSim, Python and MATLAB. Due to the flexibility of the software package, MATLAB has been selected as the programming language for the development of the computational models needed to study upper limb motion and for the characterisation of upper limb workspace with respect to dexterity.

Experimental analysis requires collecting data. The existent technological tools that can be used for human motion data acquisition are grouped into optical and non-optical systems. Non-optical systems are sensor-based including inertial, magnetic and

mechanical devices to capture motion [117]. Some devices of this type are goniometers, potentiometers, and accelerometers. Goniometers are simple manual devices that are used to measure joint range of motion. Potentiometers and electrogoniometers are more advanced instruments based on measuring a change in voltage that can be translated into angular displacement. Potentiometers tend to slightly encumber movement, whilst electrogoniometers tend to be sensitive as they are composed of finer pieces [118]. Some advantages of this electronic devices are that they are normally low cost and can provide real-time data. However, this technique may be subject to errors due to displacement of the tissue on the place of attachment or due to the incorrect alignment of the device with the plane of interest [118]. Likewise, accelerometers are transducer-based devices that can be used to measure acceleration in real time [118]. The benefits of these devices are that they are relatively inexpensive and provide real-time acceleration data, however, they do not provide joint angles or position and tend to brake easily [118].

Conversely, optical systems use cameras to detect the position of the body. This capture motion using video cameras (image sensors) to triangulate either the 2D or 3D position of the elements being recorded [117]. Most optical systems require the use of active (normally LEDs) or passive (reflective materials) markers. However, more recent systems are able to detect surface features or light contrast to accurately capture data without using markers (markerless systems) [117]. Some important aspects that need to be considered when using optical systems are camera positioning, camera speed, sampling frequency, shutter speed, synchronization of cameras, calibration of image space, digitalization, transformation of data, data filtering, anatomical models and marker sets [118]. Some examples of motion capture systems and software packages are BTS SMART, Dartfish, Digital Motion Analysis (DMAS), Hu-M-An, Kinematic Analysis Software (KA Pro), Kinovea, MaxPRO, MSMS, Templo, Vicon™ and Visual3D [117]. The reader can find further explanation of these and more software packages in the work published by Nunes [117].

Another aspect commonly assessed for human motion analysis is muscle activation, which can be measured using Electromyography (EMG), a technique used for the analysis of muscle activity. This technique measure muscle activation by placing electrodes on the skin close to the muscle (surface EMG) or by using needle electrodes (intramuscular EMG).

Complementary techniques used for the analysis of human motion are x-ray stereo photogrammetry, magnetic resonance imaging (MRI), Computed Tomography (CT), and ultrasound methods. Such techniques can provide anthropometric information such as size and geometry.

2.4 Uncertainty and sensitivity analysis

The description of a determined phenomenon requires understanding each element of the system, as well as their interactions. A system can be simplified as black box models with inputs and outputs. It is not difficult to believe that variations in the inputs of the system might affect the outputs. Sensitivity and uncertainty analysis focus on the quantification of the effect of such input variations. Sensitivity Analysis evaluates variation in the model outputs due to qualitative or quantitative variation in the input variables [119]. It helps to identify the factors that mostly contribute to output variability, the factors that are insignificant and the factors that are important for optimization [120]. Sensitivity analysis can be classified into factor screening, local, and global sensitivity analysis [120]. Screening factors help to identify influential factors that account for most of the output variability, local sensitivity analysis focuses on local impact factors by using partial derivatives of the output functions with respect to the input variables, and global sensitivity analysis apportions output uncertainty to the uncertainties in the input variables.

Some common approached to conduct sensitivity analysis are [121]:

- *Screening techniques*: this approach refers to the isolation of the elements of the system to study the system. Some techniques of this type are one-at-time (OAT) experiments, factorial, fractional factorial experiments, systemic fractional replicate design, and iterated fractional factorial.
- *Differential analysis*: basically, refers to the use of Tailor expansion series.
- *Monte Carlo analysis*: randomly inputs are studied to determine the partial and overall uncertainty of the system.
- *Variance based methods*: the study of the system through the decomposition of the overall variance into partial variances using techniques such as correlation ratios, Sobol' indices, and Fourier Amplitude of Sensitivity Test (FAST) [121].

Uncertainty is defined as a lack of certainty [122]. This uncertainty can be due to a lack of knowledge or variations in the inputs. Uncertainty Analysis focuses on the effect of uncertainty in the inputs. Uncertainty is said to be a complement of probability, or an improbability. Thus, the probability of an event E plus the uncertainty of the same event E^c must add to 1 providing the two events are exclusive (one or the other event happens at once) [122]. Probability can be defined as a branch of sciences that helps to predict the probability of an event to occur.

A powerful tool for probability analysis is the Bayes' theorem, it is centred on the fact that the probability of any event to occur can be calculated by using a the probability rules and assuming that the events are interchangeable $p(F|EK) = p(E|FK)p(F|K)/p(E|K)$ [122]. On the other hand, Bernoulli series is a powerful technique used for the study of series of events with only two possible outcomes provided that the outcome is independent from any previous results and that the probabilities for all of the outcomes in the series are equal [122].Thu, the probability of one of the two possible outcomes can be represented by θ, the probability of the complement by $(1-\theta)$ and the probability of the series by $p(x|\theta) = \theta^r(1-\theta)^{n-r}$, where r is the number of times that the first possible outcome has occurred in the series, and n the number of total outcomes [122].

Uncertainty and sensitivity analysis are important to understand and quantify the variations in the inputs and their effects on the outputs. As models represent real systems, quantifying the uncertainty of the model and identifying sensitive inputs is essential. Firstly, to determine the accuracy of the model and secondly, to understand how the real system is affected by variations in the inputs. Not many studies focused on the upper limb include sensitivity analysis, some that include it are the sensitivity analysis of dynamics of the upper limb [123], joint kinematics [124] uncertainty of wheelchair propulsion dynamics [125], and sensitivity analysis of 3D motion systems for the analysis of human motion [126].

Therefore, uncertainty and sensitivity analysis are conducted at different stages of this research work to identify influential factors and their effects on the model outputs.

2.5 Summary

This chapter provided a comprehensive literature review to identify the current state-of-the-art and research gaps for the study of human dexterity and the investigation of general human motion. Such review was divided into anatomy and physiology of the human upper limb, human hand grasp and object interaction, and human motion modelling.

The first section focused on the description of the upper limb anatomy and physiology, as well as on the review of range of motion normative data. First, for the study of upper limb motion represented as a kinematic chain, bones are considered as infinitely rigid elements, whereas joints are considered as frictionless elements that allow motion in only certain directions. For simplicity, the shoulder is commonly modelled as a ball-and-socket joint with 3-DOFs. Likewise, the elbow is commonly modelled as a hinge joint with 1-DOF, the forearm pronation-supination as a pivot joint with 1-DOF, and the wrist as a biaxial joint with 2-DOFs.

Published normative data for range of motion is confusing, unclear, and difficult to compare [39-42]. Although some researchers believe that passive assessment provides a better estimate of joint range of motion, as active assessment can be affected by pain and weakness in the limb [41], active range of motion seems to be a more reasonable measure as this is the real range in which people can perform motion by themselves. Joint range of motion normative data is inconsistent and incomplete. Consequently, future work should focus on the development of standard methods for the assessment of joint range of motion and on providing reliable normative data that can be used for human modelling. Finally, joint range of motion can be affected by aging, deformations, diseases, injuries, surgeries, etc [28, 44-46].

It is common to model the human upper limb as a kinematic chain for the study of motion [29-35]. Then, by using forward and inverse kinematics a system of equations can be obtained to describe displacement and velocity in both Cartesian and joint spaces [32, 34, 101-103].

Although, in biomechanics, upper limb workspace volumes have been mostly employed for the study of ergonomics, human-machine interactions, design of exoskeletons, and the development of rehabilitation systems [16-20]. In recent years, some authors [21-23] have started using workspace volume as a reference for comparison and optimisation purposes as such volumes provide considerable numerical and visual information about upper limb reachability.

Dexterity is usually assessed through time dependent dexterity tests [2-8]. However, such traditional dexterity tests are limited as they cannot provide data related to movement consistency, joint angles required to execute the task, regions of high dexterity, participant performance in other regions of the corresponding upper limb reachable space, and more importantly, dexterity tests cannot determine if participants are able to perform activities of daily living. Such information is essential for prescribing an adequate rehabilitation therapy, as well as for adjusting work and home spaces to facilitate the performance of activities of daily living. Likewise, such data is beneficial for the development of assistive devices.

Additionally, dexterity tests by themselves cannot be used to predict upper limb dexterity. Consequently, computational models to characterise and predict upper limb dexterity are required. Therefore, it would be worth it to explore the use of the manipulability analysis method for the characterisation of upper limb dexterity [12].

Although a wide variety of sophisticated software packages exist. Due to the flexibility of the software, MATLAB has been selected as the programming language for the development of the computational models needed to study upper limb motion and for

the characterisation of upper limb workspace with respect to dexterity. Likewise, the Vicon Motion Capture system has been selected for the recording of human motion for the experimental analysis (as this is the motion capture system available in the laboratory for human movement analysis).

3 UPPER LIMB KINEMATIC MODEL

The previous chapter of this thesis provided a comprehensive literature review. This chapter introduces and establishes a general method for the study of upper limb motion. Such method is based on the representation of the upper limb as a kinematic chain. In this chapter, the upper limb is initially represented as a simplified 2-link kinematic chain with 2-DOFs, which is upgraded in following stages of this research work. Although such simplifications may seem like a conservative approach, a simplified model is needed to ensure that the methods and the analysis are correct.

3.1 Mathematical Background - Kinematics

The science that studies position, velocity and acceleration without consideration of forces is called Kinematics [127]. For the study of motion, it is common to describe systems as kinematic chains, systems composed of rigid bodies (links) interconnected through articulated elements (joints). The distal element of a kinematic chain, which commonly perform the tasks, is called the end-effector. Thus, the movements of a kinematic chain can be described in cartesian and joint spaces. The kinematic analysis conducted to determine position and orientation of the end-effector in cartesian space given the joint values is called forward kinematics, whereas the reverse analysis is called inverse kinematics [101].

The first step for the development of a kinematic model is to define the number of segments, joints, and degrees of freedom of the kinematic chain. Once these parameters are defined, the next step is to define a global frame of reference and local frames of reference to each degree of freedom (rotational or translational motion allowed by the joint) of the system. Both local and global frames of reference are composed of three orthogonal axis x, y and z.

The matrix that maps motion and translates it from cartesian to joint space and vice versa is called a homogeneous transformation matrix [101], which combine rotation and translation operations into a single matrix multiplication [101]:

$$H = \begin{bmatrix} R & d \\ 0 & 1 \end{bmatrix}$$

Equation 3.1

Where H is the homogeneous matrix, R is the 3 X 3 rotational matrix that describes orientation, d is 3 X 1 column vector that describes translation. The rotation and translation matrices used to obtain the homogeneous matrix are [101]:

$$Trans_{x,a} = \begin{bmatrix} 1 & 0 & 0 & a \\ 0 & 1 & 0 & 0 \\ 0 & 0 & 1 & 0 \\ 0 & 0 & 0 & 1 \end{bmatrix};\ Rot_{x,\alpha} = \begin{bmatrix} 1 & 0 & 0 & 0 \\ 0 & c_\alpha & -s_\alpha & 0 \\ 0 & s_\alpha & c_\alpha & 0 \\ 0 & 0 & 0 & 1 \end{bmatrix}$$

Equation 3.2

$$Trans_{y,b} = \begin{bmatrix} 1 & 0 & 0 & 0 \\ 0 & 1 & 0 & b \\ 0 & 0 & 1 & 0 \\ 0 & 0 & 0 & 1 \end{bmatrix};\ Rot_{y,\beta} = \begin{bmatrix} c_\beta & 0 & s_\beta & 0 \\ 0 & 1 & 0 & 0 \\ -s_\beta & 0 & c_\beta & 0 \\ 0 & 0 & 0 & 1 \end{bmatrix}$$

Equation 3.3

$$Trans_{z,c} = \begin{bmatrix} 1 & 0 & 0 & 0 \\ 0 & 1 & 0 & 0 \\ 0 & 0 & 1 & c \\ 0 & 0 & 0 & 1 \end{bmatrix};\ Rot_{z,\gamma} = \begin{bmatrix} c_\gamma & -s_\gamma & 0 & 0 \\ s_\gamma & c_\gamma & 0 & 0 \\ 0 & 0 & 1 & 0 \\ 0 & 0 & 0 & 1 \end{bmatrix}$$

Equation 3.4

Where $Trans$ and Rot represent translation and rotation respectively, a, b, c are displacements on the x, y, z axes, α, β, γ represent the rotation angles with respect to the x, y, z axes, and s and c represent the sines and cosines respectively.

The position and orientation of the end-effector of a kinematic chain expressed in frame j, can be described with respect to the frame i by the homogeneous transformation matrix:

$$H = T_j^i = A_{i+1} \cdots A_j = \begin{bmatrix} R_j^i & o_j^i \\ 0 & 1 \end{bmatrix}$$

Equation 3.5

Where T_j^i represents the homogeneous matrix for the representation of position and orientation of the frame j with respect to the frame i, A_i are the homogeneous transformations from i to $i-1$, R_j^i represents the orientation of the frame j relative to the frame i, and o_j^i represents the coordinates of the origin j relative to the frame i.

Thus, the position and orientation of the end-effector of a kinematic chain can be obtained by multiplying each homogeneous transformation matrix.

3.2 Conventions and standards for the report of kinematics

Since long ago scientists from the fields of biomechanics, medicine and bioengineering have been trying to formalise the study and report results in biomechanics. Some of the most important organizations for biomechanics are the International Society of Biomechanics (ISB), the European Society of Biomechanics (ESB) and the American Society

of Biomechanics (ASB). In 1995, as a first attempt to provide standardisation, the ISB published a work that provides recommendations for standardization for the report of kinematic data [128]. The ISB proposed some general recommendations such as the use of local and global frames for orientation and displacement and the use of matrices for dynamic analysis of human motion (see Figure 3.1). In 2002, the ISB published complementary recommendations for the ankle, hip and spine [129]. Likewise, in 2005 the ISB published complementary recommendations for the shoulder, elbow, wrist and hand [130]. These works propose the terminology for the description of anatomical landmarks and present a method for the assignation of body and joint coordinate systems (see Figure 3.2).

Although the ISB has attempted to standardize the investigation and report of kinematic studies [128-130], not all researchers use the recommendations and standard proposed by the ISB. Even the ISB technical sub committees seem to differ from each other; the hand and wrist committee states that they differ from the elbow section for the assignation of frames of reference [130].

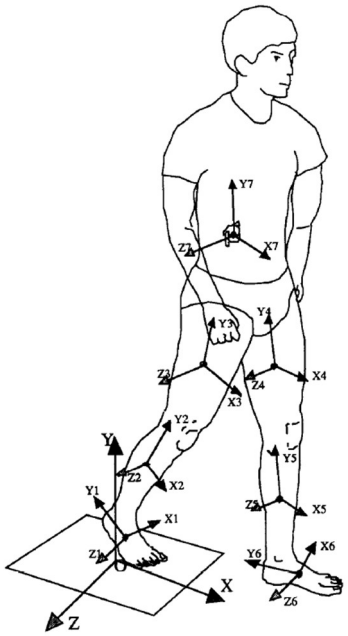

Figure 3.1. ISB Conventions for global reference frame and segmental local centre of mass reference frame. Copyright © 1995, Elsevier [11]

[11] Reprinted from Journal of Biomechanics, vol. 28, no. 10, Wu, G.; Cavanagh, P. R., "ISB Recommendations for Standardization in the Reporting of Kinematic Data", pp. 1257-1260, copyright (1995), with permission from Elsevier.

This confusion and reluctancy to the use of the standards and recommendations proposed by the ISB may come from the exclusion of other fields of science for the creation of the standards as it seems as if only clinicians and biomedical professionals were consulted for the definition of such standards without consideration of researchers from other fields of science. Some examples of the use of different conventions can be seen in the analysis of the kinematics of the hand [33], the study of wheelchair propulsion biomechanics [131], the design of exoskeletons for neural rehabilitation [132], and the study of redundancy of the arm [108].

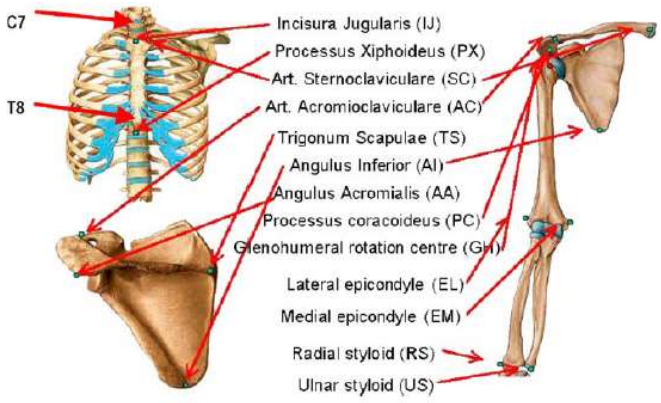

Figure 3.2. Bony landmarks and local coordinate systems of the thorax, clavicle, scapula and humerus. Copyright © 2005, Elsevier [12].

It is important to recognize the efforts made by the ISB to create standards and conventions for the report of kinematic studies and biomechanical investigations. However, failing in the adoption of such standards and conventions recommended by the ISB may be linked to the exclusion of other fields of science during the creation of such standards. The biomechanical study of the human body requires collaborative research across science; therefore, any standards and conventions should consider how they can affect modelling, computations, and use of data obtained from scientific investigations for all possible stakeholders. An example is the development of assistive devices or the study of human-machine interaction, for researchers in the field of robotics the vertical axis of the global frame of reference is commonly the z axis [101, 127, 133], whereas in the ISB recommendations it corresponds to the y axis. Although it may seem like no big deal,

[12] Reprinted from Journal of Biomechanics, vol. 38, no. 5, Wu, G. *et al.*, "ISB recommendation on definitions of joint coordinate systems of various joints for the reporting of human joint motion—Part II: shoulder, elbow, wrist and hand", pp. 981-992, copyright (2005), with permission from Elsevier.

having different standards and conventions can lead to errors and add complexity to multidisciplinary collaboration, which could be otherwise avoided by creating standards and conventions that consider other scientific fields. Therefore, one may believe that international organisations from different field of science need to work on the development of standards and conventions that can benefit the scientific community as the lack of formalization and standards slows down the scientific development.

3.3 General method

The scientific study of any phenomenon requires the establishment of the methods, standards, modelling techniques, and conventions utilized in such investigation. Therefore, this section focuses on the definition of upper limb movements, conventions, protocols, and kinematic representation used throughout this research work for upper limb modelling, simulations, and experiments.

3.3.1 Upper limb movement references and convention

Section 3.2 describe the standards and conventions recommended by the ISB for the explanation of human motion. However, such conventions have not been fully adopted as they differ from standards used in other areas of science that collaborate with biomechanics. Therefore, as the methods used in this investigation include techniques used in robotics, and in order to facilitate the cross collaboration among fields for future investigation, this research opted to assign the global frame of reference as commonly assigned in robotics and mechanics, as illustrated in Figure 3.3, where the x axis points forwards, the y axis towards the left side of the body, and the z axis points upwards.

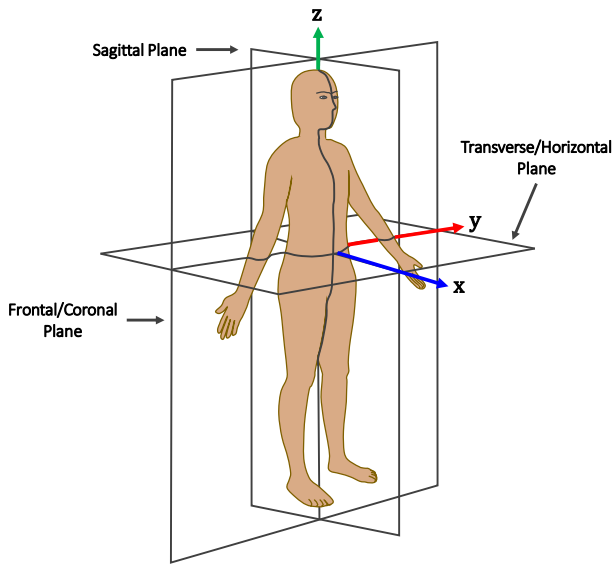

Figure 3.3. Planes of motion for the general description of human movements

However, for the upper limb models used in this research work the origin of the global frame of reference will be assigned to the shoulder as described in the next subsection (Section 3.3.2). Human motion is generally described with reference to 3 planes: the sagittal, transverse (horizontal), and frontal (coronal) planes (see Figure 3.3), which (accordingly to the global frame of reference used in this research) correspond to the x-z, x-y, and y-z planes, correspondingly.

The sagittal, transverse, and frontal planes can be used to describe general movements of the body. However, more specific movements such as shoulder abduction, elbow flexion, and wrist deviation, require defining local points of reference and neutral positions, which are defined in Figure 3.4. The figure depicts the local reference and neutral position for the movements of the right upper limb (the corresponding movements for the left limb follow the same rules). As can be observed in the figure, shoulder abduction-adduction neutral position corresponds to the limb fully extended, with the palm facing the body, and the limb parallel to the trunk pointing downwards. Shoulder abduction corresponds to the lateral movement of the extremity on the frontal plane (positive direction), whereas adduction refers to the opposite movements of the limb (negative direction). Shoulder flexion-extension neutral position occurs when the upper limb is fully extended, parallel to the trunk, and with the palm of the hand facing backwards. Shoulder flexion corresponds to the forward rotational movement of the limb on the sagittal plane from neutral position (positive direction), whereas shoulder extension refers to movements of the limb in the opposite direction (negative direction). Shoulder internal-external rotation neutral position refers to the limb in 90 degrees of shoulder abduction, 90 degrees of elbow flexion, and the palm facing downwards. Shoulder internal-external rotation corresponds to the rotational movements of the forearm on the imaginary axis formed along the upper arm segment, where external rotation refers to the upward rotational movement of the limb (positive direction), and internal rotation to the opposite rotational movement of the forearm (negative direction). Elbow flexion-extension neutral position corresponds to the upper limb fully extended, parallel to the trunk, and with the palm facing forwards. Elbow flexion refers to the rotational movement of the forearm at the elbow joint towards the shoulder (positive direction), whereas extension refers to the opposite movement of the forearm (negative direction). Forearm pronation-supination neutral position occurs when the limb is in 90 degrees elbow flexion and the thumb is pointing upwards. Forearm pronation refers to the internal rotation of the thumb/hand with the palm incrementally facing down (positive direction), whereas supination refers to the opposite movement of the forearm with the palm incrementally facing upwards (negative direction). Wrist radial-ulnar deviation neutral position corresponds to the limb in 90 degrees elbow flexion, the thumb pointing upwards (can also be with the hand

facing downwards), and the third carpal (middle finger) parallel to the forearm segment. Wrist radial deviation refers to the rotational movement of the hand towards the thumb side (positive direction), whereas wrist ulnar deviation refers to the oppositive rotation of the wrist (negative direction). Finally, wrist flexion-extension neutral position occurs when the limb is in 90 degrees elbow flexion, the thumb is pointing upwards, and the third carpal (middle finger) is parallel to the forearm segment. Wrist flexion refers to the rotational movement of the hand towards the palmar side (positive direction), whereas wrist extension refers to the opposite rotational movement of the hand towards the dorsal side of the hand (negative direction).

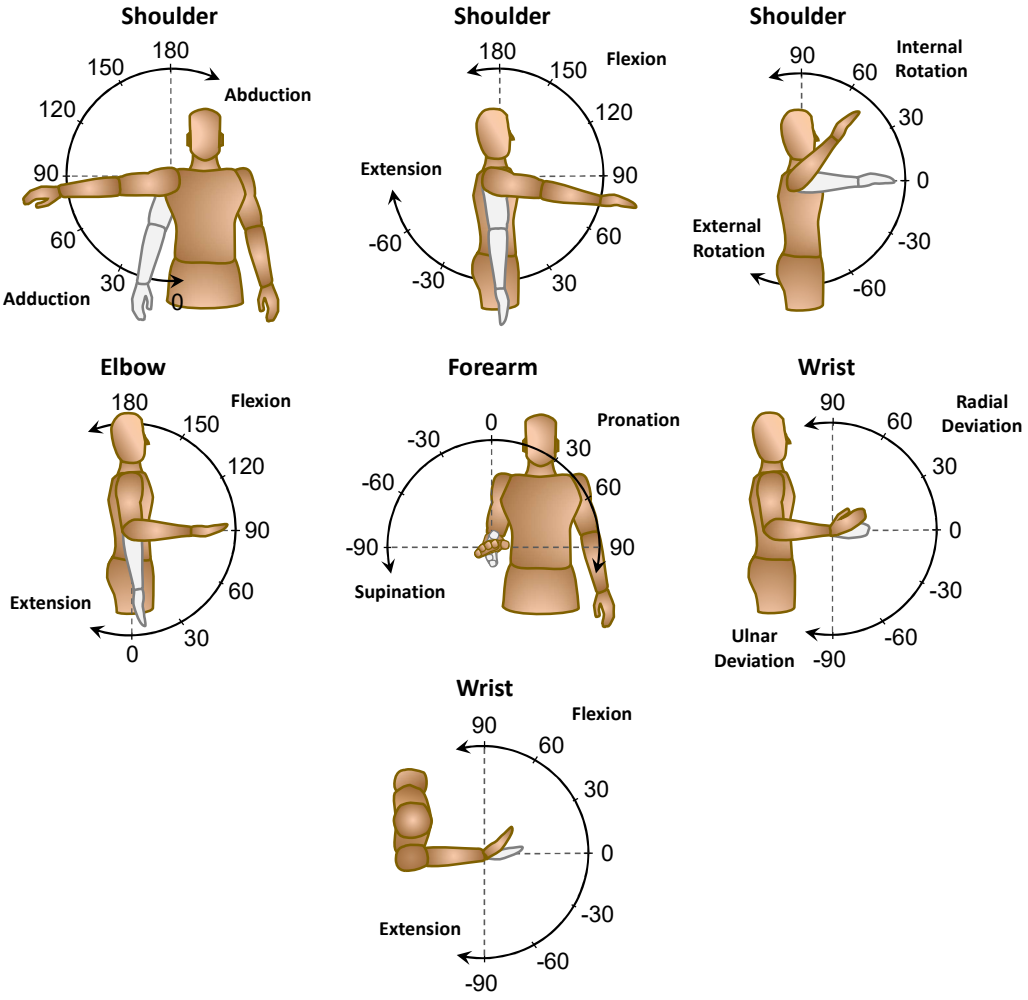

Figure 3.4. Upper limb reference for shoulder, elbow, forearm, and wrist movements. The limb in grey represents neutral positions.

3.3.2 Upper limb representation as a kinematic chain

The upper limb can be represented as a kinematic chain composed of infinitely rigid links (bones) interconnected by frictionless articulation joints which allow motion in some

directions and constrain it in others [33, 34, 97, 108, 134, 135]. Some of the general assumptions are that joint centres of rotation coincide with the axes of the segments, pronation-supination motion originates at the elbow, and wrist motion is the motion of the third metacarpal with respect to the radius [130].

The upper arm is commonly represented as a 3-link kinematic chain (arm, forearm, and hand) with 2-DOFs at the wrist, 2-DOFs at the elbow (including pronation-supination), and 3-DOFs at the shoulder. However, the number of segments and joints representing the extremity must be selected according to the scope of the study.

However, in this research, the upper limb is initially represented as a 2-link kinematic chain (upper arm and forearm) with 2-DOFs (shoulder flexion-extension and elbow flexion-extension), which is upgraded in following stages by adding 2-DOFs at the shoulder.

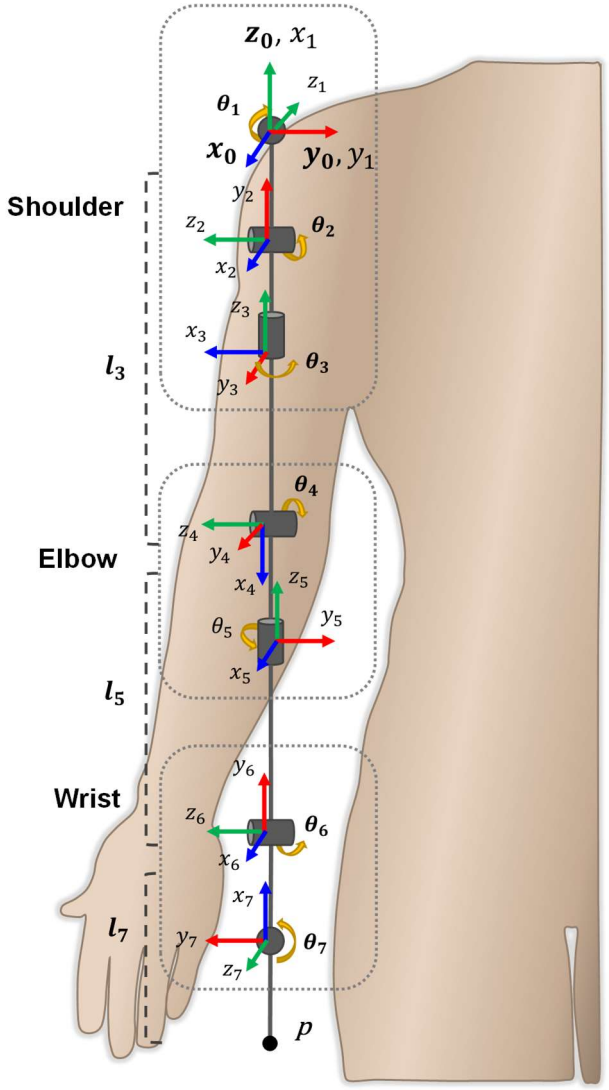

Figure 3.5. Representation of the human upper limb as a 3-link kinematic chain with 7-DOFs with a global frame of reference at the manubrium of the sternum.

The origin of the global frame of reference (x_0, y_0, z_0) is fixed at the centre of the glenohumeral joint, the z axis is parallel to the gravity and pointing upwards, the x axis points forwards as if the hand extends to reach an object to the front, finally the y axis is assigned by using the right-hand rule. The rest of the frames (x_i, y_i, z_i) are assigned as needed following the right-hand rule. Then, the homogeneous transformation matrices H_i are formed by using Equation 3.2, Equation 3.3 and Equation 3.4. Finally, the position and orientation $x = [x, y, z, \alpha, \beta, \gamma]^T$ of the end-effector (wrist) can be obtained using Equation 3.5. If position and orientation $x = [x, y, z, \alpha, \beta, \gamma]^T$ of the end-effector are known, the angles $q = [q_1, q_2, q_3, \dots, q_n]^T$ can be obtained by using inverse kinematics (see Figure 3.5 and Figure 3.6).

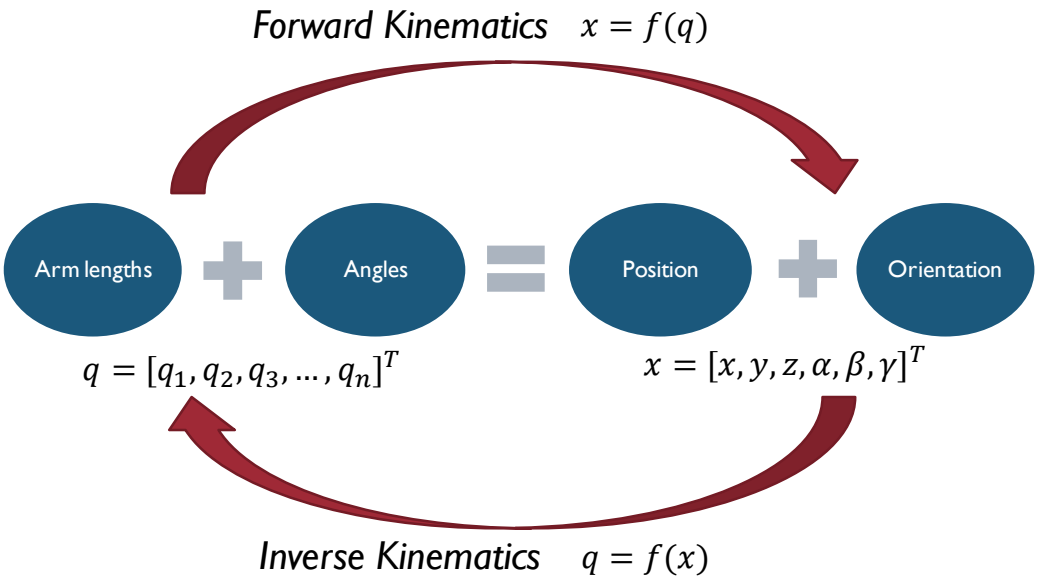

Figure 3.6. Schematic representation of the model (inputs-outputs)

3.3.3 Motion capture protocol

This research is mainly focused on the characterisation of upper limb dexterity by modelling the limb as a kinematic chain and by simulating the movements of the extremity to understand workspace and dexterity. However, Chapter 0 presents an experimental approach which requires recording participant movements. The laboratory used for the experiments conducted in this research is fitted with a motion capture system composed of 10 optical cameras (T-160, 100 Hz, Vicon Nexus 1.8.5, Vicon Motion System Ltd – Oxford, UK). The optical cameras can record the position of body landmarks by attaching reflective markers to the locations of interest. The selection of body landmarks of interest depends on the aim and scope of the experiment. Therefore, the number of markers and their attachment location vary from study to study. Some research investigations on upper limb movement analysis use as few as 6 markers,

whereas others can use above 18 markers for the study of a single limb [47, 85, 136-138]. For instance, [85] uses 6 markers for the investigation of upper limb functionality, [136] uses around 6 markers per limb to assess upper extremity kinematics during functional activities, [137] uses 9 markers for the analysis of human arm motion planning, [47] uses around 18 markers per limb for the investigation of upper limb range of motion required for activities of daily living, and [138] provides a protocol for motion capture that uses around 9 markers per limb. The selection of the number of markers and their attachment locations may pose limitations for the extraction of kinematic information and can affect the accuracy of the results. After evaluating such factors, this research adopted a modified version of the Nexus Plug-in-Gait model marker protocol [138] for the recording of participant movements. The modify version used here consists of the Nexus Plug-in Gait [138] (only the upper limb and thorax markers) and extra markers to reconstruct any missing points. Thus, the modified protocol consisting of 19 non-invasive reflective markers placed on the upper limb and thorax is illustrated and described on Figure 6.1 and Table 6.1 of Chapter 0.

However, as the computation of an accurate location of the shoulder centre of rotation is challenging, the modelling approach used in Chapter 0 assumes that the shoulder centre of rotation coincides with the position of the marker placed at the acromion. Such assumption is a limitation of the modelling approach used in the experimental analysis conducted in this research work and may affect the accuracy of the results. The rationale behind such simplification was that the complexity of computing a highly accurate shoulder centre of rotation would not significantly improve the accuracy of the computed shoulder angle for gross movements, and an approximation of shoulder and elbow angles would be sufficient to compare the results obtained from the simulation and experiments. However, future experimental analysis should explore the use of techniques and methods to increase the accuracy of the computation and analysis of the upper limb kinematics.

3.4 Summary

This chapter established a general method for the study of upper limb motion, which is used throughout this research for the investigation of upper limb motion and for the development of a novel method for the characterisation of upper limb workspace with respect to dexterity. Although the upper limb is initially represented as a simplified 2-link kinematic chain with 2-DOFs, the model is upgraded in following stages of this research work by adding 2-DOFs at the shoulder. Such simplifications may seem like a conservative approach, however, as this study aims to establish a novel method, such simplification is needed to validate that the model works correctly.

4 UPPER LIMB WORKSPACE

The previous chapter focuses on kinematic modelling methods for human motion analysis. The main inputs of such kinematic models are segment lengths, degrees of freedom, and joint range of motion. Thus, once the modelling methods are defined, the next step is to understand the nature of the input parameters and how variations in the input affect the output. Therefore, this chapter focuses on the review of anthropometry (body measurements) and range of motion (ROM) of the human upper limb. Likewise, this section explores and defines upper limb workspace. The understanding of upper limb anthropometrics and workspace limitations are a first step to comprehend the manipulability and dexterity of the extremity. The work presented in this section includes the analysis of Reach Envelope Area (REA), workspace volume and the effects of input uncertainty on the overall reachability and workspace.

4.1 Upper limb anthropometry

The human body can be divided into body segments to facilitate its study. The main parts of the body are the head, the trunk and the limbs. Likewise, each of these parts can be divided into body segments. The study of the size and shape of the body including parameters such as stature, weight, segment lengths, volume, centre of mass, and so on is called anthropometry.

During the industrial revolution and after World War II, anthropometry gained more importance as the provision of anthropometric data was important for engineering, design, ergonomics, performance optimization, rehabilitation, and for the development of military equipment and cloths. Studies published between 1950 and 1970 focused mainly on the study of anthropometrics, although, some works include range of motion and dynamic aspects of the body [139-142]. In 1978, the National Aeronautics and Space Administration (NASA) published an anthropometric source book with data obtained from surveys of 61 military and civilian populations [143, 144]. Similarly, in 1991, the Department of Defence of the United States published anthropometric data acquired from 75,000 U.S military personnel (collected in a time frame of 35 years) [145]. Likewise, in 1998 the Department of Trade and Industry of the U.K. published a handbook of adult anthropometrics and strength measurements.

The studies mentioned above are a great effort to compile anthropometric data. However, in many cases, body measurements were only obtained from military populations, commonly men, and not all body measurements for the populations were collected. Thus, the comparison, compilation and use of the data is complicated.

Body segment dimensions vary from person to person. Such variability can be attributed to various factors, such as sex, ethnicity, environment, age, secular trend, social class, occupation, among others [139, 144, 146, 147]. Such human variability can be classified into three categories [144]:

- Intra-individual: this variability includes right side-left side asymmetry and changes that occur during the adult life of an individual as a result of aging, eating habits and nutrition, environment (climate, altitude, topography, soil type), etcetera.
- Inter-individual: it refers to variability due to factors such as gender, ethnicity, and racial origin.
- Secular: changes that occur from generation to generation [144].

Therefore, in order to create accurate human models, right anthropometric data should be used according to the population being studied; one cannot assume that the body measurements are the same across populations. Moreover, the anthropometrics of an individual can vary from one side to the other (intra-individual variability) and can vary from generation to generation (secular variability). Thus, selecting the proper input data has a great effect on the validity and accuracy of a given model. When possible, the applicable statistical data should be acquired directly from the population of interest.

Table 4.1 presents males stature and upper limb lengths (acromion to fingertips) for people of 4 different nationalities. Although there are differences between the values reported by Peebles [146] and Pheasant [147], it could be said that the values agree with each other. Moreover, researchers tend to estimate values where data is not available, it may be the case for some reported values which appear to be the same for both authors (see standard deviations in Table 4.1). According to the data, and by comparing the mean values, people form the United States tend to be almost as tall as males form the United Kingdom (0.5-1.5cm difference), and both people from USA and UK seem to be from 6-10cm taller than Japanese and Hong Kong males. Similarly, male upper limb lengths for people from the United States and United Kingdom appear to be at least 5cm larger than those for Hong Kong and Japanese people.

At times, anthropometric data of a particular population is not existent or accessible. In such cases, segment length, weight, volume and mass can be estimated in function of hight or total weight; given that individual body measurements are proportional to total hight and weight. Figure 4.1 provides male body segment lengths in function of height for U.S., Mediterranean and Nordic populations.

Table 4.1. Male stature and upper limb length (acromion to fingertips) for different nationalities, source [144, 146, 147].

Population	*Stature*		*Upper limb length*		*Limb length (ratio)*	
	Peebles (1998)	*Pheasant (2006)*	*Peebles (1998)*	*Pheasant (2006)*	*Limb length / Stature*	
	(mm)	***(mm)***	***(mm)***	***(mm)***	*(-)*	*(-)*
United Kingdom	1755 (70)	1740 (70)	794 (36)	780 (36)	0.452	0.448
United States	1760 (71)	1755 (71)	796 (36)	790 (36)	0.452	0.450
Hong Kong	1690 (62)	1680 (58)	735 (32)	730 (30)	0.435	0.435
Japan	1687 (57)	1655 (58)	729 (30)	715 (29)	0.432	0.432

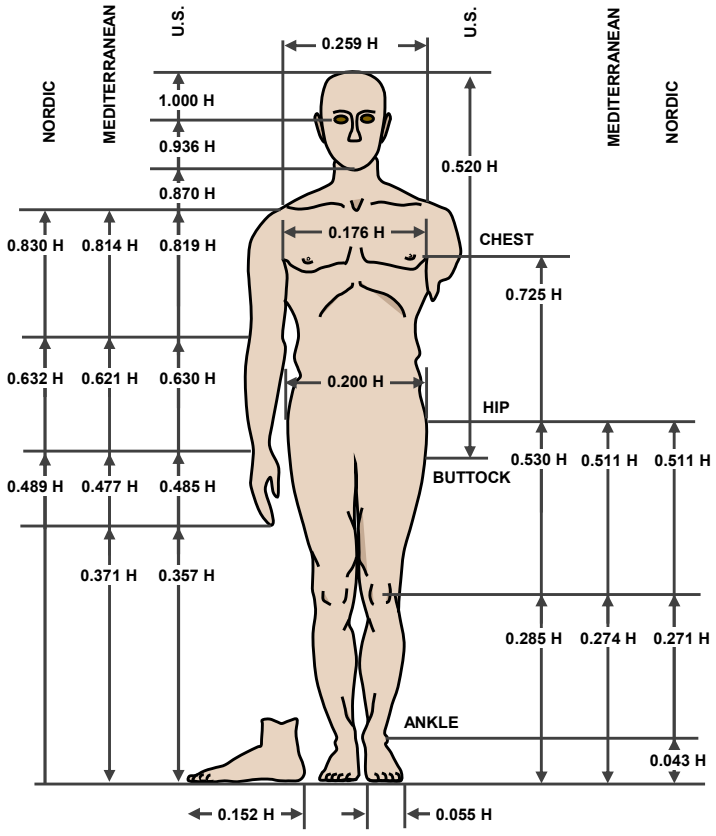

Figure 4.1. Body segment parameters in function of height for three different populations. Based on [141] Copyright © 1972 by the National Academy of Sciences.

The last 2 columns of Table 4.1 contain the upper limb segment lengths in function of stature (segment length divided by stature) according to the values of columns 2-5. Thus, the segment length of the upper limb (acromion to fingertips) in function of stature for

the United States (0.462*H) obtained from Figure 4.1 is quite close to the corresponding values in Table 4.1. Consequently, it can be said that in special circumstances where all anthropometric values of a population are not accessible, such values can be estimated in function of height (if such proportions are known). However, it is important to note that the use of such estimates will have an impact on the validity and accuracy of the study.

Therefore, when studying populations, it is recommended to use the correct statistical data according to the population of interest. If such data is not accessible, the next step is to estimate body segment parameters in function of stature. When the analysis is person-specific, if possible, the measurements of interest must be acquired directly from the individual. Thus, in this research, for population analysis, statistical data is used. However, anthropometry and range of motion values are directly obtained from the participants for the experimental studies.

4.2 Reach Envelope Area – 2-Dimensional analysis

This section focuses on the investigation of upper limb motion and workspace reachability on the horizontal plane. This limb reachability on the plane is known as reach envelope area (REA), which is constrained by the upper limb joint range of motion. Thus, the work presented in this section centres on determining and quantifying upper limb reach envelope area. Moreover, the analysis includes the quantification of input uncertainties and their effect on the overall limb reachability (2-D). The investigation presented here is a first step on the exploration of upper limb reachability, which is extended to 3 dimensions in section 4.3.

4.2.1 Methodology

The kinematic model representation of the upper limb introduced in the previous chapter was used in this parametric study to explore reach envelope area on the horizontal plane.

In this first approach, the upper limb was represented as a simplified kinematic chain composed of 2 links (upper arm and forearm) with 2-DOFs (shoulder horizontal flexion-extension and elbow flexion-extension). Thus, the reach envelope area obtained in the analysis refers to the reachability of the upper limb up to the wrist. The forearm was assumed to be fixed in supine position and the shoulder and elbow joint rotational axes perpendicular to the plane being analysed. The model inputs were the shoulder and elbow joint angles $q = [q_1, q_2]^T$ and the upper arm and forearm segment lengths $l = [l_1, l_2]$. The model outputs were the position $x = [x, y, z]^T$ of the end-effector on the cartesian space, which were used to compute the upper limb reach envelope area. The segment length values of the upper extremity were obtained from published

anthropometric data of the UK population (see Table 4.2) [146]. Likewise, Table 4.3 show the joint ROM values used in the analysis.

Table 4.2. Upper limb segment values for the British population, source [146].

Parameter	*Variable*	*Males (m)*	*Females (m)*
Upper Arm $(\boldsymbol{m})$	l_{m1}, l_{f1}	$\mu_{ml1} = 0.357, \sigma_{ml1} = 0.025$	$\mu_{fl1} = 0.321, \sigma_{fl1} = 0.018$
Forearm $(\boldsymbol{m})$	l_{m2}, l_{f2}	$\mu_{ml2} = 0.288, \sigma_{ml2} = 0.014$	$\mu_{fl1} = 0.256, \sigma_{fl1} = 0.014$

The analysis centred on reach envelope area on the horizontal plane. The only movements considered for the analysis were shoulder horizontal flexion-extension, and elbow flexion-extension. The experiment consisted of simulating upper limb motion along the plane by varying joint angles within ROM from their minimum to maximum values. The analysis was conducted in MATLAB using an algorithm that varied joint angle values from minimum to maximum obtaining as a result the reach envelope area and its boundaries (see Figure 4.2).

Table 4.3. Normal range of motion of joints in male subjects, source [39].

Element of the limb	*Movement*	*Male ROM [39]*	*Variable (Angles)*
Shoulder	Horizontal flexion	140.7 ± 5.9	$q_{8\,max}$
	Horizontal extension	45.4 ± 6.2	$q_{8\,min}$
	Abduction	184.0 ± 7.0	$q_{1\,max}$
	Adduction	- -	$q_{1\,min}$
	Flexion	166.7 ± 4.7	$q_{2\,max}$
	Extension	62.3 ± 9.5	$q_{2\,min}$
	Inward rotation	68.8 ± 4.6	$q_{3\,max}$
	Outward rotation	103.7 ± 8.5	$q_{3\,min}$
Elbow	Flexion	142.9 ± 5.6	$q_{4\,max}$
	Extension	0.6 ± 3.1	$q_{4\,min}$

4.2.2 Results

Figure 4.2 shows reach envelope area for UK males with 3 different segment lengths: mean values, mean minus 3 standard deviations, and mean plus 3 standard deviations. As can be observed in Figure 4.2, reach envelope area boundaries consist of semi-circular

segments, which was somehow expected as both joints allow only rotational motion. The total estimated reach envelope area for an upper limb with mean values (medium size) was $0.59m^2$, whereas REA for a small (-3 SD) limb was 32.9% smaller and for a large (+3 SD) limb was 39.1% larger than the medium size extremity (see Figure 4.2).

Moreover, it can be observed that reach envelope area shifts away for long limbs, increasing long-distance reachability but decreasing short-range reachability. Correspondingly, short limbs exhibit a decrease in long-distance reachability and an increase in short-distance reachability.

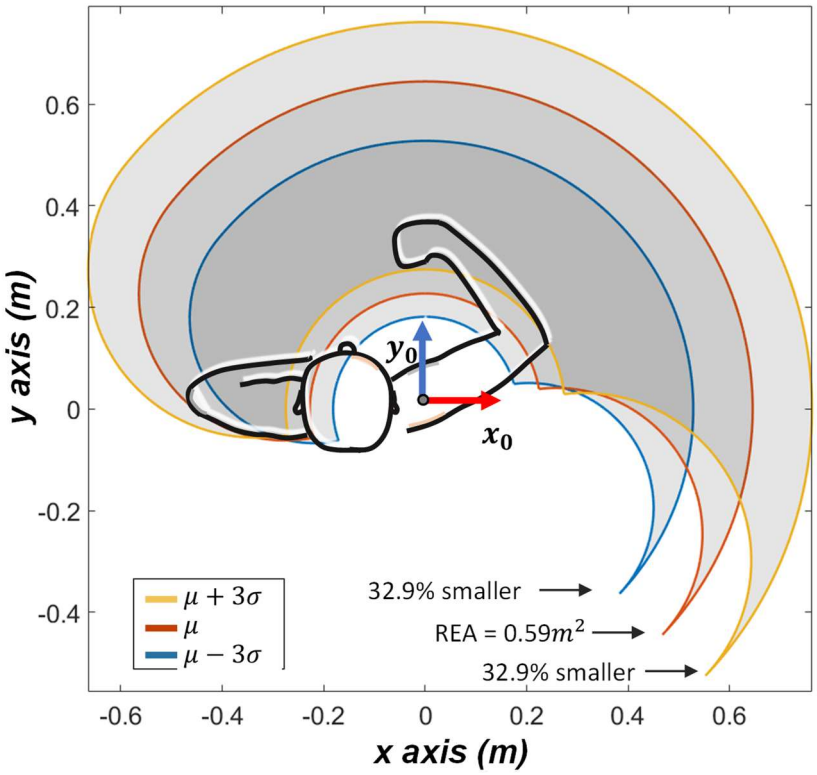

Figure 4.2. Reach envelope area of the upper limb (horizontal plane) for UK males using mean values(red), -3 SD (blue) and +3 SD (yellow).

Variations in upper limb lengths are not the only factors that affect or modify reach envelope area. Range of motion values for the analysis depicted in Figure 4.2 were fixed and only the effect of variations in segment lengths were investigated.

However, uncertainty on range of motion also affect the reachability of the upper limb and REA. Therefore, for the second part of the analysis, segment lengths were fixed to investigate how REA is affected by reductions in joint ROM. The results are shown in Figure 4.3. As can be noticed, a reduction of 15 degrees in shoulder horizontal flexion-extension decreases REA by 8.1%, regardless of which end is reduced (see Figure 4.3 a-d).

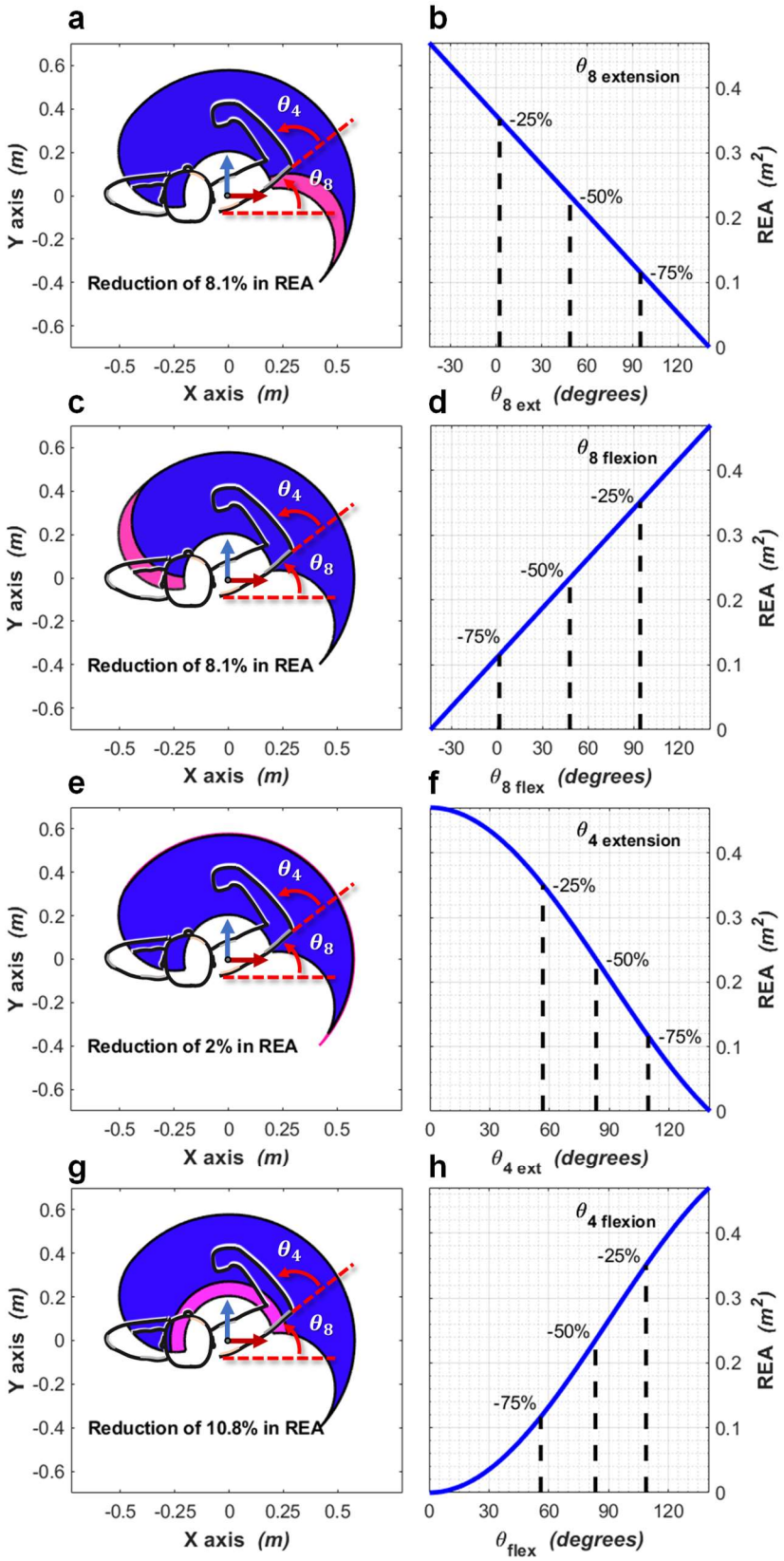

Figure 4.3. Reach Envelope Area reduction (magenta) as both extremes of the shoulder and elbow ROM are reduced by 15 degrees. (a-b) Shoulder horizontal extension; (c-d) Shoulder horizontal flexion; (e-f) Elbow extension; (g-h) Elbow flexion.

Nonetheless, a reduction of 15 degrees in elbow extension decreases REA by only 2%, whereas such the same reduction in elbow flexion decreases REA by 10.8% (see Figure 4.3 e-h). According to the results, it seems that on the plane, a reduction of 15 degrees for elbow flexion would cause a greatest reduction of REA. Furthermore, as can be seen, the reduction of elbow flexion has a direct effect in the short-distance reachability which would have a considerable effect on the performance of the limb, particularly for activities of daily living involving eating and touching the face. However, the study was conducted only on the plane and for a simplified representation of the limb (2-links with 2-DOFs) and it is possible that in real life such reductions get compensated by other joints.

Figure 4.2 and Figure 4.3, are the results obtained from studying the effects of changes in segment lengths and in joint range of motion. However, such results exhibit the separate effects of both uncertainties. Therefore, the analysis was extended to quantify the effects of propagating all input uncertainties by using the Monte Carlo method with normally distributed values for ROM and multivariate normally distributed values for the two segment lengths of the limb (see Figure 4.4).

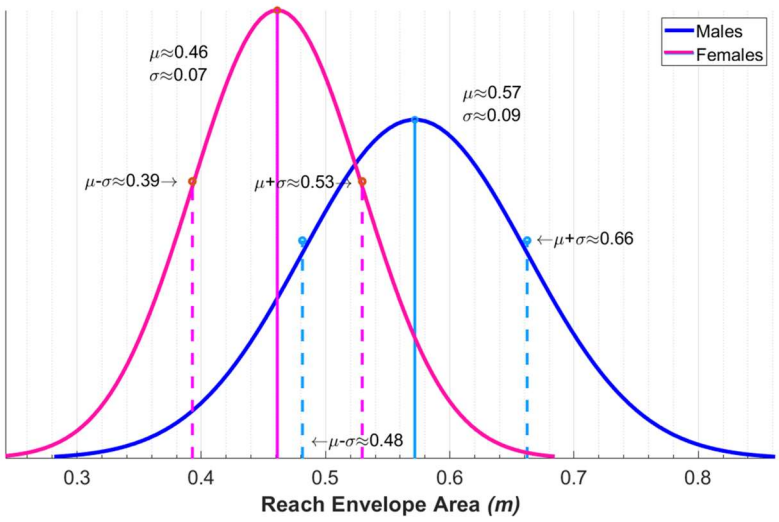

Figure 4.4. Estimated reach envelope area for males (blue) and females (magenta) using Monte Carlo analysis to propagate the input uncertainty.

Moreover, the estimated female reach envelope area was computed and compared to the corresponding male reach envelope area. The analysis was conducted by using Monte Carlo sampling from segment length distributions for both genders (see Table 4.2). However, only male ROM values were considered for both males and females as the found reported statistical values for female populations were only acquired from younger [148] or older [149] populations and not across all age groups. Therefore, the results will only show the effects of upper limb length variability given the gender of the population.

As can be appreciated, the estimated male REA is about 7% greater than the corresponding area for females. This was expected as reach envelope area depends on the size of the upper limb, which likewise relates to the stature of the individual, and according to statistical data, men tend to be taller than women (inter-individual variability, see Section 4.1). Hence, the researcher must take into consideration intra-individual variability when analysing populations as the accuracy of the results will be affected by such factors.

The results presented in Figure 4.2 and Figure 4.3, demonstrate the separate effects of variations in limb segment lengths and in ROM. The analysis was extended to estimate the combined effects on reach envelope area for the British male population. The investigation was carried out using Monte Carlo (n=10,000) and normal distributions for the input parameters (see Table 4.2 and Table 4.3). The reach envelope area boundaries were computed and are shown in Figure 4.5.

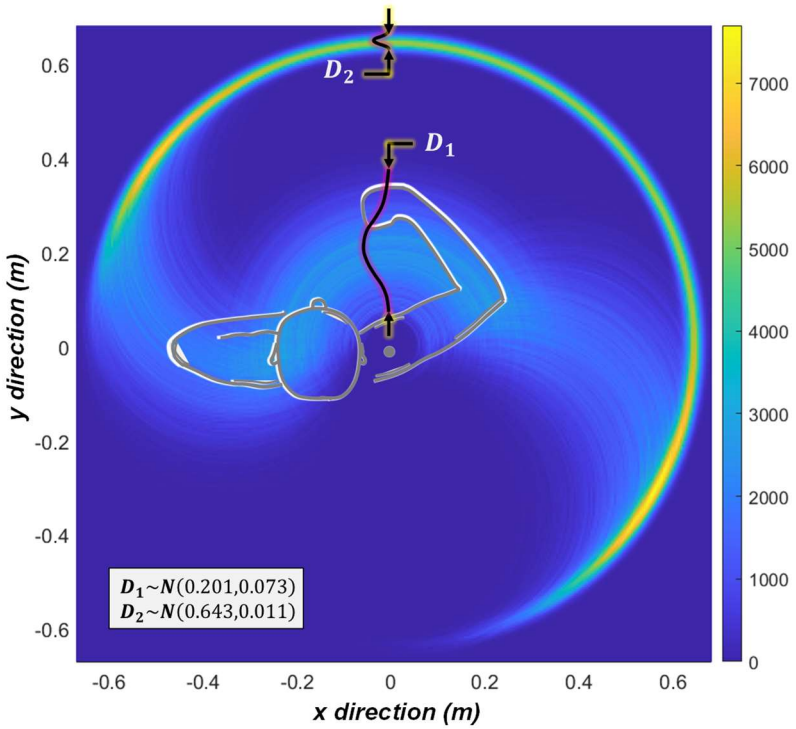

Figure 4.5. Estimated reach envelope area for British males using Monte Carlo analysis (n=10,000) and normal distributions for upper limb segment lengths and ROM.

As can be appreciated in Figure 4.5, the boundaries at the long range seem to fall relatively close to each other compared to the corresponding boundaries closer to the shoulder. The estimated mean distance for the long range boundary from the shoulder in the y direction was $\mu = 0.643m$ ($\sigma = 0.011m$) whereas, the corresponding distance for

the short range boundary was $\mu = 0.201m$ ($\sigma = 0.073m$). The deep blue surface within the boundaries is the estimated reachable surface across the sampled population.

4.2.3 Summary

The work presented in this section centred on determining and quantifying upper limb reach envelope area including uncertainties analysis.

As a result of the analysis, it has been found the combination of both effects produce high variations of REA in both shape and location. This uncertainty caused by both factors was propagated, obtaining as a result the mean and standard deviation of the predicted REA for the population, and the different REA shapes which showed that there is higher variability in the short-range than in the long-range limb reachability. These findings provide insight for the understanding of upper limb reachability and the effects of uncertainties on the reachable points on the horizontal plane. Likewise, the results presented in this section already provide information relevant for workspace design, ergonomics, and clinical analysis. However, the work presented in this section only included 2-dimensional analysis, and as the upper limb can move in 3-dimensions, a full 3-dimensional analysis of upper limb workspace is presented in the following section.

4.3 Workspace exploration – 3-Dimensional analysis

The previous section centred on the upper limb reachability on the horizontal plane (reach envelope area). However, as in reality the upper limb performs movements in 3 dimensions, this section extends the analysis presented in the previous section by adding a dimension to investigate full 3-dimentional upper limb motion. Furthermore, the study presented in this section also includes the quantification of input uncertainty and its effect on workspace (3-dimentional reachability). Understanding upper limb workspace is vital as it provides information about the potential reachable points in space, how reachability is affected by reductions in range of motion, and eventually, how all those factors can affect upper limb dexterity.

4.3.1 Workspace investigation

For the exploration of 3-dimensional reachability, the upper limb was represented as a simplified kinematic chain composed of 2 links (upper arm and forearm) with 4-DOFs (shoulder abduction-adduction, shoulder flexion-extension, shoulder internal-external rotation and elbow flexion-extension). The model inputs were the shoulder and elbow joint range of motion and the upper arm and forearm segment lengths (see Table 4.2 and Table 4.3).

The model outputs were the position $x = [x, y, z]^T$ of the end-effector on the cartesian space, which was used to compute upper limb workspace volume. The upper limb segment lengths and joint ROM values used in the analysis were obtained from published anthropometric data for the British population (see Table 4.2 and Table 4.3). However, joint range of motion published data is limited. Researchers provide ranges of motion that are commonly measured only on one plane of motion and with the rest of the segments in a single configuration as illustrated in Figure 3.4 of Section 3.3 [39-43, 148]. Nevertheless, upper limb joint range of motion is not consistent on other planes of motion and for other limb configurations. For instance, joint range of motion for shoulder abduction-adduction with the limb fully extended at 0 degrees of shoulder flexion, ranges from around 0-184 degrees (see Table 4.3), whereas shoulder abduction-adduction with the limb fully extended at 90-degrees of shoulder flexion corresponds to a joint range of motion from around -45 degrees of adduction to -90 degrees of abduction. The lack of information on human joint coupling for all possible limb configurations complicate the development of accurate human motion models.

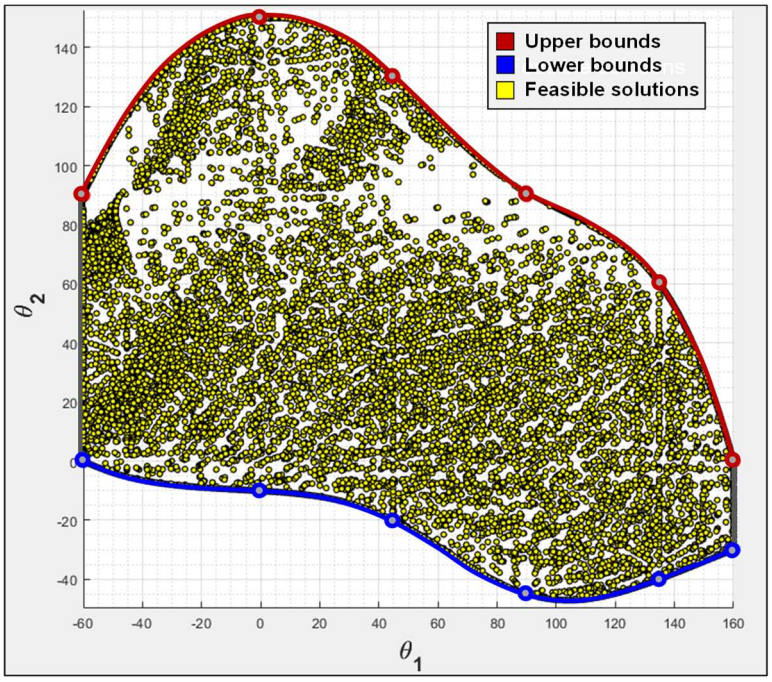

Figure 4.6. Shoulder abduction-adduction (θ_2) joint range of motion boundaries in function of shoulder flexion-extension (θ_1).

Therefore, as joint coupling data is lacking in literature and as these values were needed for upper limb workspace analysis, such range of motion values for each degree of freedom of the shoulder (3-DOFs) at various configurations were approximated by self-observation. Although such data cannot be considered as fully accurate because it was not systematically and experimentally measured, the values derived from self-

observation were a closer approach to establish a joint coupling relationship for the purpose of this study.

Likewise, these approximated values can already demonstrate the importance and applicability of such data for the improvement of upper limb models that can describe upper limb workspace, as well as more realistic limb movements. However, future work should focus on the study, definition, and accurate measure of joint range of motion in all configurations, and on establishing joint coupling relationships among each individual degree of freedom.

The joint coupling approximated values described above were used to obtain the corresponding polynomial equations that describe range of motion for each degree of freedom given the internal joint coupling (see Figure 4.6. and Figure 4.7.). This approach in combination with the statistical data presented in Table 4.3 was used to approximate the joint range of motion for each virtual individual.

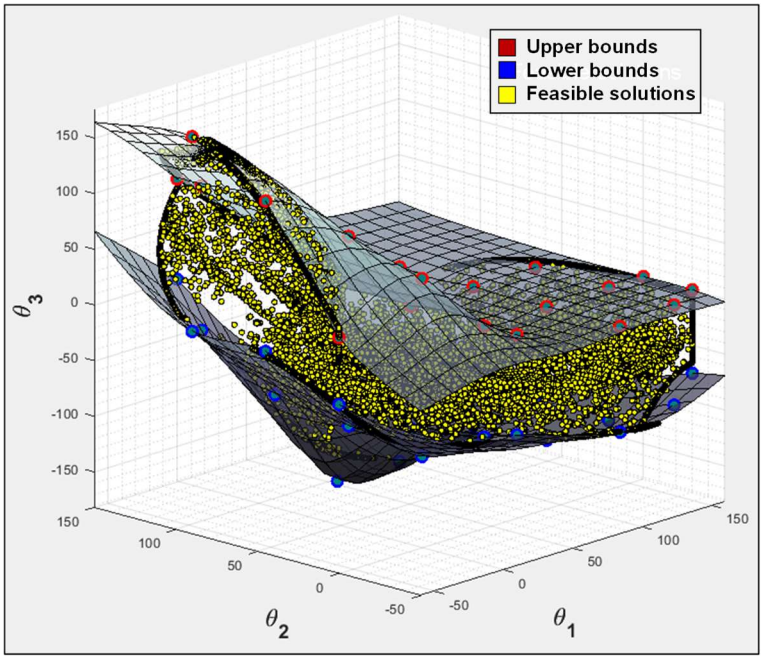

Figure 4.7. Shoulder internal-external rotation (θ_3) joint range of motion boundaries in function of shoulder flexion-extension (θ_1) and shoulder abduction-adduction (θ_2).

Table 4.4. Ranges on the X, Y, Z axes for the analysis and computation of workspace volume.

Parameter	*Variable*	*Value*
X range $(\boldsymbol{m})$	X	$-1.05(l_1 + l_2) \leq \boldsymbol{X} \leq 1.05(l_1 + l_2)$
Y range $(\boldsymbol{m})$	Y	$-1.05(l_1 + l_2) \leq \boldsymbol{Y} \leq 1.05(l_1 + l_2)$
Z range $(\boldsymbol{m})$	Z	$-1.05(l_1 + l_2) \leq \boldsymbol{Z} \leq 1.05(l_1 + l_2)$

The analysis was conducted by sampling over 5,000 points in a cubic volume 5% greater (in each direction) than the upper limb length (see Table 4.4). A Matlab algorithm was created and used to determine feasible upper limb configurations to reach each sampled point and only satisfactory reachable solutions were considered to compute workspace and manipulability.

Figure 4.8 and Figure 4.9 show the computed workspace volume for an individual with length values of $l_1 = 0.357m$ and $l_1 = 0.288m$, and with joint range of motion values of $-60° \leq \theta_1 \leq 160°$ for shoulder abduction-adduction, $-10° \leq \theta_2 \leq 150°$ for shoulder flexion-extension, -80° $\leq \theta_3 \leq$95° for shoulder internal-external rotation , $0.6° \leq \theta_4 \leq 143°$ for elbow flexion-extension. The calculated workspace volume for this individual was $v = 0.566m^2$.

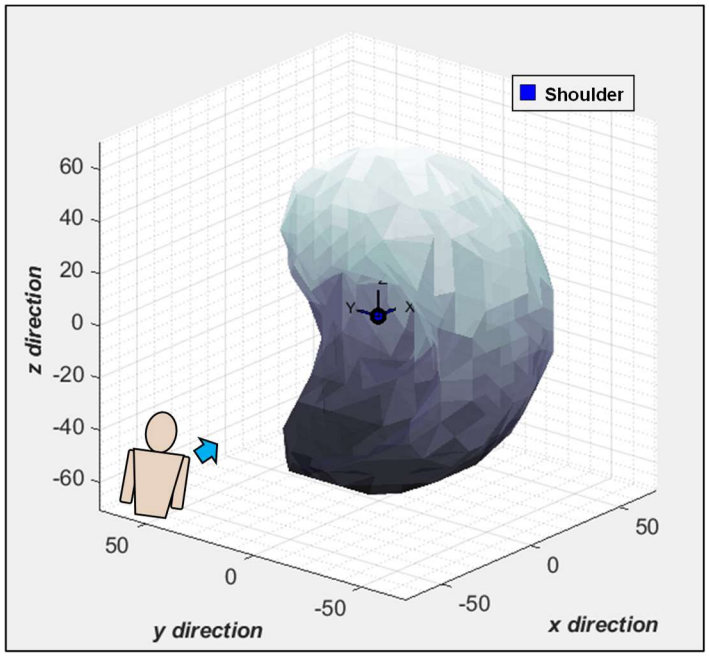

Figure 4.8. Workspace volume for an individual with input parameters: $l_1 = 0.357m$, $l_1 = 0.288m$, $\theta_{1L} = -60°$, $\theta_{1U} = 160°$ $\theta_{2L} = -10°$, $\theta_{2U} = 150°$, θ_{3L} =-80°, θ_{3U} =95°, $\theta_{4L} = 0.6°$, $\theta_{4U} = 143°$. [Shading only used to convey 3-D workspace volume].

As can be seen in Figure 4.8 and Figure 4.9, the workspace volume seems to be formed of shapes similar to the corresponding reach envelope area shapes obtained in the 2-dimensional analysis on the horizontal plane (see Section 4.2).

According to the results, for right upper limbs, the reachability appears to be greater for movements to the front and right side, whereas the reachability seems to decrease when trying to reach far to the left or backwards (see Figure 4.9).

Moreover, the upper limb end-effector (the wrist in this case) cannot reach the centre of the shoulder, this phenomenon is consistent with the results obtained in the 2-dimensional analysis in the previous section.

Likewise, backwards upper limb reachability appears to be quite constrained, it was somehow expected as the limb is near to various joint range of motion boundaries.

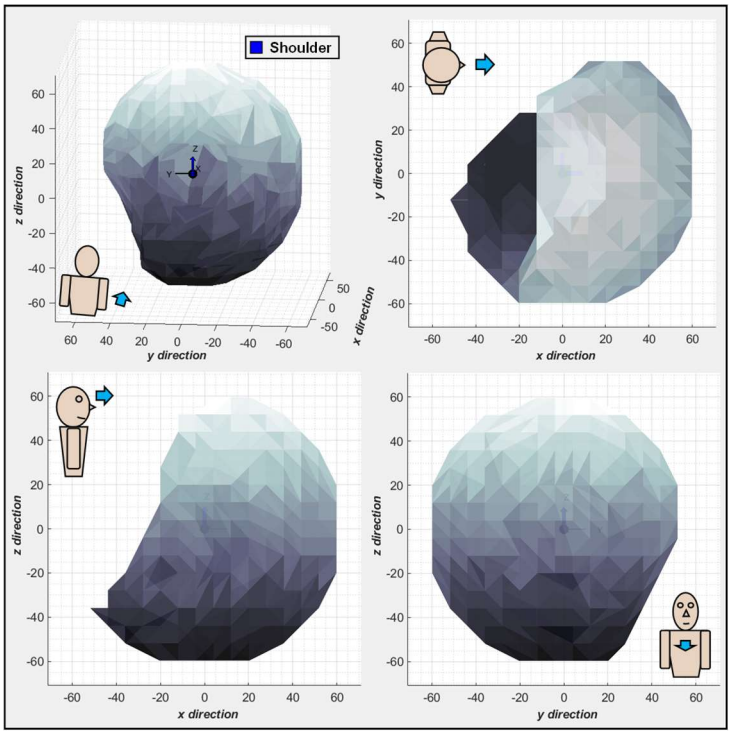

Figure 4.9. Workspace volume for an individual with input parameters: $l_1 = 0.357m$, $l_1 = 0.288m$, $\theta_{1L} = -60°$, $\theta_{1U} = 160°$ $\theta_{2L} = -10°$, $\theta_{2U} = 150°$, θ_{3L} =-80°, θ_{3U} =95°, $\theta_{4L} = 0.6°$, $\theta_{4U} = 143°$

The results presented in Figure 4.8 and Figure 4.9 are person-specific, however, the method presented in this section can be used for population analysis by using distributions based on statistical data for the input values. The following section presents a population-based example to conduct a workspace sensitivity analysis.

4.3.2 Workspace sensitivity analysis

The previous section introduced the methodology to determine upper limb workspace volume and provided a person-specific example. This section focuses on upper limb workspace sensitivity analysis. According to the properties of the model and the algorithms used for the computation of workspace volume, and based on Figure 4.10 and Figure 4.11, two methods were selected for the sensitivity analysis: the Elementary Effects (EE) screening method and a gaussian regression method using the Gaussian Emulator Machine (GEM).

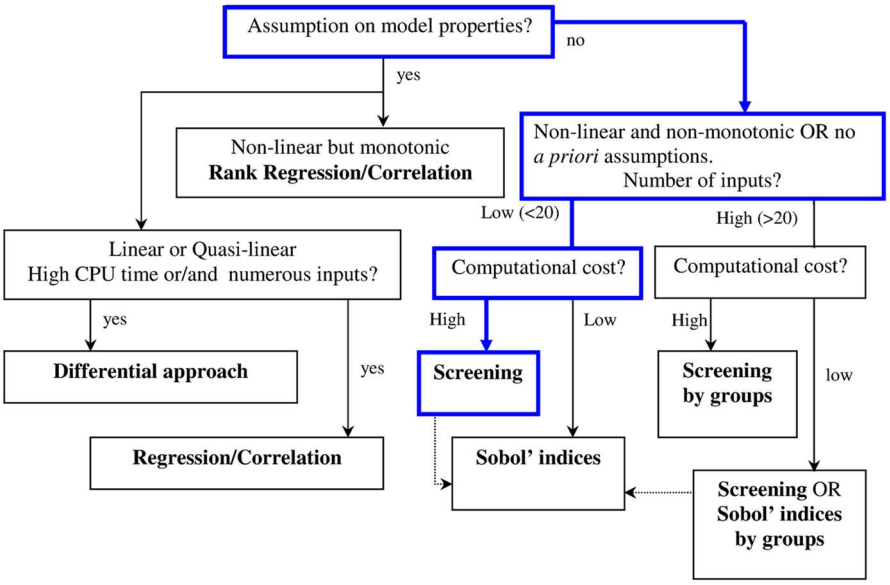

Figure 4.10. Decision tree to choose an appropriate sensitivity analysis method (meta-models can also be used with any method in the case of high computational cost). Copyright © 2008, John Wiley & Sons [13].

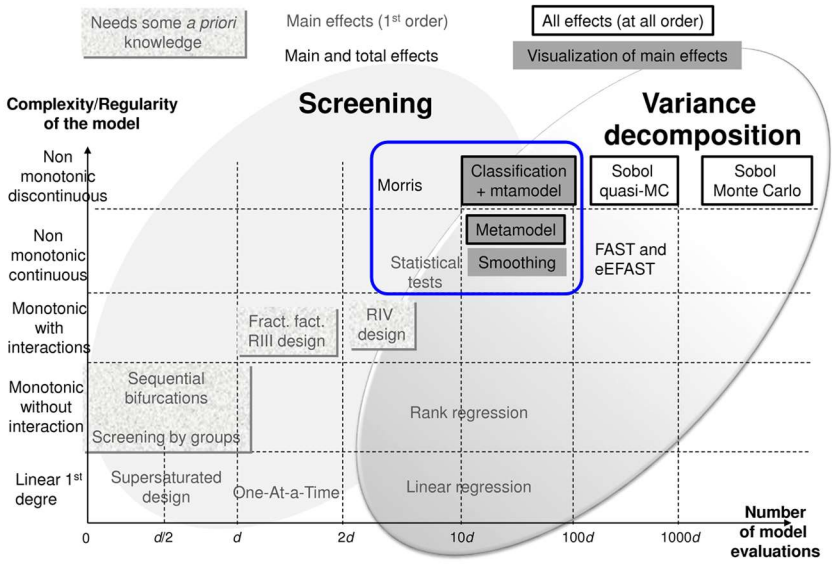

Figure 4.11. Graphical synthesis of sensitivity analysis methods. Copyright © 2015, Springer[14].

[13] Republished with permission of John Wiley & Sons, from "Uncertainty in industrial practice; a guide to quantitative uncertainty management", Rocquigny, E. et al., 2008; permission conveyed through Copyright Clearance Center, Inc.

[14] Republished with permission of Springer, from "Uncertainty in industrial practice; a guide to quantitative uncertainty management", Iooss, B.; Lemaître, P., 2015; permission conveyed through Copyright Clearance Center, Inc.

Figure 4.12. shows the methodology used to conduct the sensitivity analysis for workspace volume. The first step was to obtain mean and standard deviation values (from Table 4.2 and Table 4.3) for each of the inputs, which were used to create normal distributions. Next, Latin Hypercube (LH) and Fractional Factorial (FF) techniques were employed to sample the inputs accordingly to compute the corresponding sensitivity index. Finally, the computed index reflects how sensitive the model is to variations in the inputs.

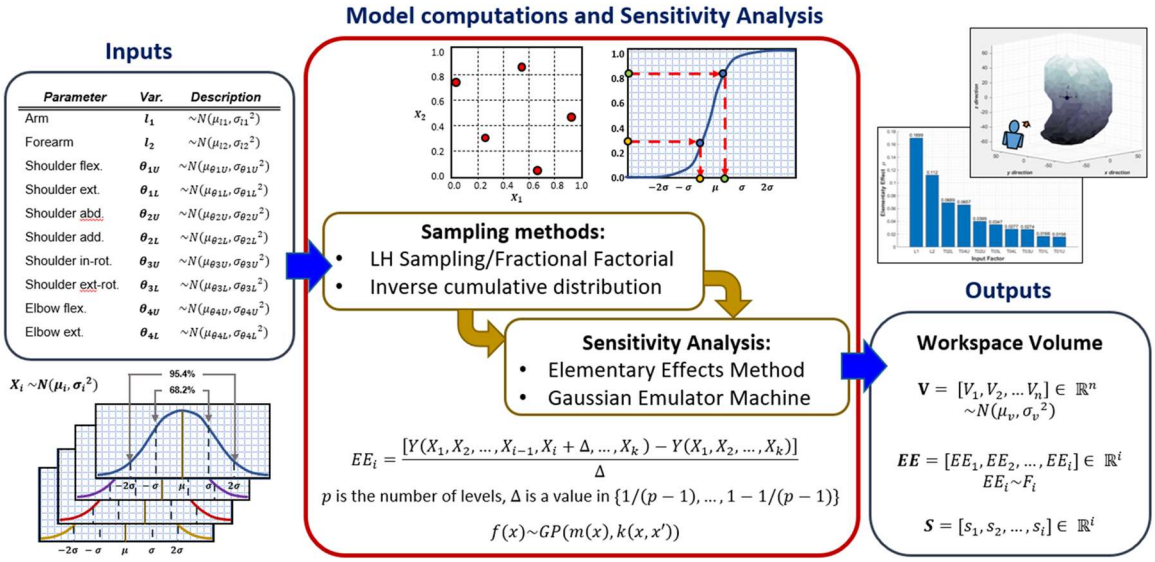

Figure 4.12. Graphical description of the methodology used to conduct sensitivity analysis for the workspace investigation.

Table 4.5. Sensitivity analysis measures for both Elementary Effects and Gaussian Emulator methods.

Input Factor	*Variable*	*Elementary Effect*	*Effect – Gaussian Emulator*
Upper arm	l_1	0.1431	59.20
Forearm	l_2	0.0895	29.90
Shoulder adduction	θ_{2L}	0.0802	12.04
Shoulder abduction	θ_{2U}	0.0389	0.31
Shoulder external rotation	θ_{3U}	0.0337	1.37
Elbow flexion	θ_{4U}	0.0331	1.75
Elbow extension	θ_{4L}	0.0330	1.32
Shoulder extension	θ_{1L}	0.0278	1.37
Shoulder internal rotation	θ_{3L}	0.0253	0.01
Shoulder flexion	θ_{1U}	0.0142	0.67

The results obtained from the sensitivity analysis are presented in Table 4.5 and Figure 4.13. As can be seen in Figure 4.13, the results obtained from the Elementary Effects Method (EEM) and the Gaussian Emulator Machine (GEM) agree with each other for the identification of the 3 most influential factors: both $\boldsymbol{l_1}$ and $\boldsymbol{l_1}$ limb lengths and $\boldsymbol{\theta_{2L}}$ shoulder adduction. However, there is some discrepancy about the influence of the rest of the factors. For instance, the EEM indicates that the next influential factor is shoulder abduction, whereas the GEM reveals that the same factor is one of the least influential. Nevertheless, it is important to mention that the results could be affected by the simplifications and assumptions of the model and methods used to compute workspace volumes, as explained in the previous sections.

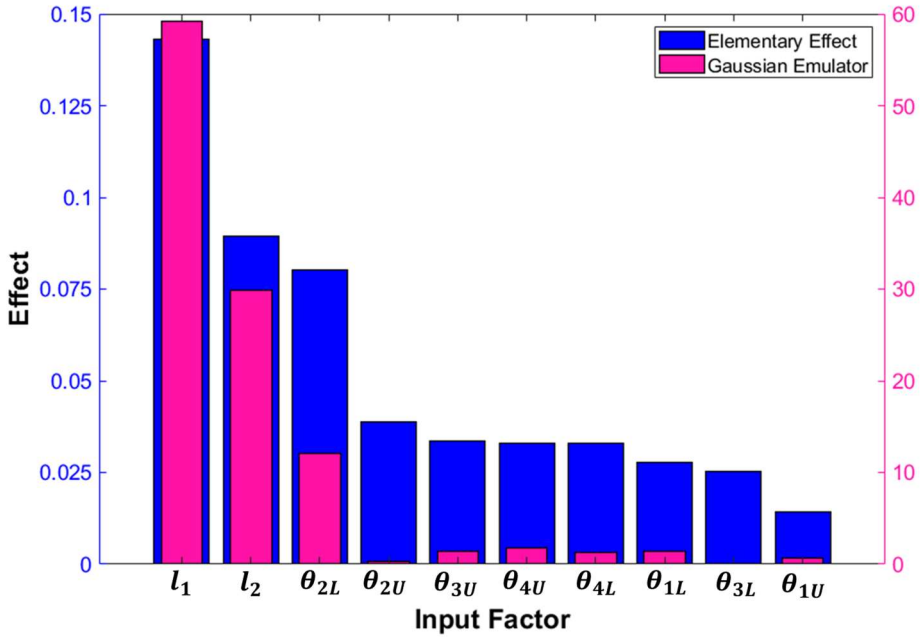

Figure 4.13. Sensitivity analysis measures for both Elementary Effects and Gaussian Emulator methods.

The effect of limb segment length variability is important for the prediction of population workspace volume. However, for person-specific clinical analysis, segment lengths will not change in most cases, therefore, joint range of motion factors become the relevant source of uncertainty for workspace analysis. Thus, shoulder adduction seems to be the most influential factor, which according to the results, is at least twice as influential as other joints.

4.3.3 Summary

The work presented in this section focused on the 3-dimensional exploration of upper limb workspace including a sensitivity analysis for upper limb workspace volume. Thus,

this chapter introduced and demonstrated the use of a method for the computation of reach envelop areas and workspace volumes.

As has been already mentioned in Section 2.3.5, studying and quantifying upper limb workspace is relevant in for the investigation of human-machine interactions, the development of rehabilitation devices, the design of assistive devices such as exoskeletons, and in ergonomics [16-20]. However, the use of workspace volumes for the evaluation of upper limb dexterity and functionality is not common in clinical analysis; although a few researchers have already attempted to introduce the use of workspace as a technique to assess the extremity [21-23, 150, 151]. Therefore, this chapter introduces and proposes a method to compute workspace volumes that provide numerical and visual information about upper limb reachability, which can be used as a reference for the evaluation of upper limb dexterity and functionality, for comparison and optimisation purposes, and for the development ergonomic and functional devices. Workspace volumes can be used as the base for the characterisation of upper limb dexterity as workspace volumes can be thought as the mapping of the extremity 3-dimensional reachable space. Therefore, dexterity measures and regions of high-low dexterity can be computed and described in terms of workspace volumes (introduced and defined in Section 5.7 and demonstrated in Chapter 7). The visual information provided by the workspace volume can be used to determine if an individual is able to reach a certain region of the space. This information is relevant as some techniques that evaluate upper limb functionality only focus on a particular region in front of the participant; however, a participant that performs well in such tests could potentially be limited in other non-evaluated regions of space. Therefore, computing the workspace volume and using it as a map can help to assign scores for the functionality of the limb across the 3-dimnsional reachable space. Moreover, the model proposed in this section can be used to characterise and predict workspace volumes for real and virtual people; however, further computational, and experimental analysis is needed in order to validate the model and the methods presented here.

One of the challenges for the creation of the computational model to compute workspace volumes was that some of the information needed for the model, such as joint coupling and joint range of motion at different configurations of the limb, is lacking in literature. Therefore, such joint coupling data to impose the upper and lower joint range of motion boundaries for all the analysed virtual participants was approximated. Therefore, future work should focus on providing joint coupling normative data.

Moreover, the sequence of joint displacements was arbitrarily imposed to simplify the model as the system is redundant and there are many rotation sequences that can get to

the same end-effector (wrist) position in cartesian space. Such simplifications and assumptions could have affected the accuracy of the results. Hence, future model versions should be more flexible and allow some level of redundancy for the model and the algorithms to find other possible solutions. It is also important to mention that the computed workspace volume corresponds to a right limb, although it can be slightly modified to evaluate a left limb. However, the shapes of the workspace volumes of the right and left extremities are expected to be mirrored and slightly different due to intra-individual variability derived from body asymmetry. The study and comparison of workspace volume for right and left limbs seems to be lacking in literature. Therefore, future work is needed in this area.

According to the results obtained from the sensitivity analysis, upper limb segment lengths and shoulder adduction are highly influential on workspace volume. Although segment length variations are relevant for the prediction workspace volumes, people joint range of motion is more likely to present variations over time due to aging, diseases, injuries, and surgeries. Therefore, more attention should be paid to shoulder adduction as according to the sensitivity analysis it is the most influential factor, which is at least twice as influential as other joints. This was also noticed in the computational analysis; reductions in shoulder adduction resulted in a significant decrease of reachability to the front-left side of the limb. This is an interesting finding that should be explored in more detail. Likewise, future work should focus on providing joint range of motion normative data including shoulder adduction range of motion for all limb configurations.

5 A NOVEL METHOD FOR THE CHARACTERISATION OF WORKSPACE WITH RESPECT TO DEXTERITY

The previous chapters gave a description of the general method for human motion modelling and studied anthropometrics, reach envelope area and workspace. Thus, providing the knowledge to create an upper limb model to describe motion in both joint and cartesian spaces and to define upper limb reachability. However, the aim of this research project is to characterise upper limb workspace with respect to dexterity. As previously defined, dexterity can be described as a motor ability to execute precise movement with a determined purpose [1]. A similar ability for robotic arms and manipulators is called "manipulability", which can be described as ease of changing the position and orientation of the end-effector of a manipulator [11, 12]. Thus, dexterity and manipulability can be said to be equal abilities. Yoshikawa [11, 12] proposed a method for the characterisation of manipulability. Although this method has been widely used in robotics [11, 12, 24-27], it has not been used much for the study of human upper limb motion. The few authors that have previously used the manipulability analysis method for human upper limb motion have used it for the study of a user-friendly rehabilitation system [13], the analysis of wheelchair propulsion [14], and for the investigation of the upper-limb during grasping [15]. Therefore, as dexterity and manipulability can be said to be equal abilities, this author proposes the use of the manipulability analysis method as a base to characterise human upper limb dexterity. The novel method proposed in this chapter, the "Dexterity Analysis Method" (DAM), is a modified version of the manipulability analysis by the incorporation of human factors in a new variable called "comfort". This comfort variable is used to penalise manipulability, and such penalised manipulability is called here "dexterity measure". Finally, it is important to clarify that upper limb reachable regions are not necessarily regions where the upper limb has high dexterity; having high dexterity can be understood as being able perform precise movements that require to translate and orientate the end-effector (in this case the wrist) of the limb.

5.1 Manipulability analysis method

This section of the chapter introduces the manipulability analysis method proposed by Yoshikawa [11, 12] including the computation of the manipulability measure and the corresponding ellipsoids.

First of all, the position and orientation of each element of a manipulator with "n" degrees of freedom can be described in joint space by a vector $q = [q_1, q_2, \cdots, q_n]^T$ where q_n represents the joint angle of the "n-th" degree of freedom. Likewise, the

position and orientation of the end-effector of a manipulator can be described in cartesian space by an m-dimensional vector $r = [r_1, r_2, \cdots, r_m]^T$. Similarly, the velocities of the manipulator, in both joint and cartesian space, can be acquired by deriving their corresponding position with respect to time.

The relationship of the velocities in joint and cartesian space is not linear, however, a transformation matrix can be used to map joint angular velocities into cartesian space (linearization). The $J(q)$ transformation matrix used for such linearization is called the Jacobian matrix:

$$\dot{r} = J(q)\dot{q}$$

Equation 5.1

where $\dot{r}$ is a vector containing velocity in cartesian space, and $\dot{q}$ is a vector describing velocity in joint space. The Jacobian matrix is written as J hereafter for simplicity.

Consequently, the manipulability measure w for a given manipulator configuration has the following properties [12]:

i. The manipulability measure w is given by

$$w = \sqrt{\det J J^T}$$

Equation 5.2

ii. When $m = n$, w reduces to

$$w = |detJ|$$

Equation 5.3

iii. Generally, $w \geq 0$ holds, and $w = 0$ if and only if $rankJ(q) < m$ (if the manipulator is in a singular configuration)

iv. When $m = n$, the set of all v realisable by a joint velocity $\dot{q}$ where

$$|\dot{q}| \leq 1, \quad i = 1,2, \dots, m$$

Equation 5.4

is a parallelepiped in m-dimensional space with a volume of $2^m w$ [12].

Moreover, manipulability ellipsoids can be derived from the Jacobian matrix by using singular value decomposition (SVD), which is denoted by:

$$J = U\Sigma V^T$$

Equation 5.5

where U and V are $m \times m$ and $n \times n$ orthogonal matrices, and Σ is a diagonal matrix containing the singular values $\sigma_1, \sigma_2, \cdots, \sigma_m$ of the Jacobian matrix J.

$$\Sigma = \begin{bmatrix} \sigma_1 & 0 & 0 & 0 \\ 0 & \sigma_2 & 0 & 0 \\ 0 & 0 & \ddots & 0 \\ 0 & 0 & 0 & \sigma_m \end{bmatrix}, \sigma_1 \geq \sigma_2 \geq \cdots \geq \sigma_m \geq 0$$

Equation 5.6

Furthermore, the u_i columns of the U vector multiplied by the corresponding singular value $u_1\sigma_1, u_2\sigma_2, \cdots, u_m\sigma_m$ provide the values of the principal axes of the manipulability ellipsoids [12] (see Figure 5.1), where the major axis of the ellipsoid represent the direction in which the end-effector of the manipulator can move easier and at higher speeds [12].

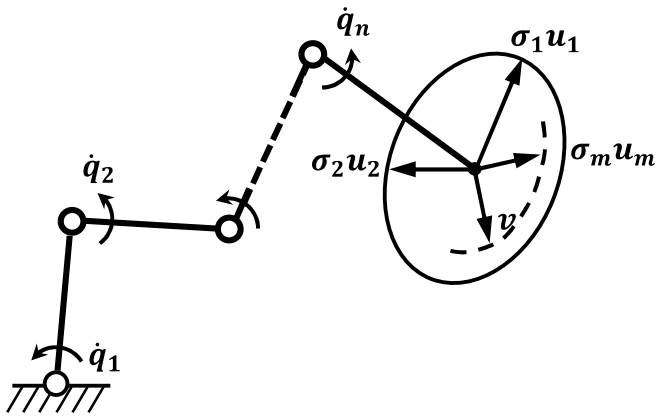

Figure 5.1. Manipulability ellipsoid. Copyright © 2003, MIT Press[15]

The manipulability measure and the corresponding manipulability ellipsoids take into consideration the individual contributions of each joint to the overall manipulator motion at the end-effector. The measure by itself can be used to determine the ease of motion of the end-effector at a given configuration, whereas the main axis of the manipulability ellipsoid describes the specific direction for such ease of motion. Although the use of this method was originally proposed for the characterisation of robotic arm manipulability, the physical characteristics of a robotic arm and a human limb, for the study of movement as kinematic chain systems, are equivalent. Thus, the manipulability measure and the manipulability ellipsoids consider the individual contributions of upper limb joints to execute movement. Therefore, it is assumed that the measure and the ellipsoids are

[15] Republished with permission of MIT Press, from "*Foundations of robotics: analysis and control [electronic resource]*", Yoshikawa, T., 2003.

intrinsically accounting for the contributions of each joint to upper limb dexterity. It is important to mention that joint contributions are initially considered to be equal, however, the model can be modified to adjust the weights of joint contributions, which might be worth considering in future work.

5.2 Manipulability analysis of a 2-link manipulator with 2-DOFs

This section focuses on the analysis of a 2-link manipulator with 2-DOFs to demonstrate how to apply the manipulability analysis method and to validate that the method has been correctly used by comparing the results to previously published studies.

The kinematic representation of the 2-link manipulator with segment length values of $l_1 = l_2 = 1$ is presented in Figure 5.2. The analysis was conducted on the x, y plane and the joints were assumed to have no range of motion constraints (can rotate 360 degrees).

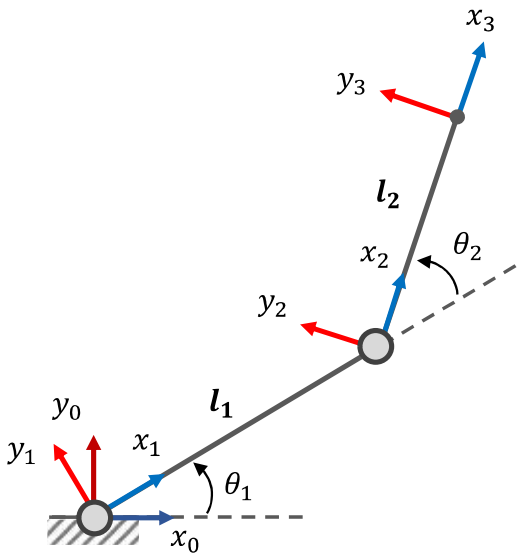

Figure 5.2. Two-link mechanism with 2-DOFs and equal segment lengths $\boldsymbol{l_1 = l_2 = 1}$.

The homogeneous matrix that describes the r position and orientation of the end-effector in cartesian space in function of the q angular joint positions is denoted by:

$$A = \begin{pmatrix} c_{12} & -s_{12} & 0 & l_2c_{12} + l_1c_1 \\ s_{12} & c_{12} & 0 & l_2s_{12} + l_1s_1 \\ 0 & 0 & 1 & 0 \\ 0 & 0 & 0 & 1 \end{pmatrix}$$

Equation 5.7

where $s_1 = \sin(q_1),\ s_{12} = \sin(q_1 + q_2),\ c_1 = \cos(q_1),\ \ c_{12} = \cos(q_1 + q_2)$

The linear and angular velocities of the end-effector (using velocity propagation from link to link) are described by:

$$\omega_3 = \begin{pmatrix} 0 \\ 0 \\ \dot{q}_1 + \dot{q}_2 \end{pmatrix}$$

Equation 5.8

$$v_3 = \begin{pmatrix} l_1 \dot{q}_1 \sin(q_2) \\ l_2(\dot{q}_1 + \dot{q}_2) + l_1 \dot{q}_1 \cos(q_2) \\ 0 \end{pmatrix}$$

Equation 5.9

where v_3 and ω_3 represent the linear and angular velocities of the end-effector, $\dot{q}_1$ and $\dot{q}_2$ represent the angular velocities of links 1 and 2 respectively, and l_1 and l_2 are the lengths of links 1 and 2.

Thus, the Jacobian matrix J was formed by obtaining the partial derivatives of Equation 5.9:

$$J = \begin{pmatrix} l_1 \sin(q_2) & 0 \\ l_2 + l_1 \cos(q_2) & l_2 \end{pmatrix}$$

Equation 5.10

Once the Jacobian matrix was obtained, the manipulator was assessed by sampling 8 equally spaced points along the x axis within the range $0 \leq x \leq (l_2 + l_2)$ (see Figure 5.3).

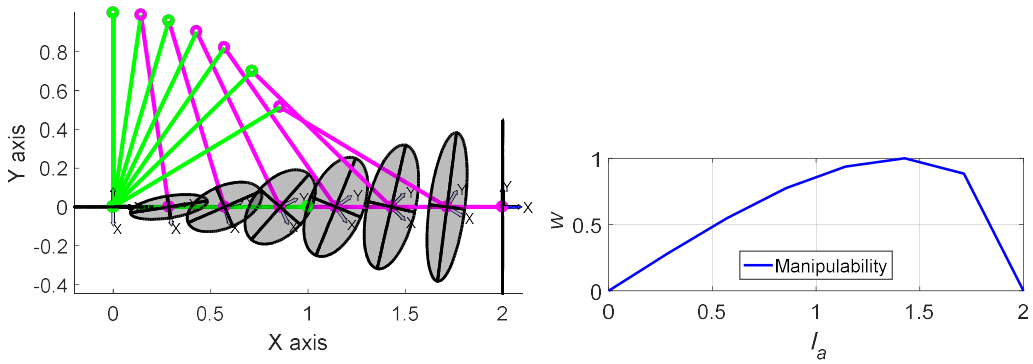

Figure 5.3. Manipulability ellipsoids of a 2-link mechanism for the execution of a linear trajectory from $x = 0$ to $x = l_1 + l_2 = 2$ (left), and Manipulability measure in function of displacement on the x axis l_a (right).

A MATLAB algorithm was created and used to determine the q angles that satisfy the task and to compute the manipulability measure (using Equation 5.3) for each sampled point (see Figure 5.3). Moreover, Equation 5.5 and Equation 5.6 were used to obtain the corresponding manipulability ellipsoids at the 8 different configurations along the task (see Figure 5.3, left).

The results show that the maximum manipulability was achieved when the end-effector was at around 1.4 on the x axis (see Figure 5.3). Conversely, the manipulability measure at $x = 0$ and $x = 2$ decreases to 0, which represents that the manipulator is in a singular configuration or that the manipulator has lost a DOF.

The manipulability measure and the corresponding manipulability ellipsoids obtained in the analysis appear to agree with the results published by Yoshikawa [12] (see Figure 5.3 and Figure 5.4), which confirms that the method has been correctly applied for the analysis presented in this section.

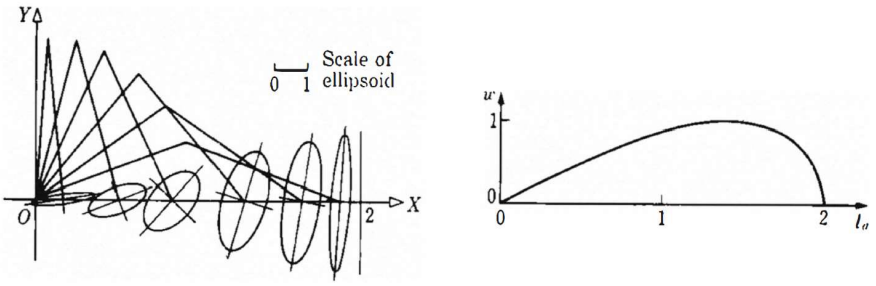

Figure 5.4. Manipulability ellipsoids and manipulability measure of a two-link mechanism. Copyright © 2003, MIT Press [16].

5.3 Manipulability on the plane (2-D analysis)

Having established the manipulability method for a 2-link kinematic chain this section focuses on developing the model in order to identify optimal areas for the execution of a given tasks on the x, y plane (see Figure 5.5).

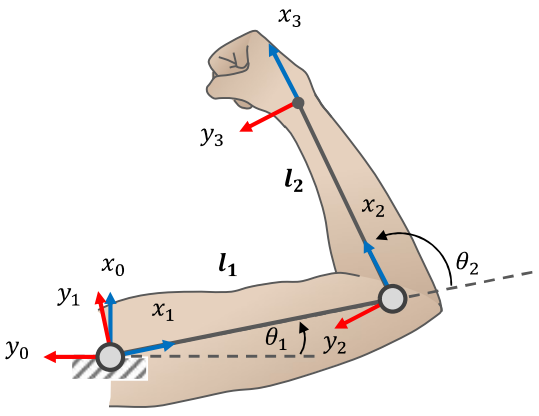

Figure 5.5. 2-link kinematic representation of the human upper limb.

[16] Republished with permission of MIT Press, from "*Foundations of robotics: analysis and control [electronic resource]*", Yoshikawa, T., 2003.

Initially the joints are assumed to have no ROM constraints (joints can rotate 360 degrees). In order to analyse how the size of the upper limb affects manipulability, 3 upper limb sizes (based on British male statistic data) were assessed: small, medium and large (see Table 5.1).

Table 5.1. British male upper limb lengths used for the study of manipulability during the execution of linear and circular trajectories [146]

Parameter	*Variable*	*Limb 1 (small)*	*Limb 2 (medium)*	*Limb 3 (large)*
Upper Arm $(\boldsymbol{m})$	l_1	$\mu_1 - 3\sigma_1 = 0.282$	$\mu_1 = 0.357$	$\mu_1 + 3\sigma_1 = 0.432$
Forearm $(\boldsymbol{m})$	l_2	$\mu_2 - 3\sigma_2 = 0.246$	$\mu_2 = 0.288$	$\mu_2 + 3\sigma_2 = 0.330$

The tasks selected for the analysis presented in this section were to execute linear and circular trajectories at different distances from the shoulder. Circular and linear trajectories were selected as everyday tasks and trajectories are often composed of this basic shapes. Moreover, it is known that the human upper limb tends to split other tasks into straight linear trajectories during the execution of tasks [35, 74, 75]. Therefore, the tasks evaluated in the analysis presented in this section were the following tasks:

i. Linear trajectories: a total of 11 equally spaced linear trajectories (lines of 1.4m of length) parallel to the y axis on the range $-0.70m \leq X \leq 0.70$.

ii. Circular trajectories: 0.20m and 0.30m diameter circular trajectories with origins in 3 different positions on the x axis.

iii. Full reach envelope area: upper limb manipulability analysis for full reach envelope area by sampling 10,000 points (evenly spaced) on the range $-0.70m \leq X \leq 0.70m$ and $-0.70m \leq Y \leq 0.70m$.

The manipulability analysis presented in this section was conducted using the methods presented in Sections 3 and 5.1.

5.3.1 Manipulability analysis for the execution of linear trajectories

This section presents the results of the manipulability analysis of the upper limb during the execution of linear trajectories as explained at the beginning of this section (Section 5.3). Figure 5.6 shows the computed manipulability measure (only 6 trajectories as the rest are symmetrical). As can be seen in Figure 5.6, the maximum manipulability value (0.87) for a linear trajectory on $x = 0.56m$ is found at about $y = 0.0m$, whereas, the maximum manipulability value (around 1.00) for a linear trajectory at $x = 0.42m$ occurs on the range $-0.25m \leq Y \leq 0.25m$. Although, the mean manipulability values appear to

be similar for some of the trajectories, the locations where the maximum values occur are different. Likewise, the manipulability values for some trajectories seem to have high variability.

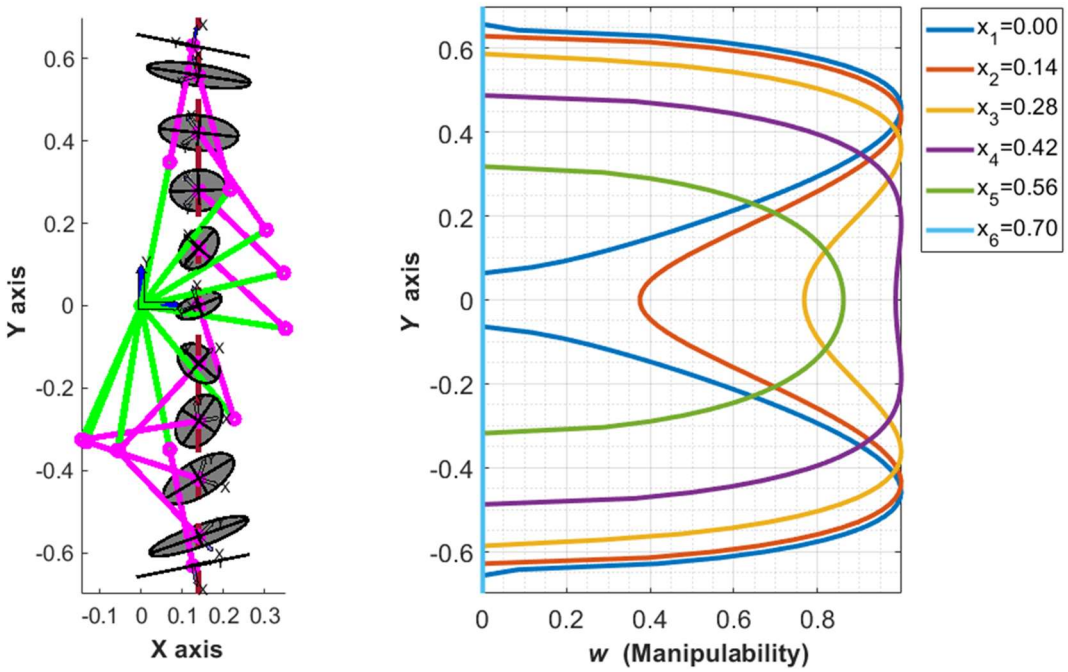

Figure 5.6. Manipulability ellipsoids for a linear trajectory at $x = 0.14$ (right) and manipulability measure for the first 6 linear trajectories parallel to the y axis (left).

Figure 5.6 (left) shows the manipulability ellipsoids for one of the linear trajectories ($x = 0.14m$). As can be seen, the shape of the manipulability ellipsoids gets completely flat when the limb is in a singular configuration, which occurs at the extremes of the trajectory.

Conversely, the shape of the manipulability ellipsoids gain area in positions where the limb has higher manipulability. According to the results, for a linear trajectory at $x = 0.14m$, the ellipsoids have a greater area at $y = -0.42m$ and $y = 0.42m$, which agree with the computed manipulability measure (see Figure 5.6, right).

Another aspect that can affect manipulability is the size of the limb. Therefore, 3 upper limb sizes were evaluated (see Table 5.1) during the execution of a linear trajectory (1.4m linear trajectory) fixed at $x = 0.14m$. The computed manipulability measure and the manipulability ellipsoids for the corresponding limbs are presented in Figure 5.7. As can be seen both the ellipsoid shapes and the manipulability values were directly affected by the size of the limbs. The manipulability measure for Limb 1 and Limb 2 decreased to 0 at the extremes of the linear trajectory as such limbs were not able to complete the task due to limb length constraints.

Conversely, the Limb 3 was able to complete the task and the manipulability measure never decreased below 0.15.

Therefore, a person with a limb with length values similar to Limb 3 is expected to complete the task and have higher performance than people with limb sizes similar to Limb 1 and 2. An interesting observation is that the main axes of the manipulability ellipsoids pointed in very similar directions for the 3 limb sizes evaluated in the analysis (see Figure 5.7).

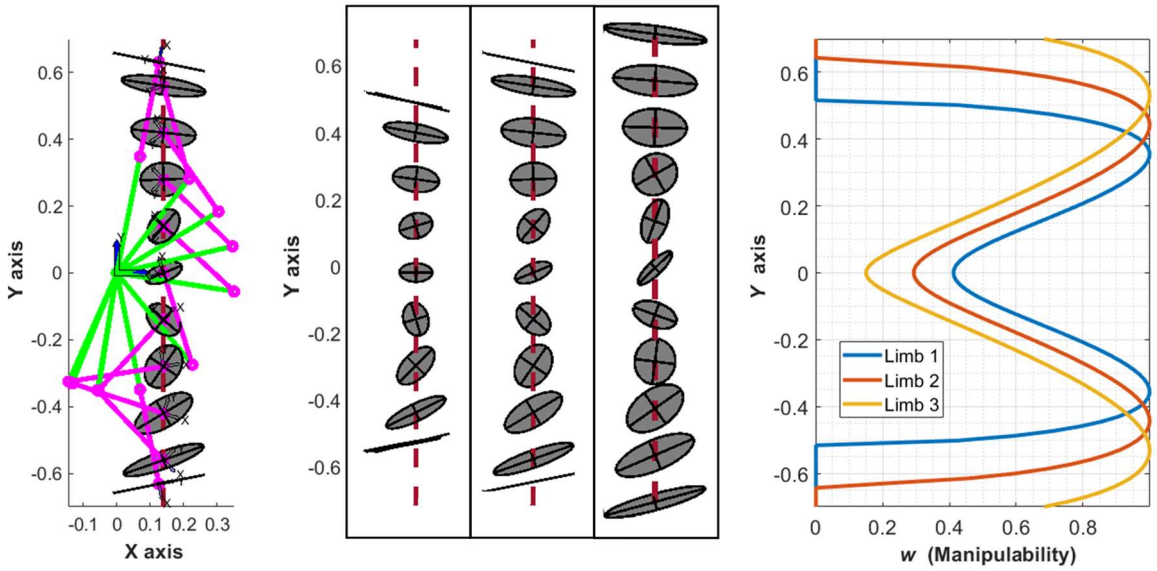

Figure 5.7. Manipulability measure and ellipsoids during the execution of a linear trajectory on x=0.14. Left: manipulability ellipsoids for Limb 2. Middle: manipulability ellipsoids for Limbs 1, 2, and 3 (left to right). Right: manipulability measure.

Thus, the results suggest that at least for linear trajectories, both position of the task and limb size affect the performance of the upper extremity.

5.3.2 Manipulability analysis for the execution of circular trajectories

This section presents the results of the manipulability analysis of the upper limb during the execution of circular trajectories as explained at the beginning of this section (Section 5.3).

Figure 5.9 and Figure 5.8 present the manipulability values and the manipulability ellipsoids along the task for the circular trajetories in the 3 different positions. As can be observed, the circular trajectory with origin $o_3(0.4,0.0)$ has the highest mean manipulability value and exhibit less variability $(0.81 \leq w \leq 1.00)$, whereas, the manipulability values for a circle with origin $o_1(0.2,0.0)$ has the highest variablity $(0.23 \leq w \leq 0.81)$ and reached a maximum manipulability value of around 0.83.

Similarly, the manipulability ellipsoids for a circular trajectory with origin $o_3(0.4,0.0)$ were larger than those for circles with origins $o_1(0.2,0.0)$ and $o_2(0.3,0.0)$ (see Figure 5.9).

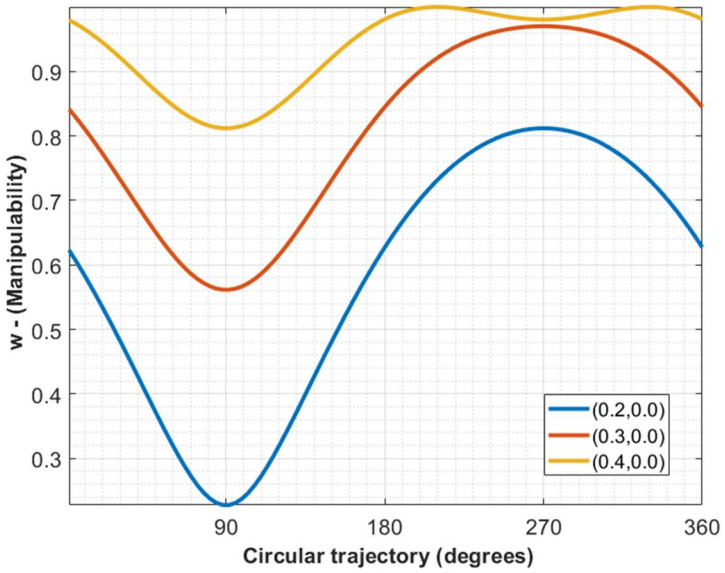

Figure 5.8. Upper limb manipulability measure during the execution of circular trajectories (0.2m-diameter) with origins on $o_1(0.2, 0.0)$, $o_2(0.3, 0.0)$ and $o_1(0.4, 0.0)$.

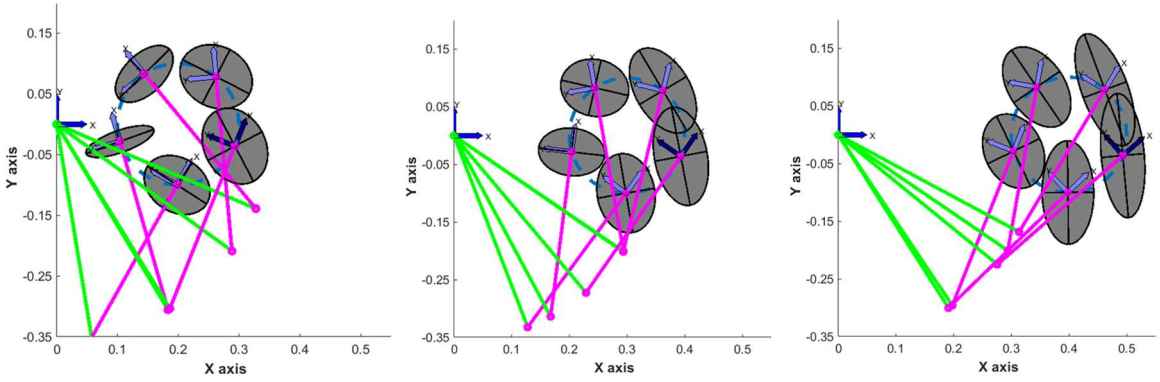

Figure 5.9. Upper limb manipulability ellipsoids during the execution of circular (0.2m-diameter) with origins $o_1(0.2, 0.0)$, $o_2(0.3, 0.0)$ and $o_1(0.4, 0.0)$.

As in the previous section, manipulability was assessed for 3 upper limb sizes (see Table 5.1) during the execution of a fixed circular trajectory (0.30m-diameter circular trajectory) with the origin fixed at $x = 0.30m$ and $y = 0.00m$. The computed manipulability measure and the manipulability ellipsoids for the corresponding limbs are presented in Figure 5.10 and Figure 5.11.

As can be noticed both the ellipsoid shapes and the manipulability values were directly affected by the size of the limbs. In this case, the larger limb (Limb 3) showed the highest variability for manipulability $(0.29 \leq w \leq 0.95)$ and had a maximum value of 0.95, whereas the mean manipulability values for Limb 1 were higher and had les variability $(0.53 \leq w \leq 1.00)$.

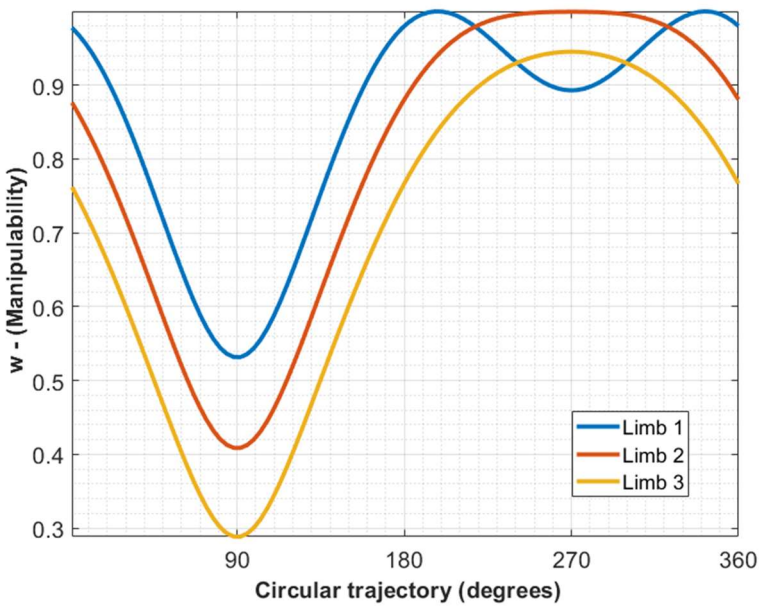

Figure 5.10. Upper limb manipulability measure for 3 limb sizes during the execution of circular trajectories (0.3m-diametre) with origin $o(0.3, 0.0)$.

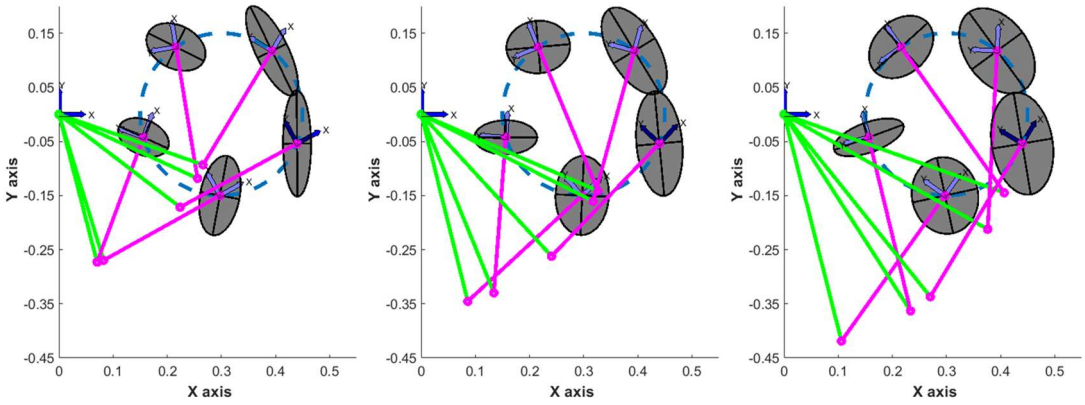

Figure 5.11. Upper limb manipulability ellipsoids for 3 limb sizes during the execution of circular trajectories (0.3m-diametre) with origin $o(0.3, 0.0)$. Limbs 1, 2 and 3 correspondingly (left to right).

Conversely, the shapes of the ellipsoids for Limb 3 were larger and more rounded than those for limbs 1 and 2 (see Figure 5.11).

However, it is important to mention that the ellipsoids by themselves do not provide the full picture of the potential performance. Although, the ellipsoids for Limb 3 are larger in comparison to the corresponding ellipsoids for the other 2 limbs, the corresponding measure for Limb 3 indicates that the full achievable manipulability was never achieved during the execution of the task. Therefore, comparing only the size of the ellipsoids to other limbs without considering the corresponding manipulability measure is not objective and should be avoided.

Finally, the upper limb manipulability analysis for the execution of circular trajectories in 3 different locations suggests that the position of the task affect manipulability. Likewise, the manipulability analysis for 3 limb sizes demonstrated that the limb size also affects manipulability. However, a large extremity does not necessarily have higher manipulability as its performance depends on the position of the task.

5.3.3 Full horizontal plane manipulability analysis

This section focuses on the investigation of manipulability on the $\boldsymbol{x}, \boldsymbol{y}$ plane in order to determine the areas of higher manipulability, therefore, higher dexterity. The analysis was conducted by sampling 40,000 points (evenly spaced) on the range $-\mathbf{0.70}\boldsymbol{m} \leq \boldsymbol{X} \leq \mathbf{0.70}\boldsymbol{m}$ and $-\mathbf{0.70}\boldsymbol{m} \leq \boldsymbol{Y} \leq \mathbf{0.70}\boldsymbol{m}$. The previous sections evaluated 3 limb sizes: small, medium, and large (see Table 5.1).

However, the upper arm and the forearm proportionality was not varied. Therefore, as the proportionality of upper limb segments may vary from person to person, this section explores both types of limbs, limbs with and without proportional upper limb segment lengths. Consequently, in this section 4 different limbs were assessed, the first 2 limbs represent medium and small size limbs with proportional segments, and the second 2 limbs represent limbs with variations in the proportions of the segments (see Table 5.2).

Table 5.2. British male upper limb lengths used for manipulability analysis on the x-y plane [146]

Parameter	*Variable*	*Limb 1*	*Limb 2*	*Limb 3*	*Limb 4*
Upper Arm $(\boldsymbol{m})$	l_1	$\mu_1 = 0.357$	$\mu_1 - 3\sigma_1 = 0.281$	$\mu_1 - \sigma_1 = 0.331$	$\mu_1 + \sigma_1 = 0.382$
Forearm $(\boldsymbol{m})$	l_2	$\mu_2 = 0.288$	$\mu_2 - 3\sigma_2 = 0.245$	$\mu_2 + \sigma_2 = 0.303$	$\mu_2 - \sigma_2 = 0.274$

The results of the analysis are presented in Figure 5.12. The areas in dark blue represent low manipulability, whereas areas in light yellow represent high manipulability values. As can be seen in Figure 5.12, limb segment lengths affect manipulability. For instance, Limb 1 has greater reachability, as well as a greater high manipulability region compared to Limb 2. However, it seems that at shorter distances Limb 2 has greater manipulability than Limb 1.

Similarly, Figure 5.12 (bottom) shows the manipulability measure for Limb 3 and Limb 4, which represent limbs with changes in the proportions of the segments. As can be seen, the manipulability of a limb with longer arm and shorter forearm (Limb 4) seems to be more affected than the manipulability of a limb with shorter arm and longer forearm (Limb 3). This observation suggests that changes in the proportions of the limb affect the

manipulability of the upper limb. Thus, people with same limb lengths but with different segment proportions are expected to obtain different manipulability values.

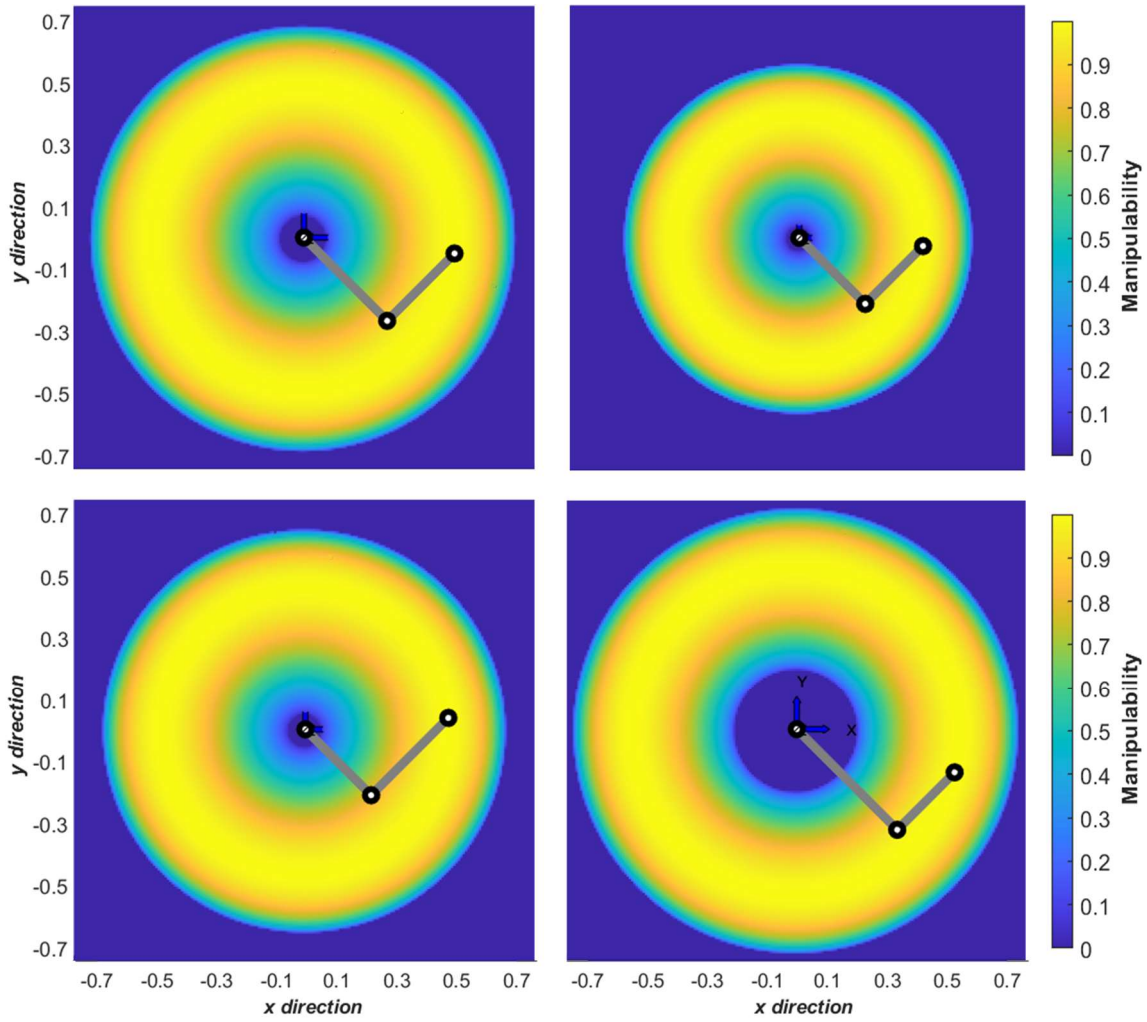

Figure 5.12. Low-high manipulability regions along the plane with ranges $-0.70m \leq X \leq 0.70m$ and $-0.70m \leq Y \leq 0.70m$. Top left: Limb 1; Top right: Limb 2; Bottom left: Limb 3; Bottom right: Limb 4. Blue and yellow represent low and high manipulability values correspondingly.

5.4 Manipulability analysis with respect to upper limb reach envelope area

The previous sections of this chapter explore manipulability without considering joint range of motion constraints. Therefore, in this section, the model is upgraded by incorporating joint range of motion constraints to determine upper limb manipulability within the corresponding reach envelope area. This is an important step in the analysis as the addition of ROM constraints to the model make it more realistic.

Table 5.3 show the shoulder and elbow range of motion values used in the analysis presented in this section. As in section 5.3.3, four different limb sizes (Table 5.2) were assessed by sampling 40,000 points (evenly spaced) on the range $-0.70m \leq X \leq 0.70m$ and $-0.70m \leq Y \leq 0.70m$.

Table 5.3. Shoulder and elbow joint range of motion [39]

Parameter	*Variable*	*Value*
Shoulder flexion	θ_{1U}	166.7
Shoulder extension	θ_{1L}	62.3
Elbow flexion	θ_{2U}	142.9
Elbow extension	θ_{2L}	0.6

Figure 5.13 illustrates the manipulability measure within the corresponding reach envelope area for the 4 limb sizes evaluated in the analysis. The low and high manipulability regions presented in Figure 5.13 are now smaller in comparison to the corresponding regions presented in Figure 5.12, this occurs due to the incorporation of joint ROM constraints to the model. Therefore, the low and high manipulability regions shown in the figures are now limited to the upper limb reach envelope area. The shapes of both reach envelope area and low and high manipulability regions have similar shapes, however, the shapes and regions shift from the shoulder according to the upper limb size and the segment length proportionality.

As can be seen Figure 5.13 (top), the upper limb reach envelope area and low and high manipulability regions proportionally increase or decrease depending on the limb size assuming the segment lengths also stay proportional. However, if the limb segments lose proportionality, as shown in Figure 5.13 (bottom), the upper limb reach envelope area, as well as the low and high manipulability regions get slightly deformed becoming thicker or thinner. As can be observed in Figure 5.13, the regions of high manipulability are in the middle sections of reach envelope area. However, high manipulability is obtained at some of the edges of reach envelope area. Consequently, the model may need to incorporate some sort of penalty to indicate that the limb is close to a limit and therefore the manipulability decreases.

The analysis presented in this section studied the effects of upper limb size and segment length proportionality on manipulability given a fixed range of motion (mean upper limb shoulder and elbow range of motion values British males). Such analysis does not include the study of variations in joint range of motion. However, Sections 4.2 investigates the

effects of variations in joint range of motion on reach envelope area, and Section 5.5 focuses on upper limb manipulability analysis and uncertainty propagation.

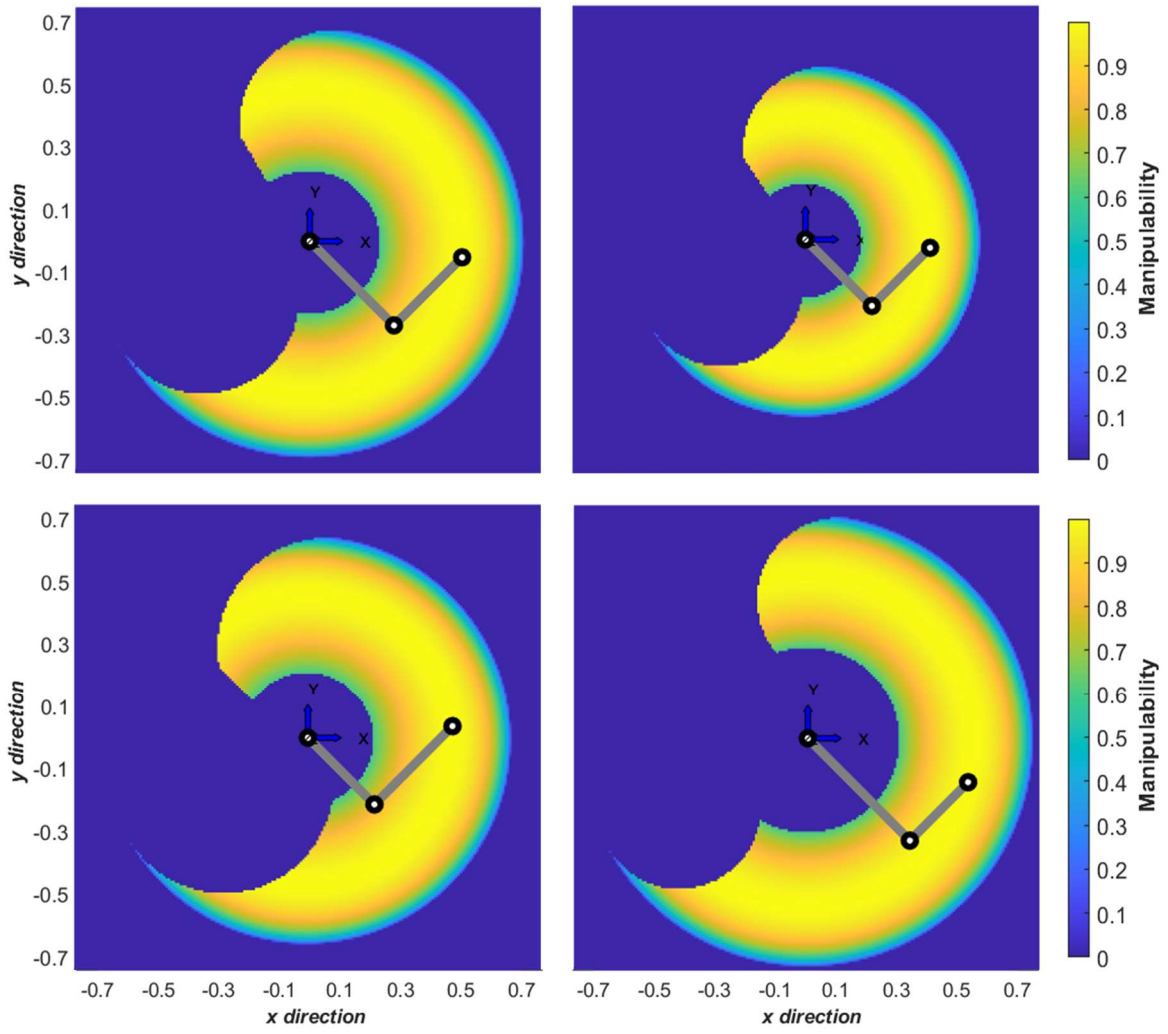

Figure 5.13. Upper limb low-high manipulability within the corresponding reach envelope area for the evaluation of 4 limbs (see Table 5.2). Blue and yellow represent low and high manipulability values correspondingly.

5.5 Upper limb manipulability analysis and uncertainty propagation

So far, the method for upper limb manipulability analysis has been established and upper limbs with discrete segment lengths have been evaluated. Nevertheless, such segment lengths and proportions can vary from person to person. Therefore, to quantify the propagation of these uncertainties, the segment length values used in the analysis presented in this section were distributions rather than fixed values. Thus, this section focused on the upper limb manipulability analysis during the execution of circular trajectories including uncertainty propagation.

In this investigation the upper limb was represented as a 2-link kinematic chain with 2-DOFs (Degrees of Freedom). Two 0.2m-diameter circular trajectories with origins $o_1(0.30,0.00)$ and $o_2(0.50,0.15)$ were selected as the tasks to be evaluated (see Figure 5.14). The input and output values used for the analysis are presented in Table 5.4 and Table 5.5. A MATLAB algorithm was created and used to obtain the Q joint angles that satisfy the task and to compute the corresponding manipulability measure, as explained in Sections 3 and 5.1.

Table 5.4. Input parameters used for the 2D case study

Parameter	*Variable*	*Description*	*Value*
Upper arm length $(\boldsymbol{m})$	l_1	$\sim N(\mu_{l1}, {\sigma_{l1}}^2)$	$\sim N(0.3565, 0.0251^2)$
Forearm length $(\boldsymbol{m})$	l_2	$\sim N(\mu_{l2}, {\sigma_{l2}}^2)$	$\sim N(0.2883, 0.0143^2)$
Circle radius $(\boldsymbol{m})$	r	*Fixed*	0.1
Circle origin on $\boldsymbol{x}$ $(\boldsymbol{m})$	a	*Fixed*	[0.30, 0.50]
Circle origin on $\boldsymbol{y}$ $(\boldsymbol{m})$	b	*Fixed*	[0.00, 0.15]

Table 5.5. Output parameters used for the 2D case study

Parameter	*Variable*	*Description*
Shoulder joint angle $(\boldsymbol{degrees})$	$Q_1 = [q_{11}, q_{12}]$	$Q_1 \in \mathbb{R}^{nxm}$
Elbow joint angle $(\boldsymbol{degrees})$	$Q_2 = [q_{21}, q_{22}]$	$Q_2 \in \mathbb{R}^{nxm}$
Manipulability $(\boldsymbol{normalised})$	W	$W \in \mathbb{R}^{nxm}$

The system of equations describing the relationship of motion in cartesian space and joint space were obtained by using forward kinematics. Thus, the following function $F(Q, L, X, Y)$ can be constructed by using such system of equations:

$$F \coloneqq \begin{bmatrix} l_2 \cos(q_1 + q_2) - x + l_1 cos(q_1) \\ l_2 \sin(q_1 + q_2) - y + l_1 sin(q_2) \end{bmatrix}$$

Equation 5.11

or

$$F \coloneqq \begin{bmatrix} \alpha_0 + \beta_0 - x \\ \alpha_1 + \beta_1 - y \end{bmatrix}$$

Equation 5.12

where $\propto_0 = l_2 \cos(q_1 + q_2),\ \propto_1 = l_2 \sin(q_1 + q_2), \beta_0 = l_1 cos(q_1), \beta_1 = l_1 sin(q_2).$

On one hand, the task (circular trajectories) expressed in cartesian coordinates was defined as:

$$\begin{bmatrix} x \\ y \end{bmatrix} = \begin{bmatrix} a - r\cos\theta \\ b - r\sin\theta \end{bmatrix}$$

Equation 5.13

where, a, b are the circle origin coordinates, r is the radius of the circle, and θ is the angular displacement (see Figure 5.14).

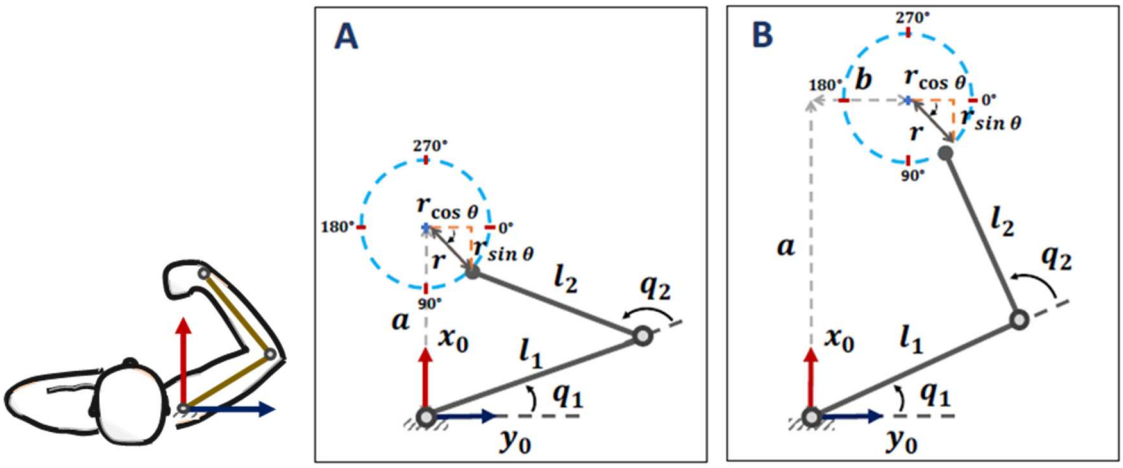

Figure 5.14. Circular trajectory followed by the end-effector of a 2-link kinematic chain representation of the upper limb.

Consequently, the Q joint angles that satisfy the task were obtained by using inverse kinematics to solve:

$$I := \begin{bmatrix} \tilde{x} \\ \tilde{y} \end{bmatrix} = \begin{bmatrix} \alpha_0 + \gamma_0 \\ \alpha_1 + \gamma_1 \end{bmatrix}$$

Equation 5.14

where the function $\boldsymbol{I}$ represents the function to solve the inverse kinematics, and $\tilde{x}$ and $\tilde{y}$ are the trajectory approximations obtained from the inverse kinematics computations.

The Q angle values used as inputs for the manipulability analysis were obtained by solving the function F (Equation 5.11) to minimize the ξ error:

$$\min_{Q \in \mathbb{R}} \left(\begin{bmatrix} \xi_0 \\ \xi_1 \end{bmatrix} = \begin{bmatrix} \tilde{x} \\ \tilde{y} \end{bmatrix} - \begin{bmatrix} x \\ y \end{bmatrix} \right)$$

Equation 5.15

The F function (Equation 5.11) was solved by using the Levenberg-Marquardt solver algorithm in MATLAB; the Levenberg-Marquardt method is an algorithm for least-squares estimation of non-linear parameters that uses Gauss-Newton direction and steepest descent direction approaches.

Once the Q joint angles values that satisfy the task were obtained, the W manipulability measure was computed using the Equation 5.3:

$$W = \begin{bmatrix} w_{11} & \cdots & w_{1j} \\ \vdots & \ddots & \vdots \\ w_{i1} & \cdots & w_{ij} \end{bmatrix}; W \in \mathbb{R}^{nxm}$$

Equation 5.16

where, the column vectors of the manipulability matrix W are the manipulability measure at each j point along the trajectory given $l_{1i}, l_{2i}; i = [1, \ldots, n]$.

The results of the analysis are presented in Figure 5.15, which shows the manipulability measure for both circular trajectories including the effects of the input uncertainties on manipulability.

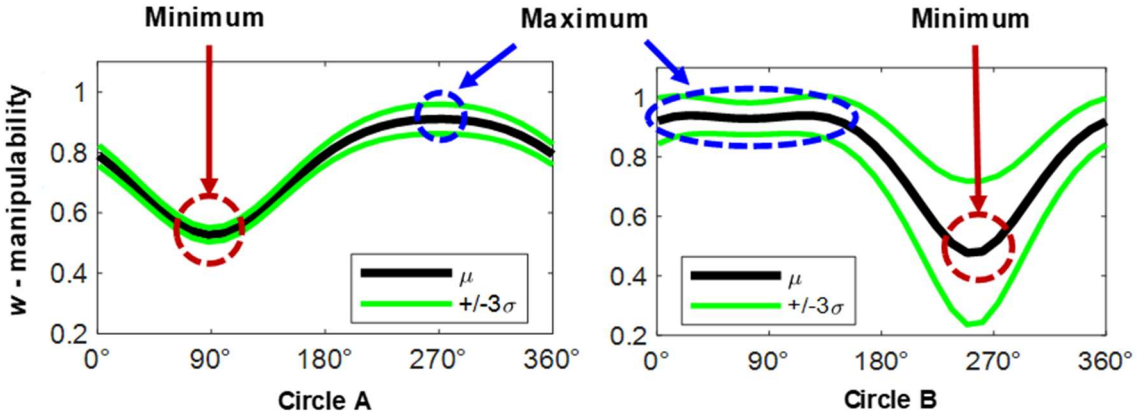

Figure 5.15. Top: q_1 joint angle values(shoulder) for the execution of the task; middle: q_2 joint angle values (elbow) for the execution of the task; bottom: manipulability

As can be seen in Figure 5.15, the maximum manipulability for Circle A is at 270° and from 0-170° for Circle B. On the other hand, the minimum manipulability for Circle A is at 90° and at 260° for Circle B. Although the mean manipulability values seem to be similar for both trajectories, the expected manipulability for trajectories on Circle B have higher variability.

Therefore, the trajectories on Circle B appear to be more affected by the uncertainties in the inputs. Thus, the results agree with the observations described in previous sections of this thesis work; the manipulability of the upper limb is affected by the position of the task on the plane, as well as, by limb segment lengths. Additionally, according to the results presented in this section, the location of the task also affects the accuracy of the prediction of regions of low and high manipulability for a given population. Therefore, this previous observation should be considered if high accuracy is needed during the study of manipulability for populations.

5.6 Manipulability in the workspace (3-D analysis)

Manipulability analysis on the horizontal plane (reach envelope area) has been addressed in the previous sections of this chapter. Such 2-dimensional analysis provides an idea of the areas where the upper limb has higher manipulability on the horizontal plane. However, upper limb tasks require 3-dimensional movements. Thus, this section extends the analysis presented previously in this chapter and centres on the investigation of manipulability within upper limb workspace (3-D analysis).

Although, in this section, the upper limb is still represented as a 2-link kinematic chain, the model is upgraded by adding 2-DOFs to the shoulder (now represented as full ball-and-socket joint). The analysis presented in this section starts with the definition of workspace (upper limb 3-D reachability) and continues with the computation of upper limb manipulability within the defined workspace.

Furthermore, this section demonstrates the versatility of the method to incorporate new variables to adjust the model and increase its accuracy to predict regions of higher manipulability, and therefore, regions of higher dexterity. Thus, this section introduces and proposes the use of a comfort variable to penalise the manipulability measure.

The investigation presented in this section is essential for the understanding and characterisation of upper limb dexterity as it incorporates new degrees of freedom at the shoulder, extends the analysis to 3 dimensions, demonstrates the versatility of the model, and proposes new variables that can improve the accuracy of the model and its predictions.

5.6.1 Manipulability analysis within the workspace

For the computation of workspace and manipulability in 3 dimensions, as in Section 4.3, the upper limb was represented as a simplified kinematic chain composed of 2 links (upper arm and forearm) with 4-DOFs (shoulder abduction-adduction, shoulder flexion-extension, shoulder internal-external rotation and elbow flexion-extension). The model inputs were the shoulder and elbow joint range of motion and the upper arm and forearm segment lengths (see Table 5.6).

The model outputs were the position $x = [x, y, z]^T$ of the end-effector on the cartesian space and the shoulder and elbow joint angles $q = [q_1, q_2, q_3, q_4]^T$, which were used to compute upper limb workspace and manipulability. A system of equations was constructed to define joint coupling for shoulder range of motion for each internal degree of freedom at any given configuration (see Section 4.3). The analysis was conducted by sampling over 5,000 points in a cubic volume 5% greater (in each direction) than the

upper limb length (see Table 5.6). A Matlab algorithm was created and used to determine feasible upper limb configurations to reach each sampled point and only satisfactory reachable solutions were used to compute workspace and manipulability.

Table 5.6. Manipulability analysis input parameters. Statistical data source [39, 146]

Parameter	*Variable*	*Value*
Upper arm length $(\boldsymbol{m})$	l_1	$\sim N(0.3565, 0.0251^2)$
Forearm length $(\boldsymbol{m})$	l_2	$\sim N(0.2883, 0.0143^2)$
X range $(\boldsymbol{m})$	X	$-1.05(l_1 + l_2) \leq \boldsymbol{X} \leq 1.05(l_1 + l_2)$
Y range $(\boldsymbol{m})$	Y	$-1.05(l_1 + l_2) \leq \boldsymbol{Y} \leq 1.05(l_1 + l_2)$
Z range $(\boldsymbol{m})$	Z	$-1.05(l_1 + l_2) \leq \boldsymbol{Z} \leq 1.05(l_1 + l_2)$
Shoulder abduction	θ_{2U}	$\sim N(184.0, 7.0^2)$
Shoulder adduction	θ_{2L}	$\sim N(45.0, 7.0^2)$*
Shoulder flexion	θ_{1U}	$\sim N(166.7, 4.7^2)$
Shoulder extension	θ_{1L}	$\sim N(62.3, 9.5^2)$
Shoulder external rotation	θ_{3U}	$\sim N(103.7, 8.5^2)$
Shoulder internal rotation	θ_{3L}	$\sim N(68.8, 4.6^2)$
Elbow flexion	θ_{4U}	$\sim N(142.9, 5.6^2)$
Elbow extension	θ_{4L}	$\sim N(0.6, 3.1^2)$

***Estimated value as statistical data for shoulder adduction is lacking in literature and is commonly omitted or reported as 0 degrees.**

Figure 5.16 (left) shows the estimated manipulability volume for an individual with mean input values (see Table 5.6). The workspace volume depicts the 3-dimensional upper limb reachability as a bubble-like envelope. Similarly, the estimated manipulability measure for each sampled point within the workspace is presented in Figure 5.16 (right). As can be seen in the figure, regions of high manipulability can be found in middle regions of the workspace and the manipulability decreases to 0 when the end-effector of the limb is further away from the shoulder.

However, manipulability values appear to be high even on the periphery of the workspace envelope where the shoulder joint has already reached the limits of range of motion. Although, these regions may still be of high manipulability for a robotic manipulator, it is hypothesised that the manipulability for human upper limbs would decrease as executing tasks in such regions may be uncomfortable due to range of motion limitations and self-weight acting on the limb.

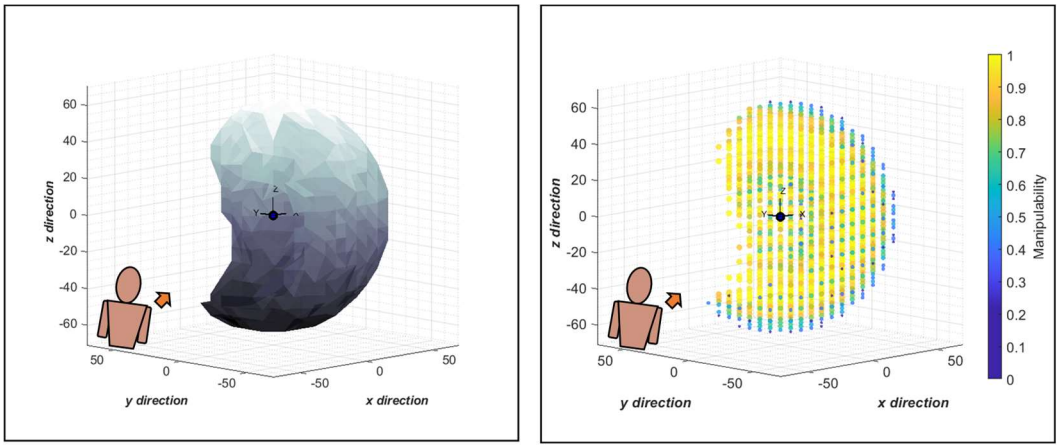

Figure 5.16. Computed workspace and low-high manipulability regions

5.7 The Dexterity Analysis Method

This section introduces the Dexterity Analysis Method (DAM), which is a modified version of the manipulability analysis method that incorporates human factors associated with comfort. The method defines upper limb workspace volume and computes manipulability and comfort to finally obtain the dexterity measure and the high dexterity regions within the corresponding workspace volume. Therefore, this section introduces the human factors that compose the proposed comfort variable and summarises the steps of the Dexterity Analysis Method.

5.7.1 Introduction of the comfort variable and computation of the dexterity measure

The manipulability analysis method is based on the contributions of each joint of a robotic manipulator to perform motion at the end-effector [11, 12]. The metric provided by this method is beneficial for the understanding of manipulability and helps to determine regions of potential high manipulability.

Although, the manipulability measure by itself is used to determine optimal positions and regions of high manipulability for a robotic arm, the use of this metric and the model proposed in this research work to determine human upper limb optimal configurations and regions of high dexterity need to incorporate other human factors. Some human factors that could improve the model to make it more humanly realistic were grouped into 8 categories: dynamics, sensorial factors, work and energy, muscle strength and activation, motor control, cognitive factors, health, ROM and anthropometry (see Figure 5.17).

Another factor to consider is the environmental conditions, which can also affect dexterity as it has been proved that upper limb performance decreases in cold temperatures [152, 153], and that protective equipment such as gloves affect upper limb

dexterity [154, 155]. Likewise, upper limb dexterity for tasks that require interaction with objects can be affected by the intrinsic properties of the object being manipulated such as material, shape, and weight [63]. For instance, holding a wet glass is harder than holding a dry glass.

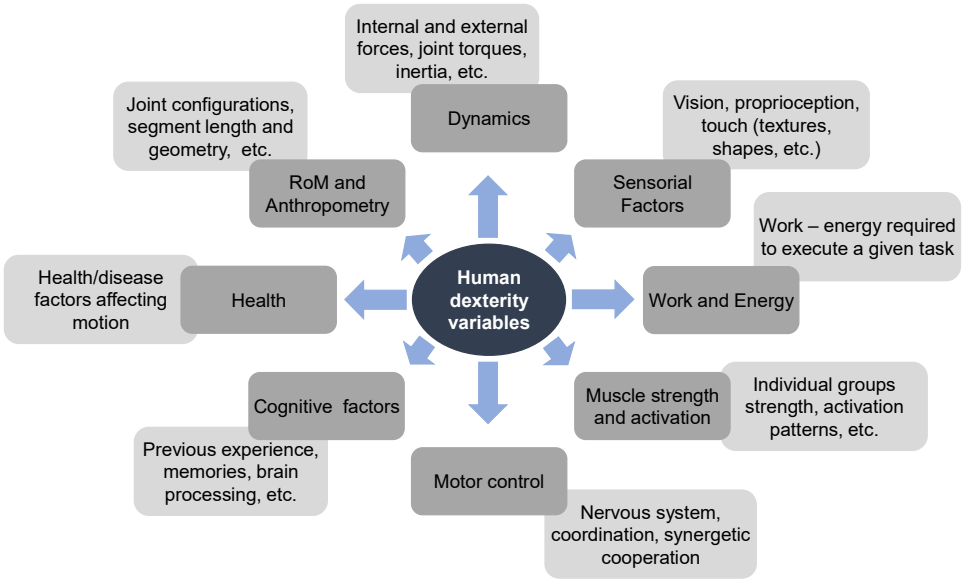

Figure 5.17. Human factors that can affect dexterity.

Although all the factors mentioned above and in Figure 5.17 are important for the study and characterisation of human dexterity, it was decided that only variables related to kinematics, dynamics and work would be added to the model as those factors are most aligned to the modelling approach and to the scope of this research project. Thus, this work proposes a new variable for the inclusion of human comfort that could be used as a penalty for the computed manipulability. Such comfort variable incorporates 3 aspects that relate to kinematics, dynamics, and work: joint configurations with respect to their corresponding ROM limits, torque force perceived at the shoulder due to upper limb self-weight, and the work needed to rise the upper limb from its neutral position (limb resting downwards) to a given configuration.

Consequently, as the 3 aspects that compose comfort need to be mathematically defined and the relationship between such aspects needs to be established, the following assumptions are proposed:

i. **Joint configurations with respect to their corresponding ROM limits**

   Upper limb joint configurations play an important role in the level of perceived comfort during the execution of a given task. It is believed that comfort decreases when the task requires joint configurations that are close to the limits of joint range of motion. Therefore, in this work, higher comfort is presumed to occur

when the upper limb joint angles are between the extremes of the corresponding joint range of motion (see Figure 5.18). Information regarding a mathematical definition of human comfort given the upper limb joint configurations with respect to the corresponding range of motion is lacking in literature. Therefore, this aspect of comfort is mathematically defined as follows:

Firstly, the middle point of range of motion for any given joint can be obtained by computing:

$$\boldsymbol{\theta_{mid}} = \boldsymbol{\theta_{max}} - \left(\frac{\boldsymbol{\theta_{max}} - \boldsymbol{\theta_{min}}}{\mathbf{2}}\right)$$

Equation 5.17

where θ_{mid} represents the middle point between the ends of the corresponding joint range of motion, and $\theta_{min}, \theta_{max}$ are the minimum and maximum range of motion values correspondingly.

On the other hand, joint angle deviation from the middle point can be defined as:

$$\theta_{dev} = \theta - \theta_{mid}$$

Equation 5.18

where θ is the joint angle at a given upper limb configuration.

Moreover, the joint angle normalised deviation can be obtained by dividing Equation 5.18 by the maximum possible deviation as follows:

$$\theta_{norm\ dev} = \frac{\theta_{dev}}{\theta_{max\ dev}}$$

Equation 5.19

where

$$\theta_{max\ dev} = \left(\frac{\theta_{max} - \theta_{min}}{2}\right)$$

Equation 5.20

Consequently, comfort for a given upper limb configuration regarding joint angle position with respect to its ROM, can be obtained by computing:

$$Comfort_{\theta} = 1 - (\theta_{norm\ dev})^2$$

Equation 5.21

Note: the normalised deviation $\theta_{norm\ dev}$ is squared to represent comfort with a quadratic behaviour as the assumption is that comfort is high at the middle point of ROM and it keeps high until the joint angle starts getting close to the ends of

ROM, where the comfort perception falls to 0. The normalised squared deviation (as it is a penalty) is subtracted from the unit as the maximum comfort value at the middle point of ROM must be 1 (see Figure 5.18).

Finally, the total comfort for an upper limb with n degrees of freedom can be obtained by computing:

$$Comfort_{\theta 1..n} = Comfort_{\theta 1} Comfort_{\theta 2}, \ldots, Comfort_{\theta n}$$

Equation 5.22

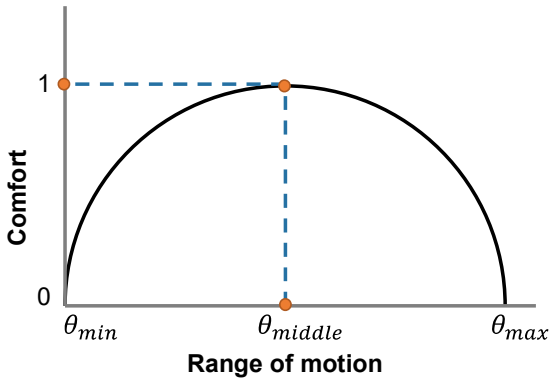

Figure 5.18. Comfort in terms of joint range of motion

ii. Torque forces perceived at the shoulder due to upper limb self-weight

Any movement executed by the upper extremity is subject to internal and external forces. Some of those forces are the moments exerted by the upper limb self-weight, which reflect as torque forces at the shoulder (pivot point of the upper limb). In this work, such torques exerted by the upper limb self-weight at the shoulder joint are presumed to have a direct impact on the perceived upper limb comfort. Thus, higher comfort, giving the upper limb self-weight, is assumed to occur when the upper extremity is in a configuration in which weight forces acting on the segment centres of mass cause the smallest moments at the shoulder joint (see Figure 5.19). Likewise, the lowest comfort is presumed to happen for configurations in which the extremity is entirely stretched at the shoulder level on the horizontal plane.

Consequently, this aspect of comfort is mathematically defined as follows:

First, the total moment of force exerted at the shoulder due to self-weight forces acting on both the upper arm and the forearm (see Figure 5.19) can be described by:

$$Mo = m_1 g\, r_1 + m_2 g\, r_2$$

Equation 5.23

where Mo is the total moment exerted at the shoulder, m_1 and m_2 are the mass of the upper arm and the forearm segments, r_1 and r_2 are the horizontal distance from the shoulder to the upper arm and forearm centres of mass (see Figure 5.19), and g corresponds to gravity.

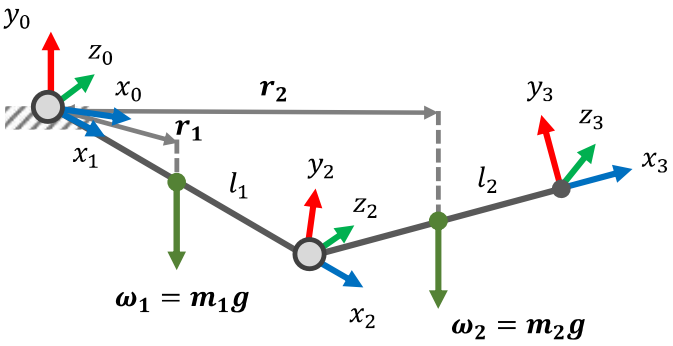

Figure 5.19. Weight forces acting on the upper limb

On the other hand, the maximum value for the total moment due to the weight forces acting on the upper extremity occurs when the limb is fully stretched at the hight of the shoulder. It can be obtained by computing:

$$Mo_{max} = m_1 g\, r_{1max} + m_2 g\, r_{2max}$$

Equation 5.24

where r_{1max} and r_{2max} are the maximum horizontal distance from the shoulder to the upper arm and forearm centres of mass, which occurs when the arm is fully stretched at the hight of the shoulder.

Therefore, the normalised moment acting at the shoulder can be obtained by dividing the total moment (Equation 5.23) by the maximum moment described by Equation 5.24 as follows:

$$Mo_{norm} = \frac{Mo}{Mo_{max}}$$

Equation 5.25

Thus, the comfort measure based on the weight forces acting on the upper limb can be obtained by computing:

$$Comfort_{Mo} = 1 - Mo_{norm}$$

Equation 5.26

Note: the normalised moment Mo_{norm} (as it is a penalty) is subtracted from the unit as the maximum comfort value must be 1.

iii. Work needed to rise the upper limb from its neutral position to a given configuration

Rising the upper limb from its neutral configuration (limb resting downwards) requires an effort which is also known as work. Such work is presumed to have a direct impact on upper limb comfort as making a higher effort translates into having less comfort during the execution of a given task.

Therefore, in this research, upper limb comfort (given the work required) is assumed to be higher when the extremity is in neutral position (resting downwards) as no work is needed to maintain the limb in such configuration (see Figure 5.20). Conversely, lower comfort is assumed to occur for configurations in which the upper limb is completely stretched all the way up as a certain amount of energy is needed to keep the limb up.

This aspect of comfort given the work required to rise the upper limb from neutral position (resting downwards) to any other upper limb configuration is mathematically defined as follows:

First, the total work required to rise the upper limb from neutral position (resting downwards) to a given height (see Figure 5.20) can be described as follows:

$$W_k = m_1 g\, h_1 + m_2 g\, h_2$$

Equation 5.27

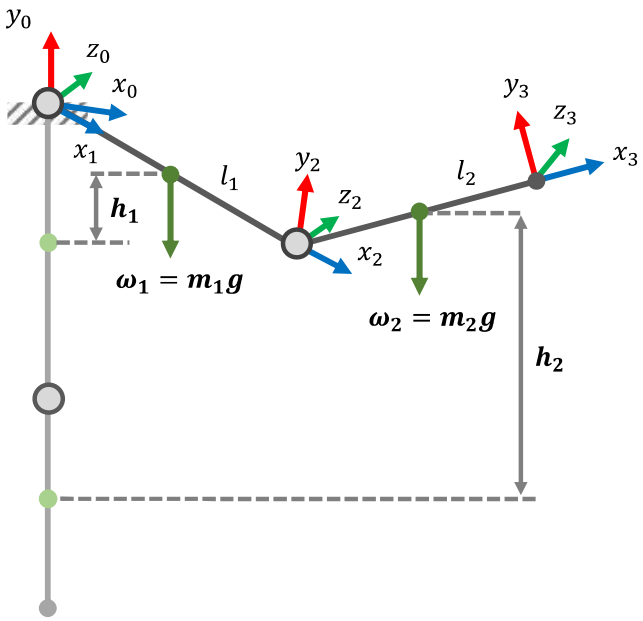

Figure 5.20. Work required to rise the upper limb.

where W_k (the subscript k is assigned to distinguish work from manipulability and weight) is the total work required to rise the arm from neutral position to a given configuration, m_1 and m_2 are the masses of the upper arm and the forearm segments, h_1 and h_2 are the vertical distances of the upper arm and forearm from their centre of mass in neutral position to their corresponding centre of mass at a given limb configuration (see Figure 5.20), and g corresponds to gravity.

On the other hand, the maximum required work (potentially) is when the limb is fully stretched all the way up. Thus, the maximum work can be obtained by computing:

$$W_{k\,max} = m_1 g\, h_{1max} + m_2 g\, h_{2max}$$

Equation 5.28

where h_{1max} and h_{2max} are the vertical distances from the upper arm and forearm centres of mass in neutral position (resting downwards) to their corresponding centres of mass when the upper limb is (potentially) fully stretched and lifted. Consequently, the normalised work required to rise the limb to any given height can be obtained by dividing the total work (Equation 5.27) by Equation 5.28 as follows:

$$W_{k\,norm} = \frac{W_k}{W_{k\,max}}$$

Equation 5.29

Thus, the comfort measure based on the work required to rise the upper limb to any given height can be obtained by computing:

$$Comfort_{W_k} = 1 - W_{k\,norm}$$

Equation 5.30

Note: the normalised work $W_{k\,norm}$ (as it is a penalty) is subtracted from the unit as the maximum comfort value must be 1.

iv. The proposed comfort variable

Although only 3 aspects are initially used for the comfort variable presented in this section, the proposed comfort variable is not limited to a certain number of aspects and factors can be added or eliminated as needed. Thus, the proposed comfort variable is mathematically defined as follows:

$$C = \sum_{i=1}^{n} \alpha_i Comfort_i$$

Equation 5.31

where $Comfort_i$ represents the i^{th} aspect of comfort, α_i is the weight of the corresponding aspect of comfort, and $\alpha_i + \alpha_{i+1} + \cdots + \alpha_n = 1$

Initially, the 3 aspects of comfort (Equation 5.22, Equation 5.26 and Equation 5.30) are considered to contribute equally $(\alpha_1 = \alpha_2 = \alpha_3 = 1/3)$. However, the weights of the corresponding aspects of comfort can be adjusted as required in order to represent the contributions as realistic as possible. As normative data to describe such aspects of comfort is lacking in literature, experimental analysis may be needed to further understand the influences of these factors.

The variable comfort described above (Equation 5.31) can be used to penalise manipulability to obtain a new measure called "dexterity measure", which can be used to determine high dexterity regions. Such dexterity measure can be computed as follows:

$$D_x = wC$$

Equation 5.32

where D_x is the dexterity measure, w is the manipulability measure, and C is the computed comfort.

This subsection introduced the comfort variable for the characterisation of dexterity. Such variable only contemplates factors related to kinematics, dynamics and work as those factors are most aligned to the modelling approach and to the scope of this research project. Thus, the modelling approach proposed in this research work only considers the musculo-skeletal physical structure of the limb represented as a kinematic chain (rigid segments and joints) and the comfort aspects described above. Therefore, this work does not cover motor control, cognition, health, and neurophysiological factors. Although this is a limitation of the current model, the modelling approach proposed in this thesis work allows incorporating such types of aspects as future improvements to create more accurate upper limb models for the characterisation of human dexterity.

5.7.2 The Dexterity Analysis Method

Previous sections of this thesis provided the background and explained in detail the concepts and theory in which the Dexterity Analysis Method is based: upper limb workspace volumes, the manipulability analysis method, the comfort variable, and the dexterity measure. Therefore, this section only summarises the steps of the Dexterity Analysis Method, which are described as follows:

I. Develop an upper limb kinematic model (Chapter 3)

II. Define joint range of motion and joint coupling.

III. Compute upper limb workspace volume (Section 4.3)

IV. Conduct manipulability analysis (Section 5.1)

V. Compute human comfort and the dexterity measure (Section 5.7)

VI. Determine high dexterity regions within the workspace volume (Section 5.7).

As explained above, these are the general steps of the Dexterity Analysis Method, and therefore, the reader is invited to review the corresponding sections to understand the techniques and methods in order to learn how to apply them accordingly.

The Dexterity Analysis Method provides numerical and visual description of workspace volumes and dexterity regions that help to the understanding and characterisation of upper limb functionality and dexterity. Such method helps to visualise how workspace volumes and dexterity regions deform and get affected by reductions in joint range of motion (and potentially by other human factors), which facilitates the identification of the most affected regions of workspace and dexterity within their corresponding volumes. Likewise, such visual information, combined with the workspace and dexterity measures, can significantly improve prosthetics, implant, ergonomics, and workstation optimisation based on the maximisation of workspace volumes and dexterity regions.

An example to illustrate the application of the Dexterity Analysis Method and to compare between manipulability and dexterity measures is presented in Figure 5.21. The input values used for this analysis are presented in Table 5.6 and Table 5.7. The figure on the left shows the manipulability measure, and as can be seen, manipulability seems to be high towards the middle regions within the volume and only decreases at the edges. Whereas, as illustrated on the right figure, dexterity decreases at the edges, in regions above shoulder hight, and regions opposite to the limb side.

Thus, the dexterity measure, by observation and intuition, seems to agree with regions that we perceive as comfortable to perform tasks: in front and below shoulder hight. Such characteristics may have been captured by the comfort factors incorporated to the method and which consider limits of range of motion, the weight forces acting on the limb, and the work required to move the extremity to a given configuration. However, it is only speculation as the method has not been fully validated, and therefore, further analysis is needed. Nonetheless, the results are quite promising, and the method seems to predict high dexterity in regions commonly perceived as comfortable to execute dexterous tasks.

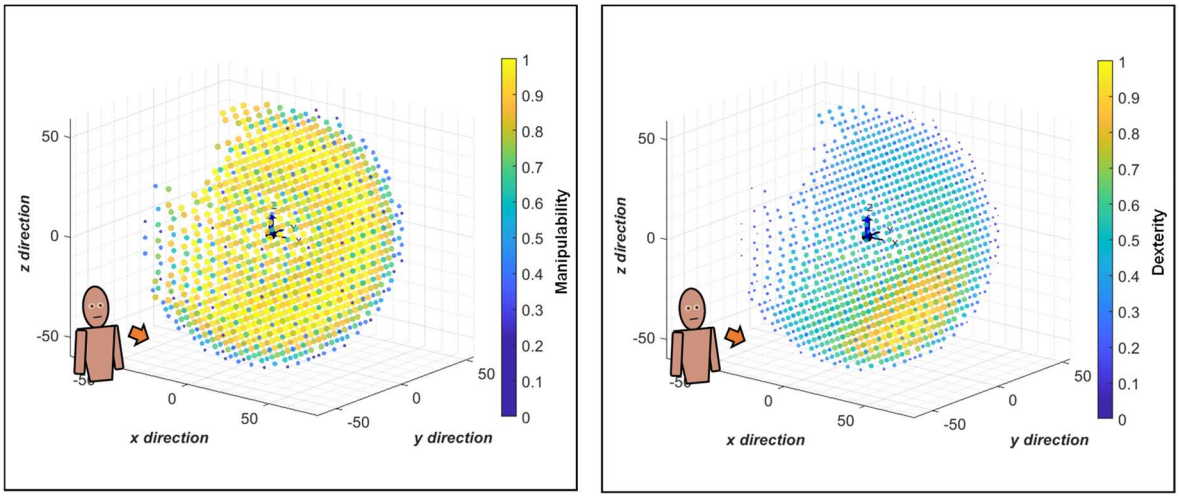

Figure 5.21. Computed low-high manipulability (left) and dexterity (right) regions of the human upper limb.

Table 5.7. Input variables used to compute comfort.

Parameter	*Variable*	*Value*
Upper Arm mass *(% body weight)*	m_1	0.58
Forearm mass *(% body weight)*	m_2	0.46
Upper arm centre of mass *(% segment length)*	r_1	0.0271
Forearm centre of mass *(% segment length)*	r_2	0.0162
Gravity *(N/kg)*	g	9.81
Body weight (mean value for British males) *(Kg)*	ω_T	83.00

5.8 Summary

The aim of this chapter was successfully accomplished as the chapter introduced and proposed a novel method for the characterisation of dexterity, the Dexterity Analysis Method, which is a modified version of the manipulability analysis method by incorporating human factors associated with comfort.

The first sections of the chapter (Sections 5.1 and 5.2) introduced and demonstrated the use of the manipulability analysis method. The manipulability analysis method considers the individual contributions of upper limb joints to execute movement. Therefore, it is assumed that the measure and the ellipsoids are inherently accounting for the contributions of each joint to upper limb dexterity. It is important to mention that so far, the individual joint contributions have been considered to be equal. Nevertheless, in future research work, the model should be modified to account for the individual joint contributions to upper limb overall motion and to dexterity.

In Section 5.3 the upper limb was represented as a 2-link kinematic chain with 2-DOFs in order to conduct manipulability analysis on the x-y plane (2-dimensional analysis). The upper limb was evaluated during the execution of linear and circular trajectories and during the exploration of the full plane by sampling evenly spaced points. The results suggested that the size of the limb, as well as the position of the task affect manipulability. A relevant observation was that the use of manipulability ellipsoids without considering their corresponding manipulability measure should not be used for the comparison of different limb manipulability predictions. As described in Section 5.3, a limb seemed to have large ellipsoids compared to other limbs, however, its manipulability measure had the highest variability, and it never achieved its higher manipulability value. Likewise, large limbs have larger low and high manipulability regions which are also proportional to their reach envelope areas. However, such regions shift from the shoulder according to the upper limb sizes. Another relevant finding was that variations on the proportionality of limb segment lengths affect the shape and size of upper limb reach envelope area and low and high manipulability regions. Therefore, people with same limb size but with different segment length proportions are expected to have different manipulability values and consequently different performance for the execution of the same task.

The analysis presented in Section 5.3 did not include range of motion constraints. Therefore, in Section 5.4, the model is upgraded by incorporating joint range of motion constraints to determine low and high manipulability regions within the corresponding upper limb reach envelope area. Thus, the manipulability analysis presented in this section describes more realistic manipulability regions as the investigation incorporated joint range of motion limits. The shapes of both reach envelope area and low and high manipulability regions have similar shapes and increase, decrease, get ticker or thinner depending on the limb size and the proportionality of the corresponding segment lengths.

Until Section 5.4, only discrete segment lengths had been evaluated. However, upper limb segment lengths and proportions can vary from person to person. Therefore, Section 5.5 focused on upper limb manipulability analysis during the execution of circular trajectories including uncertainty propagation, considering the input values as distributions rather than as fixed values. The results agreed with previous observations suggesting that manipulability is affected by the position of the task on the plane, as well as, by limb segment lengths. Moreover, it was found that the location of the task affects the accuracy for predictions of regions of low and high manipulability for a given population.

In Section 5.6, the analysis moves from 2 to 3-dimensions, and the model was upgraded by adding 2-DOFs to the shoulder and ROM constraints. As a result, regions of low and high manipulability within the workspace volume were obtained. Regions of high manipulability were found in middle regions of the workspace, whereas regions with low or no manipulability were observed on the edges of the corresponding workspace volume. However, manipulability values appeared to be high even on the periphery of the workspace envelope where the shoulder and elbow joints have already reached the joint range of motion limits.

Therefore, Section 5.7 introduced the Dexterity Analysis Method as a variation of the manipulability analysis method by incorporating human factors to make it more humanly realistic. This section presented some human factors that can affect dexterity, such factors were grouped into 8 categories: dynamics, sensorial factors, work and energy, muscle strength and activation, motor control, cognitive factors, health, ROM and anthropometry (see Figure 5.17). Only some variables related to kinematics, dynamics, and work and that are aligned to the modelling approach and to the scope of this research project were selected and incorporated in a new proposed variable called comfort. Such comfort variable is affected by joint configurations, upper limb self-weight, and the work needed to rise the limb. This research proposes the use of the comfort variable as a penalty to manipulability to obtain the “dexterity measure”. However, the variable comfort proposed in this section is based on assumptions that only consider some kinematic and dynamic aspects of motion. Although in this investigation only 3 aspects were initially used for the comfort variable, the equation to compute comfort can be adjusted to incorporate or exclude factors as needed. Likewise, the weights of the corresponding comfort aspects can be modified as required. It is relevant to mention that the individual contributions of each aspect of the variable comfort are unknown and experimental analysis is needed to better understand the influences of such factors. The modelling approach proposed here only considers the musculo-skeletal physical structure of the limb represented as a kinematic chain (rigid segments and joints) and comfort aspects, and excludes factors related to motor control, cognition, health, and neurophysiological. However, the modelling approach proposed in this thesis work allows incorporating such types of aspects as future improvements to create more accurate upper limb models for the characterisation of human dexterity.

The Dexterity Analysis Method offers numerical and visual description of workspace volumes and dexterity regions that can be used for the characterisation of upper limb functionality and dexterity. Likewise, this visual information provided by the Dexterity Analysis Method help to comprehend how workspace volumes and dexterity regions deform and get affected by reductions in joint range of motion (and potentially by other

human factors), and to identify the most affected regions of workspace and dexterity within their corresponding volumes. Additionally, such numerical and visual information considerably improve prosthetics, implant, ergonomics, and workstation optimisation based on the maximisation of workspace volumes and dexterity regions. Thus, the Dexterity Analysis Method is quite promising as it significantly contributes to the characterisation of human motion, the development of ergonomic devices, the advancement in prosthetics design, the optimisation of sports performance, and so on. However, further experimental analysis is needed to validate this novel method.

Finally, the analysis presented in this chapter was conducted using a simplified representation of the human upper limb, the joint angle values that satisfy the task in cartesian space were approximations (obtained from an optimization algorithm), and some aspects of the physical characteristics of the limb were omitted or excluded for simplification. Thus, the factors previously mentioned can affect the accuracy of the results.

6 EXPERIMENTAL ASSESSMENT OF UPPER LIMB DEXTERITY, COMFORT AND PERFORMANCE

The previous chapters of this thesis studied upper limb workspace and dexterity and established the proposed Dexterity Analysis Method for the characterisation of upper limb workspace with respect to dexterity. However, such chapters only focused on computational analysis. Conversely, this chapter centres on the experimental analysis of the upper limb to determine the accuracy of the predictions obtained from the Dexterity Analysis Method.

Thus, experimental, and computational analyses were performed in parallel. A custom test board with circular trajectories in 9 locations was designed and used to assess upper limb performance and to obtain perceived participant comfort. Likewise, participant limb lengths and joint angle values were used as inputs for the Dexterity Analysis Method to predict upper limb dexterity. As a result, three measures were obtained from the experimental analysis: prediction (from Dexterity Analysis Method), perception (perceived participant comfort), and performance (deviation from the task). Where prediction refers to the estimated dexterity for each circular trajectory obtained from the Dexterity Analysis Method, comfort refers to perceived participant comfort by ranking each of the 9 circular locations, and performance refers to task execution accuracy obtained by comparing the executed trajectory to the target test board trajectory at every given location.

Participant movements were recorded using a new custom motion capture protocol and a system of 10 optical cameras. Finally, a correlation analysis was conducted to quantify the level of agreement between the computational and experimental analysis.

6.1 Experimental Method

6.1.1 Participants

As the experimental analysis conducted in this research was only a pilot study, no exact sample size was required. A total of 23 healthy participants, reporting no injuries or impairment, were recruited for the experimental analysis (age = 31 ± 8.1 years; height = 170.1 ± 8 cm; 11 males, 14 females, all right-handed). Ethical approval was granted by the Department of Mechanical Engineering Ethics Committee at the University of Sheffield (see Appendix A). Likewise, participants provided written consent for their participation in the experiment.

6.1.2 Data acquisition and processing

Participant movements were recorded by a motion capture system composed of 10 optical cameras (T-160, 100 Hz, Vicon Nexus 1.8.5, Vicon Motion System Ltd – Oxford, UK). As explained in Section 3.3.3, the number of markers and their attachment location for data acquisition vary from study to study. In some investigations the upper limb movements are recorded using as few as 6 markers, whereas others use above 18 markers for the study of a single limb [47, 85, 136-138]. It is known that the selection of the number of markers and their attachment locations may pose limitations for the extraction of kinematic information and can affect the accuracy of the results. Therefore, after evaluating such factors, a suitable protocol was designed. Such protocol is based on the Nexus Plug-in-Gait model marker protocol [138] (only the upper limb and thorax markers) and extra markers to reconstruct any missing points: a total of 19 non-invasive reflective markers placed on the upper limb and thorax is illustrated and described on Figure 6.1 and Table 6.1. It was decided to use the Nexus Plug-in-Gait model as a reference guide for the development of the protocol used here as it considers the body landmarks that mostly describe the upper limb and are sufficient to compute kinematic data.

Data pre-processing was conducted within Nexus (Vicon Motion System software) and post-processing was performed on MATLAB (R2020a, The MathWorks, Inc. – Natick, MA, USA). The segments of the upper limb consisted of the upper arm (acromion to lateral epicondyle) and the forearm (lateral epicondyle to middle wrist). For simplicity, given that in this experiment the participants performed movements with the upper limb parallel to the horizontal plane, the centre of rotation of the elbow joint was assumed to coincide with the lateral epicondyle, whereas the glenohumeral joint was assumed to concur to the acromion. However, in reality the glenohumeral centre of rotation does not coincide with the acromion. Previously, studies focused on the computation of the glenohumeral joint centre of rotation have proven that determining the accurate centre of rotation is complex and the results can have high variability depending on the algorithms used for the computations [156-164]. The results obtained by [162] in a study that compared five functional methods for the computation of glenohumeral joint centre show that the mean distance from the angulus acromialis (AA) to the glenohumeral joint centre can range from 40-55mm on the forward(+)/backward(-) direction, -20 to 10mm on the lateral(+)/medial(-) direction, and -15 to -30mm on the upward(+)/downward(-) direction. Therefore, although the computation of the accurate glenohumeral centre could be critical for some studies focused on micro movements at the joint (e.g. for optimisation of implant location), however, [163] demonstrates that the mislocation of glenohumeral

centre has little consequence on glenohumeral kinematics. In such study [163] found a maximum root mean square error (RMSE) of 4.78°, 4.1°, and 2° in elevation, elevation plane, and axial rotation correspondingly. Therefore, assuming the glenohumeral joint at the acromion seems reasonable as errors of 5° in the upper arm angles would not have a great impact on the results. For instance, computing the dexterity measure (as explained in previous sections of this thesis) for an average British male with an elbow angle of 90° with an error of ±5° would have an effect 0.7-1.2% on the computed dexterity measure, which would not influence the results of the analysis conducted here. Thus, computing a highly accurate shoulder centre of rotation would not significantly improve the accuracy of the computed shoulder angle in the context of gross movements, and therefore, an approximation of shoulder and elbow angles would be sufficient for comparison purposed between the simulations and experiments.

Table 6.1. Description of the names and locations of the reflective markers used in this new motion capture protocol.

Marker	*Body landmark*
RAC	Right Acromion
LAC	Left Acromion
JN	Jugular Notch
C7	C7
XI	Xiphoid
RLE	Right Lateral Epicondyle
RME	Right Medial Epicondyle
RUA1	Right Upper Arm Extra 1
RUA2	Right Upper Arm Extra 2
RUA3	Right Upper Arm Extra 3
ROL	Right Olecranon
RUP	Right Ulnar Process
RRP	Right Radial Process
RFA1	Right Forearm Extra 1
RFA2	Right Forearm Extra 2
RFA3	Right Forearm Extra 3
RMW	Right Middle Wrist
RM3	Right Third Metacarpal
RM5	Right Fifth Metacarpal

Other sources of error are the inherent motion capture errors during the computations that determine marker positions, marker placement, and skin tissue artifact [165-170]. The errors from the intrinsic computations of the Vicon Motion Capture System are

relatively small if the calibration is correct, [165] evaluated the Vicon system performance and found that the system positioning error is estimated to be lower than 2mm. Whereas, according to the literature, the most significant source of error comes from skin tissue artifact [170], for instance, [169] found skin motion artifact errors of up to 16mm. Although such errors are believed to have a low impact in the outcome of the experiments, further investigation, and study of the effects of such errors on the results are required to validate the accuracy of the modelling methods presented in this research work.

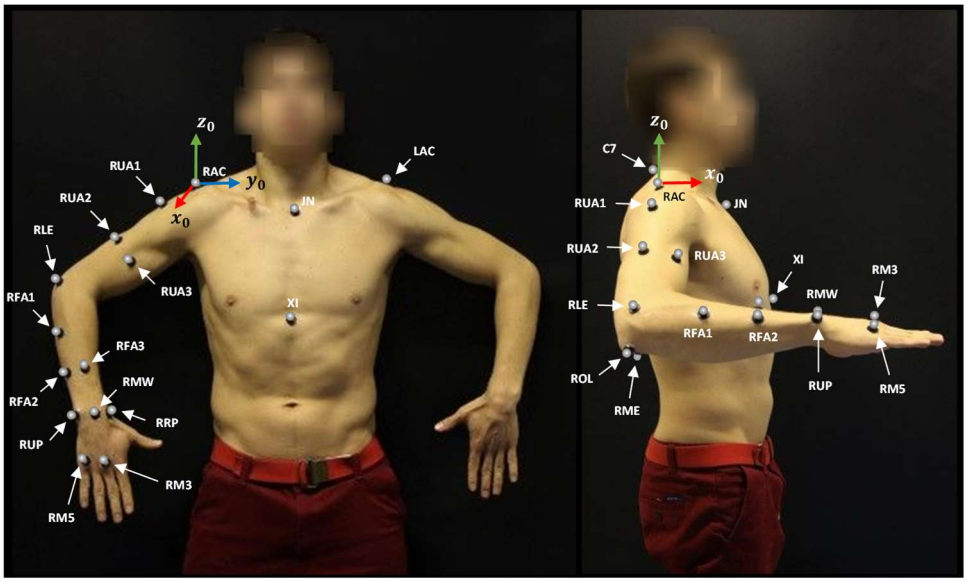

Figure 6.1. Motion capture protocol specially designed for the experimental analysis conducted in this research study.

6.1.3 Experimental protocol

Participants were asked to execute circular trajectories on a new test board that consists of circles located at 9 different positions along the board. Participants were given written and verbal instructions before and during the experiments. Moreover, participants were allowed to execute a few trajectories to familiarise with the experiment prior to the real test.

The Test Board was placed on a height-adjustable table set at participant axilla height. Prior to the execution of each task, participants were asked to stand at a distance of approximately 10cm from the test board to the participant chest and with the centre of the shoulder aligned to the centre of the test board. Next, participants were asked to grasp a handle-like stick, which had to remain vertical (aligned to the z axis and perpendicular to the test board) throughout the execution of the tasks. Participants were asked to perform 3 circular trajectories (clockwise) at each location of the board following

the alphabetic order (see Figure 6.2 and Figure 6.3). Every circular trajectory started and ended at the red-dot mark. Participants were invited to execute the tasks at comfortable steady fashion speed (as speed was not part of the performance score) without resting the limb on the board and with the rest of the body as still as possible. Next, participants were asked to rank the circular trajectory locations according to perceived comfort by assigning a number from 1 to 9 to each position (where 9 is the highest comfort score). For this evaluation of comfort, participants were allowed to repeat the task as many times as needed.

Finally, three measures were computed in this experimental analysis: prediction (from Dexterity Analysis Method), performance (deviation from the task), and perception (perceived participant comfort).

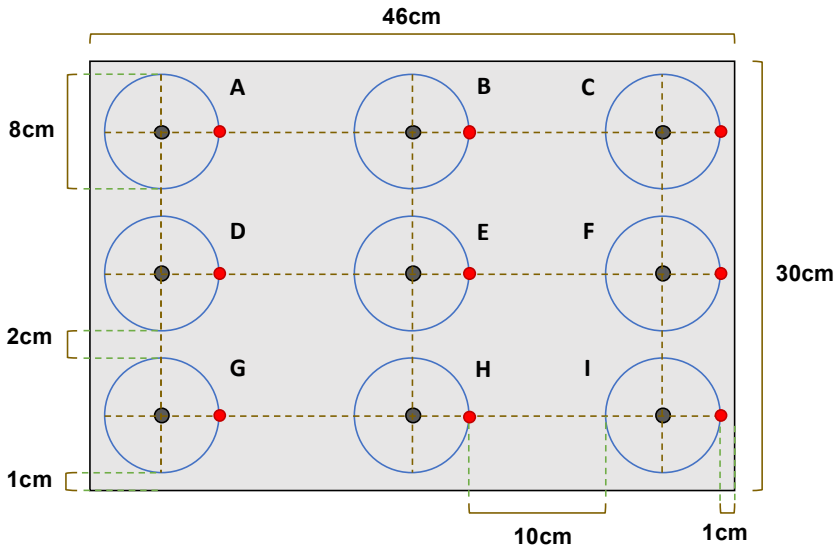

Figure 6.2. Experiment test board for circular trajectories in 9 different locations along the board.

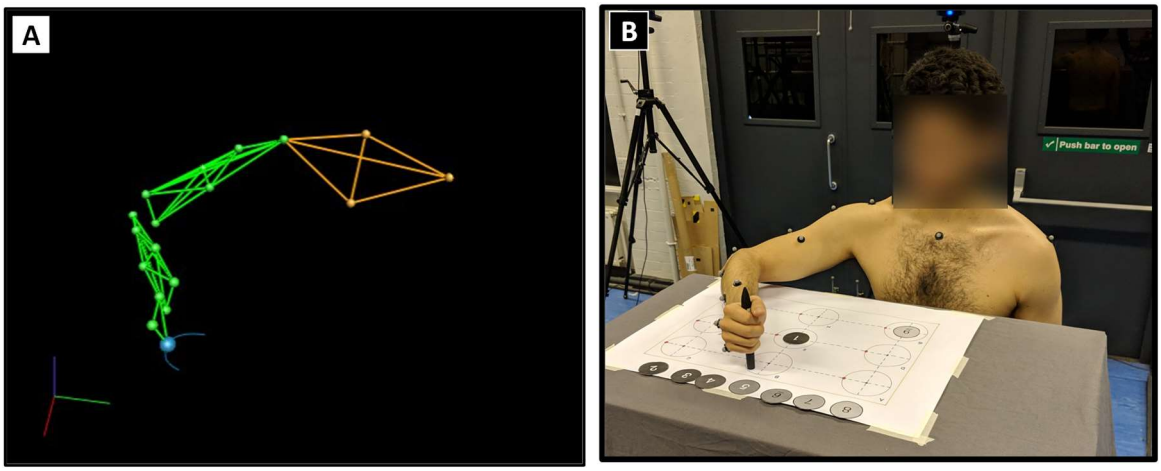

Figure 6.3. Participant motion captured by the cameras (right) and participant executing circular trajectory tasks (left).

6.2 Analysis and results

The data recorded by the motion capture system was used to reconstruct participant motion through a 4-link model composed of the clavicle, upper arm, forearm, and hand (see Figure 6.4). The global frame of reference was initially set at a fixed point on the floor of the laboratory, however, in the data processing, such global frame was transferred to the right acromion to be used as a global reference for all limb movements. The shoulder angle for horizontal flexion-extension was computed as the angle between the chest (right to left acromion) and upper arm (right acromion to olecranon) position vectors (see Figure 6.4). Likewise, the elbow angle for flexion-extension was computed as the angle between the upper arm (right acromion to olecranon) and the forearm (olecranon to ulnar process) position vectors.

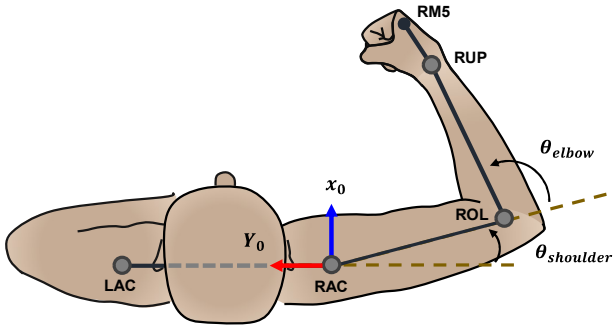

Figure 6.4. Four link model for the reconstruction of participant movements.

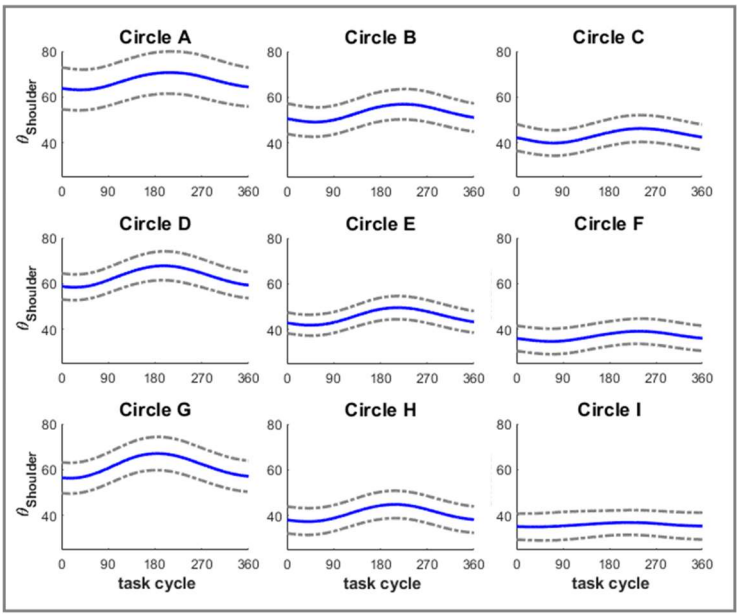

Figure 6.5. Upper limb shoulder angles for the execution of circular trajectories (mean and plus/minus a standad deviation).

The shoulder and elbow angles needed to complete the task at each circular trajectory location for all the participants are presented in Figure 6.5 and Figure 6.6. According to the results the mean values for horizontal shoulder flexion-extension and elbow flexion-extension required to complete the tasks range from approximately 30-80°, and 50-120°, respectively (see Figure 6.5 and Figure 6.6).

Some clear patters were that shoulder flexion is greater for circular trajectories on the left column, followed by the middle column, and finally by the right column. Another observation was that elbow flexion is smaller for circular trajectories further away and the required elbow flexion increases by approximately 20 degrees as the circular trajectories get closer to the body.

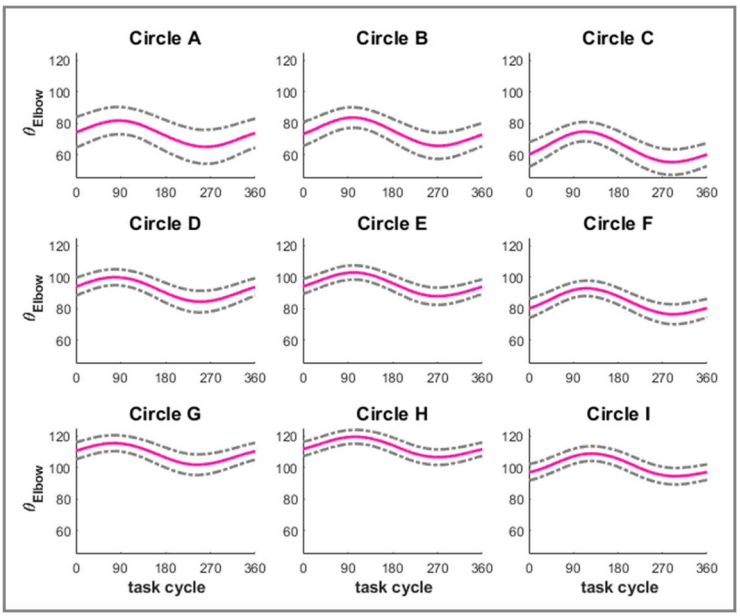

Figure 6.6. Upper limb elbow angles for the execution of circular trajectories (mean and plus/minus a standad deviation).

The shoulder and elbow angles, and participant upper limb segment lengths were used as inputs for the prediction of upper limb dexterity computed through the proposed Dexterity Analysis Method (see Chapter 5).

Figure 6.7 presents the estimated dexterity measure for all the circular trajectories. As can be noted, circular trajectories at positions D and E have high and stable dexterity values, whereas trajectories on C and H have low and unsteady dexterity values. Therefore, higher performance is expected for the execution of the task at A, D and E locations.

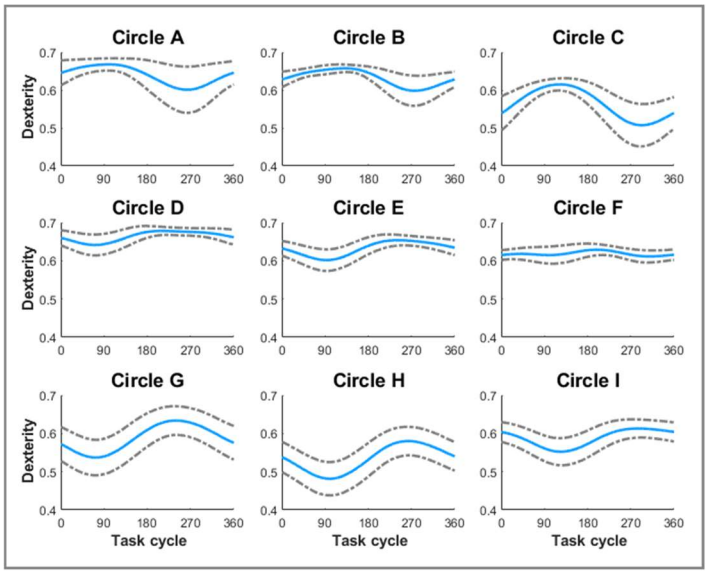

Figure 6.7. Upper limb dexterity measure for the execution of circular trajectories (mean and plus/minus a standad deviation).

Moreover, the position of the fifth metacarpal maker was used to approximate participant trajectories. Figure 6.8 illustrates the trajectories executed by a participant (blue) and the circular trajectories that should be followed (red).

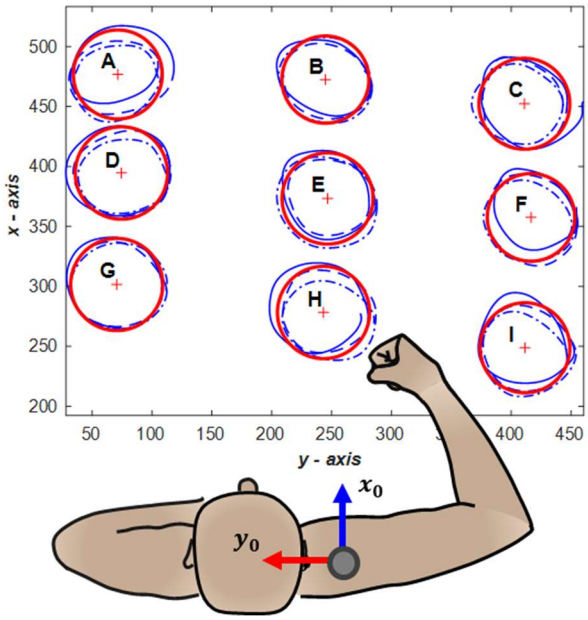

Figure 6.8. Executed trajectories by one of the participants (blue) and real circular trajectories (red).

As can be noticed, the executed participant trajectories were not exactly at the planed locations (with respect to the chest) as some participants tended to slightly rotate the trunk or move closer to the test board. However, this did not significantly affect the computation of prediction, perception and performance measures as those aspects were

assessed at the positions where the trajectories were executed, which were close to the planned locations.

Participant performance was assessed by quantifying the deviation of the trajectories executed by the participant from the target task trajectories. Such deviation from the task was obtained by computing the mean-squared-error (MSE) as follows:

$$Deviation = MSE = \frac{1}{n}\sum_{i=1}^{n}(x_i - \hat{x}_i)^2$$

Equation 6.1

Where $\hat{x}_i$ is the task trajectory, x is the trajectory executed by the participant, n is the number trajectories at each location, and i is the evaluated trajectory.

Figure 6.9 shows the mean-squared-error (MSE) for the 9 circular trajectories. As can be noticed, the curves present 2 peaks that occur mostly at the middle upper and bottom sides of the circular trajectories. During the experiments, it was also noticed that participants tend to execute ellipses instead of circles, which somehow agrees with the behaviour observed in these figures (peaks at middle sections of the trajectories).

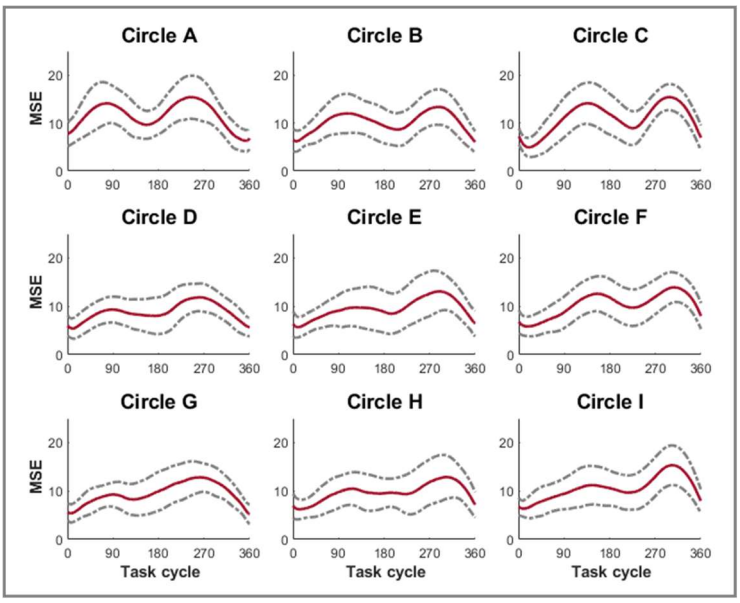

Figure 6.9. Upper limb performance measure (MSE) for the execution of circular trajectories (mean and plus/minus a standad deviation)

As participant trajectories tend to be elliptical instead of circular, an ellipse fit function was used to further analyse this aspect. As a result, it was observed that the elliptical trajectories executed by all the participants presented a similar behaviour, the ellipse main axis show a consistent angle of inclination. Therefore, it was decided to compute the manipulability ellipsoids to determine if there was a correlation between the ellipse fit

axis and the manipulability ellipsoids (see Section 5.1) that determine the directions of higher manipulability (see Figure 6.10). The results from the correlation analysis confirmed that the ellipse fit axis and the manipulability ellipsoid axis have a strong correlation coefficient of 0.87 with p value = 0.002. Therefore, it is believed that the upper limb tends to overshoot in directions of higher manipulability, which could be linked to the ease of performing movements in such directions. This implies the upper limb has less control in the directions in which it can move with more ease. However, this finding could be also linked to other factors such as muscle activation, muscle strength, and vision.

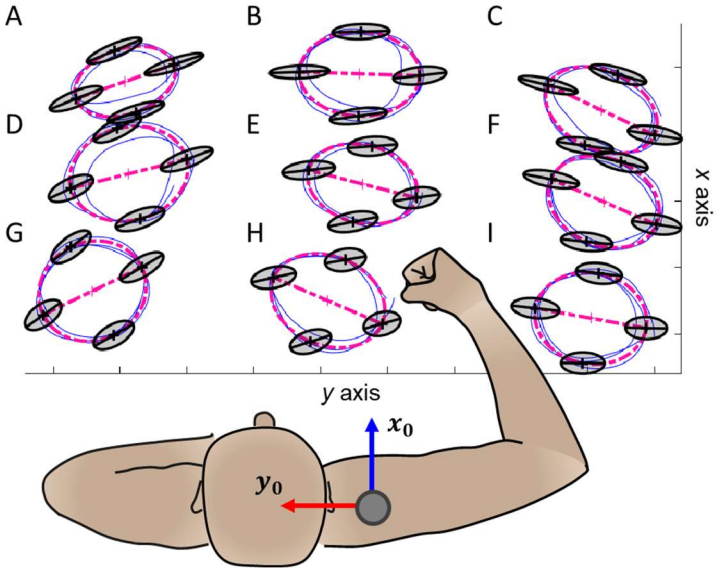

Figure 6.10. Trajectories executed by one of the participants (blue), participant trajectory ellipse fit (magenta), manipulability ellipsoids (grey).

Furthermore, participants were asked to rank circular trajectory positions from 1 to 9 based on comfort (where 9 is the highest). For this evaluation of comfort, participants were allowed to repeat the task as many times as needed.

Once prediction (dexterity), perception (comfort), and performance (accuracy) measures were obtained, a correlation analysis was conducted. However, as perception data was ordinal, prediction and performance data were also converted into ordinal data in order to conduct Spearman's rank correlation analysis for these 3 measures. Figure 6.11 show prediction, perception, and performance (ordinal data) for all circular trajectories and for all the participants. Likewise, Table 6.2 presents the correlation coefficients for the 3 measures.

As can be observed in Figure 6.11 and Table 6.2, the results cannot statistically prove nor disprove the hypothesis of the relationship between prediction (dexterity), perception

(comfort), and performance (accuracy). Although the results cannot demonstrate such relationships and the full potential of the analysis, these are only early indications but not a strong case to discard the potential of the methods proposed in this work. Likewise, the sample size is not sufficiently large to rely on the conducted statistical analysis. Nevertheless, by observation Figure 6.11, some interesting patterns and correlations can be clearly seen across participants like the perception of comfort for which most participants indicated that they perceived higher comfort for the positions “E” and “F” which are immediately in front and closer to the shoulder, whereas low comfort was perceived for positions further away and on the opposite side of the limb (positions “A”, ”B”, ”C”, ”D”, and “G”) . Similarly, the 3 measures for participants 3, 4 and 5, visually seem to be more related than what the numbers suggest. However, performance seems to have higher variability across participants, but at least visually, some correlations between prediction, perceptions and performance can be observed. For instance, both prediction and performance across participants seems to be higher for positions “D” and “E”, which indicate some sort of correlation.

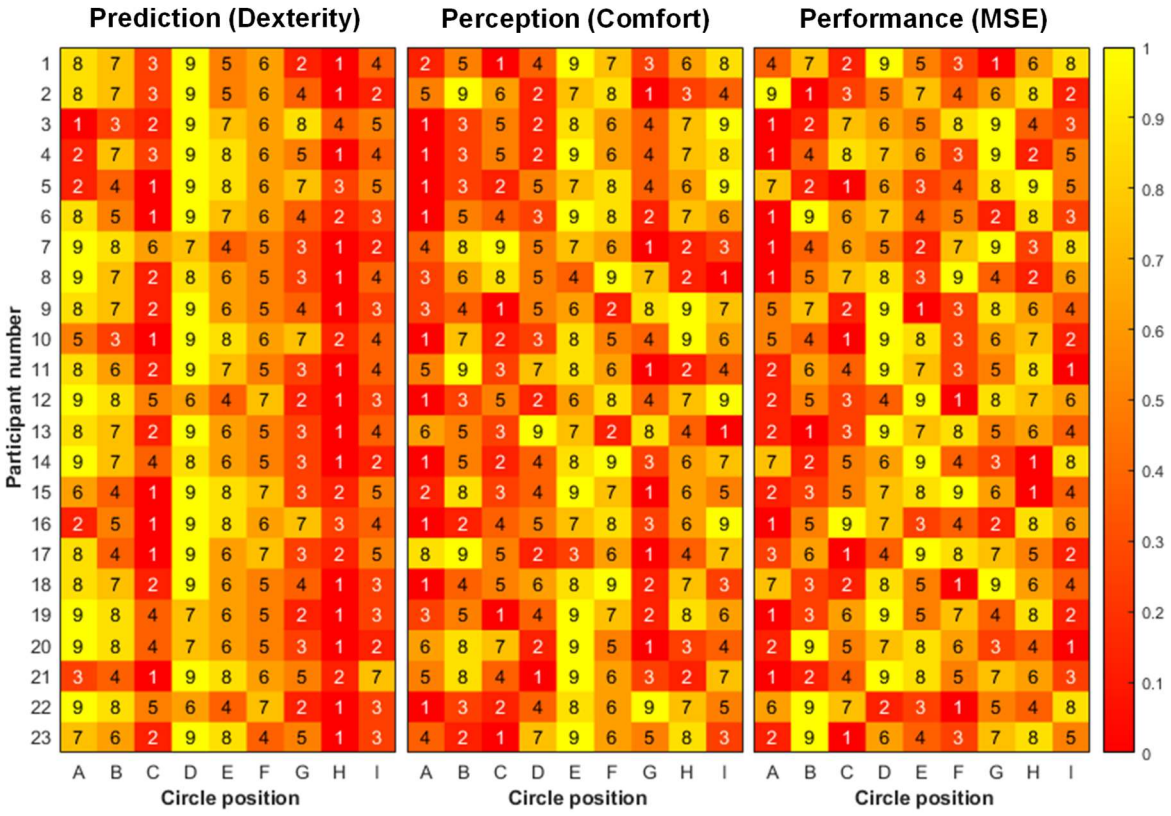

Figure 6.11. Prediction (dexterity), perception (comfort) and performance (MSE) ordinal data. High numbers in light yellow colour represent high values.

As can be seen in Table 6.2, the correlation values for prediction, perception and performance are inconsistent. Most participants have a positive correlation for

prediction-performance and perception-performance; however, some participants show a negative correlation (6 participants for each). Likewise, the correlation coefficient for prediction-perception is even more unbalanced with around 50% negative correlation coefficients.

Table 6.2. Spearman's rank correlation coefficients for prediction-performance, prediction-perception, and perception-performance. Sample size n=23, healthy participants.

N	$r_{pred/perf}$	p value	$r_{pred/perc}$	p value	$r_{perc/perf}$	p value
1	0.43	*0.25*	-0.07	*0.88*	0.42	*0.27*
2	0.05	*0.91*	0.20	*0.61*	-0.40	*0.29*
3	0.60	*0.10*	0.17	*0.68*	0.13	*0.74*
4	0.42	*0.27*	-0.03	*0.95*	0.07	*0.88*
5	0.13	*0.74*	0.52	*0.16*	0.07	*0.88*
6	-0.20	*0.61*	-0.17	*0.68*	0.33	*0.39*
7	-0.40	*0.29*	0.55	*0.13*	-0.25	*0.52*
8	-0.03	*0.95*	-0.07	*0.88*	0.58	*0.11*
9	0.33	*0.39*	-0.30	*0.44*	0.38	*0.31*
10	0.67	*0.06*	-0.10	*0.81*	0.25	*0.52*
11	0.12	*0.78*	0.75	*0.03*	0.22	*0.58*
12	-0.73	*0.03*	-0.55	*0.13*	0.20	*0.61*
13	0.07	*0.88*	0.48	*0.19*	0.25	*0.52*
14	0.33	*0.39*	-0.32	*0.41*	0.08	*0.84*
15	0.57	*0.12*	0.32	*0.41*	0.22	*0.58*
16	-0.27	*0.49*	0.25	*0.52*	0.30	*0.44*
17	0.18	*0.64*	0.07	*0.88*	-0.30	*0.44*
18	0.28	*0.46*	-0.13	*0.74*	-0.45	*0.23*
19	-0.30	*0.44*	-0.12	*0.78*	0.22	*0.58*
20	0.45	*0.23*	0.47	*0.21*	0.48	*0.19*
21	0.55	*0.13*	0.18	*0.64*	-0.38	*0.31*
22	0.08	*0.84*	-0.73	*0.03*	-0.45	*0.23*
23	0.02	*0.98*	0.30	*0.44*	0.20	*0.61*

Finally, the results presented in this section are only an early indication and not a strong positive or negative case in terms of validity for the methods. It is possible that the discrepancies occurred as a result of some model assumptions and the model parameters that still need calibration because some of the parameter values are approximation as such data is lacking in literature. Moreover, participants commonly struggled to appropriately rank the trajectory locations according to perceived comfort, maybe because we are not naturally trained to rank how we perceive things. Additionally, performance is strongly dependent on participants effort to execute the movements as precise as possible, participants could be fatigued, bored, or not willing to execute the

task as requested. Lastly, the accuracy of the result can be also affected by the experimental design, for instance, it was particularly difficult to fix participants torso or to keep the upper arm always a 100% parallel to the test board.

6.3 Summary

This chapter focused on the experimental analysis of the upper limb to determine the accuracy of the predictions obtained from the Dexterity Analysis Method. Therefore, 23 healthy participants were evaluated through experimental analysis that consisted of executing circular trajectories at 9 different locations on a new designed test board. As a result, 3 measures were obtained: prediction (dexterity), perception (comfort), and performance (accuracy). Finally, a correlation analysis was conducted to quantify the level of agreement for those measures.

First, although written and verbal instructions were given to the participants throughout the experiments, it was noticed that participants tend to slightly rotate the trunk and to move from the test board, which partly displaced the positions of the trajectories. However, this did not considerably affect the calculation of prediction, perception, and performance measures (as those were computed at the real location of the executed trajectory).

The required shoulder flexion for the execution of the circular trajectories was greater positions on the left column of the test board (around 60°), which proportionally decreased for the middle and right columns, respectively. Similarly, the required elbow flexion was smaller for circular trajectories on the row that is further away (around 70°) and increased by approximately 20 degrees as the circular trajectories got closer to the body. This joint angle characteristics for the execution of circular trajectories could be used for comparison of healthy and non-healthy populations.

Another finding is that the deviation of the participant trajectories from the corresponding task trajectories showed 2 peaks that occur mostly at the middle top and bottom sides of the circular trajectories, which somehow agrees with the observation of elliptical rather than circular trajectories.

The results of the correlation analysis are not conclusive. Although most participants showed a positive correlation for prediction-performance and perception-performance, other participants exhibited negative correlations. Similarly, the coefficient correlation for prediction-perception was around 50% negative and 50% positive. Discrepancies may have occurred as a result of model assumptions and the model parameters that still need calibration as some of the parameter values are approximation. Likewise, participants commonly struggled to appropriately rank the trajectory locations according to perceived

comfort, whereas performance was strongly dependent on participants effort to execute the movements (participants could be fatigued, bored, or not willing to execute the task as requested). Furthermore, experimental design related factors could also affect the results as it was hard to prevent participants from moving their torso whilst executing the movements. It is important to mention that the results presented in this section are only an early indication and not a strong positive or negative case in terms of validity for the methods. However, future work should consider the aspects previously mentioned and the possibility of appropriately modifying the experimental set up to increase the accuracy of the analysis.

Finally, an interesting finding was that the axis of the ellipse fit for participant trajectories and the axis of the manipulability ellipsoids have a strong correlation coefficient of 0.87 with p value = 0.002. This finding suggests that upper limbs tend to overshoot in directions of higher manipulability (ease of performing movements), which indicates that upper limbs have less control in such directions. Therefore, this finding is an interesting venue for further exploration of the use of the manipulability ellipsoids for the characterisation of human motion.

7 UPPER LIMB WORKSPACE WITH RESPECT TO DEXTERITY IN REVERSE SHOULDER ARTHROPLASTY (CASE STUDY)

The proposed novel method for the characterisation of human upper limb dexterity and its applicability to determine regions of low-high dexterity in both 2 and 3-dimentional spaces has been established and demonstrated in the previous chapters of this thesis work. The input values used in such previous analysis correspond to upper limb segment lengths and joint range of motion of healthy populations. However, the novel method proposed in this research can be used to analyse healthy and non-healthy individuals or populations. Therefore, a real case study is analysed in this section to demonstrate applicability of the method to real life situations such as clinical interventions for reverse shoulder arthroplasty. Arthroplasty refers to surgical interventions to repair joint functionality, whereas the term reverse shoulder refers to reversing the natural ball and socket mechanism of the shoulder by inverting the position of these elements (an artificial ball is attached to the anatomical socket and vice versa). Hence, the aim of the study presented here was to determine human upper limb workspace with respect to dexterity in reverse shoulder arthroplasty based on the scientific paper published by Keener et al. [28]. In such published work various implant configurations for glenoid and humeral reverse shoulder arthroplasty were evaluated in order to find the corresponding implant optimal positions. The paper provides all the values for joint range of motion given the evaluated implant configurations [28]. Such joint range of motion values were used here as inputs to determine upper limb workspace with respect to dexterity. Thus, the study presented in this section can be considered an extension to the investigation conducted by Keener et al. [28] and a demonstration of the applicability of the novel method proposed in this thesis work.

People with reverse shoulder arthroplasty suffer from reductions in joint range of motion. Therefore, in this research study, workspace volumes and high dexterity regions for non-healthy populations (with reverse shoulder arthroplasty) are believed to be directly impacted by reductions in joint range of motion and to be smaller than those for healthy populations. Likewise, high dexterity regions are anticipated to be proportional to workspace volume. The reductions in range of motion are quite dramatic for some implant configurations and that is expected to be clearly illustrated by the computed workspace volumes and high dexterity regions. Furthermore, it is assumed that the computed workspace volumes and high dexterity regions will be able to indicate which are the most affected workspace regions due to joint range reductions. Finally, the optimal implant position defined by Keener et al. [28] is believed to be close to the corresponding optimal implant position determined in this study.

7.1 Methodology and experimental protocol

The joint range of motion values used here as inputs to determine upper limb workspace with respect to dexterity were acquired from the work published by Keener et al. [28]. The author stated that the results presented in such investigation were obtained by studying shoulder computed tomography scans from 10 male participants (mean age = 61.5 years) with osteoarthritis and advanced posterior erosive glenoid deformities, such scans were analysed with Glenosys (Imascap, Brest, France) and Ascend Flex (Tornier; Bloomington, MN, USA) software to conduct range of motion analysis for various implant configurations in reverse shoulder arthroplasty. The implant variables investigated by Keener et al. [28] were glenoid component retroversion, glenoid base lateralization, humeral angle of inclination and humeral offset [28] (see Figure 7.1 and Table 7.1 and Table 7.2).

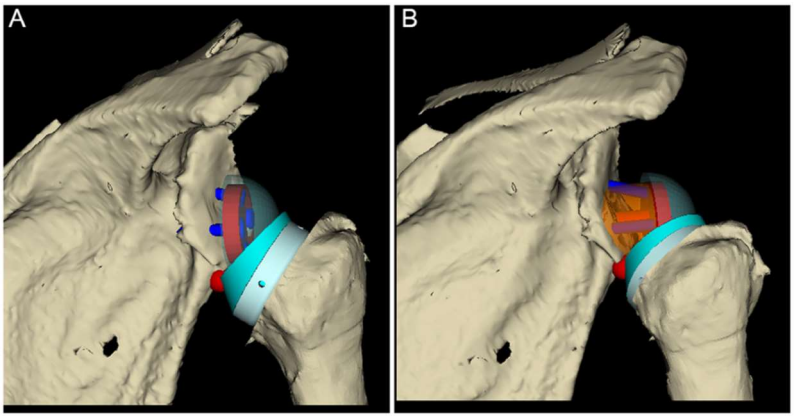

Figure 7.1. Glenoid and humeral implants for reverse shoulder arthroplasty with a base plate at 0mm lateralisation and 5° retroversion (left) and with a base plate at 10mm lateralisation (right). Mechanical contact is remarked with a red sphere. Copyright © 2018, Elsevier[17]

First, glenoid retroversion refers to the angle formed by the glenoid implant base and an imaginary line across the scapula on the horizontal plane. Second, glenoid base lateralization refers to the implant offset from the glenoid towards the lateral side of the body. Third, humeral angle of inclination (AOI) refers to the angle formed between the humeral implant and the imaginary humerus axis. Finally, the humerus offset refers to the distance of the plate from the prepared surface on the humerus head. The glenoid implant variables were independently studied to determine the optimal implant configu-

[17] Reprinted from Journal of Shoulder and Elbow Surgery, vol. 27, no. 2, Keener, J. D. et al., "Optimizing reverse shoulder arthroplasty component position in the setting of advanced arthritis with posterior glenoid erosion: a computer-enhanced range of motion analysis", pp. 339-349, copyright (2018), with permission from Elsevier.

Table 7.1. Joint range of motion (in degrees) for various glenoid implant configurations, source [28]. Data expressed as mean (standard deviation).

Lat (mm)	*Ret* (deg)	*Add* (deg)	*Abd* (deg)	*I.R.* (deg)	*E.R.* (deg)	*Ext* (deg)	*Fle* (deg)
0	***0***	1.2 (2)	79 (8.4)	33 (36)	4.3 (7.4)	6.1 (19)	74 (5.3)
0	***5***	1.1 (2)	82 (8.3)	39 (39)	3.5 (6.2)	5.6 (18)	80 (13)
0	***10***	0.9 (2.1)	84 (7.7)	47 (41)	2.2 (5.1)	1.1 (2.5)	86 (15)
0	***15***	0.8 (2)	84 (7.8	52 (45)	1.7 (4.2)	0.8 (2)	96 (18)
0	***20***	0.6 (1.4)	84 (9)	60 (47)	1 (2.3)	0.5 (1.2)	102 (20)
5	***0***	11 (7.7)	88 (10)	60 (29)	26 (17)	17 (14)	109 (34)
5	***5***	11 (8.2)	90 (10)	68 (27)	23 (16)	15 (13)	119 (32)
5	***10***	11 (8.6)	92 (11)	75 (27)	19 (16)	13 (11)	135 (26)
5	***15***	10 (9.7)	92 (12)	81 (28)	15 (15)	10 (10)	137 (23)
5	***20***	8.5 (10)	91 (13)	86 (28)	12 (13)	8.3 (9.3)	138 (19)
10	***0***	24 (10)	95 (11)	70 (19)	45 (13)	42 (25)	156 (29)
10	***5***	25 (11)	97 (12)	75 (18)	42 (12)	34 (15)	157 (22)
10	***10***	26 (12)	98 (13)	81 (17)	38 (12)	30 (13)	156 (19)
10	***15***	26 (15)	98 (13)	85 (16)	34 (12)	26 (12)	153 (17)
10	***20***	27 (17)	97 (14)	88 (15)	30 (11)	23 (11)	150 (17)

***Lat*, Lateralisation; *ret*, retroversion; *add*, adduction; *abd,* abduction; *i.r.,* internal rotation; *e.r.,* external rotation; *ext*, extension; *fle*, flexion.**

Table 7.2. Joint range of motion for various humeral implant configurations, source [28]. Data expressed as mean (standard deviation).

AOI (deg)	*Offset* (mm)	*Add* (deg)	*Abd* (deg)	*I.R.* (deg)	*E.R.* (deg)	*Ext* (deg)	*Fle* (deg)
135	***-3.5***	37 (11)	90 (11)	75 (11)	52 (9.1)	80 (36)	163 (19)
135	***0.0***	37 (11)	90 (11)	75 (11)	52 (9.1)	80 (36)	164 (18)
135	***3.5***	37 (11)	90 (13)	75 (11)	52 (9.1)	80 (36)	166 (13)
145	***-3.5***	22 (10)	98 (11)	69 (15)	40 (12)	33 (14)	155 (26)
145	***0.0***	22 (10)	97 (11)	69 (15)	40 (12)	33 (14)	155 (25)
145	***3.5***	22 (10)	97 (13)	69 (15)	40 (12)	33 (14)	157 (25)
155	***-3.5***	8.6 (9)	102 (11)	54 (30)	22 (17)	12 (12)	143 (27)
155	***0.0***	8.6 (9)	101 (11)	54 (30)	22 (17)	12 (12)	144 (27)
155	***3.5***	8.6 (9)	101 (13)	54 (30)	22 (17)	12 (12)	146 (28)

***AOI*, angle of inclination; *offset, medialised (-3.5), neutral (0) and lateralised (3.5) humerus*; *add*, adduction; *abd,* abduction; *i.r.,* internal rotation; *e.r.,* external rotation; *ext*, extension; *fle*, flexion.**

-rations (using a 145° humeral angle of inclination with no implant offset) [28]. Similarly, once the glenoid implant optimal position was determined, humeral implant configurations were investigated with fixed glenoid implant values at the corresponding optimal configuration (10mm of lateralization and 5° of retroversion) [28]. The estimated joint range of motion for shoulder abduction, adduction, flexion, extension, internal and external rotation given the various glenoid and humeral implant configurations are presented in Table 7.1 and Table 7.2 correspondingly. The data presented in Table 7.1 and Table 7.2 are the joint range of motion evaluated here to determine workspace and high dexterity regions. No information regarding implant joint coupling to determine range of motion for all configuration combinations has been provided by Keener et al. [28]. Therefore, such joint coupling was modelled under the assumptions and the method described in Section 4.3. Furthermore, Table 7.3 contains the complementary input values for upper limb segment lengths, limb segment weights (as a percentage of body weight), limb centres of mass (as a percentage of segment length), participant body weight, evaluated volume and gravity force. The upper limb segment lengths and the participant body weight presented in Table 7.3 correspond to mean values for British males.

Table 7.3. Upper limb anthropometric values, *x, y, z* ranges of the evaluated volume, and gravity force value. Statistical data source [39, 146]

Parameter	*Var.*	*Value*
Upper arm length (m)	$\boldsymbol{l_1}$	0.356
Forearm length (m)	$\boldsymbol{l_2}$	0.288
X range (m)	$\boldsymbol{X}$	$-1.05(l_1 + l_2) \leq \boldsymbol{X} \leq 1.05(l_1 + l_2)$
Y range (m)	$\boldsymbol{Y}$	$-1.05(l_1 + l_2) \leq \boldsymbol{Y} \leq 1.05(l_1 + l_2)$
Z range (m)	$\boldsymbol{Z}$	$-1.05(l_1 + l_2) \leq \boldsymbol{Z} \leq 1.05(l_1 + l_2)$
Upper Arm mass *(% body weight)*	$\boldsymbol{m_1}$	0.58
Forearm mass *(% body weight)*	$\boldsymbol{m_2}$	0.46
Upper arm centre of mass *(% segment length)*	$\boldsymbol{r_1}$	0.0271
Forearm centre of mass *(% segment length)*	$\boldsymbol{r_2}$	0.0162
Gravity *(N/kg)*	$\boldsymbol{g}$	9.81
Body weight (mean for British males) *(Kg)*	$\boldsymbol{\omega_T}$	83.00

Finally, high dexterity regions within the corresponding workspace volume for all the evaluated implant configurations were computed following the methods presented in Chapter 5. In the analysis presented in this chapter, high dexterity regions refer to the regions where the dexterity measure D_x is greater than 0.7 (in the scale 0-1, where 1 is the highest).

7.2 Analysis of human upper limb workspace with respect to dexterity in reverse shoulder arthroplasty

This section presents the results of the analysis conducted to determine upper limb workspace volumes and high dexterity regions for various implant configurations in reverse shoulder arthroplasty (following the methods described above). The results of the study are shown in Table 7.4 and Figure 7.3, Figure 7.4 and Figure 7.2.

Table 7.4. Workspace and high dexterity volumes for various glenoid implant configurations in reverse shoulder arthroplasty.

ID	*Implant side*	*Lat (mm)*	*Retro (deg)*	*AOI (deg)*	*Offset (mm)*	V_w (m^3)	V_{Dx} (m^3)
1	Glenoid	0	0	145	0	0.110	0.022
2	Glenoid	0	5	145	0	0.125	0.030
3	Glenoid	0	10	145	0	0.148	0.030
4	Glenoid	0	15	145	0	0.164	0.034
5	Glenoid	0	20	145	0	0.180	0.033
6	Glenoid	5	0	145	0	0.244	0.051
7	Glenoid	5	5	145	0	0.256	0.056
8	Glenoid	5	10	145	0	0.280	0.069
9	Glenoid	5	15	145	0	0.276	0.054
10	Glenoid	5	20	145	0	0.271	0.054
11	Glenoid	10	0	145	0	0.394	0.066
12	**Glenoid**	**10**	**5**	**145**	**0**	**0.403**	**0.081**
13	**Glenoid**	**10**	**10**	**145**	**0**	**0.406**	**0.078**
14	Glenoid	10	15	145	0	0.390	0.078
15	Glenoid	10	20	145	0	0.380	0.075
16	**Humeral**	**10**	**5**	**135**	**-3.5**	**0.462**	**0.065**
17	**Humeral**	**10**	**5**	**135**	**0**	**0.462**	**0.065**
18	**Humeral**	**10**	**5**	**135**	**3.5**	**0.463**	**0.065**
19	Humeral	10	5	145	-3.5	0.387	0.067
20	Humeral	10	5	145	0	0.386	0.079
21	Humeral	10	5	145	3.5	0.387	0.080
22	Humeral	10	5	155	-3.5	0.292	0.064
23	Humeral	10	5	155	0	0.292	0.067
24	Humeral	10	5	155	3.5	0.294	0.064

The first 15 rows of Table 7.4 correspond to the evaluated glenoid configurations, whereas rows 16 to 24 refer to the assessed humeral variables. The last two columns correspond to workspace volumes and high dexterity regions, respectively. A consistent increase in both workspace volume and high dexterity region was noticed while

lateralisation increased. Likewise, both workspace volumes and high dexterity regions steadily decreased as the humeral angle of inclination increased. In order to quantify such relationship, a correlation analysis was conducted, as a result, it was found that workspace volumes and high dexterity regions strongly correlate to glenoid lateralisation with coefficients of 0.99 and 0.96, respectively (Table 7.5). Similarly, a strong negative correlation of -1.00 between workspace volumes and humeral angle of inclination was found.

Table 7.5. Correlation analysis of glenoid lateralisation, glenoid retroversion, humeral angle of inclination and humeral offset on workspace volume and high dexterity regions.

	Lateralisation	*Retroversion*	*AOI*	*offset*
Workspace volume	0.99	0.10	-1.00	0.01
High dexterity regions	0.96	0.11	0.01	0.28

Figure 7.3, Figure 7.4 and Figure 7.2 illustrate workspace volumes (grey) and high dexterity (yellow) regions for various glenoid and humeral implant configurations in reverse shoulder arthroplasty. Each individual figure was identified with a number which corresponds to the evaluated implant configurations presented in Table 7.4. As can be observed in Figure 7.3 and Figure 7.2, the first 5 volumes show a very reduced workspace volume which demonstrate how limited the extremity would be with an implant with such parameter values. The workspace volumes and high dexterity regions for configurations 6-10 are larger than the previous volumes (1-5), with some volumes twice as large. As can be observed, the highest estimated workspace volume and high dexterity region for the evaluated glenoid configurations were achieved with 10mm glenoid lateralisation and 5-15° glenoid retroversion.

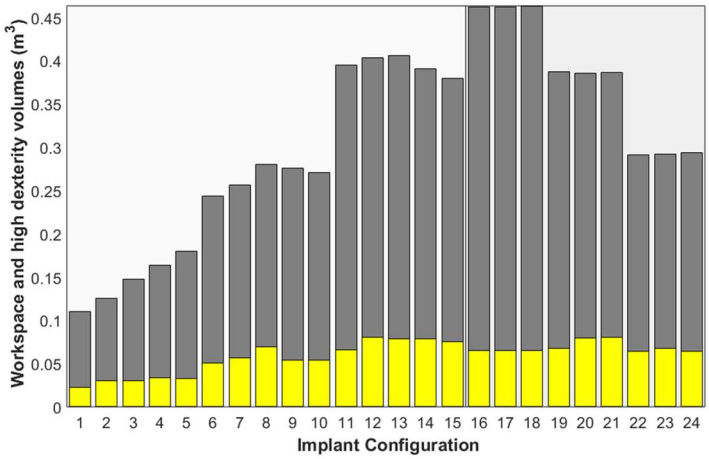

Figure 7.2. Workspace volumes (grey) and high dexterity regions (yellow) for various glenoid (1-15) and humeral (16-24) implant configurations.

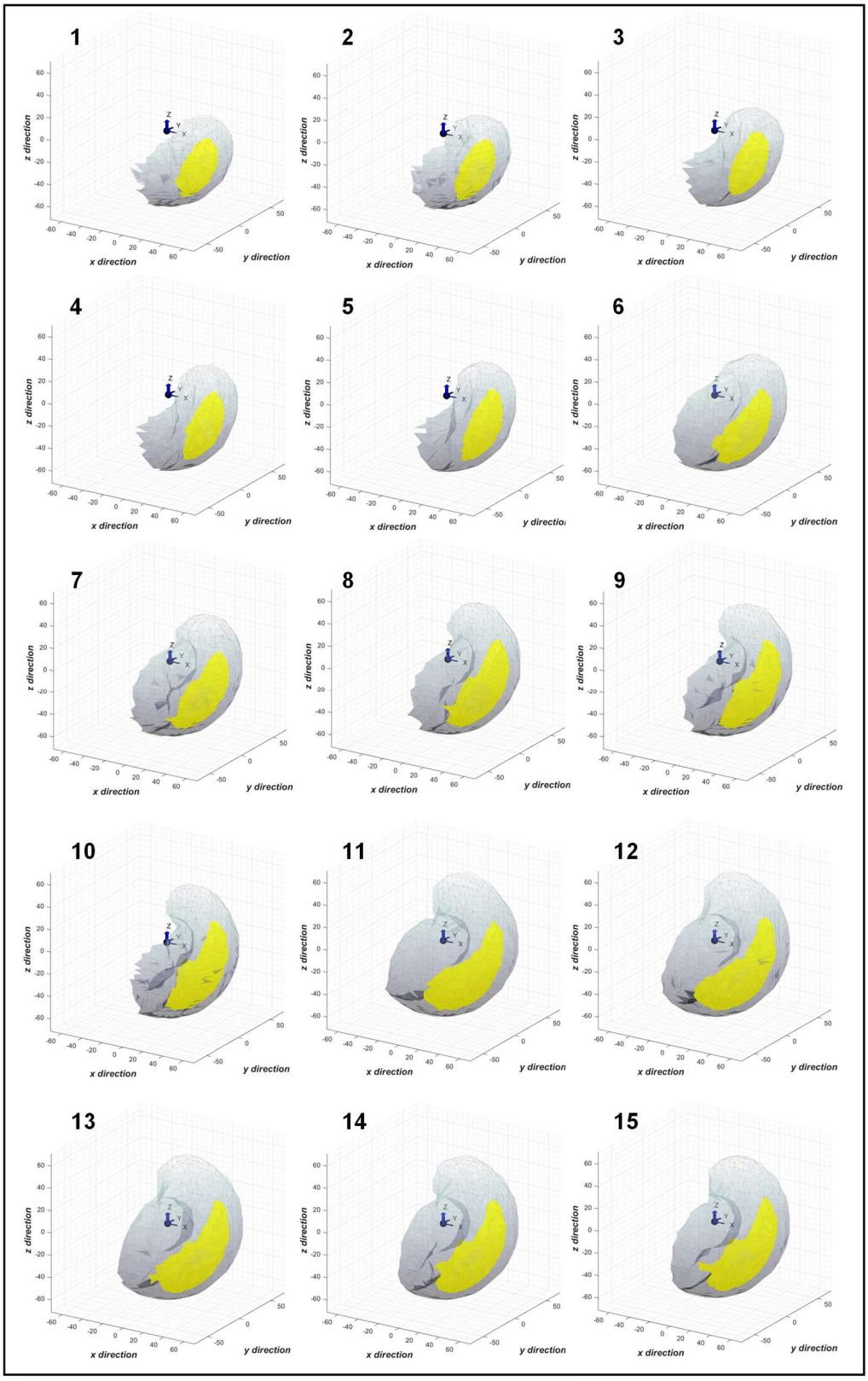

Figure 7.3. Workspace (grey) and high dexterity regions (yellow) for various glenoid implant configurations in reverse shoulder arthroplasty using a 145° humeral angle of inclination and no humeral implant offset.

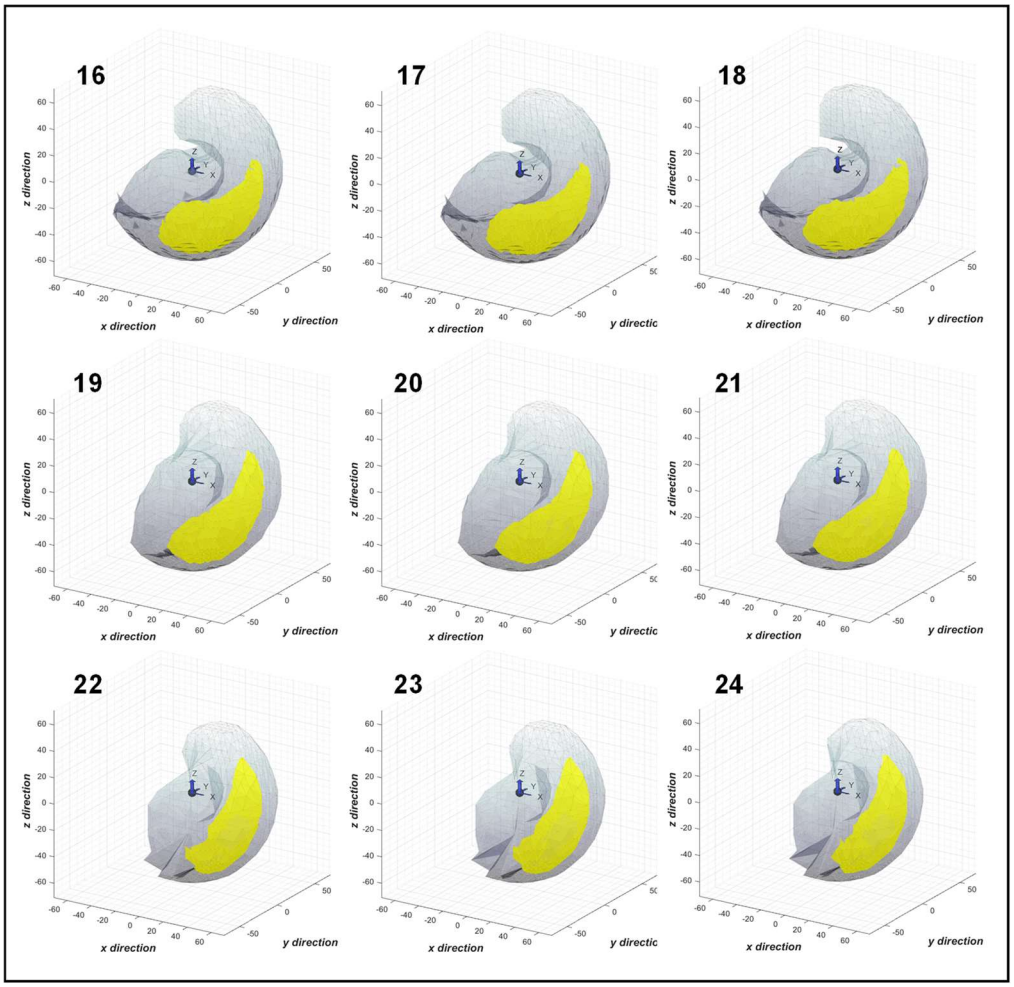

Figure 7.4. Workspace volumes (grey) and high dexterity regions (yellow) for various humeral implant configurations in reverse shoulder arthroplasty given an optimised glenoid position with 10mm of lateralization and 5° of retroversion.

However, as illustrated in Figure 7.4 and Figure 7.2, the largest workspace volume (given the optimal glenoid implant configuration) for the assessed humeral configurations was attained with a 135° humeral angle of inclination for any humeral lateral offset, whereas, the largest high dexterity region was achieved with a 145° humeral angle of inclination and 0-3.5mm humeral offset.

Therefore, the results suggest that optimal implant configuration with respect to workspace is attained with a 10mm glenoid lateralisation, 5-10° glenoid retroversion, 135° humeral angle of inclination, and any (-3.5 to 3.5mm) humeral lateralisation (see Table 7.4 and Figure 7.3, Figure 7.4 and Figure 7.2). However, according to the results, the optimal implant configuration with respect to high dexterity regions is achieved with 10mm glenoid lateralisation, 5-15° glenoid retroversion, 145° humeral angle of inclination, and 0-3.5mm humeral offset. Hence, the selection of the best implant

parameter values should consider both workspace volumes and high dexterity regions as, according to the results, only one of those aspects can be fully maximised. As the proposed dexterity measure may need adjusting and has not been fully validated, the recommendation is to give priority to workspace volume over high dexterity regions. Nevertheless, when possible and if increasing high dexterity regions do not sacrifice a great amount of workspace volume, both aspects should be balanced.

The first part of the study presented in this chapter focused on the evaluation of people with reverse shoulder arthroplasty. However, workspace and dexterity for healthy and non-healthy populations should be evaluated to understand and quantify the impacts of reverse shoulder arthroplasty on such aspects. Therefore, the second part of the study presented here analyses a healthy individual and an individual with reverse shoulder arthroplasty (optimal implant configuration with respect to workspace, configuration 17 in Table 7.4). The estimated workspace and high dexterity regions for both individuals are illustrated in Figure 7.5 and Figure 7.6.

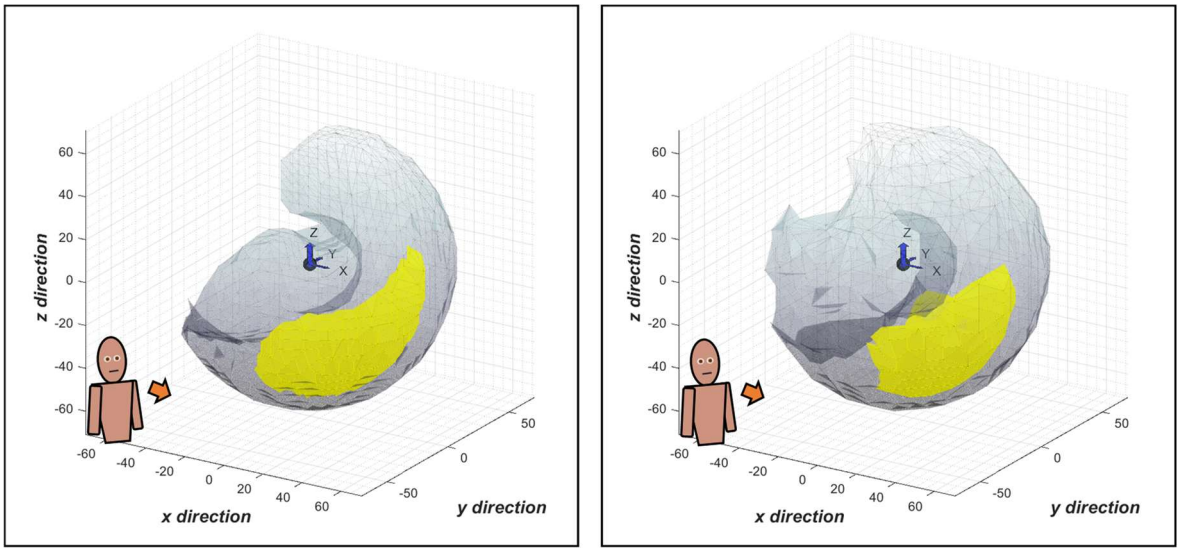

Figure 7.5. Estimated workspace volumes (grey) and high dexterity regions (yellow) for: an individual with optimal implant position in reverse shoulder arthroplasty (left) and a healthy individual(right). One view.

The estimated workspace volumes for the healthy individual and the individual with reverse shoulder arthroplasty were 0.611m^3 and 0.463m^3, and the high dexterity regions were 0.083m^3 and 0.065m^3, respectively. Thus, the workspace volume for a healthy individual is around 32% larger than the corresponding volume for an individual with reverse shoulder arthroplasty (optimal implant configuration). This is a significant difference for upper limb workspace reachability between the 2 individuals. As can be seen in Figure 7.6, it is noticeable that the workspace volume for the individual with reverse shoulder arthroplasty reduces primarily on the top right side of the workspace

volume. Similarly, the expected high dexterity region for a healthy individual is around 27% larger that the corresponding region for an individual with the selected implant configuration. Nevertheless, an individual with implant configuration 12 (see Table 7.4) and a healthy individual have similar high dexterity regions. However, the individual with the implant with such configuration would have a smaller workspace volume compared to an individual with implant configuration 17.

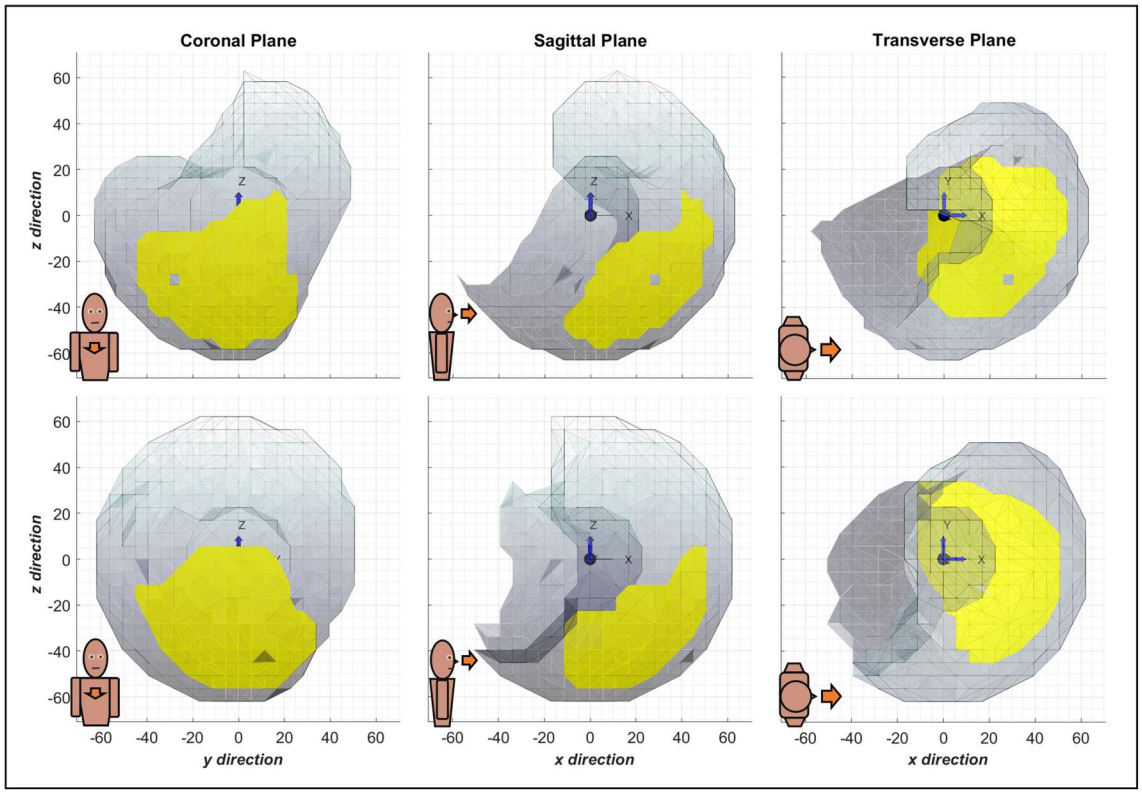

Figure 7.6. Estimated workspace volumes (grey) and high dexterity regions (yellow) for: an individual with optimal implant position in reverse shoulder arthroplasty (top row) and a healthy individual (bottom row). Three views: Coronal, Sagittal and Transverse planes.

7.3 Summary

This research work established a novel method for the characterisation of workspace with respect to dexterity, which can be used to analyse healthy and non-healthy individuals or populations. Therefore, in order to demonstrate the applicability of the method, this chapter centred on the study of human upper limb workspace with respect to dexterity in reverse shoulder arthroplasty based on the scientific paper published by Keener et al. [28].

First of all, no information related to the shoulder implant joint coupling with respect to range of motion for all configuration combinations was provided by Keener et al. [28]. Therefore, such joint coupling was modelled under the assumptions and the method

described in Section 4.3; the implant was assumed to have a similar behaviour than the human shoulder joint as it remains mechanically similar. However, further research should be conducted to determine if implant and human joints have similar mechanical behaviour, and to define the corresponding joint coupling. Understanding these aspects of both implant and human joints is essential for the creation of more realistic upper limb models.

A total of 24 implant configurations (see Table 7.4) including glenoid lateralisation, glenoid retroversion, humeral angle of inclination, and humeral offset were evaluated to determine upper limb workspace volumes and high dexterity regions. According to the results, workspace volumes and high dexterity regions strongly correlate to glenoid lateralisation with coefficients of 0.99 and 0.96, respectively. This finding suggests that greater glenoid lateralisation produce joint ranges of motion that result in larger workspace volumes and high dexterity regions. Similarly, a strong negative correlation of -1.00 between workspace volumes and humeral angle of inclination was found, which indicates that smaller humeral angles of inclination result in larger workspace volumes. However, the optimal value for humeral angle of inclination with respect to high dexterity regions seems to be 145°. Therefore, it is unknown if such behaviour and correlations remain for other non-evaluated values.

Furthermore, the results suggest that optimal implant configuration with respect to workspace is attained with a 10mm glenoid lateralisation, 5-10° glenoid retroversion, 135° humeral angle of inclination, and any (-3.5 to 3.5mm) humeral lateralisation. Whereas the optimal implant configuration with respect to high dexterity regions is achieved with 10mm glenoid lateralisation, 5-15° glenoid retroversion, 145° humeral angle of inclination, and 0-3.5mm humeral offset. This finding suggests that workspace volumes and high dexterity regions are not necessarily proportional, which opposes to the assumption of workspace volume and high dexterity region proportionality mentioned in the introduction of this chapter. Therefore, the best implant parameter values should be cautiously selected as, according to the results, only workspace volume or high dexterity region can be fully maximised. It is recommended to prioritise workspace volume as the proposed dexterity measure may need adjusting and has not been fully validated, and when possible, to keep workspace and high dexterity regions balanced (if increasing high dexterity regions do not sacrifice a great amount of workspace volume).

It is important to mention that the estimated optimal implant position described in the previous paragraph only predicts the best location in terms of upper limb reachability within the corresponding workspace. However, an optimal implant position should also

consider other factors such as joint stability, internal bone, and muscle interactions, torques and forces. Nevertheless, the inclusion of such factors in the analysis presented here was not part of the scope of this study.

Moreover, the analysis presented in this chapter was limited to the values provided by Keener et al. [28]. In the work published by Keener et al. [28], only the glenoid or the humeral variables were varied at a time whilst keeping the others fixed. In such study, the author used fixed 145° humeral angle of inclination and 0mm humeral offset to evaluate glenoid lateralisation and glenoid retroversion. However, it was observed that a 135° humeral angle of inclination can produce larger workspace volumes. Consequently, future work should explore implant configurations that include all possible combinations of glenoid and humeral parameters (and any other relevant variables).

The second part of the study comprehended the analysis of a healthy and a non-healthy individual (with reverse shoulder arthroplasty, implant configuration 17 in Table 7.4) to quantify the impact of reverse shoulder arthroplasty on workspace and dexterity. The results show that the estimated workspace volume for a healthy individual is around 32% larger than the corresponding volume for an individual with reverse shoulder arthroplasty (optimal implant configuration), which is a significant difference. This finding agrees with the assumption described in the introduction of this chapter in which healthy populations were expected to obtain larger workspaces volumes. According to the results, the most affected workspace region for an individual with implant would be the top-front-right side. Range of motion reductions on such region would complicate the execution of upper limb movements for activities that require reaching that side of workspace such as storing objects at high levels, operating machinery, changing a bulb, climbing, swimming, playing tennis, baseball, basketball, and volleyball.

Similarly, it was observed that the estimated high dexterity region for a healthy individual is around 27% larger than the corresponding region for an individual with reverse shoulder arthroplasty (optimal implant configuration). However, an individual with an implant configuration with 135° humeral angle of inclination (configuration 12 in Table 7.4) seem to have smaller workspace volume compared to an individual with optimal implant configuration (configuration 17 in Table 7.4) but larger high dexterity regions, similar to those for healthy populations. As already mentioned above, it is possible that other glenoid and humeral implant variable combinations can provide a more optimal implant configuration that can offer both workspace volumes and high dexterity regions closer to those for healthy populations.

The estimated optimal implant configuration with respect to workspace (in this study) agrees with the corresponding optimal implant location proposed by Keener et al. [28], as

initially assumed. However, the analysis presented in this section offers deeper insight regarding upper limb reachability and indicates which workspace regions are the most affected. Additionally, the analysis conducted here estimated high dexterity regions for all implant configurations to investigate the effect of implant location on upper limb performance. As can be noticed in the results, larger workspace volumes do not necessarily translate into greater high dexterity regions.

Finally, this chapter demonstrated the applicability of the novel method proposed in this thesis work to real life situations. The results indicate that the proposed method and its measure are quite promising as they can be used to define upper limb workspace volume and high dexterity regions for both healthy and non-healthy populations. The proposed method can be used to quantify 3-dimensional upper limb reachability and to identify the most affected workspace regions due to reductions in joint range of motion. Such method can also estimate regions of high dexterity within the corresponding workspace, which offer information regarding the regions where the upper limb is expected to have higher performance. Therefore, this method can be used in real life to optimise implant location, to predict upper limb performance, to compare and assess limb workspace and dexterity regions before and after surgery, as a reference for upper limb rehabilitation, for the design of limb prosthetics, for ergonomics, and for the design of workspace stations. Although the proposed novel method and its measure are quite promising, further research needs to be conducted in order to validate it.

8 DISCUSSION

The aim of the work presented in this thesis was to propose a novel method for the characterisation of human upper limb workspace with respect to dexterity, which was successfully established. This novel method, the Dexterity Analysis Method, is based on the representation of the upper limb as a kinematic chain, and on the principles of the manipulability analysis method [11, 12], widely used in robotics for robotic arm performance assessment. Moreover, the Dexterity Analysis Method incorporates a new comfort variable that is composed of various motion aspects associated with range of motion, limb self-weight and work. Such comfort variable had to be designed for this model as no published work defining comfort within the workspace was found. Therefore, human comfort is a concept that still needs to be explored and characterised in future research. In the experimental part of this research, participants were found to struggle to rank comfort across the experimental test board. Ranking comfort was expected to be an easy task; however, it was observed that comfort perception can be confusing, a probable reason is that self-evaluation of such subtle aspects is rarely requested. Finally, the designed comfort variable was added to the model as a penalty term alongside manipulability to obtain the proposed "dexterity measure". The dexterity measure encapsulates information regarding upper limb anthropometrics (segment lengths and joint range of motion), manipulability, and comfort, with reference to upper limb workspace volume. Until now there was no method that has proposed integrating manipulability, comfort, dexterity, and workspace. Thus, this work has coupled dexterity and workspace and thus established a novel method for the characterisation of upper limb workspace with respect to dexterity. This method enables surgeons to assess patients before and after clinical interventions, implant designers and surgeons to optimise implants based on its impact on workspace and dexterity, and designers to develop more ergonomic and efficient, devices, workplace stations and homes.

This research was both computational and experimental. Firstly, this research used a computational model that encodes the physical properties of the upper limb in terms of segment length and joint range of motion to simulate upper limb movements to compute workspace volume and high dexterity regions according to the dexterity analysis method. This computational modelling allows to study individuals by providing specific values of the person being studied, as well as specific populations based on published statistical data. Secondly, a novel experiment was designed for experimental testing to study upper limb performance, comfort, and dexterity, in order to establish a relationship among such factors and as an initial validation method.

Although some discussion was provided throughout this thesis work, this chapter focuses on the discussion of the most relevant findings of this research. The discussion is organised into 5 subsections to address upper limb motion modelling, joint range of motion, workspace, the dexterity analysis method, and future research. The upper limb motion modelling section focuses on the representation of the extremity as a kinematic chain, the assumptions, validity, and the importance of selecting an appropriate number of rigid and articulated elements to represent the system. The joint range of motion section addresses the importance of reliable range of motion statistical data and the characterisation of joint coupling for the development of accurate models. The workspace section focuses on previous work on the field and highlights the importance of incorporating workspace for the objective evaluation of upper limb performance and dexterity across 3-dimensional space. The dexterity analysis method section addresses the proposed novel method established in this research including a description of previous approaches, its application, strengths and weaknesses, and future improvements. Finally, the last subsection focuses on future work given the identified research gaps found in the literature review conducted for this study, and in the findings of this research.

8.1 Upper limb motion modelling – Kinematic chain representation

The study of upper limb motion is complex and challenging as the execution of movements requires of the cooperation of many systems of the body. Creating models that consider all the interactions among such systems would be ideal. However, in many cases, simplified models can be sufficient as long as they resemble the upper limb movement properties according to the aim of the study. The aim of this research project was to study and characterise workspace with respect to dexterity, in which the extremity is modelled as a system at the organism structural level; a system composed of the upper arm, forearm, and their corresponding interconnecting joints. Therefore, the extremity was modelled as a kinematic chain composed of 2 rigid elements (upper arm and forearm) and 2 joints (shoulder and elbow) with a total of 4 degrees of freedom. For simplicity, the current model represented the shoulder as a ball-and-socket joint, which a is common assumption for the analysis of the overall motion of the upper limb [29-35]. However, such assumption may not be valid for studies focused on the investigation of shoulder complex internal interactions, which require the addition of other rigid elements such as the clavicle and scapula. An example is the work published in [171] which models the extremity as 6 rigid elements (thorax, clavicle, scapula, humerus, ulna, and radius) constrained by 6 anatomical joints (3 degrees of freedom for each joint) for the study of joint muscle and joint reaction forces. Likewise, [172] models the shoulder as 3 segments

(clavicle, scapula, humerus) articulating at the sternum to study the motion coupling relationship between glenohumeral joint centre displacement relative to the thorax. The factors previously mentioned, as well as, other shoulder factors would be worth exploring in future versions of the model, particularly the translation of the glenohumeral joint centre of rotation as it could have a direct impact on upper limb workspace. However, it is unknown if such slight changes in the 3-dimensional limb reachability would have a relevant impact in the execution of activities of daily living.

Moreover, the current model excludes the hand for simplicity, as adding all the elements of the hand would represent including at least 19 more segments and at least another 15 joints. The reason behind such assumption is that the hand stays mostly fixed in a grasp position shape when performing activities that require object translation and manipulation. For instance, when drinking water from a glass the hand stays mostly in the same position after grasping the glass, or when hammering the hand also stays in a grasp shape. Therefore, adding the hand and all its elements in this first version of the model would add much complexity that could overshadow the results and validity of the model. However, future versions of the model should include the hand as some specific tasks such as drawing, writing, and manipulating watchmaker tools do require in-hand manipulation. An interesting observation is that relevant in-hand and full limb object manipulation and dexterity seem to happen rather separately. For example, watchmakers may slightly move their wrists whilst manipulating their tools, however, wrist location keeps mostly fixed, and the fine control of the tool mostly occurs in-hand. It does not mean that they never occur together, nevertheless, it seems reasonable to separate the study of in-hand and full limb object manipulation and dexterity, at least for first model iterations. However, it is relevant to evaluate the effects of the inclusion/exclusion of elements on upper limb workspace and dexterity. Therefore, future models should explore the interactions and effects of such elements.

Another important factor is the representation of the joint centre of rotation and the corresponding segment lengths. The values of such parameters were obtained from statistical data for the simulations and were estimated from the markers attached at specific body landmarks for the experimental analysis. In the model, the segments of the upper limb consisted of the upper arm (acromion to lateral epicondyle) and the forearm (lateral epicondyle to middle wrist). For simplicity, given that in this experiment the participants performed movements with the upper limb parallel to the horizontal plane, the centre of rotation of the elbow joint was assumed to coincide with the lateral epicondyle (a common assumption), whereas the glenohumeral joint was assumed to concur to the acromion. Although it is common to assume the elbow joint axis of rotation at the epicondyles, the real glenohumeral centre of rotation does not coincide with the

acromion. Published research work has demonstrated that estimation of the accurate centre of rotation of the glenohumeral joint is not trivial and such estimations have therefore high variability [156-164]. [162] found that the glenohumeral joint centre from the angulus acromialis (AA) ranges from 40-55mm on the forward(+)/backward(-) direction, -20 to 10mm on the lateral(+)/medial(-) direction, and -15 to -30mm on the upward(+)/downward(-) direction. However, [163] demonstrates that slight errors in the estimation of glenohumeral centre of rotation has little consequence on glenohumeral kinematics (root mean square error (RMSE) of 4.78°, 4.1°, and 2° in elevation, elevation plane, and axial rotation correspondingly). The effect of such an error (±5° on shoulder angle) for an average British male with an elbow angle of 90° would have an effect 0.7-1.2% on the computed dexterity measure in such limb configuration, which would not greatly impact the results. Thus, considering the shoulder and elbow at the acromion and epicondyles is sufficient for this preliminary studies.

Representing the extremity as a kinematic chain allows to explore and apply knowledge from other fields of science. One of the methods explored and implemented here was the manipulability analysis method [11, 12], which is widely used in robotics to evaluate the performance of robotic arms. Such method encodes the mechanical properties of the robotic arm, or in this case the limb, to mathematically define optimal configurations given the inherent kinematic and dynamic properties of the arm (further discussion on manipulability and how it was implemented in this study is addressed in Section 8.4). Likewise, the kinematic chain modelling approach allows multi-collaborative research across many fields of science to develop assistive devices, exoskeletons, machinery, and prosthetics. For instance, [173] studies robot programming via human arm motion, [132] develops an arm exoskeleton for neural rehabilitation, [174, 175] develop prosthetics that mimic the human extremity.

However, comparative analysis and the use of published data is sometimes confusing and complicated as terminology and standards differ across fields of science. In an attempt to provide standards for the report of kinematic data in biomechanics, the international society of biomechanics (ISB) published some recommendations. In [128] they promoted the use of global and local frames of reference to describe displacement and orientation of body movements, and in [129, 130] they proposed the use of specific terminology, defined anatomical landmarks, and a method for the assignation of body and joint coordinate systems for the upper and lower limbs. However, the adoption of such recommendations commonly fails, even the ISB technical sub committees seem to differ from each other, as clearly stated in [130] where the hand and wrist committee stated that they differ from the elbow section for the assignation of frames of reference. One reason why many researchers still fail or oppose to adopt the standards and conventions

proposed by the ISB could be that the committees responsible for the consensus of such recommendations may have a clinical and medical background and favour commonly used standards from such fields, and therefore exclude or have little consideration of standards used in other fields of science. As can be deducted, there is a need of collaborative effort among fields of science to adopt common standards and conventions to benefit the scientific community as the lack of formalization and standards slows down the scientific development.

In conclusion, representing a system as a kinematic chain is powerful as it allows to analyse the systems kinematics and dynamics. However, it is important to select the number segments and joints that represent the system according to the required accuracy and the aim of the study. Likewise, joint centres of rotation and body landmark references should be selected appropriately. Finally, the assignment of frames of reference and the conventions used in the study should also be carefully selected to benefit the fields that collaborate the most with the research being conducted.

8.2 Joint range of motion

Joints are probably the most important elements of a system in terms of motion, without articulated elements the system would not be able to perform motion. For simplicity, the current upper limb kinematic model, used to characterise workspace and dexterity, represents the shoulder and the elbow as a ball-and-socket and hinge joint with 3 and 1 degrees of freedom correspondingly. The limits of shoulder and elbow joint range of motion were assigned based on published statistical data. However, such published statistical data is inconsistent, difficult to objectively compare, and for some aspects such as joint coupling, lacking.

First, researchers measure joint range of motion using various methods and instruments, different body landmarks as reference, only on one plane of motion, with segments in a single configuration, for specific populations (only females/males, old/young, healthy/non-healthy, specific ethnicity), in active or passive mode, and consider only a few joints or degrees of freedom [39-43]. For instance, some researchers measure joint range of motion for internal-external shoulder rotation with the upper arm at 90° abduction and 0° adduction, whereas others measure it at 0° abduction and 0° adduction. Moreover, in some cases, authors do not even report sample size, sampling methods, and standard deviation [39-43]. Therefore, the objective comparison of the reported data is complicated. In this research, joint range of motion and anthropometric values were defined based on the published data provided by [39, 146]. Such values were used as a reference for the analysis of the British population. However, the ranges of motion

provided in such studies correspond only to males and the values may be slightly different from the current population due to secular variability. When possible, such values should be directly obtained from the individual or the population of interest to increase the accuracy of the results.

The combination of degrees of freedom of the shoulder and elbow joints allows the limb to reach the same locations with multiple limb configurations, and to perform tasks using different strategies without varying its overall performance. This concept of having more than one possible solution for the execution of a task is known as redundancy. Upper limb redundancy has been actively studied with the purpose of developing rehabilitation devices and exoskeletons [108, 112-116]. However, the investigation of redundancy and its relationship to upper limb dexterity is lacking in literature. The current model inherently accounts for upper limb redundancy when mapping 3-dimensional space to determine workspace volume, as the algorithm solves the inverse kinematics of the system to find a feasible solution given the mechanical properties of the extremity that include joint range of motion. The algorithm saves the mapped location for the computation of workspace volume if at least one feasible solution was found. However, a specific and explicit analysis and quantification of redundancy was not performed in this study. Thus, the study of redundancy and its effect on workspace and dexterity is a relevant research venue that should be explored in future investigations.

Another important factor when modelling upper limb motion is defining joint coupling, which refers to establishing internal joint interactions and absolute range of motion for each corresponding degree of freedom for every possible limb configuration. For instance, shoulder abduction-adduction range of motion is measured on the frontal plane with the limb fully extended and the palm facing forwards (0° shoulder flexion-extension). However, the limits of abduction-adduction range of motion are different when measured with 90° shoulder flexion, which is effectively being measured on the horizontal plane now. That may be the reason why some studies measure shoulder horizontal range of motion, in an attempt to provide extra information on the reachability of the upper limb given the lack of knowledge on shoulder joint coupling. Defining joint coupling is relevant for the creation of upper limb models that can accurately describe real limb behaviour. However, information about joint coupling and joint range of motion for all possible limb configurations is lacking in literature, which complicates the development of accurate human motion models. As joint coupling was needed in this research, shoulder range of motion for multiple limb configurations was approximated by self-observation. Such values were used to mathematically describe joint coupling by using a system of polynomial equations (see Section 4.3). Finally, this system of equations was used to approximate joint coupling for each virtual individual. The estimation of shoulder joint

coupling allowed the model and the algorithms to explore and quantify the upper limb workspace considering the mechanical properties of the limb. However, the values used to create the system of equations that describe the coupling are only an approximation, which could affect the accuracy of the results presented in this research. Therefore, reliable normative data is needed to establish valid models to describe the coupling of each joint of the body. Similar computational modelling approaches have been proposed in previous studies [30, 31, 176-178], which are based on the method established in [177]. Such works model shoulder joint coupling as a series of rotations that start with abduction-adduction, followed by flexion-extension, and finally rotation, in which joint range of motion depends on the prior joint configurations. Similar to the approach used in this thesis. However, [177] do not clearly explain how they derived joint limit values and how they validated the model. Alternative approaches use a globe coordinate system to represent shoulder motion as presented in [47] which describes shoulder abduction-adduction and flexion-extension as humeral elevation and humeral plane of elevation. The author states that such approach facilitates visual interpretation, however, describing the shoulder motion using a globe coordinate system would not solve the problem of creating a mathematical description of joint coupling.

In conclusion, joints are the most important elements of the body in terms of motion. Information regarding joint coupling is relevant for the development of realistic human motion models. However, such information is lacking in literature. This research contributes to closing such knowledge gap by proposing to measure joint range of motion with the limb in many (or all) configurations and then deriving a system of equations to define joint coupling as described in Section 4.3. Nevertheless, the values used to define joint coupling were only an approximation from self-observation and therefore future research should focus on providing normative data and creating validated joint coupling models.

8.3 Upper limb workspace

Upper limb workspace is directly related to joint range of motion, therefore, one of the main challenges to overcome to characterise workspace was defining a kinematic model and joint ranged of motion, as well as joint coupling. These aspects were discussed in previous subsections; thus, the following paragraphs only focus on workspace.

In this thesis work, workspace was estimated by mapping 3-dimensional space through simulations using the upper limb kinematic model, anthropometric and range of motion statistical data, and the joint coupling approach introduced in Chapter 4. A computational algorithm was created to simulate upper limb movements given its mechanical properties

defined in the kinematic model. Only feasible solutions were considered as reachable locations, then the cloud of reachable points was used to define the corresponding workspace volume. The novel approach to compute workspace established in this research contributes to closing knowledge gaps on the understanding of 3-dimensional reachability considering joint coupling within the analysis. However, the joint coupling values were approximations by self-observation as such data is lacking in literature. Moreover, the accuracy of the estimated workspace volume obtained in this study was not validated. However, both the shape and measure of the estimated workspace volume ($v = 0.566m^3$) are similar to the results obtained in [31] ($v = 0.667m^3$), although the results cannot be directly compared as the parameter values and the methodologies are slightly different, and whilst [31] considers some sort of joint coupling within the analysis, their approach is different.

The modelling approach established here to estimate workspace is a very powerful tool as it allows to evaluate 3-dimensional reachability of individuals and populations using direct measures or statistical data. Likewise, this type of computational models can help to study non accessible populations and to explore the effects of changes in the proportionality of the limb segments for the development of prosthetic devices. Workspace volumes provide visual and quantitative information regarding upper limb 3-dimensional reachability, which can help to analyse how the workspace volume shapes get affected by variations in joint range of motion derived from diseases, injuries, surgery, and aging. It was demonstrated in Chapter 7 which investigated how joint range of motion is affected by implants in reverse shoulder arthroplasty and illustrates how workspace volumes get deformed as a result of reductions in joint range of motion. Therefore, this research promotes the use of workspace volume as an objective measure and reference to evaluate and characterise upper limb performance and dexterity.

This research also investigated which parameters are more influential on workspace by conducting a sensitivity analysis (see Chapter 4). The results suggest shoulder adduction has the greatest impact on the upper limb 3-dimensional reachability, which compared to other joint limits is at least twice as influential. Unfortunately, the effect of shoulder adduction on upper limb performance was not found in scientific publications, and therefore, further analysis should be conducted to validate such finding.

It is important to mention that the computed workspace volume corresponds to a right limb. However, the methods presented in this research can be easily adjusted to estimate workspace volume for the left limb. Although, assuming that both limbs are healthy, the workspace volumes corresponding to a left extremity and their shapes are expected to be

similar but mirrored with slight variations due to intra-individual variability derived from body asymmetry.

In conclusion, workspace volumes can quantify and visually describe upper limb 3-dimensional reachability, and more importantly, can help to identify the most affected regions of workspace as a result of reductions in joint range of motion. However, little is unknown about the effects of reductions in specific regions of workspace on the upper limb performance and the execution of activities of daily living. This research has contributed to closing this gap by providing a method for the computation of workspace and by promoting the use of workspace volumes as an objective measure and to map other factors such as healthiness and dexterity within such workspace volumes. Nevertheless, future work should improve and validate the methods proposed here.

8.4 The Dexterity Analysis Method

This research focuses on the characterisation of upper limb workspace with respect to dexterity. Therefore, this thesis established a novel method for the characterisation of dexterity by developing a kinematic model that allows mimicking upper limb motion. Likewise, this work provided a method to define upper limb workspace volume taking into consideration shoulder joint coupling. Finally, a novel method was established to characterise workspace with respect to dexterity, which provides quantitative and visual information that can help to understand how segment lengths and joint range of motion affect upper limb 3-dimensonal reachability and dexterity. Thus, the novel method presented in this research can be a powerful tool to evaluate performance, assess healthiness, optimise implants and prosthetic devices, design ergonomic workplaces and homes, develop assistive devices, and conduct pre- and post-surgery evaluations.

Up until this research, the most common approach to evaluate upper limb dexterity is through time-dependent dexterity tests such as the Box and Block Test (BBT), Perdue Pegboard Test (PPT), Motor-free Visual Perceptual Test, Functional Dexterity Test, and Strength Dexterity Test [2-10]. Such tests focus on assessing the execution of tasks that require placing objects into their corresponding shapes/positions or moving objects from point a to point b, and although, such tests allow to quantify certain aspects of dexterity including grasp patterns and the ability to perform tasks over specific periods of time, they cannot distinguish movement consistency and movement variations among participants that have obtained similar scores. Likewise, such tests commonly evaluate dexterity in a single position in front of the participant at a fixed hight and cannot provide information on how participants perform across the full reachable 3-dimensional space. Another limitation of such tests is that they are time-dependent, and therefore cannot

determine if a person can actually perform a fine dexterous task regardless of time. For instance, high dexterity can be an important ability for a watchmaker, however, a watchmaker my not be interested in movement speed but rather on precision. Therefore, a time dexterity text may not be able to capture such ability as having a poor performance on a time-dependent test may not necessarily translate into lower dexterity, because such individual could be inherently slow or not being trained to conduct high speed tasks. Therefore, this research focused on establishing a method to contribute to close this knowledge gap by developing a time-independent novel method, the Dexterity Analysis Method (DAM), capable of characterising dexterity across the full reachable -3-dimensional space (workspace volume).

The dexterity analysis method starts by representing the upper limb as a kinematic chain, in which the rigid and articulated elements that represent the upper limb should be carefully selected according to the aim of the study. In this research the upper limb was represented as 2 rigid segments (upper arm and the forearm) interconnected through the shoulder (3-DOF) and elbow (1-DOF) joints. The next step is to define joint range of motion and joint coupling. Joint coupling is an important factor particularly for ball-and-socket joints or joint complexes composed of multiple internal joints. However, as up until now joint coupling data is lacking in literature, this aspect can be approximated by estimating joint range of motion for different limb configurations and by using polynomial equations to describe it (see Section 4.3). Then, workspace volume is computed by mapping the 3-dimensional space to find feasible solutions given the mechanical properties of the extremity (see Section 4.3). Subsequently, the manipulability analysis, a method widely used in robotics to evaluate the dexterity of robotic arms [11, 12, 24-27], is conducted to quantify upper limb manipulability within its workspace volume (see Chapter 5). The manipulability analysis was selected as it provides relevant information regarding performance and dexterity by mathematical analysis of the mechanical properties of kinematic chains, which was therefore explored and applied to characterise human dexterity. This method was previously used in biomechanics for the assessment of a user-friendly rehabilitation system [13], the analysis of wheelchair propulsion [14], and for the investigation of the upper-limb during grasping [15]. However, such studies directly apply the manipulability analysis method to study specific tasks and do not consider human factors. The Dexterity Analysis Method takes advantage of the information provided by the manipulability analysis, incorporates human factors included in a new variable called “comfort”, and provides a new measure called “dexterity measure”. Finally, the last step of the DAM is to map and assign the dexterity measure to its corresponding workspace volume location to provide quantitative and visual information regarding workspace and dexterity (see Section 5.7).

The dexterity analysis method is a powerful tool. The method is flexible, versatile, and scalable. It can be used to analyse real or virtual individuals or populations using direct measures or statistical data. Likewise, the DAM allows including and excluding segments and joints by modifying the kinematic model representation of the extremity, which do not require changes in the subsequent steps of the DAM. Moreover, the DAM allows adding human factors as penalisations, as well as assigning different weights to each factor, which permit adjustment and calibration as more precise information becomes available. Therefore, this research promotes the use of the dexterity analysis method for the characterisation of upper limb dexterity.

Chapter 7 demonstrated the applicability of the dexterity analysis method to a real-life situation by studying human upper limb workspace with respect to dexterity in reverse shoulder arthroplasty (based on the scientific paper published by Keener et al. [26]). In such study, 24 implant configurations were investigated including the glenoid lateralisation, glenoid retroversion, humeral angle of inclination, and humeral offset variables. As a result, the dexterity analysis method produced workspace volumes and high dexterity regions that allowed to determine the most optimal implant configuration. Moreover, a virtual healthy individual was compared to an individual with an optimal implant. The results indicate that workspace volumes and high dexterity regions for healthy individuals are expected to be around 32% and 27% larger than those for an individual with optimal implant. It was also found that larger workspace volumes do not necessarily translate into greater high dexterity regions. This finding is quite interesting as at the beginning of this research, workspace volume and high dexterity regions were believed to be proportional to each other. Therefore, it would be exciting to investigate why high dexterity regions can be in some cases larger for a smaller workspace volume compared to those for larger workspace volumes.

Although the dexterity analysis method is promising, it is not perfect and there are still areas for improvement. First of all, an experimental set up was designed to analyse the validity of the dexterity analysis method. The experiments consisted of executing circular trajectories on a test board specifically designed to study upper limb motion at 9 positions on the horizontal plane. Movements were recorded using a marker-based motion capture system. The participants were also asked to rank the 9 positions according to comfort. The movements were analysed following the dexterity analysis method to compute the dexterity measure for each location on the board. As a result, three measures were obtained: prediction (dexterity measure), performance (deviation from the task), and perception (relative comfort ranked by participants). Both performance and perception were hypothesised to be correlated to prediction or dexterity; however, the preliminary results were not conclusive, and therefore, the

dexterity analysis method could not be validated. Nonetheless, some patterns can be observed across participants. For instance, participants indicated that they perceived higher comfort for the positions “E” and “F” which are immediately in front and closer to the shoulder, whereas low comfort was perceived for positions further away and on the opposite side of the limb (positions “A”, “B”, “C”, “D”, and “G”). Likewise, both prediction and performance across participants seems to be higher for positions “D” and “E”, which indicate some sort of correlation. However, these are only early indications but not a strong case to discard the potential of the methods proposed in this work. Moreover, discrepancies could be derived from assumptions and the model parameters that still need calibration. Additionally, ranking locations according to perceived comfort was confusing to participants, one reason of this maybe that we are not naturally trained to rank how we perceive things. On the other hand, performance is strongly dependent on participants effort to execute the movements as precise as possible, participants could be fatigued, bored, or not willing to execute the task as requested. Other factors that could have affected accuracy are artifacts derived from the experimental design, an example was preventing participants to rotate their torso or to keep the upper limb completely parallel to the horizontal plane, which was particularly challenging. Finally, the experimental sample size is not sufficiently large to rely on the conducted statistical analysis.

Another important aspect is the oversimplification of the upper limb. The current model represents the upper limb with 2 segments (upper arm and forearm) interconnected through the shoulder and elbow with 3- and 1-DOFs correspondingly. However, the extremity is composed of 32 bones that connect to the trunk, and of more than 20 joints. For instance, the shoulder is represented here as a ball-and-socket joint, but in reality, it is composed of the scapula, clavicle and the head of the humerus, and each of these elements interconnect at the sternum, acromion, thorax, and glenoid. Hence, describing the internal interactions of the shoulder is challenging. Moreover, the analysis conducted in this research only focused on the right upper extremity, and therefore, the results are only valid for the right extremity. This concept referring to the use of the left or right extremity is called “handedness”, which is estimated to have a 1:10 ratio of left- versus right-handers worldwide. Handedness has been studied in previous research studies such as the work published by [179] which found that sinistral subjects had significantly smaller mean discrepancy scores in performance between their hands and much greater variance in performance than dextral subjects, [180] studied innate dexterity for endoscopic manipulations in medical students and found that right-handed males exhibited a greater level of ambidexterity, more-efficient task performance as measured by execution time, but no significant difference in terms of precision control and fine movements between

the three groups, and [181] studied handedness influence in bilateral shoulder range of motion in nonathlete adult women and found a statistically significance difference in external rotation (mean = 4.74°) and internal rotation (mean = 3.52°) between dominant and non-dominant shoulders. Therefore, as intra-variability is inherent in humans, left and right limbs are expected to have different values for segment lengths and joint range of motion, and therefore, workspace volumes and dexterity measures for a left extremity are expected to have variations, but to be generally similar in shapes and values but mirrored. Although the current model was developed for a right limb, the model can be easily adjusted to account for the variations derived from handedness.

As mentioned in the previous paragraphs, the current model is a simplified representation of the upper extremity and do not account for some of the factors already described. However, for the preliminary analysis produced in this research work, such simplification was necessary to reduce the variables of the model with the purpose of exploring and establishing a novel method for the characterisation of dexterity, which is by itself inherently challenging. Thus, the current model allowed to explore new methods such as the manipulability analysis method and facilitated experimental comparison between the results obtained from simulations and experiments. Nonetheless, future iterations of the model should include other elements and factors to improve the accuracy of the model and to investigate the influence of the excluded elements and factors in the overall workspace and dexterity.

In conclusion, the dexterity analysis method is a powerful tool to characterise upper limb workspace with respect to dexterity, which can help to evaluate performance, assess healthiness, optimise implants and prosthetic devices, design ergonomic workplaces and homes, develop assistive devices, and conduct pre- and post-surgery evaluations. The novel method proposed here promotes the use of workspace as an objective reference to map functionality, performance, healthiness, and dexterity. Likewise, this research promotes the use of the dexterity analysis method to characterise upper limb workspace with respect to dexterity with a time-independent approach. Therefore, this novel method directly contributes to closing the knowledge gaps on the understanding and quantification of motion, workspace, and dexterity. However, the method still needs to be fully validated as the experimental results obtained in this research with such purpose were not conclusive.

8.5 Future research

Knowledge gaps were identified whilst conducting this research work. Such gaps complicate the development of realistic human motion models and affect the accuracy of

the analysis in the field as some data is lacking in literature or require validation. The most relevant gaps regarding human motion are listed and described here as follows:

i. Establishment of standard methods for the report of results from human motion investigations. The International Society of Biomechanics [128-130] has attempted to implement a standard for the report of human kinematics; however, researchers in the field still report the results from human motion investigations using different standards and conventions. As discussed in Section 8.1, one reason for not following the recommendations published by the ISB may be that the standards do not agree with other conventions of fields that collaborate with biomechanics and human motion researchers. Independently of the reason behind the reluctancy to adopt the recommendations proposed by the ISB, clear standards and conventions are needed for the benefit of the scientific community as the lack of such standards slow down the progress in the field.

ii. Acquisition and report of reliable human normative data for human modelling. May studies have published anthropometric and joint range of motion data [39-43]; however, in such studies, the authors use various methods, instruments, reference points, study specific populations, and for range of motion, in many cases, only a few joints or degrees of freedom are reported. Nonetheless, complete, reliable, and accurate data are vital for the development of realistic human models for the study of motion. Although research to provide such kind of data may be boring or tedious, this information is still needed.

iii. Investigation and mathematical definition of human joint coupling. This aspect was probably one of the most relevant knowledge gaps to this research work because such information was vital to develop a realistic model to study and characterise upper limb 3-dimensional space and to map its corresponding dexterity within the workspace volume. However, information related to joint coupling is lacking in literature. Without such data, its difficult to establish the mathematical description and rules that joints must obey, and therefore, the exclusion of joint coupling results in unrealistic 3-dimensional movements.

iv. Investigation and report of typical workspace volumes for healthy populations. Workspace volumes are not commonly used in biomechanics and biomedical science to assess the upper extremity; however, workspace volumes are a powerful tool as they allow to characterise 3-dimensional reachability, and therefore, can be potentially used to map other measures related to healthiness, functionality, and dexterity, within their corresponding volume. However, information regarding workspace volume (3-dimensional reachability) for healthy

subjects was not found in literature. Nonetheless, the provision of such data would be very beneficial as it would serve as a reference for clinicians, ergonomic designers, assistive device developers, and for human motion researchers in general.

v. Investigation and quantification of human factors that affect dexterity including human comfort. Information regarding human comfort across the upper limb workspace is lacking in literature. Therefore, the dexterity analysis method established in this research designed a variable called comfort, which considers the configuration of the limb with respect to joint range of motion, and the forces action on the limb due to the segments self-weight. However, this variable is only an estimation of comfort given the lack of data on this factor. Therefore, accurate and validated data regarding comfort and other human factors would allow creating more realistic human modes based. Likewise, it would be interesting to investigate if such factors are individual or universal.

vi. Investigation and quantification of minimum, maximum, and typical joint angular velocities, accelerations, forces and torques for each degree of freedom of the upper limb individually. Such factors have been studied in previous investigations [14, 50, 51, 54, 131, 182, 183]. However, they only focus on the performance of specific tasks, movement synergies, and on the resultant values produced by the combination of all degrees of freedom. However, in order to create realistic models, such variables must be measured independently for every degree of freedom. For instance, the overall resultant shoulder velocity cannot be used as the velocity limit for the 3 degrees of freedom of the glenoid joint as the individual speeds that can be produced by each degree of freedom are expected to be different and dependent on movement direction. Therefore, future investigations should focus on the investigation and provision of such normative data.

vii. Investigation of scapulothoracic rhythm. The understanding and description of this aspect of the shoulder complex is challenging as its internal interactions depend on the combination of movements of the clavicle, scapula, and humerus. The understanding of scapulothoracic rhythm is limited and its mathematical description is lacking in literature. However, more complete and detailed models aiming to incorporate all segments and aspects of the upper extremity require reliable data and a correct mathematical description of scapulothoracic rhythm.

9 CONCLUSION

This chapter outlines the final conclusions, summarises the contributions of this research work to close knowledge gaps regarding human dexterity, and indicates venues for future work. The aim of this study was to establish a novel method for the characterisation of upper limb workspace with respect to dexterity. Therefore, after conducting a comprehensive literature review, defining a kinematic model for the analysis of upper limb motion, and investigating the factors that affect upper limb performance, a novel method called the "Dexterity Analysis Method" was successfully established. The Dexterity Analysis Method consists of 5 main steps: creating a kinematic model representation of the extremity, defining joint range of motion and joint coupling, computing workspace volume, obtaining the manipulability measure, and computing the dexterity measure to map it across workspace volume and to define high dexterity regions. The dexterity analysis method can help to optimise task location within the workspace volume, to optimise implant position based on workspace maximisation and high dexterity regions, to visually and quantifiably define how reductions in range of motion regions would affect workspace and dexterity volumes, to optimise sports performance, to assess and compare healthy and non-healthy individuals in terms of workspace and dexterity, to optimise workstation and home design, and to improve prosthetics development.

The main conclusions from this study are summarised as follows:

i. Human dexterity is a complex phenomenon associated with physiological and cognitive factors that affect the execution of precise movements. Capturing all aspects of dexterity in human models is quite challenging. Therefore, the inclusion and exclusion of dexterity factors in human modelling should be carefully considered depending on the scope of the study.

ii. Published normative data for joint range of motion is confusing, unclear, and difficult to compare. Moreover, not all authors report statistical information such as sample size, sampling methods and standard deviation. Furthermore, joint coupling and the corresponding joint ranges of motion for all possible limb configurations is lacking in literature. The lack of such information is quite problematic as it is needed for the creation of human models with realistic limb capabilities. Therefore, future work should focus on the development of standard methods for the assessment and report of human normative, as well as on conducting experimental analysis to provide reliable human normative data that can be used for human modelling. Consequently, open access research and data

are needed for the advancement in science and to close research gaps for the investigation of human motion.

iii. The Dexterity Analysis Method offers numerical and visual description of workspace volumes and dexterity regions that can be used for the characterisation of upper limb functionality and dexterity. Likewise, this visual information provided by the Dexterity Analysis Method help to comprehend how workspace volumes and dexterity regions deform and get affected by reductions in joint range of motion (and potentially by other human factors), and to identify the most affected regions of workspace and dexterity within their corresponding volumes. The dexterity analysis method is flexible, versatile, and scalable, that can be used to analyse real or virtual individuals or populations using direct measures or statistical data. Likewise, the dexterity analysis method can be easily adapted to include or exclude segments and joints, as well as to add, remove, and calibrate the model human factors as more precise information becomes available. Therefore, this research promotes the use of the dexterity analysis method for the characterisation of upper limb dexterity. Thus, the dexterity analysis method is a powerful tool to characterise upper limb workspace with respect to dexterity, which can help to evaluate performance, assess healthiness, optimise implants and prosthetic devices, design ergonomic workplaces and homes, develop assistive devices, and conduct pre- and post-surgery evaluations. However, the current model is based on a simplified upper limb representation and the method still needs to be fully validated as the experimental results obtained in this research were not conclusive.

iv. Upper limb reachability is commonly described by measuring joint range of motion on a single plane and with the limb segments in a single configuration (normally in neutral configuration). However, joint range of motion cannot fully portray 3-dimensional upper limb reachability. Therefore, this work proposes the use of workspace volumes, as an augmented method for the assessment of upper limb 3-dimensional reachability and as an objective reference to map other factors such as healthiness, performance, and dexterity, within such volumes.

v. This work introduced a “comfort” variable, which include human factors linked to dexterity. Such variable is composed of 3 comfort aspects associated with joint configuration with respect to the corresponding joint ROM, torques perceived at the shoulder due to limb self-weight, and work needed to rise the limb. The current comfort variable is composed of 3 aspects related to joint range of motion and limb self-weight; however, the variable can be easily modified to include or

exclude biomechanical and cognitive factors that may affect comfort and dexterity, and to adjust factor weights for each aspect of comfort as required. It is important to mention that the current comfort variable is only an estimation as information regarding comfort across workspace is lacking in literature. Therefore, further experimental analysis is needed to understand and quantify this, and other human factors associated with dexterity.

vi. According to the results, workspace volumes for healthy populations are expected to be significantly larger than those for non-healthy populations (individuals with injuries, surgeries, or diseases). However, it was found that larger workspace volumes do not necessarily translate into greater high dexterity regions, which indicate that people with similar workspace volumes do not necessarily have comparable performance. On the contrary, it is possible that people with smaller workspace volumes can have even greater dexterity than those with larger workspace volumes.

vii. The effect of reductions in range of motion on the overall upper limb reachability depends on the extreme at which such reductions occur. According to the results, a decrease of 15° in elbow extension reduces 2% of upper limb reach envelope area (2-dimensional reachability), whereas a decrease of 15° in elbow flexion reduces 10.8% of upper limb reach envelope area. Therefore, surgeons should be cautious when deciding which extreme of the range of motion should be reduced in cases of surgery, reconstruction, and implant position optimisation. As demonstrated in Chapter 7, the proposed Dexterity Analysis Method can help to assess the impacts of reductions in joint range of motion and therefore, to provide advice to surgeons before clinical intervention.

In conclusion, the development of human models that can accurately describe dexterity is extremely challenging. Therefore, this research work has established a novel method (Dexterity Analysis Method) for the characterisation of upper limb workspace with respect to dexterity. Such method is a direct contribution to closing the knowledge gaps on human motion and dexterity. Finally, although the Dexterity Analysis Method is quite promising, further experimental analysis is needed to fully validate this novel method as the results conducted here with such purpose were not conclusive.

REFERENCES

[1] M. L. Latash, M. T. Turvey, and N. A. Bernshteĭn, *Dexterity and its development*. Mahwah, N.J.: Erlbaum, 1996.

[2] D. D. N. Natta, E. Alagnidé, T. G. Kpadonou, C. Detrembleur, T. M. Lejeune, and G. G. Stoquart, "Box and block test in Beninese adults," *J REHABIL MED,* vol. 47, no. 10, pp. 970-973, 2015, doi: 10.2340/16501977-2023.

[3] F. Şahin, N. Ş. Atalay, N. Akkaya, and S. Aksoy, "Factors affecting the results of the functional dexterity test," *J HAND THER,* vol. 30, no. 1, pp. 74-79, 2016, doi: 10.1016/j.jht.2016.04.005.

[4] V. Gonzalez, J. Rowson, and A. Yoxall, "Development of the Variable Dexterity Test: Construction, reliability and validity," *INT J THER REHABIL,* vol. 22, no. 4, pp. 174-180, 2015.

[5] V. Gonzalez, J. Rowson, and A. Yoxall, "Analyzing finger interdependencies during the Purdue Pegboard Test and comparative activities of daily living," *J HAND THER,* vol. 30, no. 1, pp. 80-88, 2016, doi: 10.1016/j.jht.2016.04.002.

[6] C.-S. Song, "Relationship between visuo-perceptual function and manual dexterity in community-dwelling older adults," *J PHYS THER SCI,* vol. 27, no. 6, pp. 1871-1874, 2015, doi: 10.1589/jpts.27.1871.

[7] S. V. Duff, D. H. Aaron, G. R. Gogola, and F. J. Valero-Cuevas, "Innovative evaluation of dexterity in pediatrics," *J HAND THER,* vol. 28, no. 2, pp. 144-9; quiz 150, 2015, doi: 10.1016/j.jht.2015.01.004.

[8] Y. M. Choi, "Comparison of Grip and Pinch Strength in Adults with Dexterity Limitations to Normative Values," *Procedia Manufacturing,* vol. 3, pp. 5326-5333, 2015, doi: doi: 10.1016/j.promfg.2015.07.637.

[9] K. Kontson, I. Marcus, B. Myklebust, and E. Civillico, "Targeted box and blocks test: Normative data and comparison to standard tests," *PLoS One,* vol. 12, no. 5, p. e0177965, 2017, doi: 10.1371/journal.pone.0177965.

[10] P. Feys *et al.*, "The Nine-Hole Peg Test as a manual dexterity performance measure for multiple sclerosis," *Mult Scler,* vol. 23, no. 5, pp. 711-720, 2017, doi: 10.1177/1352458517690824.

[11] T. Yoshikawa, "Manipulability of Robotic Mechanisms," *The International Journal of Robotics Research,* vol. 4, no. 2, pp. 3-9, 1985, doi: 10.1177/027836498500400201.

[12] T. Yoshikawa, *Foundations of robotics : analysis and control / [electronic resource]*. Cambridge, Massachusetts : MIT Press, 2003.

[13] M. Yamashita, "Robotic Rehabilitation System for Human Upper Limbs Using Guide Control and Manipulability Ellipsoid Prediction," *Procedia Technology,* vol. 15, pp. 559-565, 2014, doi: 10.1016/j.protcy.2014.09.016.

[14] J. Jacquier-Bret, N. Louis, N. Rezzoug, and P. Gorce, "Manipulability of the upper limb during wheelchair propulsion," (in English), *Computer Methods in Biomechanics and Biomedical Engineering,* Meeting Abstract vol. 14, pp. 87-89, 2011, doi: 10.1080/10255842.2011.596350.

[15] J. Jacquier-Bret, N. Rezzoug, and P. Gorce, "Manipulability of the upper limb during grasping," *Computer Methods in Biomechanics and Biomedical Engineering,* vol. 13, no. sup1, pp. 73-75, 2010, doi: 10.1080/10255842.2010.493729.

[16] S. C. Venema and B. Hannaford, "A probabilistic representation of human workspace for use in the design of human interface mechanisms," *IEEE/ASME Transactions on Mechatronics,* vol. 6, no. 3, pp. 286-294, 2001, doi: 10.1109/3516.951366.

[17] A. Schiele and F. C. T. van der Helm, "Kinematic Design to Improve Ergonomics in Human Machine Interaction," *IEEE Trans Neural Syst Rehabil Eng,* vol. 14, no. 4, pp. 456-469, 2006, doi: 10.1109/TNSRE.2006.881565.

[18] E. Piña-Martínez, R. Roberts, S. Leal-Merlo, and E. Rodriguez-Leal, "Vision system-based design and assessment of a novel shoulder joint mechanism for an enhanced workspace upper limb exoskeleton," *Applied bionics and biomechanics,* vol. 2018, 2018, doi: 10.1155/2018/6019381.

[19] D. B. Chaffin, "Digital Human Modeling for Workspace Design," *Reviews of Human Factors and Ergonomics,* vol. 4, no. 1, pp. 41-74, 2008, doi: 10.1518/155723408X342844.

[20] M. A. Laribi, G. Carbone, and S. Zeghloul, "On the Optimal Design of Cable Driven Parallel Robot with a Prescribed Workspace for Upper Limb Rehabilitation Tasks," *Journal of Bionic Engineering,* vol. 16, no. 3, pp. 503-513, 2019, doi: 10.1007/s42235-019-0041-4.

[21] G. Kurillo, J. J. Han, R. T. Abresch, A. Nicorici, P. S. Yan, and R. Bajcsy, "Development and Application of Stereo Camera-Based Upper Extremity Workspace Evaluation in Patients with Neuromuscular Diseases," (in English), *Plos One,* Article vol. 7, no. 9, p. 10, Sep 2012, Art no. e45341, doi: 10.1371/journal.pone.0045341.

[22] R. P. Matthew, G. Kurillo, J. J. Han, and R. Bajcsy, "Calculating reachable workspace volume for use in quantitative medicine," vol. 8927, ed, 2015, pp. 570-583.

[23] J. Bai and A. Song, "Measurement and Analysis of Upper Limb Reachable Workspace for Post-stroke Patients," vol. 10984, ed, 2018, pp. 225-234.

[24] B. Bayle, J. Y. Fourquet, M. Renaud, and Ieee, "Manipulability analysis for mobile manipulators," in *IEEE International Conference on Robotics and Automation*, Seoul, South Korea, May 21-26 2001, NEW YORK: Ieee, in Ieee International Conference on Robotics and Automation, 2001, pp. 1251-1256. [Online]. Available: <Go to ISI>://WOS:000172615800200

[25] I. Mansouri and M. Ouali, "A new homogeneous manipulability measure of robot manipulators, based on power concept," (in English), *Mechatronics,* Article vol. 19, no. 6, pp. 927-944, Sep 2009, doi: 10.1016/j.mechatronics.2009.06.008.

[26] B. Siciliano, "The Tricept robot: Inverse kinematics, manipulability analysis and closed-loop direct kinematics algorithm," (in English), *Robotica,* Article vol. 17, pp. 437-445, Jul-Aug 1999, doi: 10.1017/s0263574799001678.

[27] Y. Tanaka, N. Yamada, K. Nishikawa, I. Masamori, and T. Tsuji, "Manipulability analysis of human arm movements during the operation of a variable- impedance controlled robot," ed. USA, 2005, pp. 1893-1898.

[28] J. D. Keener, B. M. Patterson, N. Orvets, A. W. Aleem, and A. M. Chamberlain, "Optimizing reverse shoulder arthroplasty component position in the setting of advanced arthritis with posterior glenoid erosion: a computer-enhanced range of motion analysis," *Journal of Shoulder and Elbow Surgery,* vol. 27, no. 2, pp. 339-349, 2018, doi: 10.1016/j.jse.2017.09.011.

[29] D. Haering, M. Raison, A. Arndt, and M. Begon, "Kinematic model and elbow flexion interaction on shoulder range of motion," *COMPUT METHOD BIOMEC,* vol. 17 Suppl 1, pp. 84-85, 2014, doi: 10.1080/10255842.2014.931150.

[30] N. Klopcar, M. Tomsic, and J. Lenarcic, "A kinematic model of the shoulder complex to evaluate the arm-reachable workspace," *J BIOMECH,* vol. 40, no. 1, pp. 86-91, 2007, doi: 10.1016/j.jbiomech.2005.11.010.

[31] N. Klopčar and J. Lenarčič, "Kinematic Model for Determination of Human Arm Reachable Workspace," (in eng), *Meccanica,* vol. 40, no. 2, pp. 203-219, 2005, doi: 10.1007/s11012-005-3067-0.

[32] B. Tondu, "A closed- form inverse kinematic modelling of a 7R anthropomorphic upper limb based on a joint parametrization," ed, 2006, pp. 390-397.

[33] X. Wang, "Three- dimensional kinematic analysis of influence of hand orientation and joint limits on the control of arm postures and movements," *Biological Cybernetics,* vol. 80, no. 6, pp. 449-463, 1999, doi: 10.1007/s004220050538.

[34] R. Raikova, "A general approach for modelling and mathematical investigation of the human upper limb," *Journal of Biomechanics,* vol. 25, no. 8, pp. 857-867, 1992, doi: 10.1016/0021-9290(92)90226-Q.

[35] P. Morasso, "Spatial control of arm movements," (in English), *Experimental Brain Research,* Note vol. 42, no. 2, pp. 223-227, 1981.

[36] G. J. Tortora, *Principles of anatomy & physiology*, 14th; EMEA ed. (Principles of anatomy and physiology). Hoboken, NJ: Wiley, 2014.

[37] S. J. Hall, *Basic biomechanics*, 6th; International ed. New York: McGraw-Hill, 2012.

[38] S. J. Hall, *Basic biomechanics*, Seventh; International ed. New York, NY: McGraw-Hill Education, 2015.

[39] D. C. Boone and S. P. Azen, "Normal range of motion of joints in male subjects," *The Journal of bone and joint surgery. American volume,* vol. 61, no. 5, p. 756, 1979.

[40] I. Gûnal, N. Köse, O. Erdogan, E. Göktürk, and S. Seber, "Normal range of motion of the joints of the upper extremity in male subjects, with special reference to side," *The Journal of bone and joint surgery. American volume,* vol. 78, no. 9, p. 1401, 1996.

[41] J. M. Soucie *et al.*, "Range of motion measurements: reference values and a database for comparison studies," *Haemophilia,* vol. 17, no. 3, pp. 500-507, 2011, doi: 10.1111/j.1365-2516.2010.02399.x.

[42] N. B. Stubbs, J. E. Fernandez, and W. M. Glenn, "Normative data on joint ranges of motion of 25- to 54- year- old males," *International Journal of Industrial Ergonomics,* vol. 12, no. 4, pp. 265-272, 1993, doi: 10.1016/0169-8141(93)90096-V.

[43] N. Doriot and X. G. Wang, "Effects of age and gender on maximum voluntary range of motion of the upper body joints," (in English), *Ergonomics,* Article vol. 49, no. 3, pp. 269-281, Feb 2006, doi: 10.1080/00140130500489873.

[44] M. F. Welsh, R. T. Willing, J. W. Giles, G. S. Athwal, and J. A. Johnson, "A rigid body model for the assessment of glenohumeral joint mechanics: Influence of osseous defects on range of motion and dislocation," *Journal of Biomechanics,* vol. 49, no. 4, pp. 514-519, 2016, doi: 10.1016/j.jbiomech.2015.11.001.

[45] R. T. Willing, M. Nishiwaki, J. A. Johnson, G. J. W. King, and G. S. Athwal, "Evaluation of a computational model to predict elbow range of motion," *COMPUT AIDED SURG,* vol. 19, no. 4-6, pp. 57-63, 2014, doi: 10.3109/10929088.2014.886083.

[46] S. Gutiérrez *et al.*, "Evaluation of abduction range of motion and avoidance of inferior scapular impingement in a reverse shoulder model," *Journal of Shoulder and Elbow Surgery,* vol. 17, no. 4, pp. 608-615, 2008, doi: 10.1016/j.jse.2007.11.010.

[47] D. Gates, L. Walters, J. Cowley, J. Wilken, and L. Resnik, "Range of Motion Requirements for Upper- Limb Activities of Daily Living," *The American Journal of Occupational Therapy,* vol. 70, no. 1, pp. 1-50, 2016, doi: 10.5014/ajot.2016.015487.

[48] A. M. Oosterwijk, M. K. Nieuwenhuis, C. P. van der Schans, and L. J. Mouton, "Shoulder and elbow range of motion for the performance of activities of daily living: a systematic review," *Physiotherapy theory and practice,* vol. 34, no. 7, pp. 505-528, 2018, doi: 10.1080/09593985.2017.1422206.

[49] S. A. F. Taylor, A. E. Kedgley, A. Humphries, and A. F. Shaheen, "Simulated activities of daily living do not replicate functional upper limb movement or reduce movement variability," *J Biomech,* vol. 76, pp. 119-128, 2018, doi: 10.1016/j.jbiomech.2018.05.040.

[50] G. S. Fleisig *et al.*, "Kinetic comparison among the fastball, curveball, change-up, and slider in collegiate baseball pitchers," (in English), *American Journal of Sports Medicine,* Article vol. 34, no. 3, pp. 423-430, Mar 2006, doi: 10.1177/0363546505280431.

[51] B. Elliott, G. Fleisig, R. Nicholls, and R. Escamilia, "Technique effects on upper limb loading in the tennis serve," (in English), *Journal of Science and Medicine in Sport,* Article vol. 6, no. 1, pp. 76-87, Mar 2003, doi: 10.1016/s1440-2440(03)80011-7.

[52] B. M. Joseph, G. L. Kevin, R. P. Maria, P. B. James, and M. L. Scott, "Glenohumeral Range of Motion Deficits and Posterior Shoulder Tightness in Throwers With Pathologic Internal Impingement," (in eng), *The American journal of sports medicine,* vol. 34, no. 3, pp. 385-391, 2006, doi: 10.1177/0363546505281804.

[53] E. Shanley, M. J. Rauh, L. A. Michener, T. S. Ellenbecker, J. C. Garrison, and C. A. Thigpen, "Shoulder Range of Motion Measures as Risk Factors for Shoulder and Elbow Injuries in High School Softball and Baseball Players," (in eng), *The American journal of sports medicine,* vol. 39, no. 9, pp. 1997-2006, 2011, doi: 10.1177/0363546511408876.

[54] K. Laudner, R. Wong, D. Evans, and K. Meister, "The effects of restricted glenohumeral horizontal adduction motion on shoulder and elbow forces in collegiate baseball pitchers," (in eng), *Journal of shoulder and elbow surgery,* vol. 30, no. 2, pp. 396-400, 2021, doi: 10.1016/j.jse.2020.05.029.

[55] M. Marzke, "Precision grips, hand morphology, and tools," *American journal of physical anthropology,* vol. 102, no. 1, pp. 91-110, 1997, doi: 10.1002/(SICI)1096-8644(199701)102:1<91::AID-AJPA8>3.0.CO;2-G.

[56] J. M. Landsmeer, "Power grip and precision handling," *Annals of the rheumatic diseases,* vol. 21, pp. 164-170, 1962.

[57] N. J. R., "The prehensile movements of the human hand," *The Journal of Bone and Joint Surgery. British volume,* vol. 38-B, no. 4, pp. 902-913, 1956.

[58] J. Napier, "The evolution of the hand," *Scientific American,* vol. 207, pp. 56-62, 1962.

[59] N. Kamakura, M. Matsuo, H. Ishii, F. Mitsuboshi, and Y. Miura, "Patterns of static prehension in normal hands," *The American journal of occupational therapy : official publication of the American Occupational Therapy Association,* vol. 34, no. 7, p. 437, 1980, doi: 10.5014/ajot.34.7.437.

[60] M. R. Cutkosky, "On grasp choice, grasp models, and the design of hands for manufacturing tasks," *Robotics and Automation, IEEE Transactions on,* vol. 5, no. 3, pp. 269-279, 1989, doi: 10.1109/70.34763.
[61] M. Cutkosky and P. Wright, "Modeling manufacturing grips and correlations with the design of robotic hands," vol. 3, ed, 1986, pp. 1533-1539.
[62] T. Feix, J. Romero, H.-B. Schmiedmayer, A. M. Dollar, and D. Kragic, "The GRASP Taxonomy of Human Grasp Types," *Human-Machine Systems, IEEE Transactions on,* vol. 46, no. 1, pp. 66-77, 2016, doi: 10.1109/THMS.2015.2470657.
[63] J. B. J. Smeets and E. Brenner, "A new view on grasping," (in English), *Motor Control,* Article vol. 3, no. 3, pp. 237-271, Jul 1999, doi: 10.1123/mcj.3.3.237.
[64] R. N. Lemon, R. S. Johansson, and G. Westling, "Corticospinal control during reach, grasp, and precision lift in man," *The Journal of neuroscience : the official journal of the Society for Neuroscience,* vol. 15, no. 9, p. 6145, 1995.
[65] M. Santello, M. Flanders, and J. Soechting, "Postural Hand Synergies for Tool Use," *Journal of Neuroscience,* vol. 18, no. 23, pp. 10105-10115, 1998.
[66] V. Gonzalez Sanchez, "Development of a dexterity assessment method," ed. Sheffield, UK: University of Sheffield;Faculty of Engineering (Sheffield);Mechanical Engineering (Sheffield), 2016.
[67] A. Yoxall *et al.*, "Getting to grips with packaging: using ethnography and computer simulation to understand hand–pack interaction," *Packaging Technology and Science,* vol. 20, no. 3, pp. 217-229, 2007, doi: 10.1002/pts.755.
[68] A. Yoxall, J. Luxmoore, J. Rowson, J. Langley, and R. Janson, "Size does matter: further studies in hand– pack interaction using computer simulation," *Packaging Technology and Science,* vol. 21, no. 2, pp. 61-72, 2008, doi: 10.1002/pts.778.
[69] J. Rowson and A. Yoxall, "Hold, grasp, clutch or grab: Consumer grip choices during food container opening," *Applied Ergonomics,* vol. 42, no. 5, pp. 627-633, 2011, doi: 10.1016/j.apergo.2010.12.001.
[70] J. Z. Zheng, S. De La Rosa, and A. M. Dollar, "An investigation of grasp type and frequency in daily household and machine shop tasks," ed, 2011, pp. 4169-4175.
[71] I. M. Bullock, J. Z. Zheng, S. D. L. Rosa, C. Guertler, and A. M. Dollar, "Grasp Frequency and Usage in Daily Household and Machine Shop Tasks," *Haptics, IEEE Transactions on,* vol. 6, no. 3, pp. 296-308, 2013, doi: 10.1109/TOH.2013.6.
[72] R. Deimel and O. Brock, "A novel type of compliant and underactuated robotic hand for dexterous grasping," *The International Journal of Robotics Research,* vol. 35, no. 1-3, pp. 161-185, 2016, doi: 10.1177/0278364915592961.
[73] M. Benati, S. Gaglio, P. Morasso, V. Tagliasco, and R. Zaccaria, "Anthropomorphic robotics," *Biological Cybernetics,* vol. 38, no. 3, pp. 125-140, 1980, doi: 10.1007/BF00337402.
[74] W. Abend, E. Bizzi, and P. Morasso, "Human arm trajectory formation," *Brain,* vol. 105, no. 2, pp. 331-348, 1982, doi: 10.1093/brain/105.2.331.
[75] P. Morasso, "Three dimensional arm trajectories," *Biological Cybernetics,* vol. 48, no. 3, pp. 187-194, 1983, doi: 10.1007/BF00318086.
[76] G. Redding and B. Wallace, "Adaptive spatial alignment and strategic perceptual-motor control," *Journal of Experimental Psychology,* vol. 22, no. 2, p. 379, 1996, doi: 10.1037/0096-1523.22.2.379.

[77] M. Kawato, "Internal models for motor control and trajectory planning," *Current Opinion in Neurobiology,* vol. 9, no. 6, pp. 718-727, 1999, doi: 10.1016/S0959-4388(99)00028-8.

[78] L. Williams, N. Pirouz, J. C. Mizelle, W. Cusack, R. Kistenberg, and L. A. Wheaton, "Remodeling of cortical activity for motor control following upper limb loss," *Clin Neurophysiol,* vol. 127, no. 9, pp. 3128-3134, 2016, doi: 10.1016/j.clinph.2016.07.004.

[79] E. Musk, "An Integrated Brain-Machine Interface Platform With Thousands of Channels," *J Med Internet Res,* vol. 21, no. 10, p. e16194, 2019, doi: 10.2196/16194.

[80] S. A. Jax, D. A. Rosenbaum, J. Vaughan, and R. G. J. Meulenbroek, "Computational Motor Control and Human Factors: Modeling Movements in Real and Possible Environments," *Human Factors: The Journal of Human Factors and Ergonomics Society,* vol. 45, no. 1, pp. 5-27, 2003, doi: 10.1518/hfes.45.1.5.27226.

[81] R. Garcia-Rosas, D. Oetomo, C. Manzie, Y. Tan, and P. Choong, "On the Relationship Between Human Motor Control Performance and Kinematic Synergies in Upper Limb Prosthetics," *Conf Proc IEEE Eng Med Biol Soc,* vol. 2018, pp. 3194-3197, 2018, doi: 10.1109/EMBC.2018.8512992.

[82] J. W. Sensinger and S. Dosen, "A Review of Sensory Feedback in Upper-Limb Prostheses From the Perspective of Human Motor Control," *Frontiers in neuroscience,* vol. 14, 2020, doi: 10.3389/fnins.2020.00345.

[83] J. W. Keller, A. Fahr, J. Balzer, J. Lieber, and H. J. A. van Hedel, "Validity and reliability of an accelerometer-based assessgame to quantify upper limb selective voluntary motor control," *Journal of neuroengineering and rehabilitation,* vol. 17, no. 1, pp. 1-11, 2020, doi: 10.1186/s12984-020-00717-y.

[84] R. H. Leigh *et al.*, "Reach and grasp by people with tetraplegia using a neurally controlled robotic arm," *Nature,* vol. 485, no. 7398, p. 372, 2012, doi: 10.1038/nature11076.

[85] M. Caimmi *et al.*, "Normative Data for an Instrumental Assessment of the Upper-Limb Functionality," (in eng), *BioMed research international,* vol. 2015, pp. 484131-14, 2015, doi: 10.1155/2015/484131.

[86] A. de los Reyes-Guzmán *et al.*, "Novel kinematic indices for quantifying upper limb ability and dexterity after cervical spinal cord injury," *Med Biol Eng Comput,* vol. 55, no. 5, pp. 833-844, 2017, doi: 10.1007/s11517-016-1555-0.

[87] W.-S. Kim, S. Cho, D. Baek, H. Bang, and N.-J. Paik, "Upper Extremity Functional Evaluation by Fugl-Meyer Assessment Scoring Using Depth-Sensing Camera in Hemiplegic Stroke Patients," *PLoS One,* vol. 11, no. 7, p. e0158640, 2016, doi: 10.1371/journal.pone.0158640.

[88] C. Colomer, R. Llorens, E. Noé, and M. Alcañiz, "Effect of a mixed reality-based intervention on arm, hand, and finger function on chronic stroke," *J Neuroeng Rehabil,* vol. 13, no. 1, p. 45, 2016, doi: 10.1186/s12984-016-0153-6.

[89] J. Xu, Q. Kun, H. Liu, and X. Ma, "Hand Pose Estimation for Robot Programming by Demonstration in Object Manipulation Tasks," vol. 2018-, ed: Technical Committee on Control Theory, Chinese Association of Automation, 2018, pp. 5328-5333.

[90] C. Melchiorri, "GLOBAL TASK SPACE MANIPULATABILITY ELLIPSOIDS FOR MULTIPLE-ARM SYSTEMS AND FURTHER CONSIDERATIONS - COMMENTS," (in English), *Ieee*

Transactions on Robotics and Automation, Letter vol. 9, no. 2, pp. 232-235, Apr 1993, doi: 10.1109/70.238288.

[91] P. K. Artemiadis, P. T. Katsiaris, M. V. Liarokapis, and K. J. Kyriakopoulos, "On the effect of human arm manipulability in 3D force tasks: Towards force- controlled exoskeletons," ed, 2011, pp. 3784-3789.

[92] J. D. Humphrey, *An introduction to biomechanics : solids and fluids, analysis and design*. London: Springer, 2003.

[93] A. B. Schultz, J. A. Faulkner, and V. A. Kadhiresan, "A simple Hill element-nonlinear spring model of muscle contraction biomechanics," *J APPL PHYSIOL,* vol. 70, no. 2, pp. 803-812, 1991.

[94] R. Cohen and D. Rosenbaum, "Prospective and retrospective effects in human motor control: planning grasps for object rotation and translation," *An International Journal of Perception, Attention, Memory, and Action,* vol. 75, no. 4, pp. 341-349, 2011, doi: 10.1007/s00426-010-0311-6.

[95] T. Emanuel and I. J. Michael, "Optimal feedback control as a theory of motor coordination," *Nature Neuroscience,* vol. 5, no. 11, p. 1226, 2002, doi: 10.1038/nn963.

[96] R. Shadmehr and J. Krakauer, "A computational neuroanatomy for motor control," *Experimental Brain Research,* vol. 185, no. 3, pp. 359-381, 2008, doi: 10.1007/s00221-008-1280-5.

[97] C.-y. Wu, K.-c. Lin, H.-c. Chen, I. h. Chen, and W.-h. Hong, "Effects of Modified Constraint- Induced Movement Therapy on Movement Kinematics and Daily Function in Patients With Stroke: A Kinematic Study of Motor Control Mechanisms," *Neurorehabilitation and Neural Repair,* vol. 21, no. 5, pp. 460-466, 2007, doi: 10.1177/1545968307303411.

[98] M. Vidyasagar, *Nonlinear systems analysis*, 2nd ed. Englewood Cliffs, N. J. : London: Prentice Hall ; London:Prentice Hall International, 1993.

[99] P. A. Cook, *Nonlinear dynamical systems*, 2nd ed. New York ; London: Prentice Hall, 1994.

[100] S. A. Billings *et al.*, *Non-linear system design*. London: Peregrinus on behalf of the Institution of Electrical Engineers, 1984.

[101] M. W. Spong, *Robot modeling and control*. Hoboken, N.J.: Wiley, 2006.

[102] H. Ehsani, M. Rostami, and M. Parnianpour, "A closed- form formula for the moment arm matrix of a general musculoskeletal model with considering joint constraint and motion rhythm," *Multibody Syst Dyn,* vol. 36, no. 4, pp. 377-403, 2016, doi: 10.1007/s11044-015-9469-4.

[103] G. Shuxiang, Z. Wu, W. Wei, G. Jian, J. Yuehui, and W. Yunliang, "A kinematic model of an upper limb rehabilitation robot system," ed. Takamatsu, Japan, 2013, pp. 968-973.

[104] B. Masih-Tehrani and F. Janabi-Sharifi, "Kinematic modeling and analysis of the human workspace for visual perceptibility," *International journal of industrial ergonomics,* vol. 38, no. 1, pp. 73-89, 2008, doi: 10.1016/j.ergon.2007.09.006.

[105] M. Laitenberger, M. Raison, D. Périé, and M. Begon, "Refinement of the upper limb joint kinematics and dynamics using a subject-specific closed-loop forearm model," *Multibody System Dynamics,* vol. 33, no. 4, pp. 413-438, 2015, doi: 10.1007/s11044-014-9421-z.

[106] R. Postacchini *et al.*, "Kinematic analysis of reaching movements of the upper limb after total or reverse shoulder arthroplasty," *Journal of Biomechanics,* vol. 48, no. 12, pp. 3192-3198, 2015, doi: 10.1016/j.jbiomech.2015.07.002.

[107] L. Ho Shing and S. S. Q. Xie, "An upper limb exoskeleton with an optimized 4R spherical wrist mechanism for the shoulder joint," ed: IEEE, 2014, pp. 269-274.

[108] L. M. Hyunchul Kim, N. Miller, G. Byl, J. Abrams, and J. Rosen, "Redundancy Resolution of the Human Arm and an Upper Limb Exoskeleton," *Biomedical Engineering, IEEE Transactions on,* vol. 59, no. 6, pp. 1770-1779, 2012, doi: 10.1109/TBME.2012.2194489.

[109] V. Meel, P. Sagi, M. C. Spalding, S. W. Andrew, and B. S. Andrew, "Cortical control of a prosthetic arm for self- feeding," *Nature,* vol. 453, no. 7198, p. 1098, 2008, doi: 10.1038/nature06996.

[110] S. Cai, G. Huang, L. Huang, and L. Xie, "Kinematics analysis, design, and simulation of a dual-arm robot for upper limb physiotherapy," vol. 397, ed, 2018, p. 12049.

[111] M. A. Admiraal, W. P. Medendorp, and C. C. A. M. Gielen, "Three-dimensional head and upper arm orientations during kinematically redundant movements and at rest," (in eng), *Experimental brain research,* vol. 142, no. 2, pp. 181-192, 2002, doi: 10.1007/s00221-001-0897-4.

[112] C. T. Freeman, P. L. Lewin, E. Rogers, and D. H. Owens, "Iterative learning control of the redundant upper limb for rehabilitation," ed: IEEE, 2010, pp. 1278-1283.

[113] H. Kim and J. Rosen, "Predicting Redundancy of a 7 DOF Upper Limb Exoskeleton Toward Improved Transparency between Human and Robot," (in eng), *J Intell Robot Syst,* vol. 80, no. S1, pp. 99-119, 2015, doi: 10.1007/s10846-015-0212-4.

[114] J. M. P. Gunasekara, "Dexterity Measure of Upper Limb Exoskeleton Robot with Improved Redundancy," *International Conference on Industrial and Information Systems.,* pp. 548-+, 2013.

[115] J. M. P. Gunasekara, "Redundant Upper Limb Exoskeleton Robot with Passive Compliance," *International Conference on Information and Automation for Sustainability,* 2014.

[116] S. Yang, B. P.-Y. Hsiao, M. Ji, and J. Rosen, "Upper limb redundancy resolution under gravitational loading conditions: Arm postural stability index based on dynamic manipulability analysis," ed: IEEE, 2017, pp. 332-338.

[117] J. Nunes, P. Moreira, and J. Tavares, "Human Motion Analysis and Simulation Tools: A Survey " *ResearchGate,* vol. September, Chapter 12, 2015, doi: 10.4018/978-1-4666-8823-0.ch012.

[118] J. Richards, *Biomechanics in clinic and research : an interactive teaching and learning course*. Edinburgh ; New York: Churchill Livingstone/Elsevier, 2008.

[119] S. Marino, I. B. Hogue, C. J. Ray, and D. E. Kirschner, "A methodology for performing global uncertainty and sensitivity analysis in systems biology," *Journal of Theoretical Biology,* vol. 254, no. 1, pp. 178-196, 9/7/ 2008, doi: http://dx.doi.org/10.1016/j.jtbi.2008.04.011.

[120] A. Saltelli, K. Chan, E. M. Scott, K. Chan, and A. Saltelli, *Sensitivity analysis*. Chichester: Wiley, 2000.

[121] A. Saltelli, K. Chan, and M. Scott, "Preface," *Computer Physics Communications,* vol. 117, no. 1, pp. xi-xiv, 1999/03/01 1999, doi: http://dx.doi.org/10.1016/S0010-4655(98)00150-7.

[122] D. V. Lindley, *Understanding uncertainty*. Hoboken, N.J.: Wiley, 2006.
[123] K. Chen, R. A. Foulds, and Asme, "Sensitivity analysis of dynamics system in the upper limb movement control," (in English), *International Mechanical Engineering Congress and Exposition,* Proceedings Paper vol. 2: Biomedical and Biotechnology, pp. 429-434, 2012.
[124] M. M. Ardestani, M. Moazen, and Z. Jin, "Sensitivity analysis of human lower extremity joint moments due to changes in joint kinematics," 2015.
[125] R. A. Cooper, M. L. Boninger, D. P. VanSickle, R. N. Robertson, and S. D. Shimada, "Uncertainty analysis for wheelchair propulsion dynamics," *IEEE Trans Rehabil Eng,* vol. 5, no. 2, pp. 130-139, 1997.
[126] S. Kim, M. Mazumder, and S. J. Park, "Uncertainty analysis of 3D motion data available from motion analysis system," *Int. J. Phys. Sci.,* vol. 5, no. 7, pp. 1191-1199, 2010.
[127] H. Rahnejat, *Multi-body dynamics : vehicles, machines, and mechanisms*. London: Professional Engineering, 1998.
[128] G. Wu and P. R. Cavanagh, "ISB RECOMMENDATIONS FOR STANDARDIZATION IN THE REPORTING OF KINEMATIC DATA," (in English), *Journal of Biomechanics,* Note vol. 28, no. 10, pp. 1257-1260, Oct 1995, doi: 10.1016/0021-9290(95)00017-c.
[129] G. Wu *et al.*, "ISB recommendation on definitions of joint coordinate system of various joints for the reporting of human joint motion— part I: ankle, hip, and spine," vol. 35, ed, 2002, pp. 543-548.
[130] G. Wu *et al.*, "ISB recommendation on definitions of joint coordinate systems of various joints for the reporting of human joint motion— Part II: shoulder, elbow, wrist and hand," *Journal of Biomechanics,* vol. 38, no. 5, pp. 981-992, 2005, doi: 10.1016/j.jbiomech.2004.05.042.
[131] Y. Vanlandewijck, D. Theisen, and D. Daly, "Wheelchair Propulsion Biomechanics," *Sports Medicine,* vol. 31, no. 5, pp. 339-367, 2001, doi: 10.2165/00007256-200131050-00005.
[132] Y. Mao and S. K. Agrawal, "Design of a cable- driven arm exoskeleton (CAREX) for neural rehabilitation," *IEEE Transactions on Robotics,* vol. 28, no. 4, pp. 922-931, 2012, doi: 10.1109/TRO.2012.2189496.
[133] J. J. Craig, *Introduction to robotics : mechanics and control*, 2nd ed. Reading, Mass. ; Wokingham: Addison-Wesley, 1989.
[134] M. Viceconti, *Multiscale modeling of the skeletal system*. Cambridge: Cambridge University Press, 2012.
[135] W. Maurel and D. Thalmann, "Human shoulder modeling including scapulo-thoracic constraint and joint sinus cones," (in English), *Computers & Graphics-Uk,* Article vol. 24, no. 2, pp. 203-218, Apr 2000, doi: 10.1016/s0097-8493(99)00155-7.
[136] K. Petuskey, A. Bagley, E. Abdala, M. A. James, and G. Rab, "Upper extremity kinematics during functional activities: Three-dimensional studies in a normal pediatric population," (in eng), *Gait & posture,* vol. 25, no. 4, pp. 573-579, 2006, doi: 10.1016/j.gaitpost.2006.06.006.
[137] M. Hyosang, H. Nguyen, N. P. Robson, and R. Langari, "Human arm motion planning against a joint constraint," ed: IEEE, 2012, pp. 401-406.
[138] V. M. Systems, "Vicon Nexus Reference Guide," ed, 2020.

[139] W. T. Dempster, "The anthropometry of body action," *Annals of the New York Academy of Sciences,* vol. 63, no. 4, pp. 559-585, 1955, doi: 10.1111/j.1749-6632.1955.tb32112.x.
[140] R. Contini, R. J. Drillis, and M. Bluestein, "Determination of body segment parameters," (in English), *Human Factors,* Article vol. 5, no. 5, pp. 493-504, 1963, doi: 10.1177/001872086300500508.
[141] R. Contini, "Body segment parameters, part II," *Artificial Limbs,* vol. 16, 1, pp. 1-19, 1972.
[142] C. R. Drillis R., Bluestein M., "Body segment parameters. A survey of measurement techniques," *Artificial limbs,* vol. 25, pp. 44-66, 1964.
[143] *Anthropometric source book. Volume 2: A handbook of anthropometric data*. United States: NASA Scientific and Technical Information Office, 1978.
[144] E. Churchill, L. L. Laubach, J. T. Mcconville, and I. Tebbetts, *Anthropometric source book volume I: Anthropometry for designers*. Houston, Tex., United States: NASA Scientific and Technical Information Office, 1978.
[145] U. S. D. o. Defense, *Military Handbook Anthropometry of U.S. Military Personnel (metric)*. U.S. Department of Defense, 1991, p. 531.
[146] L. Peebles, *Adultdata : the handbook of adult anthropometric and strength measurements : data for design safety*. U.K.: Department of Trade and Industry, 1998.
[147] S. Pheasant, *Bodyspace : anthropometry, ergonomics, and the design of work*, 3rd ed. ed. Boca Raton, Fla. ; London: Boca Raton, Fla. ; London : CRC, 2006, 2006.
[148] T. S. Ellenbecker, E. P. Roetert, P. A. Piorkowski, and D. A. Schulz, "Glenohumeral joint internal and external rotation range of motion in elite junior tennis players," (in English), *Journal of Orthopaedic & Sports Physical Therapy,* Article vol. 24, no. 6, pp. 336-341, Dec 1996, doi: 10.2519/jospt.1996.24.6.336.
[149] J. M. Walker, D. Sue, N. Miles-Elkousy, G. Ford, and H. Trevelyan, "Active Mobility of the Extremities in Older Subjects," *Physical Therapy,* vol. 64, 6, pp. 919-923, 1984.
[150] J. J. Han, G. Kurillo, R. T. Abresch, A. Nicorici, and R. Bajcsy, "Validity, Reliability, and Sensitivity of a 3D Vision Sensor-based Upper Extremity Reachable Workspace Evaluation in Neuromuscular Diseases," (in English), *PLoS currents,* vol. 5, 2013, doi: 10.1371/currents.md.f63ae7dde63caa718fa0770217c5a0e6.
[151] J. J. Han, G. Kurillo, R. T. Abresch, E. De Bie, A. Nicorici, and R. Bajcsy, "Upper extremity 3-dimensional reachable workspace analysis in dystrophinopathy using Kinect," (in English), *Muscle & Nerve,* Article vol. 52, no. 3, pp. 344-355, Sep 2015, doi: 10.1002/mus.24567.
[152] W.-L. Chen, Y.-C. Shih, and C.-F. Chi, "Hand and Finger Dexterity as a Function of Skin Temperature, EMG, and Ambient Condition," (in eng), *Human factors,* vol. 52, no. 3, pp. 426-440, 2010, doi: 10.1177/0018720810376514.
[153] M. D. Muller *et al.*, "Cold habituation does not improve manual dexterity during rest and exercise in 5 °C," (in eng), *Int J Biometeorol,* vol. 58, no. 3, pp. 383-394, 2014, doi: 10.1007/s00484-013-0633-3.
[154] Q. Geng, F. Chen, and I. Holmér, "The Effect of Protective Gloves on Manual Dexterity in the Cold Environments," (in eng), *International journal of occupational safety and ergonomics,* vol. 3, no. 1-2, pp. 15-29, 1997, doi: 10.1080/10803548.1997.11076362.

[155] D. Preece, R. Lewis, and M. J. Carré, "Effects of Mucin on the dexterity and tactile sensitivity of medical glove users," (in eng), *Biotribology (Oxford),* vol. 24, p. 100146, 2020, doi: 10.1016/j.biotri.2020.100146.

[156] M. Stokdijk, J. Nagels, and P. M. Rozing, "The glenohumeral joint rotation centre in vivo," (in eng), *Journal of biomechanics,* vol. 33, no. 12, pp. 1629-1636, 2000, doi: 10.1016/S0021-9290(00)00121-4.

[157] R. M. Ehrig, W. R. Taylor, G. N. Duda, and M. O. Heller, "A survey of formal methods for determining the centre of rotation of ball joints," (in eng), *Journal of biomechanics,* vol. 39, no. 15, pp. 2798-2809, 2006, doi: 10.1016/j.jbiomech.2005.10.002.

[158] T. Monnet, E. Desailly, M. Begon, C. Vallée, and P. Lacouture, "Comparison of the SCoRE and HA methods for locating in vivo the glenohumeral joint centre," (in eng), *Journal of biomechanics,* vol. 40, no. 15, pp. 3487-3492, 2007, doi: 10.1016/j.jbiomech.2007.05.030.

[159] A. C. Campbell, J. A. Alderson, D. G. Lloyd, and B. C. Elliott, "Effects of different technical coordinate system definitions on the three dimensional representation of the glenohumeral joint centre," (in eng), *Med Biol Eng Comput,* vol. 47, no. 5, pp. 543-550, 2009, doi: 10.1007/s11517-009-0467-7.

[160] A. C. Campbell, D. G. Lloyd, J. A. Alderson, and B. C. Elliott, "MRI development and validation of two new predictive methods of glenohumeral joint centre location identification and comparison with established techniques," (in eng), *Journal of biomechanics,* vol. 42, no. 10, pp. 1527-1532, 2009, doi: 10.1016/j.jbiomech.2009.03.039.

[161] M. Lempereur, F. Leboeuf, S. Brochard, J. Rousset, V. Burdin, and O. Rémy-Néris, "In vivo estimation of the glenohumeral joint by functional methods : accuracy and repeatability assessment," (in eng), *Journal of biomechanics,* vol. 43, no. 2, pp. 370-374, 2010, doi: 10.1016/j.jbiomech.2009.09.029.

[162] M. Lempereur, S. Brochard, and O. Rémy-Néris, "Repeatability assessment of functional methods to estimate the glenohumeral joint centre," (in eng), *Computer methods in biomechanics and biomedical engineering,* vol. 16, no. 1, pp. 6-11, 2013, doi: 10.1080/10255842.2011.597386.

[163] M. Lempereur, F. Leboeuf, S. Brochard, and O. Rémy-Néris, "Effects of glenohumeral joint centre mislocation on shoulder kinematics and kinetics," (in eng), *Computer methods in biomechanics and biomedical engineering,* vol. 17, no. sup1, pp. 130-131, 2014, doi: 10.1080/10255842.2014.931539.

[164] B. Michaud, M. Jackson, A. Arndt, A. Lundberg, and M. Begon, "Determining in vivo sternoclavicular, acromioclavicular and glenohumeral joint centre locations from skin markers, CT-scans and intracortical pins: A comparison study," vol. 38, ed, 2016, p. 290.

[165] P. Merriaux, Y. Dupuis, R. Boutteau, P. Vasseur, and X. Savatier, "A Study of Vicon System Positioning Performance," (in eng), *Sensors (Basel, Switzerland),* vol. 17, no. 7, p. 1591, 2017, doi: 10.3390/s17071591.

[166] M. K., S. A., and K. S., "Evaluating motion capture accuracy for gait analysis," presented at the 2017 International Symposium on Micro-NanoMechatronics and Human Science (MHS), Nagoya, Japan, 2017.

[167] S. L. Raghu, C.-k. Kang, P. Whitehead, A. Takeyama, and R. Conners, "Static accuracy analysis of Vicon T40s motion capture cameras arranged externally for motion capture in constrained aquatic environments," (in eng), *Journal of biomechanics,* vol. 89, pp. 139-142, 2019, doi: 10.1016/j.jbiomech.2019.04.029.
[168] C. Nester *et al.*, "Foot kinematics during walking measured using bone and surface mounted markers," (in eng), *Journal of biomechanics,* vol. 40, no. 15, pp. 3412-3423, 2007, doi: 10.1016/j.jbiomech.2007.05.019.
[169] R. Shultz, A. E. Kedgley, and T. R. Jenkyn, "Quantifying skin motion artifact error of the hindfoot and forefoot marker clusters with the optical tracking of a multi-segment foot model using single-plane fluoroscopy," (in eng), *Gait & posture,* vol. 34, no. 1, pp. 44-48, 2011, doi: 10.1016/j.gaitpost.2011.03.008.
[170] A. Leardini, L. Chiari, U. Della Croce, and A. Cappozzo, "Human movement analysis using stereophotogrammetry. Part 3. Soft tissue artifact assessment and compensation," (in eng), *Gait & posture,* vol. 21, no. 2, pp. 212-225, 2005.
[171] C. Quental, J. Folgado, J. Ambrósio, and J. Monteiro, "Critical analysis of musculoskeletal modelling complexity in multibody biomechanical models of the upper limb," (in eng), *Computer methods in biomechanics and biomedical engineering,* vol. 18, no. 7, pp. 749-759, 2015, doi: 10.1080/10255842.2013.845879.
[172] C. Zhang, M. Dong, J. Li, and Q. Cao, "A Modified Kinematic Model of Shoulder Complex Based on Vicon Motion Capturing System: Generalized GH Joint with Floating Centre," (in eng), *Sensors (Basel, Switzerland),* vol. 20, no. 13, p. 3713, 2020, doi: 10.3390/s20133713.
[173] A. Jha, S. S. Chiddarwar, V. Alakshendra, and M. V. Andulkar, "Kinematics-based approach for robot programming via human arm motion," (in eng), *Journal of the Brazilian Society of Mechanical Sciences and Engineering,* vol. 39, no. 7, pp. 2659-2675, 2017, doi: 10.1007/s40430-016-0662-z.
[174] J. L. Pons *et al.*, "The MANUS-HAND Dextrous Robotics Upper Limb Prosthesis: Mechanical and Manipulation Aspects," (in eng), *Autonomous Robots,* vol. 16, no. 2, pp. 143-163, 2004, doi: 10.1023/B:AURO.0000016862.38337.f1.
[175] X. Zhe, V. Kumar, and E. Todorov, "A low-cost and modular, 20-DOF anthropomorphic robotic hand: design, actuation and modeling," ed: IEEE, 2013, pp. 368-375.
[176] N. Klopcar and J. Lenarcic, "Bilateral and unilateral shoulder girdle kinematics during humeral elevation," (in eng), *Clinical biomechanics (Bristol),* vol. 21, pp. S20-S26, 2006, doi: 10.1016/j.clinbiomech.2005.09.009.
[177] J. Lenarcic and A. Umek, "Simple model of human arm reachable workspace," (in eng), *T-SMC,* vol. 24, no. 8, pp. 1239-1246, 1994, doi: 10.1109/21.299704.
[178] J. Lenarčič and N. Klopčar, "Positional kinematics of humanoid arms," (in eng), *Robotica,* vol. 24, no. 1, pp. 105-112, 2006, doi: 10.1017/S0263574705001906.
[179] M. Verdino and S. Dingman, "Two measures of laterality in handedness: the Edinburgh Handedness Inventory and the Purdue Pegboard test of manual dexterity," *PERCEPT MOTOR SKILL,* vol. 86, no. 2, pp. 476-478, 1998, doi: 10.2466/pms.1998.86.2.476

info:doi/10.2466/pms.1998.86.2.476.
[180] F. H. F. Elneel, F. Carter, B. Tang, and A. Cuschieri, "Extent of innate dexterity and ambidexterity across handedness and gender: Implications for training in

laparoscopic surgery," *SURG ENDOSC,* vol. 22, no. 1, pp. 31-37, 2008, doi: 10.1007/s00464-007-9533-0

info:doi/10.1007/s00464-007-9533-0.

[181] A. L. F. Conte, A. P. Marques, R. A. Casarotto, and S. M. Amado-João, "Handedness influences passive shoulder range of motion in nonathlete adult women," *J MANIP PHYSIOL THER,* vol. 32, no. 2, pp. 149-153, 2009, doi: 10.1016/j.jmpt.2008.12.006

info:doi/10.1016/j.jmpt.2008.12.006.

[182] S. F. Glenn *et al.*, "Kinetic Comparison Among the Fastball, Curveball, Change-up, and Slider in Collegiate Baseball Pitchers," (in eng), *The American journal of sports medicine,* vol. 34, no. 3, pp. 423-430, 2006, doi: 10.1177/0363546505280431.

[183] Z. Bańkosz and S. Winiarski, "Correlations between Angular Velocities in Selected Joints and Velocity of Table Tennis Racket during Topspin Forehand and Backhand," *Journal of sports science & medicine,* vol. 17, no. 2, pp. 330-338, 2018.

APPENDIX A

Ethics approval for research undertaken

The University Of Sheffield.

Downloaded: 19/09/2020
Approved: 01/10/2018

Ulises Daniel Serratos Hernandez
Registration number: 160108167
Mechanical Engineering
Programme: PhD Mechanical Engineering

Dear Ulises Daniel

PROJECT TITLE: Subject relative comfortability and its relation to the manipulability approach
APPLICATION: Reference Number 022879

On behalf of the University ethics reviewers who reviewed your project, I am pleased to inform you that on 01/10/2018 the above-named project was **approved** on ethics grounds, on the basis that you will adhere to the following documentation that you submitted for ethics review:

- University research ethics application form 022879 (form submission date: 20/09/2018); (expected project end date: 01/10/2020).
- Participant information sheet 1051307 version 1 (11/09/2018).
- Participant consent form 1051204 version 1 (04/09/2018).

If during the course of the project you need to deviate significantly from the above-approved documentation please inform me since written approval will be required.

Your responsibilities in delivering this research project are set out at the end of this letter.

Yours sincerely

Anne Bradford
Ethics Administrator
Mechanical Engineering

Please note the following responsibilities of the researcher in delivering the research project:

- The project must abide by the University's Research Ethics Policy: https://www.sheffield.ac.uk/rs/ethicsandintegrity/ethicspolicy/approval-procedure
- The project must abide by the University's Good Research & Innovation Practices Policy: https://www.sheffield.ac.uk/polopoly_fs/1.671066!/file/GRIPPolicy.pdf
- The researcher must inform their supervisor (in the case of a student) or Ethics Administrator (in the case of a member of staff) of any significant changes to the project or the approved documentation.
- The researcher must comply with the requirements of the law and relevant guidelines relating to security and confidentiality of personal data.
- The researcher is responsible for effectively managing the data collected both during and after the end of the project in line with best practice, and any relevant legislative, regulatory or contractual requirements.

APPENDIX B

Publication outputs

Publications

Serratos, U., Barthorpe, R. and Rowson, J., "Upper limb manipulabilty analysis and uncertainty propagation," in *25th Congress of the European Society of Biomechanics*, Vienna, Austria, P. Thurner, D. Pahr, and C. Hellmich, Eds., 2019: TU verlag an der Technischen Universität Wien, p. 289

Forthcoming Publications

Serratos, U., Barthorpe, R. and Rowson, J., " Upper limb manipulability analysis, performance and perception assessment for model validation" in *26th Congress of the European Society of Biomechanics*, Milan, Italy (submitted for podium presentation, Congress postponed to 2021 due to coronavirus pandemic)

Serratos, U., Russell, L., Barthorpe, R. and Rowson, J., " Maximum Joint Angular Velocities of the Upper Limb - A Contribution to Human Normative Data", potential journal: Journal of Biomechanics, status: draft (experiments and analysis completed).

UPPER LIMB MANIPULABILITY ANALYSIS AND UNCERTAINTY PROPAGATION

Ulises Serratos (1,2), Robert Barthorpe (2), Jennifer Rowson (1,2)

1. INSIGNEO Institute for in silico Medicine, University of Sheffield, Sheffield, UK; 2. Dynamics Research Group, Department of Mechanical Engineering, The University of Sheffield, UK.

Introduction

The study of the dexterity of human upper limbs is complex as it is affected by body sensing, information processing, muscle activation, anthropometry, range of motion, motor control, etc. This author proposes the use of the manipulability approach [1], mathematical modelling of limb physical characteristics, for the characterization of dexterity, providing a manipulability metric. Thus, this work focuses on the manipulability of the upper limb, represented here as kinematic chain, including uncertainty propagation. Circular trajectories are used to examine how manipulability is affected by changing the position of the task in the workspace. This investigation serves as a precursor to experimental analysis and to more complex modelling work.

Methods

In this investigation the arm is represented as a 2-link kinematic chain with 2-DoF (Degrees of Freedom). Two 0.2m-diameter circular trajectories with origins $A(0.30,0.00)$ and $B(0.50,0.15)$ were selected as the tasks to be evaluated (see Figure 1).

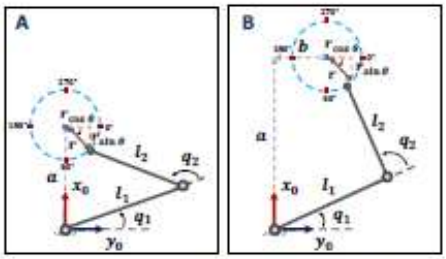

Figure 1: Circular trajectories followed by the limb.

The relationship between the task in cartesian space and in joint coordinate system is described by:

$$x = f(q) \qquad (1)$$

Where, $x = [x_1, x_2, \dots, x_n]^T$ and $q = [q_1, q_2, \dots, q_m]^T$ are the manipulation and joint vectors respectively and the superscript T represents the transpose. The equations describing velocity can be obtained by deriving equation 1, then, the Jacobian matrix J can be formed by computing the partial derivatives of the linear velocity:

$$J = \begin{pmatrix} l_1 sin(q_2) & 0 \\ l_2 + l_1 cos(q_2) & l_2 \end{pmatrix} \qquad (2)$$

Where, l_1, l_2 are the segment lengths and q_1, q_2 the joint angles. Finally, the manipulability measure w can be obtained by computing:

$$w = |\det(J)| \qquad (3)$$

Furthermore, for the analysis of uncertainty propagation, multivariate normal distributions are assumed for the segment length values which are based on statistical data [2], enabling expected manipulability for a population of subjects to be evaluated.

Results

The predicted maximum manipulability value (around 0.9) is obtained at 270° for circle A, whereas, for circle B it is obtained from 0-170° (see Figure 2). On the other hand, the predicted minimum manipulability value is around 0.5 (at 90° for circle A and 260° for circle B). The two tasks have similar manipulability values; however, circle B shows higher variability (particularly at 260°). The results show that position in space can affect manipulability.

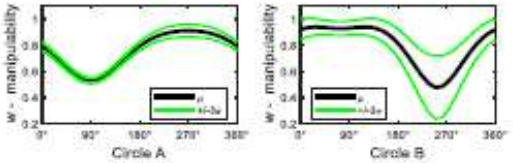

Figure 2: Manipulability measure for two circular tasks.

Discussion

This work introduces a new manipulability metric for the characterization of dexterity of the human upper limb. Such metric can help to determine suitable areas for the execution of a given task for a specific subject or for a determined population. This method and its measure have a great impact on clinical analysis, ergonomics, prosthetics, sport performance, etc. However, this is just a first step and further investigation needs to be conducted to determine the validity of the method. Thus, in future work, this author will conduct subject experimental trials to be compared with the simulation analysis presented here. Likewise, comfortability will be included in future work.

References

1. T. Yoshikawa, "Manipulability of Robotic Mechanisms," The International Journal of Robotics Research, vol. 4, no. 2, pp. 3-9, 1985
2. L. Peebles, Adultdata: the handbook of adult anthropometric and strength measurements: data for design safety. U.K.: Department of Trade and Industry, 1998.

Acknowledgements

This work was supported by CONACYT (Mexico).

APPENDIX C

Supplementary material available on request

1. Documents
   - 1.1. Experiment documentation
     - 1.1.1. Ethics approval letter
     - 1.1.2. Ethics application form
     - 1.1.3. Participant consent form
     - 1.1.4. Participant information sheet
     - 1.1.5. Motion Capture Lab risk assessment
     - 1.1.6. Vicon risk assessment
   - 1.2. Publications and posters
     - 1.2.1. Conference paper for the European Society of Biomechanics 2019 Congress
     - 1.2.2. Poster for the Dynamics Research Group 2018 Showcase
     - 1.2.3. Poster for the INSIGNEO (Institute for in silico Medicine) 2019 Showcase
     - 1.2.4. Poster for the INSIGNEO (Institute for in silico Medicine) 2019 Summer Research Programme
2. Experiment row data
3. MATLAB code
   - 3.1. Code to compute reach envelope area (2-D reachability) with respect to dexterity
   - 3.2. Code to compute workspace volume (3-D reachability) with respect to dexterity
   - 3.3. Experimental analysis – computation of Prediction, Performance, and Perception

Access to supplementary materials can be requested on the following link:

https://drive.google.com/drive/u/1/folders/0AJiZXncbdmpDUk9PVA